Towards an algorithm for the prediction of non-contact Anterior Cruciate Ligament injuries

Prepared by:

Shaun Fickling

Department of Biomedical Engineering

Faculty of Health Sciences

University of Cape Town

Prepared for:

Dr Lester John

and

Dr Sudesh Sivarasu

Department of Biomedical Engineering

Faculty of Health Sciences

University of Cape Town

December 2014

Submitted to the Faculty of Health Sciences at the University of Cape Town in fulfilment of the academic requirements for a Master of Medicine degree in **Biomedical Engineering**

Key Words: Anterior Cruciate Ligament, Non-contact Injury, Strain, Prediction

The financial assistance of the National Research Foundation (NRF) towards this research is hereby acknowledged. Opinions expressed and conclusions arrived at, are those of the author and are not necessarily to be attributed to the NRF.

Declaration

I, Shaun Dean Fickling, hereby declare that the work on which this dissertation is based is my original work (except where acknowledgements indicate otherwise) and that neither the whole work nor any part of it has been, is being, or is to be submitted for another degree at this or any other university. I empower the university to reproduce for the purpose of research either the whole or any portion of the contents in any manner whatsoever.

The Harvard referencing style was used for citation and referencing. Each contribution to, and quotation from the work(s) of other people has been cited and referenced.

Signature of Author: Signed by candidate

Date: 7 December 2014

Abstract

Background: The anterior cruciate ligament (ACL) of the knee is one of the most frequently injured ligaments in the body. 70% of ACL injuries are sustained without any direct contact to the knee, during the early stance phase of a rapid deceleration movement. Females have a significantly greater risk of injury than males participating in the same activities. In the years following injury, ACL deficient individuals are likely to experience lasting joint pain, functional instabilities and the onset of osteoarthritis. The best practice model for management of ACL injuries is a continued emphasis on prevention, which is currently limited by an incomplete understanding of how the injuries occur.

Hypothesis: Body biomechanics occurring during the terminal swing phase of a dynamic deceleration movement can predict the resulting weight acceptance phase ACL loading in both ligament bundles. This will further the understanding of the sequence of events that result in non-contact ACL injuries.

Methods: For a preliminary feasibility study, a musculoskeletal model was developed in OpenSim incorporating both anteromedial (AMB) and posterolateral (PLB) bundles of the ACL. Motion capture data of female soccer players (n = 10, mean age = 19.60 ± 1.49 years) performing unanticipated side-step cutting movements were recorded. Instantaneous, three dimensional joint angles and angular velocities at the mid-swing stage of the side-step were selected as the independent variables. The dependent variables were the maximum stance-phase AMB and PLB strains. Multiple pairwise correlation analyses were used to quantify linear relationships between these variables. To evaluate the overall potential to predict ACL strain, a best subsets linear regression model was implemented using only the significantly correlated independent variables. Each ligament bundle was analysed independently.

Results: Hip internal rotation at the mid-swing stage explained 79.1% (95% CI: 59.9% - 98.2%) of the variance in maximum stance-phase anteromedial bundle strain ($p = 0.0006$). Mid-swing knee varus position and knee valgus velocity combined explained 83.3% (95% CI: 69.2% - 97.3%) of the variance in maximum stance-phase posterolateral bundle strain ($p = 0.0019$).

Conclusions: Swing-phase body kinematics during a side-step movement can provide meaningful predictive information as to the future strain in both bundles of the ACL. They are thus useful components in understanding and exploring elements of the inciting event, particularly a kinematic “sequence of no return” that directly precedes the injury. The results validate continued research in this area, where the

relationships identified in this preliminary investigation can guide the development of a priori hypotheses for future studies to be completed at higher levels of evidence.

Clinical Relevance: A more comprehensive understanding of the variables that result in non-contact ACL injuries will allow for the design and implementation of more effective preventative measures. For example, knowledge of the "sequence of no return" could be used in sophisticated statistical systems to predict ACL injury events in real-time. This could be used to trigger an active knee brace to apply external support to the knee, preventing damage to the ligament. The long-term outcome of this project is to move towards reducing the risk and incidence of ACL injuries and the associated negative effects, preserving knee-vitality and ensuring quality of life for athletes and active individuals.

Acknowledgements

Firstly, to all of my academic advisors, thank you for all the guidance and inspiration over the years. To the engineers, Jeremy, Kieran and Tim, thanks for all the lunch, coffee and pub breaks (in no particular order). I am truly honoured to have shared this experience with you. To my parents and my sister, I could not ask for a more supportive and loving family. Thank you for always being there for me and for believing in me. Finally, to my incredible girlfriend, Nikita, I would never have managed this without you. Thank you for being by my side during this journey.

(And here's to you, Mrs Robinson)

Table of Contents

List of Figures

List of Tables

List of Equations

Chapter 1: The Anterior Cruciate Ligament

1.1: Introduction

The knee is one of the most complex joints in the human body. It operates with six degrees-of-freedom, three translations (anterior-posterior, lateral-medial, and superior-inferior) and three rotations (flexion-extension, varus-valgus and external-internal rotation) in all three planes of motion (sagittal, frontal and transverse). The orientations of these movements relative to the knee joint are illustrated in Figure 1.1 and the location of the planes of motion within the human body is illustrated in Figure 1.2.

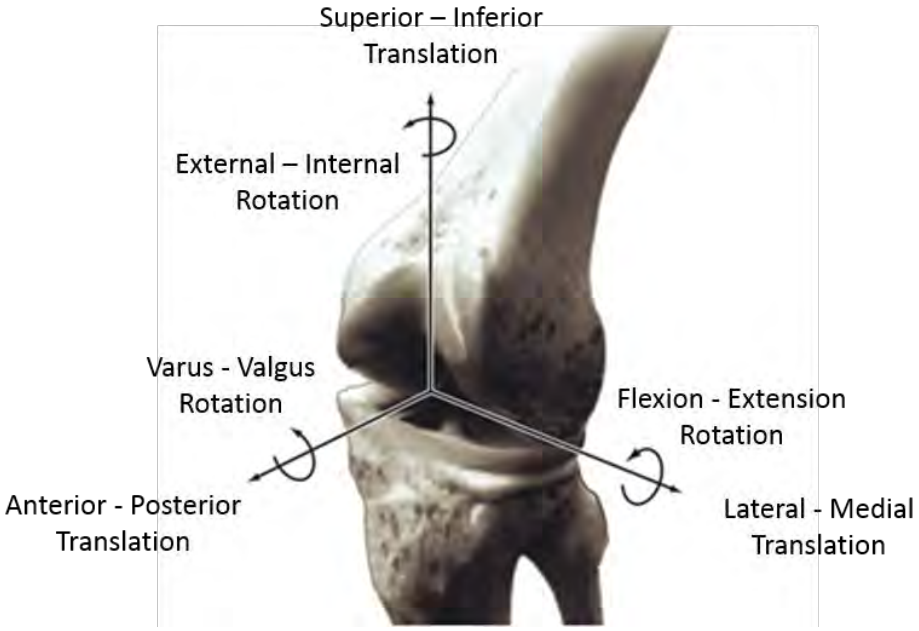

Figure 1.1: Illustration of the six degrees of freedom that the (left) knee articulates around, consisting of three translations and three rotations (Firestein et al. 2008). The word listed first in each pair corresponds with the direction of the related arrow. The second word corresponds with the opposite direction.

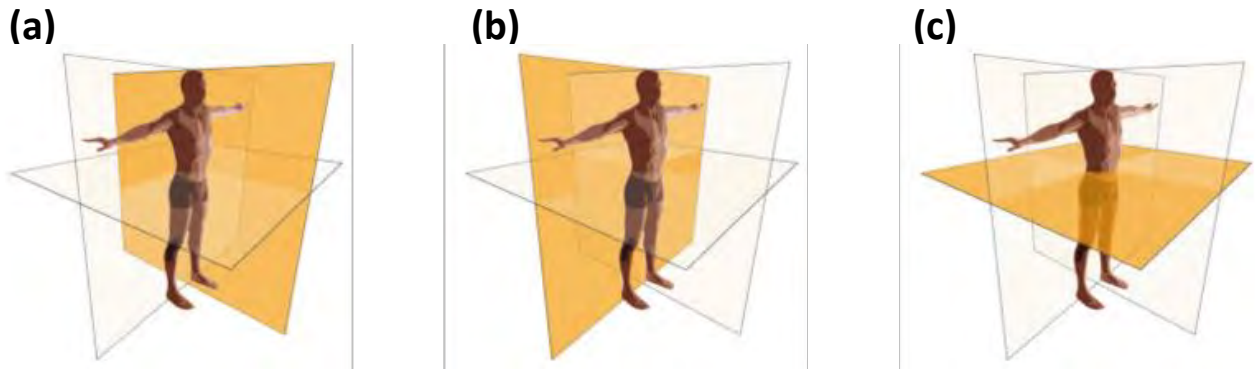

Figure 1.2: Illustration of the Sagittal (a), Frontal (b) and Transverse (c) planes of motion relative to the orientation of the human body (Swinnen 2014).

The knee is required to move fluidly through these coordinates while being stable[1] enough to support multiple times the weight of the body. Dynamic movements that require high maneuverability[2] compromise the stability of the knee which is already limited by its location between the two longest levers in the body, the tibia and the femur (McGinty et al. 2000; Lin et al. 2011). As a result, the knee is often considered to be one of the most frequently injured joints in the human body, particularly during sporting or athletic activity (Butler 1989; Meyer & Haut 2005; Majewski et al. 2006).

The ligaments within the knee perform functions that address both of these mechanical requirements of the knee, stability and maneuverability. There are four primary ligaments in the knee, the anterior cruciate ligament (ACL), posterior cruciate ligament (PCL), medial collateral ligament (MCL) and the lateral collateral ligament (LCL). These are purely tensile elements and are not functional in compression or when shortened below their resting length (Solomonow 2004). The ligaments ensure that the bones maintain articular contact, thereby controlling and guiding stable joint movement throughout the normal range of motion. They also act as tensional restraints to resist abnormal movement outside of these limits in order to maintain joint stability (Huiskes & Blankevoort 1992; O'Connor & Zavatsky 1995).

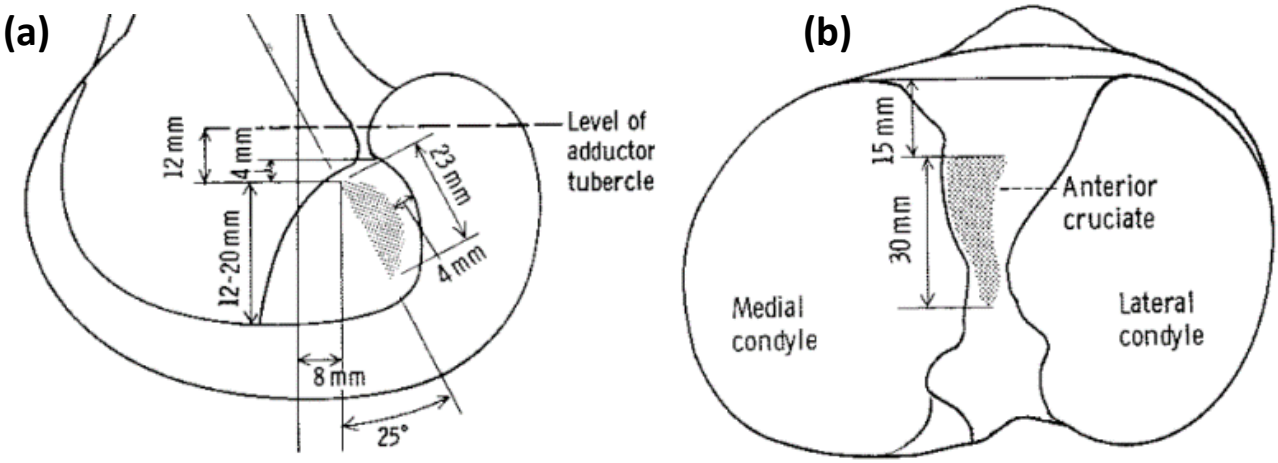

Figure 1.3: The femoral origin (a) and tibial insertion (b) zones of the ACL in the (right) knee joint capsule, shaded in grey (Girgis et al. 1975).

Of the ligaments in the knee joint, the ACL is one of the most frequently injured. An epidemiological study of 7769 knee injuries discovered that ACL lesions accounted for 20.3% of the total, with injuries to all of

[1] Stability refers to the ability of the joint to maintain a particular state without failing (Huang & Ahmed 2011)
[2] Maneuverability is defined as the ability to generate purposeful changes in motion (Huang & Ahmed 2011)

the other ligaments combined making up only 9.65% (Majewski et al. 2006). An understanding of the anatomy of the ACL is fundamental in evaluating how it can be injured (Arnoczky 1983). The ACL originates from an oval zone (Figure 1.3a) along the notch of the posterior, medial surface of the lateral femoral epicondyle. It inserts onto the medial intercondylar tubercle (Figure 1.3b), located anterior and lateral to the medial tibial spine (Girgis et al. 1975; Amis & Dawkins 1991; Luites et al. 2007). This tibial zone is larger than the zone of origin in the femur as well as the mid-section of the ligament itself. This results in a visible "fanning" pattern in the individual collagen fibrils that make up the ligament fascicles as they attach to the tibia (Duthon et al. 2006; Petersen & Zantop 2007; Scuderi 2010).

Whilst the ligament is made up of a continuous range of fibres, a different set of which are taut throughout the entire range of knee motion, it can be considered to consist of two sections, the anteromedial bundle (AMB) and the posterolateral bundle (PLB) (Arnoczky 1983; Odensten & Gillquist 1985). These are not necessarily physiologically separable but, functionally, can be viewed to be discrete. The relative origins and insertions of these bundles are illustrated in Figure 1.4. The AMB originates on the anterior, superior aspect of the femoral zone (Figure 1.4, area A) and inserts on the anterior, medial aspect of the tibial insertion zone (Figure 1.4, area B). The PLB originates posterior and inferior to the AMB on the femur (Figure 1.4, area C) and inserts posterior and lateral to the AMB on the tibia (Figure 1.4, area D).

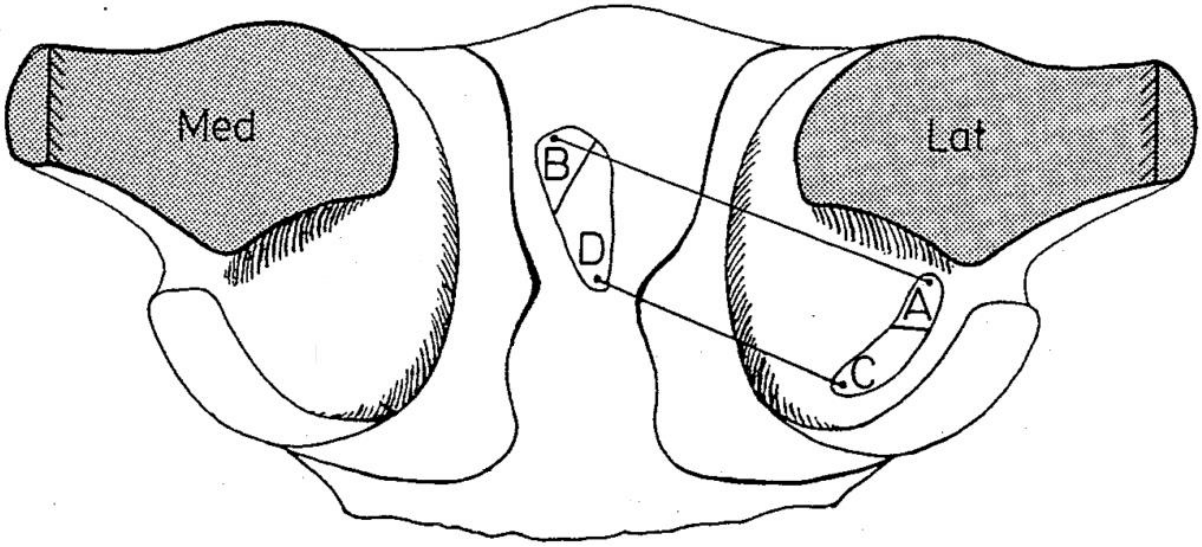

Figure 1.4: Cut away of a superior view of the knee joint illustrating of the origins and insertions of the Anterior Cruciate Ligament bundles within the knee. The anteromedial bundle (AMB) runs from A to B. The posterolateral bundle (PLB) runs from C to D (Huiskes & Blankevoort 1992).

During non-weight bearing flexion-extension tasks, the AMB is taut in knee flexion and lax in extension whereas the PLB is initially slack in flexion and tightens as the knee extends (Girgis et al. 1975; Huiskes & Blankevoort 1992). However, it has been shown that these bundles perform more complementary roles

to resist external loads occurring during weight-bearing tasks (Wu, Hosseini, et al. 2010; Wu, Seon, et al. 2010). In this scenario, both bundles experience maximum elongation when the knee is close to full extension.

There have also been reports on the presence of a third, intermediate bundle which remains the same length throughout flexion (Amis & Dawkins 1991; Hollis et al. 1991). However, other studies have failed to consistently identify this bundle and the two bundle model is thus typically regarded as the best approximation of ligament function (Takahashi et al. 2006; Duthon et al. 2006).

Neural elements relating to sensorimotor or proprioceptive functions are known to be present within the ligament (Tsuda et al. 2001; Adachi et al. 2002). These are used as afferent neural input to assist in sending the relevant activation signals to the muscles. This is required for fine neuromuscular control and motor coordination (Beard et al. 1993; Solomonow 2004; Ghez 2011).

1.2: Injury Statistics

It is estimated that approximately 80,000 anterior cruciate ligament tears occur every year in the United States alone. With the mean cost per surgery recently reported at $8574, this totals over $685m spent on ACL injury recovery every year just in the USA (Griffin & Agel 2000; Gianotti et al. 2009). Figure 1.5 illustrates that the vast majority of ACL injuries occur to people between the ages of 15 and 45 (Gianotti et al. 2009). It also indicates considerably higher rates of injury in females than in males.

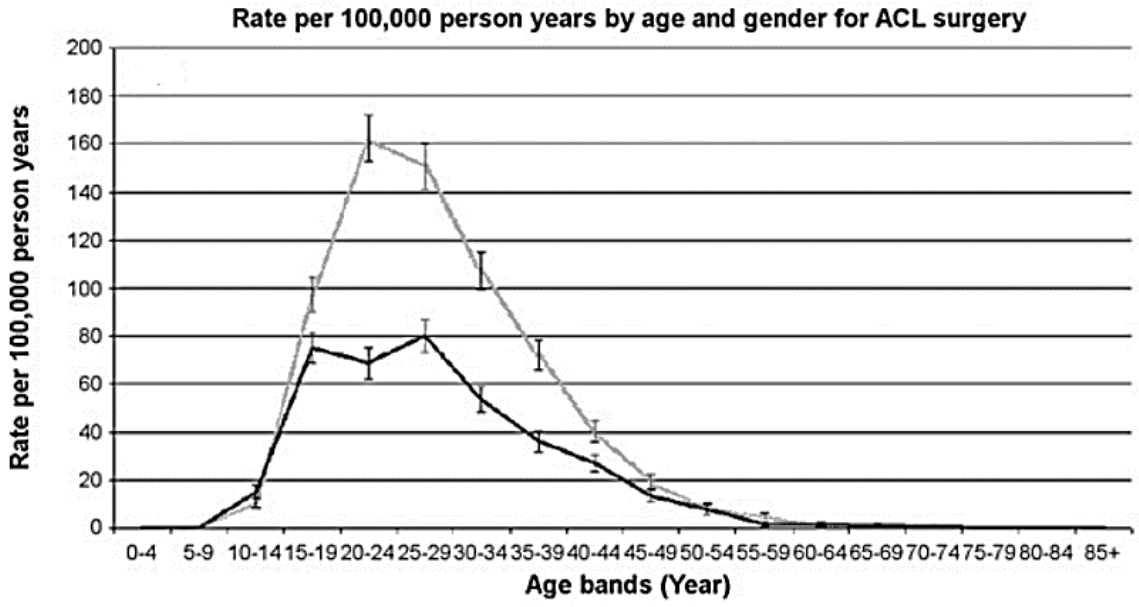

Figure 1.5: Incidence (per 100 000 person years) of ACL surgery in females (grey) and males (black) of different age groups (Gianotti et al. 2009).

There are two categories of ACL injury: contact and non-contact. Contact injuries typically result from an externally applied force as a result of a collision with an object or another player, whereas non-contact injuries take place without a direct impact to the knee joint. The non-contact condition is the most common, responsible for approximately 70% of all ACL injuries (Ireland 1999; Arendt et al. 1999; Olsen 2004; Krosshaug, Slauterbeck, et al. 2007).

Patients typically report hearing or feeling a "pop" within the knee at the moment of injury. Within 24 hours this is followed by the onset of acute haemarthrosis and swelling. Most patients are unable to continue sport or activity immediately after the injury (Noyes et al. 1989; Renstrom et al. 2008). Diagnosis of the injury is predominantly made through clinical assessment and radiography although many clinicians also make use of Magnetic Resonance Imaging (MRI) and arthroscopy (Mirza et al. 2000).

Conservative (i.e. non-surgical) solutions are often recommended for children, senior citizens and less-active patients (Mirza et al. 2000; Renstrom et al. 2008). However, a report by Strehl and Eggli (2007) revealed that almost two thirds of conservatively treated ACL injuries ultimately progressed to a point where surgical reconstruction was required. At the end of that study period only 16% of the non-operative patients were successfully treated and only 20% of this group returned to high risk sports. Furthermore, Mather et al. (2014) observed that patients who underwent surgery sooner after their injuries had higher quality-adjusted life-years[3] (QALYs) at a lower expense than those who delayed the procedure.

Surgical interventions tend to be advised for highly active individuals such as competitive athletes or patients who have also damaged other knee structures. Patients recovering from ACL reconstruction surgery typically face lengthy periods of time before they are fully healed. Hartigan et al. (2010) found that only 5% of ACL deficient athletes were able to return-to-play 3 months post operation, with 46% returning at 6 months and 78% at 1 year. The authors concluded that some individuals may never be able to return to high-level activity after an ACL injury. Similarly, Shelbourne et al. (2014) reported that only 74% of ACL deficient high school and collegiate athletes and 62% of adults in non-competitive leagues were able to return to the same level of activity.

[3] Quality Adjusted Life Years (QALYs) is a metric used when making decisions between different treatment methods. It reflects the additional years of life - adjusted for quality - that each potential treatment option would provide a patient (Broome 1993).

Professional athletes also experience similar setbacks. Analysing a 5 year period in the National Football League, Carey et al. (2006) reported that over 20% of all running backs and wide receivers who sustained ACL injuries never returned to a competitive game in the league. Those that did return only played their next game an average of more than a year after the injury and their power rating[4] per game dropped significantly from their pre-injury level. In a similar study of elite soccer players, 94% of athletes with ACL reconstructions returned to training within 10 months of surgery and 89% played a competitive fixture within 12 months (Waldén et al. 2011).

In addition to the ACL, other structures within the knee are often damaged either as part of the initial injury or later on as a result of functional instabilities. As described by Wang et al. (2009), *"The injury of ACL can change the load transmission of the knee joint, resulting in the load re-distribution of the inter-articular tissues and the damages of other tissues and structures."* The longer term secondary effects of ACL injury are worrying, with a very high prevalence of osteoarthritis, joint pain and functional instability recorded in patients a decade post-injury (Lohmander et al. 2004). For example, in a 14 year follow up study of patients who had undergone ACL reconstruction surgery on one knee, Barenius et al. (2014) found that osteoarthritis was three times more likely to develop in the injured knee than in the uninjured knee. Neither surgical nor conservative treatment has shown to be able to prevent the onset of these secondary symptoms (von Porat 2004).

[4] The Power Rating score for each player was calculated as the total (annual) yards ran divided by 10 plus total touchdowns scored multiplied by 6 (Carey et al. 2006).

Chapter 2: Injury Mechanisms

2.1: The Running Gait Cycle

The gait cycle refers to the repetitive pattern of human movement, it is the interval between two successive instances of one of the characteristic events of locomotion (Levine et al. 2012). This period can be divided into two discrete stages for each limb: swing phase, where the foot is in the air, and stance phase, where the foot is in contact with the ground (Rose & Gamble 2006).

Using the standard recommended by DeVita (1994), the swing phase can be considered to occur first. "Toe-off" is the first aspect of the swing phase, beginning the gait cycle where one foot leaves the ground and "swings" forward. During the majority of this stage the other foot is in contact with the ground (completing its own cycle - albeit out of phase). However, due to the speed of the running movement, there are two short periods at the start and end of the swing phase where neither leg is in contact with the ground known as "float" (Novacheck 1998). "Initial contact", when the foot returns to the ground, marks the beginning of the stance phase. The stance phase then ends at toe-off, initiating the swing phase of the following gait cycle. One full gait cycle is illustrated in Figure 2.1.

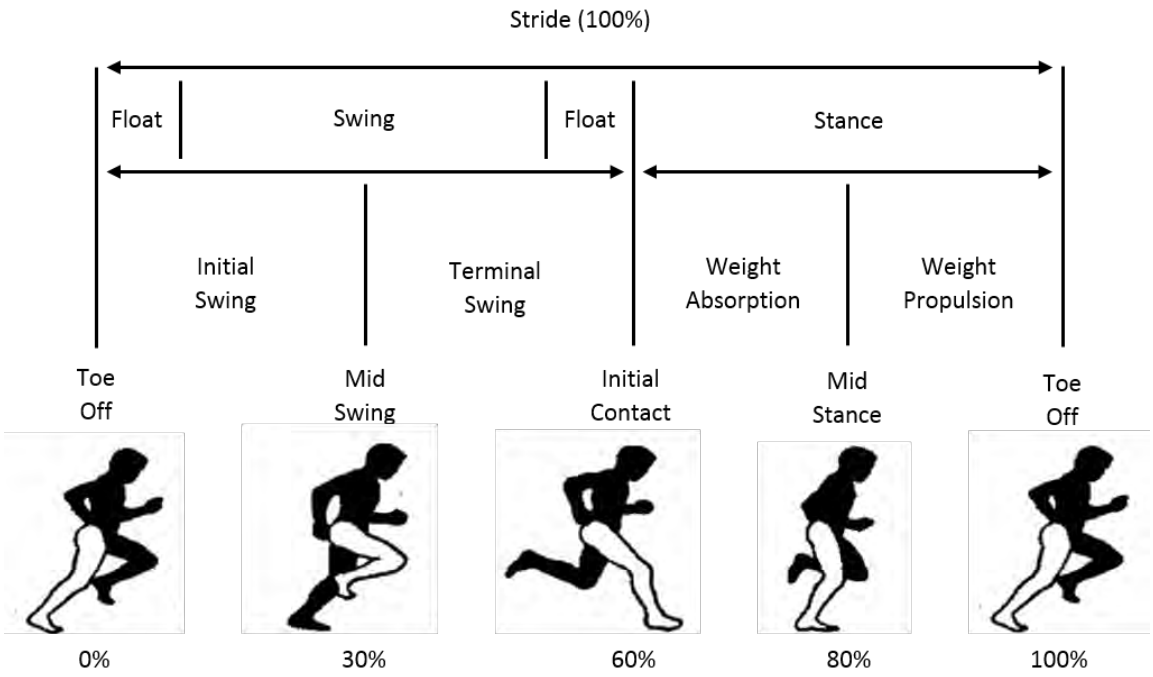

Figure 2.1: The Running Gait Cycle, from toe-off to toe-off, adapted from Ounpuu (1994), Yam et al. (2004) and Dugan and Bhat (2005).

The relative timing of these phases depends on the speed of the movement. The duration of the swing phase increases at higher speeds with a decrease in the duration of the stance phase. In normal walking,

the swing phase represents about 40% of the total duration, with the stance phase taking up the remaining 60%. However, when running, the timing is approximately reversed (Ounpuu 1994; Novacheck 1998).

Each of these phases of movement can be further subdivided into two stages. “Initial swing” is the first component of the swing phase. “Terminal swing” takes place next, as the body positions itself to prepare for landing. “Mid-swing”, where the knee reaches its maximum flexion angle, divides these two stages (Perry et al. 1996; Dugan & Bhat 2005; Rose & Gamble 2006). The first half of the stance phase consists of the weight absorption stage, where the body absorbs the ground reaction force resulting from impact. At the “mid-stance” point, the weight propulsion stage then begins as the body is propelled forwards into toe-off.

2.2: ACL Loading

The oblique spatial orientations of the ACL bundles (Figure 1.4) within the synovial capsule of the knee are related to their function as restraints of loading in multiple directions of motion. Markolf et al. (1995) reported that anterior translation of the tibia relative to the femur (Figure 2.2a) is the most direct loading mechanism of the ACL. However, these sagittal plane forces in isolation cannot realistically create loads large enough to rupture the ligament (McLean et al. 2004; Wang et al. 2009). The general thought behind ACL loading mechanisms is that a combination of loads in multiple planes of motion presents the greatest risk of injury (Griffin et al. 2006; Quatman & Hewett 2009).

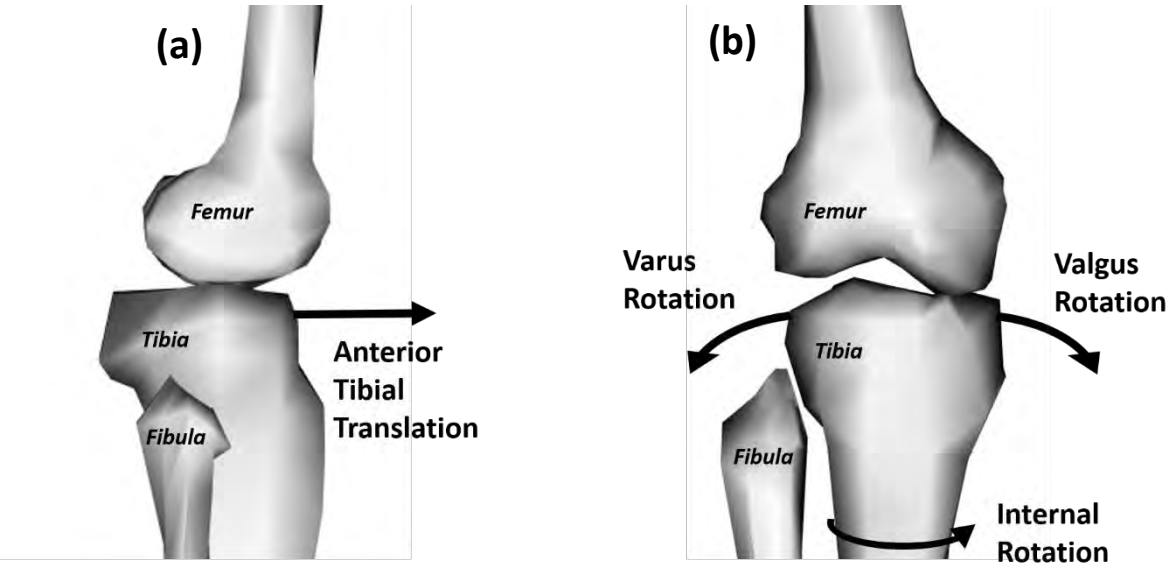

Figure 2.2: Sagittal (a) and frontal (b) plane views of the right leg illustrating the movements at the knee joint that load the ACL.

The results from Markolf's study support this concept. The authors observed that internal tibial rotation (Figure 2.2b) in combination with anterior translation created *"dramatic increases"* in ligament forces in the fully extended knee. They also investigated the effects of isolated frontal plane rotations in the knee, determining that both knee varus and valgus movements (Figure 2.2b) have the potential to load the ACL, albeit at different flexion angles. Knee varus rotation loaded the ACL in the extended knee whereas knee valgus loaded the ligament in the flexed knee. Oh et al. (2012) investigated how these frontal plane movements affected the ACL when combined with loading in the transverse plane. They determined that both varus and valgus rotations created significantly greater loads when coupled with internal tibial rotation in the extended knee. They observed that isolated knee valgus moments force the knee into internal rotation due to a mechanical coupling of the femoral and tibial contact surfaces. This is supported in earlier results published by McLean et al. (2004), who showed that neuromuscular perturbations designed to create valgus loads at the knee also resulted in both anterior translation and internal rotation moments.

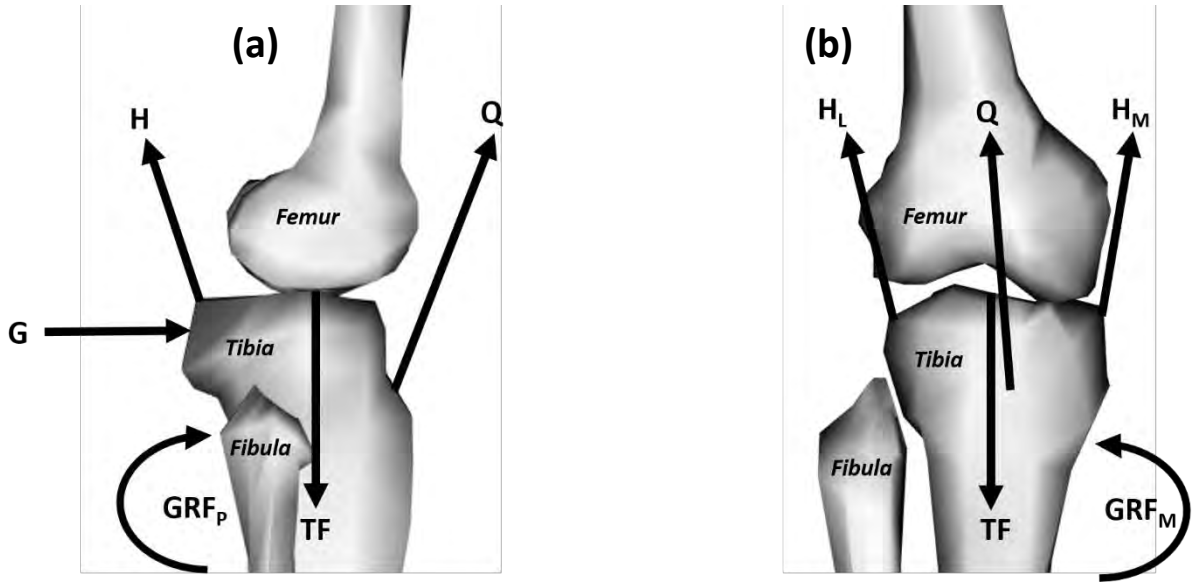

Figure 2.3: Free body diagram of the forces applied to the tibia in the sagittal (a) and frontal (b) planes where: H = Hamstrings, G = Gastrocnemius, TF = Tibiofemoral Compressive Force, Q = Quadriceps, GRF_P = Anterior translation moment arising from a posteriorly directed ground reaction force, H_L = Lateral Hamstrings, H_M= Medial Hamstrings, GRF_M = Moment arising from a medially directed ground reaction force.

The forces primarily responsible for creating moments within the knee are the ground reaction force, the tibiofemoral compressive force (Figure 2.3, TF) and the muscle forces applied by quadriceps (Figure 2.3, Q), hamstrings (Figure 2.3, H), and gastrocnemius (Figure 2.3, G). Two free body diagrams of the kinetic variables at the knee that affect loading in the ACL are illustrated in Figure 2.3, in the sagittal (Figure 2.3a) and frontal (Figure 2.3b) planes (Pflum et al. 2004; Kernozek & Ragan 2008).

During the stance phase (Chapter 2.1) of a dynamic movement, the ground reaction force applied to the foot is required to generate meaningful changes in direction. (Rose & Gamble 2006). The vertical component of this force is a function of the inertia and the relative upward and downward accelerations of the body during the movement. Additional components in the anterior-posterior and medial-lateral directions arise from the friction between the foot and the ground.

This force creates moments at the knee joint, the magnitude of which is a function of the magnitude of the ground reaction force as well as the distance between the angle of the force and the centre of rotation of the knee (Donnelly et al. 2012). For example, a force directed posterior and medial to the knee of the ground reaction force would create moments that would attempt to increase the anterior translation (Figure 2.3, GRF_P) and knee varus position (Figure 2.3, GRF_M), respectively. Similarly, a laterally directed component of the ground reaction force would create a valgus moment at the knee.

The tibiofemoral compressive force is created by the vertical component (relative to the tibial plateau) of the ground reaction force. This creates an anterior shift and internal rotation of the tibia relative to the femur due to the physical interaction between the surface contours of the tibia and the femur and the slope of the tibial plateau (Meyer & Haut 2005; Shao et al. 2011).

Under non-weight bearing conditions, the quadriceps and gastrocnemius muscles strain the ligament by drawing the tibia anteriorly relative to the femur (DeMorat 2004; Kevin B Shelburne et al. 2004). The hamstrings counteract this loading on the ACL by applying a posteriorly directed force on the tibia (Kernozek & Ragan 2008; Podraza & White 2010). The hamstrings also have both medial (Figure 2.3b, H_M) and lateral (Figure 2.3b, H_L) insertions which provides additional rotational stability to the knee joint (Hewett et al. 2010). However, during weight bearing tasks, both quadriceps and gastrocnemius activations have been shown to reduce the maximum resulting loads in the ligament by increasing joint stiffness to provide stability against the external loads (Wu, Seon, et al. 2010; Hashemi et al. 2010; Morgan et al. 2014).

The rate of loading is also thought to increase the risk of injury. Strain-rate in the ACL has been shown to alter the mechanical resistance of ligaments, with higher rates of strain creating higher tensions (Lee & Hyman 2002). This is evident in that fast, dynamic motions are known to result in more incidents of ligament damage than static movements (R.H. Peterson 1986). Eversull et al. (2001) demonstrated that up to 50% more tension was developed in a given length of the supraspinous ligament when stretched at

200% per second compared to 25% per second. Rapid stretching of the ACL may thus create dangerous loading levels while still remaining within a physiologically safe length (Solomonow 2004).

2.3: A framework for examining Injury Events

Meuwisse (1994) proposed a multivariate model for studying athletic injuries, expanding the work of Hennekens and Buring (1987). The purpose of this model is to analyse the contribution of various factors to injury etiology and to explore the interactions between these factors. It takes the form of a causation chain of increasing risk, with accumulated exposure to specific factors and events resulting in an athlete's progression towards sustaining an injury. This sequence is depicted in Figure 2.4.

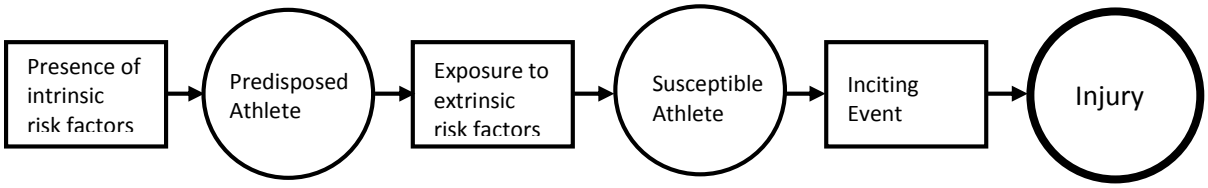

Figure 2.4: The Meeuwisse (1994) framework for injury causation. This causation chain, read from left to right, illustrates the types of factors (rectangle blocks) that lead to different categories of risk (circles) and, ultimately, an injury event.

The first part of the chain describes the intrinsic risk factors that, if present, defines a "predisposition" to an injury. These are anatomical, hormonal or neuromuscular variables that are specific to an individual (Hewett et al. 2005; Hewett et al. 2006). Subsequent exposure to extrinsic risk factors, those related to the environment around the individual, creates a "susceptibility" to an injury. Any variable that affects the loading patterns on the ACL (2.2) constitutes a risk factor for injury. Similarly, any variable that inhibits the body's ability to withstand these loads is also a risk factor (McIntosh 2005).

After a four-year evaluation of military cadets by Uhorchak et al. (2003), it was observed that the presence of one of more identified risk factors greatly increased a cadet's risk of injury. All of the female cadets with some combination of risk factors went on to sustain ACL injuries. However, exposure to one or many of these risk factors alone is not enough to produce an injury. The final link in the causation chain is the inciting event, regarded as the physical mechanism that creates the failure in the ligament (Bahr & Krosshaug 2005). This framework is implemented in the following chapters to describe and evaluate the current body of knowledge in literature regarding non-contact ACL injuries.

2.4: Risk Factors

2.4.1: Intrinsic Risk Factors

The mechanical tolerance of a ligament defines its ability to withstand forces. Subjected to the same load levels, weaker ligaments would be more prone to rupture than those which are inherently stronger. Noyes and Grood (1976) observed that the strength of the ACL decreases significantly with age. It is also thought that a narrower notch space between the femoral condyles is likely to house a smaller and thus weaker ACL (Uhorchak et al. 2003; Renstrom et al. 2008). Another theory is that the ACL can become impinged on the femoral condyle under certain conditions, excessively loading the ligament under what might normally appear to be safe movement conditions (Olsen 2004).

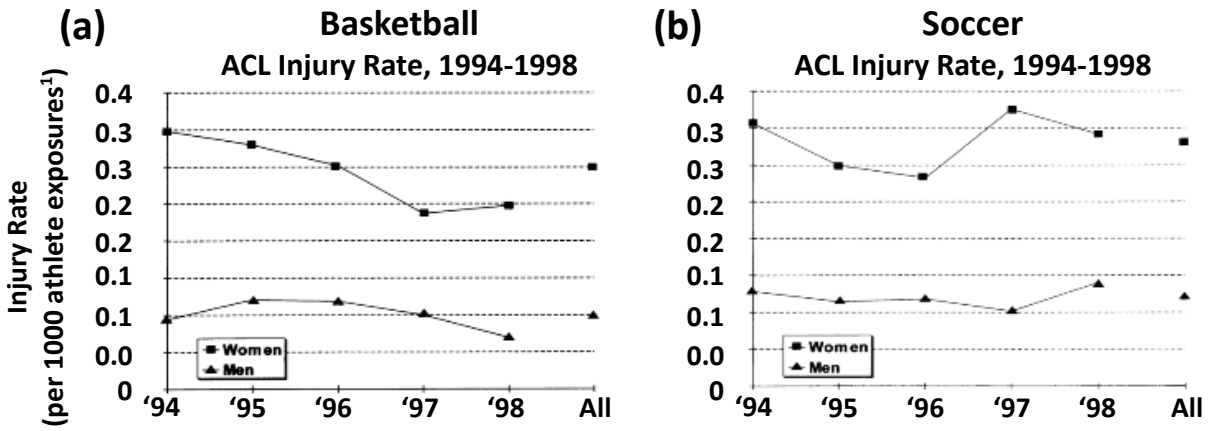

Figure 2.5: Difference in ACL injury rates between Men and Women per 1000 athlete exposures[5] over a five season study period in Basketball (a) and Soccer (b) (Arendt et al. 1999). This clearly illustrates the increased prevalence of injuries amongst female populations, signifying that gender is an important risk factor.

Gender is also a significant factor in the incidence of ACL injuries. Women are 2 - 5 times more likely to sustain these injuries than men participating in the same activities, as depicted in Figure 2.5. This disparity remains fairly constant in the literature over a variety of different sports and activities (Arendt et al. 1999; Kernozek & Ragan 2008; Waldén et al. 2011). Chandrashekar et al. (2006) measured female ACLs to be significantly weaker than those of males when controlling for age, ligament size and body anthropometric measurements. The authors concluded that, "*the lower mechanical properties of the female ACL is a central factor because it affects all existing theories."* Women have also been shown to have significantly

[5] An exposure was defined by Arendt (1999) as "the participation of one athlete in one practice or game where he or she is exposed to the possibility of athletic injury."

narrower femoral notches than men, with height and weight as covariates (Shelbourne 1998). However, Anderson et al. (2001) found no differences in notch width between genders.

A large Q-angle (Figure 2.6a), the angle between the imaginary line from the anterior-superior iliac spine to the centre of the patella and the line from the patella to the tibial tubercle, may place the knee in an increased valgus position (McLean et al. 1999; Alentorn-Geli et al. 2009). Arendt et al. (1999) measured female Q-angles to be an average of 5 degrees larger than those of males.

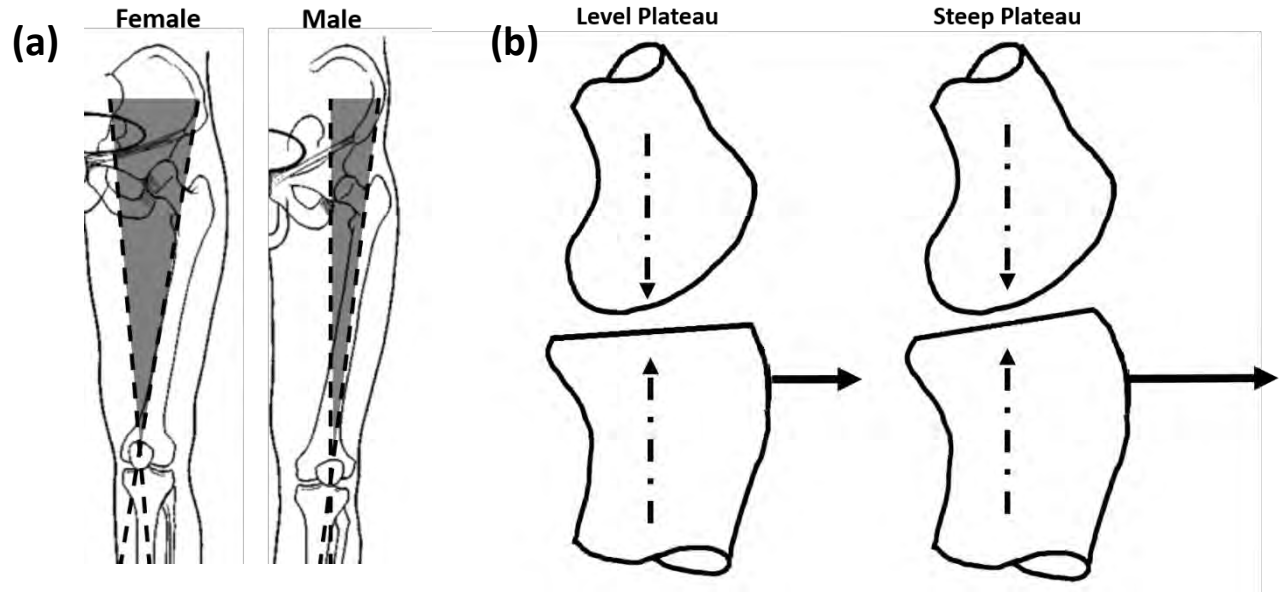

Figure 2.6: Two potential intrinsic risk factors for non-contact ACL injury. The difference in Q-Angle between genders (a), adapted from Griffin and Agel (2000). The increase in anterior displacement resulting from a steeper tibial plateau (b), adapted from Meyer & Haut (2005).

Individuals with a steeper tibial slope (Figure 2.6b) would experience larger anterior displacements of the tibia and thus increased ligament loading (Chapter 2.2) than those with a more level gradient under the same tibial compressive force (Meyer & Haut 2005; Shao et al. 2011).

The level of experience and skill of an individual athlete has shown to affect the risk of an ACL injury. Shelbourne (1998) found that military cadets playing sports at a competitive level had roughly 5 times lower risk of injury than those playing socially. This is supported my McLean et al. (1999), who found that lack of experience was a predictor of variability in knee kinematics during dynamic movements.

Footedness, or the preference of an athlete to favour a particular leg, may also be a risk factor for ACL injury. Some studies have recorded side-to-side differences in neuromuscular strength (Hewett et al.

1996) and knee joint moments (Kar & Quesada 2013), but others have observed no difference in kinematic patterns between dominant and non-dominant limbs (Ford et al. 2005; Stone et al. 2014).

The ground reaction force created during a dynamic movement (Chapter 2.2) is typically much greater than the weight of the athlete due of the inertia of the body (Hewett et al. 2010). Individuals with a high Body Mass Index (BMI)[6] would thus experience larger joint forces than leaner athletes under the same kinematic conditions. This has been shown to increase the risk of ACL injuries, particularly in women (Uhorchak et al. 2003).

Fatigue affects muscle strength and activation patterns to significantly alter the mechanics of movement (Rozzi et al. 1999). Kernozek et al. (2008) reported that fatigued participants, when landing from a jump, displayed kinematic patterns that are known to increase the risk of ACL injury (Chapter 2.6). This effect was present in both genders, although it was noted to be more pronounced in women. Deficits in proprioception have also been linked to functional instabilities within the knee and an increased risk for knee ligament injury (Beard et al. 1993; Zazulak et al. 2007).

Static postural factors can also affect the risk of a non-contact ACL injury. Woodford-Rogers (1994) observed that joint laxity (the natural kinematic variability within the knee) and a pronation of the subtalar joint were significantly more prominent in a cohort of ACL injured athletes. This was an extension of the results published by Tiberio (1987) and Coplan (1989) suggesting that these two properties are fundamentally linked. Louden and Jenkins (1996) also found athletes who had sustained ACL injuries to demonstrate greater subtalar pronation than non-injured athletes. Furthermore, the injured group also displayed greater knee recurvatum (hyper-extension) when standing upright than the uninjured group. Women have also been shown to have fundamentally greater knee joint laxity than men (Rozzi et al. 1999). Laxity can be measured directly at the knee through the use of arthrometers (Rozzi et al. 1999; Uhorchak et al. 2003) or with more generic tests such as the Beighton Score[7] (Simpson 2006).

Finally, a personal history of ACL injury is known to be one of the strongest predictors of a repeat occurrence. Athletes who have undergone an ACL reconstruction are up to 12 times more likely to sustain

[6] Body Mass Index (BMI) is represented as the mass of an individual (kilograms) divided by the square of their height (metres) (WHO 1995)

[7] The Beighton Score is a measure of generalized joint laxity that is calculated when testing range-of-motion during the execution of 5 simple joint movements (Simpson 2006).

an additional injury within the first year than those with no prior history and 4 times more likely thereafter (Orchard et al. 2001).

2.4.2: Extrinsic Risk Factors

Seventy percent of all ACL injuries occur during athletic activity (Senter & Hame 2006). Athletes have a 10-20 times greater risk of sustaining an ACL injury in a match rather than at a practice session, despite the fact that total training hours were far longer than those of match play (Arendt et al. 1999; Waldén et al. 2011). Most injuries occur during the first and last fifteen minutes of matches which is an indication of the intensity of play early on and then the potential effect of fatigue (Chapter 2.4.1) towards the end of the game (Rahnama et al. 2002).

Non-contact ACL injuries typically occur when athletes attempt rapid deceleration movements combined with an attempt to change direction (Griffin et al. 2006). These high-risk movements such as cutting, pivoting, and landing from a jump occur frequently during sporting activity, making up as much as seventy percent of the active part of a basketball game (Ford et al. 2005). Variations in technique such as speed, cutting width and cutting angle can also significantly increase the risk of injury (Kristianslund et al. 2013).

The position of the foot when landing, a factor related to technique, changes the direction of the ground reaction force (Chaudhari & Andriacchi 2006). For example, making ground contact with the heel of the foot results in this vector being directed posterior to the knee, creating an anterior shear force which loads the ACL (Chapter 2.2). Making ground contact with the toes rather than the heel or flat foot ensures that the ground reaction force vector is directed anteriorly, preventing this loading condition (Griffin & Agel 2000).

Modern footwear are designed to increase performance by maximising friction with the playing surface underfoot (Silvers & Mandelbaum 2011). However, this appears to place the ACL at risk because an increase in friction would subsequently increase the frontal and transverse plane moments at the knee (Chapter 2.2). Scranton et al (1997) observed that over 95% of ACL injuries in American Football occurred on a dry field and that more injuries happened on natural grass than on artificial grass. The higher rate of injuries was accredited to the increased friction coefficients of the dry fields. Orchard et al (2003) similarly reported that fewer injuries occurred on both types of turf when the weather was cold, concluding that the temperature reduced the traction between player footwear and the field surface to lower the risk of injury. For indoor surfaces, Olsen (2004) found that there were more ACL injuries when handball fixtures

were played on synthetic floors than on wooden floors. Again, this was attributed to the higher friction coefficient of the synthetic floor.

Very little is known about how more abstract factors such as rules, referees or coaching influence injury risk (Renstrom et al., 2008).

2.5: The Non-Contact ACL Injury Mechanism

In this study, the injury mechanism is referred to as the sequence of events that result in a non-contact ACL injury. It consists of variables that lead up to the actual, physical means by which the ligament is strained beyond its tensile strength. The two primary types of movements that result in non-contact ACL injuries are side-step (plant and cut) and jump-landing movements. Failed side-step attempts are the most common, typically involved in 60% of ACL injuries (Arendt et al. 1999; Olsen 2004). Athletes often report being disturbed or out of balance at the time of injury (Ireland 1999; Krosshaug, Nakamae, et al. 2007).

Retrospective analyses of video footage and player reports of ACL injury events have shown that the basic sequence of the injury event is fairly consistent and non-contact injury patterns are similar between men and women (Ireland 1999). At initial contact (Chapter 2.1) with the ground, the foot is firmly planted on the floor and the knee is at or near full extension (Olsen 2004; Krosshaug, Slauterbeck, et al. 2007). The rupture typically occurs after initial contact, during the weight acceptance phase (Chapter 2.1) of the side-step movement (Pflum et al. 2004; Kernozek & Ragan 2008; Taylor et al. 2011).This coincides with the timing of the maximum vertical ground reaction force (Cerulli et al. 2003; Krosshaug, Nakamae, et al. 2007; Koga et al. 2010). However, analysis of video evidence remains unsubstantiated as it is difficult to confirm that the observed injury mechanisms were the underlying cause or simply visible as a result of the injury (Olsen 2004).

Ultimately, the sequence(s) of biomechanics that result in for non-contact ACL injuries are not well understood. The overriding consensus in literature is that these injuries result from complex interactions between body biomechanics in multiple planes of motion (Griffin et al. 2006; Quatman & Hewett 2009).

2.6: Kinematic[8] factors related to the Injury Mechanism

2.6.1: Introduction

ACL injuries are known to occur around the same time as the peak ground reaction force in a side-step movement (Chapter 2.5). The positions of each of the links in the kinetic chain, relative to the direction of this force, affects the magnitude of the resulting moment at the knee and subsequently the loading applied to the ACL (Chapter 2.2). This indicates that the alignment of the body at the point of impact with the ground may be a crucial aspect in furthering the understanding of how non-contact injuries occur.

2.6.2: The Position of No Return

Ireland (1999) first proposed the concept of a "position of no return" for ACL injuries. This represents the general kinematic alignment of the body at initial contact that presents the greatest risk for ACL injury during a cutting or pivoting movement. This concept has since been expanded upon by multiple authors, investigating the relationship between body position at initial contact and the subsequent risk of injury to gain a better understanding of non-contact ACL injuries.

In the upper body, Chaudhari et al. (2005) showed that the position of the arms can influence loading in the knee to potentially put the ACL at risk. This was related to the position of the torso at the point of contact with the ground. Dempsey et al. (2009) observed that a more upright torso position at landing was correlated with decreased knee moments. In a later study, Dempsey et al. (2012) reported that lumbar bending and rotation away from the new direction of travel (i.e. towards the planting foot) at initial contact is strongly related to an increase in valgus moments in the knee. Similarly, Kristianslund et al. (2013) found that lumbar bending towards the support leg increased valgus moments in the knee. Dempsey et al. also found that lumbar bending towards the new direction of motion (i.e. away from the planting foot) increased the internal rotation moments in the knee. Frank et al. (2013) reported that lumbar rotation towards the new direction of motion increases the varus moment in the knee. Thus, any displacement of the trunk away from the mid-line can influence potentially harmful moments within the knee.

[8] Kinematics describes the motion of the joints in the human body without referring to the underlying forces that create the movement (Novacheck 1998; Woo et al. 1999; Levine et al. 2012).

At the hip joint, studies have observed that athletes who exhibit higher degrees of hip abduction and internal rotation at initial contact also exhibit larger frontal and transverse plane knee moments (McLean et al. 2005; Sigward & Powers 2007; Dempsey et al. 2012).

Landing with an extended knee is one of the most commonly observed aspects of the non-contact ACL injury. This is likely because both bundles of the ACL are maximally loaded in the extended knee during weight bearing tasks (Chapter 1.1). Podraza and White (2010) reported that an extended knee at initial contact creates significantly larger ground reaction forces than landing with a flexed knee. Making contact with the ground with an increased knee valgus angle has shown to be highly predictive of the onset of a large knee valgus moment during the stance phase (McLean et al. 2005; Kristianslund et al. 2013). Finally, landing with the knee externally rotated is a predictor of large, subsequent internal rotation moments (Dempsey et al. 2012).

Sigward and Powers (2007) observed that athletes who exhibited large knee valgus moments during side-step movements also exhibited more internally rotated foot progression angles[9] at initial contact. Ford (2005) observed athletes to demonstrate an inverted ankle position at initial contact which then shifted to an everted position during the stance phase. This eversion in combination with tibial rotation were determined to be major factors influencing knee valgus positioning. Similarly, Dempsey (2012) found a strong correlation between the degree of ankle inversion at initial contact and stance-phase internal rotation moments.

Joint angles are not the only kinematic variables that have been linked to ACL injuries. The angular velocities of both hip and knee extension at initial contact have been shown to be highly correlated with the posterior and vertical ground reaction forces (Yu et al. 2006).

One theory about the position of no return outlines a set of joint alignments known as “dynamic valgus” (Hewett et al. 2005). This predominantly details the respective frontal plane positions of hip (femoral) adduction, knee valgus (abduction) and ankle eversion, as illustrated in Figure 2.7. An increase in any one of these joint angles, with the ground reaction force directed laterally to the knee would theoretically increase the valgus moment at the knee (Hewett et al. 2010). Dynamic valgus is not just limited to frontal

[9] Foot progression angle was defined as the angle from the forward direction of movement to the longitudinal axis of the foot at initial contact.

plane alignments, it also refers to hip internal rotation, tibial external rotation and tibial anterior translation (Hewett et al. 2006).

In recent years, studies have primarily focused on a knee valgus loading mechanism for non-contact ACL injuries (Oh et al. 2012). However, this is merely one theory of many plausible injury mechanisms. Both Chaudhari and Andriacchi (2006), and Van de Pol et al. (2009) demonstrated that a knee varus alignment at initial contact could place the ligament at risk. It has also been theorised that a predominantly sagittal-plane mechanism was responsible for injuries in men, although there is little evidence to support this claim (McLean et al. 2004). Ultimately, what is known about non-contact ACL injuries is that the stability of the knee is exceptionally sensitive to changes in body alignment at initial contact.

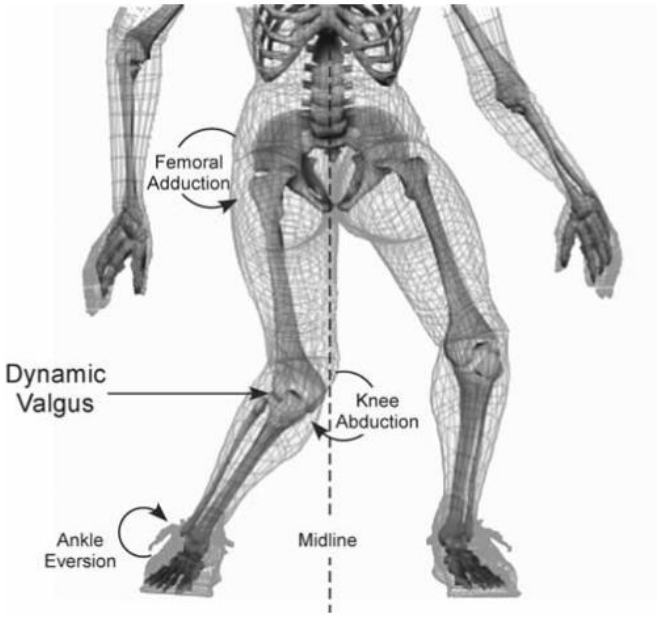

Figure 2.7:The Dynamic valgus alignment proposed by Hewett et al. (2005) indicating the combined joint angles of hip (femoral) adduction, knee valgus (abduction) and ankle eversion that may form part of the non-contact injury mechanism.

The safest techniques when attempting dynamic deceleration movements are those that minimise the propagation of reaction forces and moments up the kinetic chain, which typically involves a neutrally aligned lower extremity (Podraza & White 2010). This consists of flexed hips and knees with the body well balanced over both feet. This alignment has been proven to reduce the load on the ACL (Chaudhari & Andriacchi 2006; van de Pol et al. 2009).

2.7: Other Factors related to the Injury Mechanism

2.7.1: Neuromuscular control and ligament dominance

Since the musculature of the body is the driving force behind motor function, it plays a crucial role in creating and inhibiting forces in the ACL (Chapter 2.2). A balance between the muscle groups at the knee is ideal for optimal joint stability as well as maintaining safe load levels within the ACL (Winter 2009). For example, Weinhandl et al. (2012) demonstrated that the load in the ACL increases considerably when the hamstrings are weakened. Hamstring activation also initiates the knee flexor mechanism, which has been shown to reduce the risk of injury by preventing landing with an extended knee (Chapter 2.6.2).

If the knee muscles are not adequately contracted to stabilise the joint, the ligaments are required to provide the additional stabilizing force and absorb the balance of the impact forces. This is known as ligament dominance, which allows the ground reaction force to dictate the movement of the joint after contact. This could be exacerbated by a unfavourable lower extremity alignment (Chapter 2.6) or any other factor which results in an increase in landing forces (Chapter 2.4) (Ford et al. 2005). A balanced landing technique has been shown to reduce the maximum force in the ACL compared to a more ligament-dominant landing style. Landing with an extended knee creates a mechanical disadvantage which can be rectified by employing a softer, more flexed landing strategy with the knee musculature contracted to stabilize the joint (Hashemi et al. 2010; Wu, Seon, et al. 2010; Bulluck 2010; Laughlin et al. 2011).

Neuromuscular fatigue (Chapter 2.4.1) can also result in a worst case scenario for ACL loading. Decreased muscle strength creates a more unstable knee, with a reliance on the ligamentous structures to absorb the joint forces. (Borotikar et al. 2008). Matching for age, skill and gender, Kernozek et al. (2008) observed lower knee extension angles at initial contact in fatigued athletes, thought to be a key component in the injury mechanism (Chapter 2.6.2).

2.7.2: Unplanned Movements

Athletes often have to react to sudden changes in game dynamics like the unexpected movement of an opponent or the ricochet of a ball. With little time in which to execute the movement with appropriate technique, this can result in a situation where the athlete positions their body in an unfavourable manner (Chapter 2.6.2) with inhibited neuromuscular control (Chapter 2.7.1) (Olsen 2004).

Motor control is achieved through a combination of feed-forward or feedback systems. Feed-forward systems are faster and are used to execute planned movements, such as the process of moving the hand into the correct position to intercept a ball. Feedback systems are inherently slower as they are controlled

based on instantaneous stimuli, such as those used to stabilize the hand and arm once a ball has been caught (Ghez 2011). Muscle activations in planned movements are executed through the feed-forward systems. Unplanned movements, conversely, are more reflexive and thus rely on the slower feedback systems (Silvers & Mandelbaum 2011).

The muscle activation strategy for planned movements involves selective, timed contractions of the knee musculature to stabilize the knee against the applied load. In unplanned movements, this coordinated pattern is replaced with a more general co-contraction, with total muscle activation increasing by between 10 and 20%. However, this appears to substantially increase the knee joint moments in comparison to pre-planned movements (Weinhandl et al. 2013). Besier et al. (2001) observed that knee moments in both the frontal and transverse planes approximately doubled during unplanned movements.

2.8: Gender Factors related to the Injury Mechanism

The increased risk of ACL injuries in women is well documented (Chapter 2.4.1). The difference in injury rates between sexes is primarily as a result of multiple interrelated factors, both intrinsic as well as kinematic and neuromuscular factors related to the inciting event (Anderson et al. 2001).

Females typically display greater variability in knee joint angles and larger maximum moments (normalized to body weight) in the frontal plane when compared to males participating in the same deceleration tasks (McLean et al. 1999; Ford et al. 2005; McLean et al. 2005). James et al. (2004) observed that female athletes averaged less knee flexion at initial contact and greater maximum ground reaction forces than males. The authors concluded that technique and variables related to body positioning were the major contributing factors to this difference. Sigward & Powers (2006) also reported significantly lower knee flexion angles in women during side-step cutting. Ford et al. (2005) found no difference in flexion angles between genders but did, however, observe significantly larger maximum ankle eversion angles in females.

2.9: Current Concepts on ACL Injury Mechanisms

Although many studies have investigated kinematic (Chapter 2.6) and neuromuscular (Chapter 2.7) effects on ACL injury risk, the precise biomechanic sequences that lead up to non-contact ACL injuries are still not well understood (Sigward & Powers 2007; Hashemi et al. 2011). The overriding opinion in the literature is that it is likely a combination of multiple factors occurring along the causation chain (Chapter 2.3) - with no unique feature solely responsible (Arendt et al. 1999). The International Olympic Committee (Renstrom

et al. 2008) released a current concepts statement in 2008, concluding that the most probable components for the non-contact ACL injury mechanism include:

"most or all of the force on a single leg or foot with the foot displaced away from the body's centre of mass and increased trunk motion"

The risk for re-injury as well as the long-term onset of osteoarthritis (Chapter 1.1) does not seem to be declining, despite improvements in surgical and rehabilitation practices. Multiple studies have described the best practice model for dealing with ACL injuries as continued focus on the improvement of injury prevention methods, emphasizing a need for a better understanding of the events leading up non-contact injuries (Lohmander et al. 2004; Griffin et al. 2006; Hashemi et al. 2011).

Chapter 3: Current Preventative Measures:

3.1: Knee Bracing

There are two primary types of knee braces used to try and protect the ACL: prophylactic braces and functional braces. Prophylactic braces are typically used to prevent an injury to a healthy or mildly injured knee. These are made with a neoprene sleeve reinforced with medial and lateral hinged bars to provide external support to the knee (Figure 3.1a). Functional braces (Figure 3.1b) are more rigid structures to prevent excessive motion and provide stability to an already unstable knee, such as after an ACL injury (Ramsey et al. 2001; Wright & Fetzer 2007; Chew et al. 2007; Pietrosimone et al. 2008).

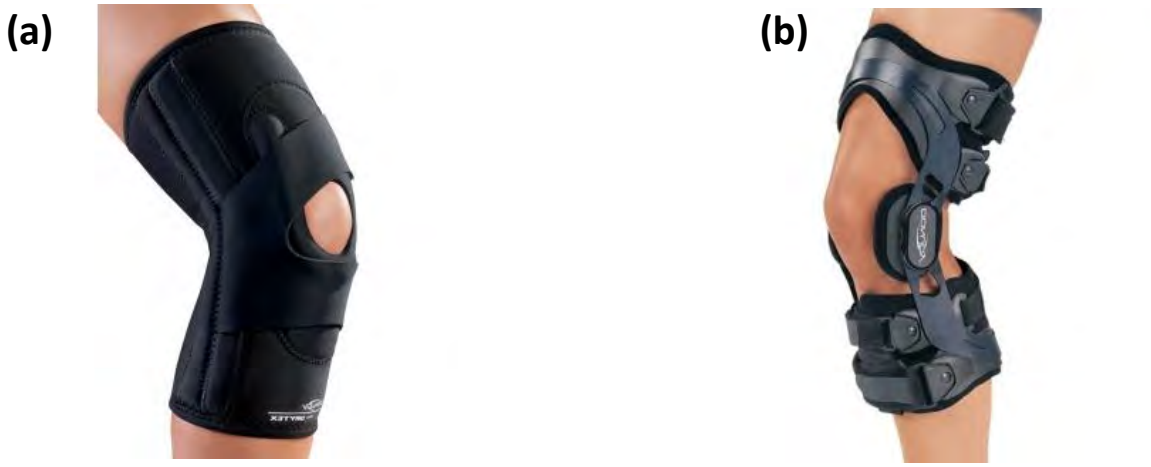

Figure 3.1: Examples of commercially available prophylactic (a) and functional (b) braces (DJO Global, Vista, CA).

In a randomized controlled trial of functional and prophylactic brace use after ACL surgery, Birmingham et al. (2008) observed no significant differences in quality of life and activity level between either group at 1 or 2 year follow ups although the functional brace group demonstrated higher self-reported ratings of confidence. Participants from both groups sustained repeat injuries during the study period but the sample size was too small to conclude a statistical relationship. A meta-analysis of studies published in six electronic databases from their inception until May 2012 concluded that there was insufficient data to make objective conclusions about the effect of bracing after ACL surgery (Kinikli et al. 2014). The authors described the general quality of the studies as poor and limited in design.

In an Editorial for the Clinical Journal of Sport Medicine, Hagel and Meeuwisse (2004) expressed concern that commercialised protective equipment such as knee braces do not require the same level of scientific evidence that is usually required in the field of health research. There are also fears that the use of a brace could lead to greater risk taking behaviour due to a false sense of security, known as risk homeostasis (Wilde 1994; Chew et al. 2007).

3.1.1: Prophylactic Braces

In an assessment of 1396 Military Cadets, Sitler (1990) observed a significant decrease in all knee injuries in defensive football players who wore prophylactic knee braces but not in offensive players when compared to a non-braced control group. They measured no difference in injury severity between those injured wearing a brace and those without.

There is very little research on the use of bracing to prevent first-time ACL injuries in a previously un-injured population. One study required players in a major college football team to wear prophylactic knee braces during all practice and match sessions. The results actually indicated higher incidences of ACL injuries when athletes wore the braces. Furthermore, the athletes also reported increased episodes of muscle cramping and had to repeatedly be reminded to wear the braces (Rovere et al. 1987).

Pietrosimone et al. (2008) conducted an exhaustive literature search of journal entries from 1970-2006 on the effect of prophylactic knee braces on ACL injury reduction. Based on their findings, the authors could neither categorically support nor discourage the use of prophylactic braces to prevent ACL injuries and highlighted a need for better-quality studies.

3.1.2: Functional Braces

Wojtys et al. (1994) and Yeow et al. (2010) both demonstrated that functional braces can decrease anterior tibial shift and axial rotation under the low loading conditions characteristic of day-to-day use. However, both studies concluded that these braces need to be tested under more dynamic loading conditions to truly assess their effect on preventing injuries in sport.

In a two-year follow up on patients after ACL reconstruction surgeries, McDevitt (2004) recorded no differences in stability, isokinetic strength, range of motion and functional testing between functionally braced and non-braced groups. There was no significant difference found in re-injury rates between the groups.

A systematic review of 12 randomized controlled trials of functional knee bracing by Wright and Fetzer (2007) found no evidence that pain, range of motion, graft stability or rate of re-injury were affected. None of the studies demonstrated that these braces had the potential to reduce strain in the ACL under the higher loading conditions typical of athletic activity. The overwhelming consensus in the literature is that there is currently no conclusive evidence to prove that functional knee braces can prevent the occurrence of ACL injuries (Wright & Fetzer 2007; Boyer 2011; Silvers & Mandelbaum 2011).

3.2: Screening Algorithms

Intrinsic risk factors are inherently difficult to correct but - through an understanding of injury epidemiology, anatomy and biomechanics - procedures can be developed to screen for high-risk individuals and prescribe them to targeted intervention programs (Renstrom et al. 2008; Hewett et al. 2010).

Hewett et al. (2005) used stance phase kinetics and kinematics to predict, with 73% sensitivity and 78% specificity[10], which athletes would suffer ACL injuries later in their careers. A similar algorithm was developed by Myer et al. (2010) using five clinical variables (knee flexion ROM, body mass, tibia length and hamstring/quadriceps ratio). This achieved 73% sensitivity and 70% specificity although the same authors had previously reported values of 85% and 90% respectively, through the use of equipment and methods typically unavailable in a clinical setting. The calculation tool - known as a nomogram -for the clinical test along with the operational instructions are in Appendix A.1.

These screening algorithms are not developed as real-time implementations. They are only designed to predict the risk of future injury and not the actual injury event. To actually reduce the rate of non-contact ACL injuries, these programs need to be combined with an effective preventative measure.

3.3: Injury Prevention Training Programs

The performance of voluntary, goal-directed movements improves as the motor control system learns through repetition (Ghez 2011). It is thought that technique and neuromuscular control are thus the most modifiable risk factors for non-contact ACL injuries (Hewett et al. 2006; Podraza & White 2010). To decrease the moments in the knee, either the overall magnitude of the ground reaction force or distance between this force and the centre of the knee must be reduced. This can be achieved by avoiding stiff, extended landings (Chapter 2.7.1) and unfavourable body alignments (Chapter 2.6.2) respectively (Dempsey et al. 2009; Donnelly et al. 2012; Kristianslund et al. 2013). Training programs have been developed to address these issues in an attempt to prevent ACL injuries. The fundamental goals of these programs are to:

[10] Sensitivity and specificity are terms used to classify the accuracy of a clinical test. Sensitivity refers to the ability of the test to correctly classify a true positive (i.e. detect an athlete who will go on to sustain an ACL injury). Specificity, on the other hand, is the ability of the test to correctly classify a true negative (i.e. an athlete who will not sustain an injury) (Parikh et al. 2008; Lalkhen & McCluskey 2008).

- Focus on correct, balanced techniques and body positioning (Chapter 2.6.2)
- Increase hamstring muscle group strength (Chapter 2.7.1)
- Improve balance, proprioception and neuromuscular control (Chapter 2.7.1)
- Improve reaction time, visual processing of stimuli and ensure familiarity with unanticipated movements (Chapter 2.7.2)
- Enhance athletic performance, and
- Educate athletes in ACL injury mechanisms

These tests take approximately 15 minutes per session to complete and consist of a variety of warm-up routines, targeted muscle stretches, lectures, dynamic movements and exercises focusing on strength, plyometrics and agility. (T F Besier et al. 2001; Myklebust et al. 2003; Mandelbaum et al. 2005; Renstrom et al. 2008; Boyer 2011). A sample program, initially published by Hewett et al. (1999), is attached to Appendix A.2.

The reported effects of these programs vary. Many studies have shown improvements in proprioception, neuromuscular control, side-to-side imbalances, co-contraction indices, technique and athletic performance (Hewett et al. 1996; Dempsey et al. 2009; Lee et al. 2014). However, other studies found no benefit on performance or landing technique after 6-8 weeks of training (Grandstrand et al. 2006; Vescovi & VanHeest 2010). One study reported multiple kinematic and neuromuscular improvements as a result of the training program but also observed higher knee valgus moments (Chapter 2.2) in the intervention group, known to be related to the injury mechanism (Lim et al. 2009). Another report observed significant improvements in hip kinematics but no difference in knee valgus or flexion angles after an entire intervention season (Pollard et al. 2006).

The underlying concept is that participation in these programs will translate to reduced injury rates. Hewett et al. (1999) observed significant decreases in the incidence of non-contact knee injuries in female. However, this was still not found to be significantly different to that of a control group of untrained male athletes. Mandelbaum et al. (2005) observed an 88% decrease in ACL injuries during the first twelve months of a training program and 74% reduction in the next year. However, both authors noted various

limitations in their study designs. The subjects in Mandelbaum's study were enrolled voluntarily[11], whereas Hewett had an unequal distribution of participants with more volleyball players in the intervention group. Neither study was randomized, blinded or controlled for multiple confounding factors. Hewett only included female athletes with no record of knee injuries whereas Mandelbaum - also using female athletes - only controlled for age and skill. Both posited that selection bias could have affected the results. Both had low sample sizes and decreased statistical power.

A similar intervention study was conducted by Myer et al. (2007) who used a screening program to divide the test population into high and low risk groups. Half of each group then completed an injury prevention program, with the remainder serving as the control subjects. After 7 weeks, there were no significant changes in the low risk intervention group and the control subjects in both groups. The high risk group who participated in training exhibited a 13% decrease in knee valgus moments, but this was still not reduced to levels similar to the low risk group.

A neuromuscular intervention study aimed the top three divisions (Elite, Division II, Division III) of Handball players in Norway by Myklebust et al. (2003) recorded no significant reduction in ACL injuries overall, although a trend to decrease was evident. A significant improvement in injury rates was only seen in the elite division with the participants who completed the program. This was attributed to the fact that elite athletes have 5-10 training sessions per week and benefitted more from increased exposure to the program. This is corroborated by Sugimoto et al. (2014) who concluded from a meta-analysis of 14 studies that the effectiveness of injury prevention programs is related to the duration and frequency of training. The limitations of Myklebust's study were similar to those of Hewett and Mandelbaum.

To determine the general effect of injury prevention programs on ACL injury rates, Stevenson et al. (2014) extracted relevant journal articles published in Medline, Cochrane, and CINAHL databases from 1995 to 2011. Only two out of the ten included studies successfully reduced ACL injury incidence rates over the entire intervention population. A further two studies only reported significant decreases in subgroups

[11] Voluntary enrollment may lead to the "Hawthorne Effect" which was defined by Mandelbaum et al. (2005) as, *"A significant positive effect that turns out to have no causal basis in the theoretical motivation for the intervention but is owing to the effect on the participants of knowing themselves to be studied in connection with the outcomes measured."*

within the study population. Four could only indicate a trend towards a reduction in injury rates and the final two studies actually observed an increase in injuries as a result of the program.

The variance in these results is likely due to methodological differences among the studies. Noyes and Barber-Westin (Noyes & Barber-Westin 2014) completed a systematic review of retraining programs published from 1994-2013 and concluded that, *"There was wide variability among all programs in the frequency, duration, and timing of training; how training was conducted, supervised, or controlled; the components of the program; how exposure data were calculated; noncontact ACL injury incidence rates in the control groups; and compliance with training."*

Chapter 4: Summary

ACL ruptures frequently result in extended absence, cost and disability. Participation in athletic activities is unlikely to decrease and there is presently no evidence to suggest that current surgical practices can either reduce the incidence of re-injury or the onset of osteoarthritis (Chapter 1.2). There are multiple intrinsic (Chapter 2.4.1) and extrinsic (Chapter 2.4.2) risk factors that are characteristic of predisposed and susceptible individuals. Similarly, there are multiple biomechanical factors, many occurring simultaneously, that could potentially initiate a non-contact ACL injury event. The "position of no return" concept (Chapter 2.6.2) is one of the most explored risk factors of the injury event, but there remains a lot of uncertainty over the precise mechanism of injury. The unanimous agreement in the literature is that a continued emphasis on prevention is needed to address the poor long-term outcomes of an ACL injury.

Knee braces have not shown a consistent, objective reduction in injuries during dynamic loading conditions typical of athletic activity (Chapter 3.1). There is a critical lack of compelling evidence to justify routine brace use in sporting activity and multiple review articles have questioned the quality of the existing research in knee bracing. Screening tests have shown to be reasonably successful in identifying high risk individuals, but need to be combined with effective preventative measures to be useful in reducing the incidence of non-contact ACL injuries (Chapter 3.2).

Unfortunately, the influence of preventative training programs on the rate of non-contact ACL injuries is inconclusive. Studies that have presented positive effects have design limitations that severely impact their reliability (Chapter 3.3). These programs are also time and labour intensive and require the commitment of multiple stakeholders for optimising the chances of success. This may be feasible at a professional level, but seems unachievable for amateur athletes (Myer et al. 2007; Renstrom et al. 2008). Training an athlete to improve their technique and neuromuscular control may improve their risk of injury during planned movements, however there is no evidence to suggest that these programs have an improvement on the athlete's response to unexpected disturbances.

Chapter 5: Problem Statement

5.1: The Inciting Event

The best practice model for the management of ACL injuries is a continued focus on prevention. However current preventative measures have not proven to be effective. A more comprehensive understanding of the sequence of events leading up to the injury will advance the body of knowledge to improve current prevention methods and move towards the design and innovation of entirely new strategies. This is a widely held position throughout literature (Meeuwisse 1994; Arendt et al. 1999; Ireland 1999; Bahr & Krosshaug 2005; Griffin et al. 2006; Sigward & Powers 2007; Bulluck 2010; Hewett et al. 2010).

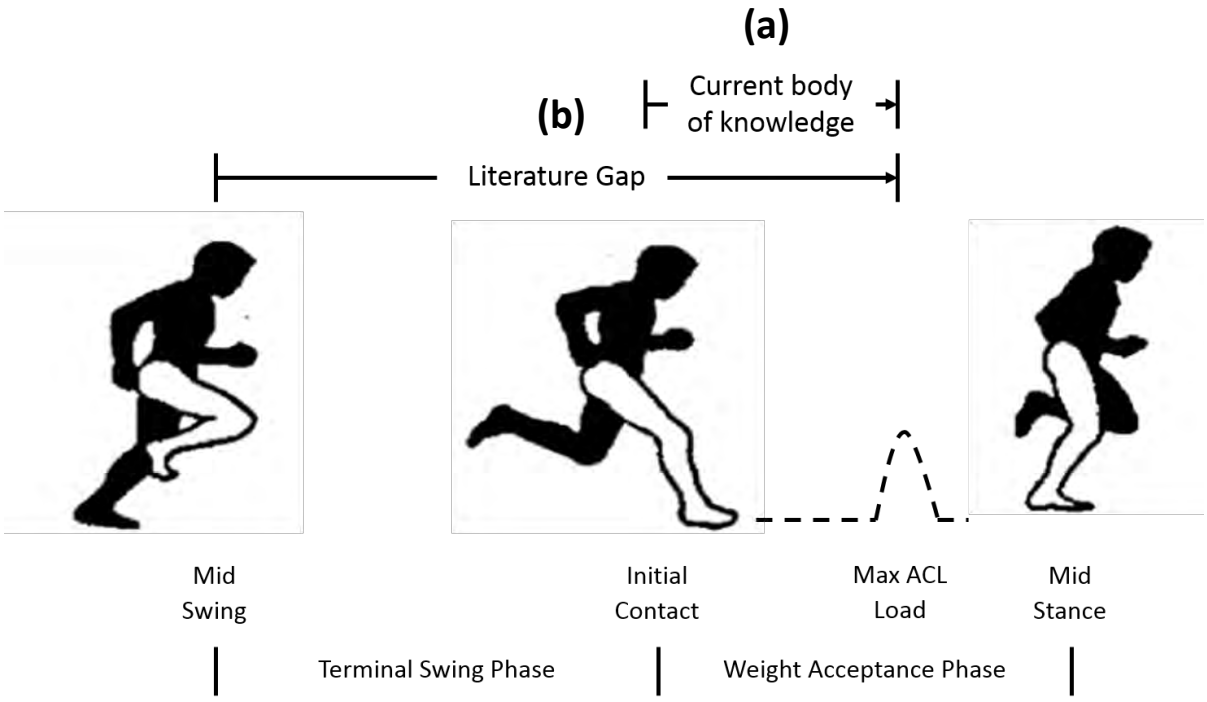

Figure 5.1: Illustrating the current body of knowledge (Chapter 2.6) of the relationship between initial contact kinematics and subsequent weight acceptance phase ACL loading (a) and the gap in the literature of the effect of swing phase kinematics (represented in this image by the terminal swing phase) on weight acceptance phase ACL loading (b).

The relationships between body kinematics at initial contact and ACL loading during the weight acceptance phase, when non-contact injuries typically occur (Chapter 2.5), are well documented (Chapter 2.6.2). However, movement is not a discrete function. There must exist a sequence of swing-phase kinematics, prior to initial contact, which precedes the "position of no return". This is currently undocumented in the literature, no studies to date have investigated the presence of predictive

relationships between swing-phase biomechanics and subsequent stance phase ACL loading[12]. This literature gap is indicated in Figure 5.1

This relationship, if present, would lead to the formation of a "sequence of no return" concept rather than the singular "position of no return". This expansion would considerably increase the amount of information available to researchers to further the understanding of events leading up to non-contact ACL injuries. The subsequent applications are discussed in more detail in Chapter 10.4.

5.2: Dual-bundle Ligament Strain

There is also a lack of research detailing strains occurring in both bundles of the ACL (Chapter 1.1) during dynamic[13] activity, particularly for side-step movements which are known to account for a large percentage of all non-contact ACL injuries (Chapter 2.5). Most studies do not model the different bundles independently, assuming them to have similar characteristics (Kar & Quesada 2013). This is evident in Table A.1 and Table A.2.

Table A.1 lists studies, in chronological order, which have investigated various kinematic and neuromuscular risk factors for non-contact ACL injuries occurring during dynamic movements. The table indicates if an ACL was directly modelled in the study, what type of dynamic movement(s) were performed by the participants and whether or not these were planned or unplanned. Table A.2 lists those studies which performed purely observational analyses of variables related to non-contact anterior cruciate ligament injuries. Studies that implemented invasive methods as well as those that only analysed static movements were not considered in the review.

Of the 31 studies that investigated the effects of various risk factors on ACL loading (Table A.1), only Kar and Queseda (2012) investigated ligament strain. However, the movement that was tested was a jump landing and the ligament was only considered as a single bundle. For strictly observational studies (Table A.2), Cerulli et al. (2003), Zhang et al. (2010), Taylor et al. (2011) and Kar and Queseda (2013) all investigated ligament strain occurring during jump landings, although Zhang et al. were the only study to consider the ligament as a dual-bundle structure. The only study found in the literature search that

[12] ACL loading is typically measured directly through strain or force or indirectly through observing the knee valgus moments, internal rotation moments or anterior shear forces.

[13] Studies investigating ACL loading during static movements were not considered in the review as non-contact ACL injuries typically occur during dynamic movements (2.5)

analysed dual bundle ACL strain patterns during a side-step cut is from Zhang et al. (2011), however this was a case study using only a single test subject.

5.3: Summary

There are thus two primary gaps in the literature that need to be addressed:

- The effect of swing phase kinematic components on stance phase ACL loading, and
- The strain occurring in both bundles of the ACL during a side-step cutting movement

Chapter 6: Hypothesis

6.1: Research Aims

- Quantify linear relationships between mid-swing kinematics and the resulting maximum stance-phase ACL bundle strains during a side-step movement.
- Evaluate the overall capability of swing phase kinematics to predict these future maximum ACL bundle strains.
- To examine differences in loading patterns between the anteromedial and posterolateral bundles during side-step cutting.

6.2: Research Hypothesis

The fundamental hypothesis is that kinematics occurring during the swing phase of a side-step movement can predict the resulting maximum stance phase ACL strain in both ligament bundles. Specifically, it is hypothesised that instantaneous kinematics at the mid-swing aspect of a side-step movement are significant ($p < 0.05$) predictors of the subsequent maximum. This will be tested in a linear regression model.

6.3: Research Outcomes

Rejecting the null hypothesis (that these kinematics are not significant predictors of ligament strain) will further the understanding of the sequence of events that results in non-contact ACL injuries. The specific implications are discussed in more detail in Chapter 10.4.

6.4: Additional Research Question

Since the anteromedial and posterolateral bundles experience different loading patterns due to their respective locations and orientations within the knee joint (Chapter 1.1), analysing the ligament as a complex structure rather than a single contractile unit is potentially important in furthering our understanding of the ACL injury mechanism. The research question in this regard is to determine if different loading patterns exist between the bundles of the ACL during the stance phase of a side-step. This has not been well defined in the literature (Chapter 5.2).

6.5: Project Scope

6.5.1: Study Design

This study is presented as a preliminary feasibility investigation. No published studies were found categorizing the relationships between swing phase components and resultant stance-phase ACL loading

(Chapter 5.1). Therefore the focus of this study is to build a predictive model to establish *a posteriori* knowledge of these relationships. The results from this preliminary investigation can then guide the development of *a priori* hypotheses for future studies, which can be completed at higher levels of evidence.

6.5.2: Participants

The participants for this study will be drawn from a population of female soccer players. Females are at a higher risk of suffering non-contact ACL injuries than males, due to various intrinsic (Chapter 2.4.1), kinematic (Chapter 2.8) and neuromuscular factors (Chapter 2.8). Soccer players are at a particularly high risk of injury. This is supported by Waldén et al. (2011), who concluded that, *"Preventive research should primarily address the young female football player".* For consistency and to control for possible side-to-side imbalances (Chapter 2.4.1), only right leg dominant athletes will be used.

6.5.3: Movement

Non-contact ACL injuries typically occur when athletes attempt rapid deceleration movements combined with a change in direction such as a side-step, which accounts for 60% of such injuries. Athletes typically describe being disturbed or having had to react to an unexpected situation (Chapter 2.5). ACL loading has been shown to drastically increase during unanticipated side-step cutting in comparison to pre-planned movements (Chapter 2.6.2). For these reasons, this project will investigate athletes completing unanticipated side-step movements.

6.5.4: Biomechanics Investigated

Body kinematics (Chapter 2.6) and neuromuscular control (Chapter 2.7.1) are the two primary measurable factors responsible for the ACL injury inciting event. These two aspects are fundamentally related, since movement is generated by the underlying muscle activations. For the scope of this project, body kinematics were chosen for the investigation because they can be rapidly and accurately measured using modern techniques (Chapter 7.2). The kinematic variables that will be analysed are the instantaneous three dimensional joint angles and velocities of the lumbar, right hip, right knee, right ankle and right subtalar joints. These kinematics will be extracted from the mid-swing aspect of the swing-phase. Mid-swing was chosen as it is easily definable where the knee reaches its maximum flexion angle and it marks the beginning of the terminal swing phase, the final segment before initial contact (Chapter 2.1). Analysis of kinematics occurring at the upper body as well as the non-dominant limb will not be included in this study.

6.5.5: Means of determining ACL loading

This study will investigate the maximum strain occurring in both ligament bundles over the stance phase of the movement. Studies looking at relationships between kinematics and ACL loading or injury risk have typically quantified one of: strain, force, knee valgus moment, internal rotation moment or anterior shear force (Table A.1). For the scope of this project, strain will be analysed as the dependent variable for multiple reasons. Firstly, there is a lack of published data on dual bundle ACL strain during dynamic deceleration movements, particularly investigating possible predictive relationships (Chapter 5.2). Secondly, ACL loading is known to take place in multiple coordinates (Chapter 2.2) and individual loads cannot simply be superposed to produce a general estimate because that does not account for the interaction between loading conditions (Markolf et al. 1995; Oh et al. 2012).

Strain may thus be a better metric than simply analysing kinetics in individual planes of motion as it automatically and simultaneously evaluates all planes of motion in the model, relative to the ligament orientation. Furthermore, strain is purely a function of the change in ACL length, relative to its zero-load length (Chapter 7.3.4). This is directly related to the instantaneous position of the knee joint which makes it a better fit for analyses of body kinematics. While strain can also be estimated through the resolution of joint and muscle forces, this approach requires prior knowledge of more subject-specific mechanical properties such as ligament thickness, modulus of elasticity etc. (Appendix B.2). Furthermore, since swing-phase joint kinematics are hypothesised as the predictors of future stance-phase ACL strain (Chapter 6.1), the use of stance-phase kinematics to determine ACL strain is a more direct and logical approach.

Chapter 7: Methodology

7.1: Methodological Objectives

The primary methodological objectives of this study are outlined in Figure 7.1 as a progressive sequence of stages. The first objective is to collect kinematic data of female athletes attempting unanticipated side-step maneuvers. These kinematics then need to be applied to a model to calculate the stance-phase strain in both bundles of the ACL throughout the movement. The third stage is to identify the presence of linear relationships between mid-swing kinematics and the maximum stance phase ACL strains. Finally, the overall potential of the identified kinematic components to predict ACL strain in both the anteromedial and posterolateral bundles should be evaluated.

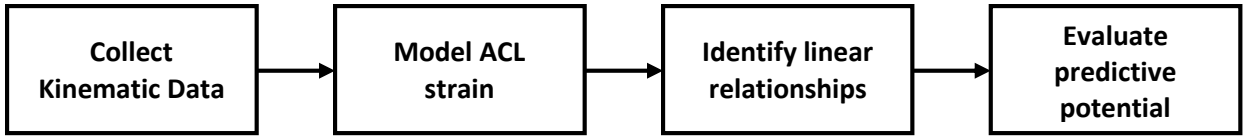

Figure 7.1: Pipeline of methodological objectives from the collection of kinematic data through to the evaluation of the overall predictive potential of these kinematics to predict ACL strain in both ligament bundles.

7.2: Collection of Kinematic Data

The ability to quantitatively record, recreate and analyse human movement is a useful clinical and experimental tool (Kadaba et al. 1990; Kirk et al. 2005). The de-facto motion capture technology over the last decade is marker-based optical motion capture (Schönauer et al. 2011). This is an accurate, non-invasive and relatively low risk method.

This technique employs an array of high speed digital cameras to triangulate the three-dimensional (3D) positions of set of active or passive markers placed at locations on a test subject (Sandholm et al. 2009). Active markers transmit light, ultrasonic or electromagnetic signals to the camera arrays (Hemmerich et al. 2006; Lo et al. 2008). Passive markers are made from a retro-reflective material and reflect infrared light emitted by a source co-located with each camera. Active systems are bulkier with more wiring and require the participant to be connected to a power source. Passive systems are less restrictive but require more sophisticated calibration techniques (Kirk et al. 2005; Sandholm et al. 2009). Force plates are typically embedded in the ground to record the direction and magnitude of the ground reaction forces occurring during movement (Vicon Motion Systems 2006; Sandholm et al. 2009; Levine et al. 2012).

For each point in time, each marker needs to be in full view of at least two of the cameras (Vicon Motion Systems 2006). Thus, most capturing systems tend to use a redundant array of cameras to minimize the possibility of marker occlusion (Kirk et al. 2005). Each body part of interest requires a minimum of three

markers to be fixed to it to be accurately tracked in 6 degrees of freedom (3 translations, 3 rotations) within the experimental coordinate space (Lu & O'Connor 1999; Schönauer et al. 2011).

There are two types of error associated with optical motion capture. The first, instrumentation error, refers to the errors resulting from the digitization of then 3D coordinates of a marker. This can result from noise, optical distortion, poor calibration or mathematical rounding (Cappozzo 1991). This error can be reduced by running multiple trials for redundancy, which can be done very quickly, as well as by implementing accurate calibration and post processing methods (Vicon Motion Systems 2006). The second type, marker error, results from movement of the marker attached to soft surface tissue relative to the underlying bone (Cappozzo 1991; Lu & O'Connor 1999). This error, known as soft-tissue artefact, can be mitigated through practical marker placement on palpable, bony landmarks close to the skin as well as through the use of redundant marker arrays to improve the accuracy of inverse kinematic algorithms (Chapter 7.3.2). Ultimately, continuing developments in computational hardware, software and mathematical reconstruction routines allows for highly accurate capture of motion (Zhang et al. 2011).

For a brief description of other motion-capture methods not considered for this study, refer to Appendix B.1

7.3: Modelling the ACL and calculating ACL strain

It is impractical and invasive to directly measure knee ligament responses *in vivo*, however models can be used to represent these structures and emphasize their most important characteristics (Pandy et al. 2007; Fregly et al. 2012). These can be more effective than purely experimental methods when investigating cause and effect relationships as they can analyse variables that are often difficult to measure (Delp et al. 2007; Seth et al. 2011). Models of the knee have been used for many years to simulate and investigate knee joint motion (Wismans et al. 1980; O'Connor & Zavatsky 1995; Toutoungi et al. 1997). Breakthroughs in computer hardware and software routines allow for complex models to be developed rapidly at low cost (Pandy 2001).

OpenSim[14] (Stanford University, Stanford, CA) is an open-source software package which consists of a standardized set of file formats for creating and editing musculoskeletal models to simulate and analyse movement (Delp et al. 2007). Each model is built with multiple different components including: body segments, articulating joints, contact elements, ligaments, and muscle fibres. Virtual markers are placed on the model to match the locations of the experimental markers used in the motion capture trials (Seth et al. 2011).

For a description of other methods to determine ACL loading that were not considered for this study, refer to Appendix B.2.

7.3.1: OpenSim - Model Scaling

To create subject-specific models which better approximate the individual anthropometry of each participant, the size and mass distributions of a generic model can be scaled. Each body segment in the model is scaled independently according the ratio of distances between experimental markers (Figure 7.2a) placed on the test subject and the corresponding virtual markers (Figure 7.2b) on the generic model (Delp et al. 2007; Bulluck 2010; Anderson et al. 2012).

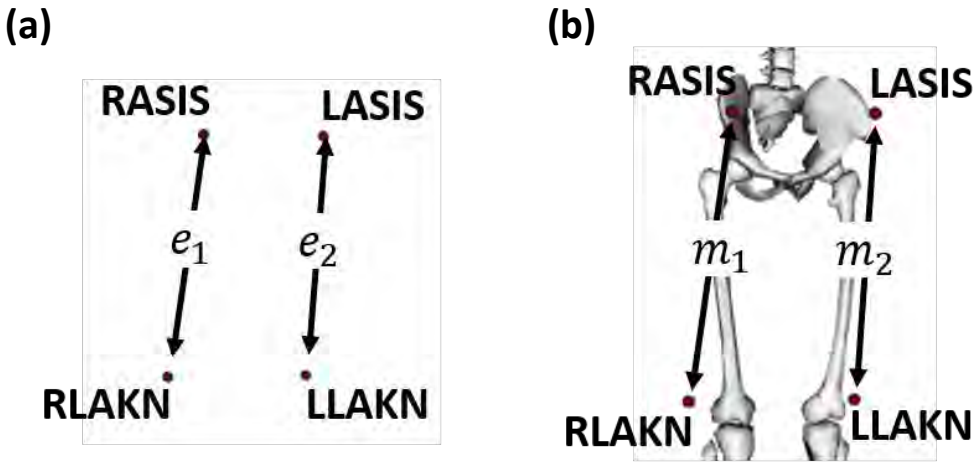

Figure 7.2: The derivation of equation parameters to calculate the model scaling ratio (Equation 7.1) for the thigh segment from the relative distances of experimental markers on the participant (a) and the corresponding markers on the virtual model (b), adapted from Anderson et al. (2012).

[14] OpenSim is funded by NIH Roadmap grant U54 GM072970, the NIH research infrastructure grant R24 HD065690, and the DARPA Warrior Web Program.

Origin and insertion sites of ligaments and muscles on different segments in the model are then scaled accordingly. The scaling ratio (Equation 7.1) is averaged from measurements on both sides of the model to maintain bilateral symmetry:

$$Scaling\ Ratio = \frac{(\frac{e1 + e2}{2})}{(\frac{m1 + m2}{2})} \qquad \textit{Equation 7.1}$$

Where $e1$ and $e2$ refer to the coordinates of the experimental marker pairs during motion capture and $m1$ and $m2$ refer to the corresponding marker pairs on the virtual model.

The collection of scaling ratios used to scale the virtual model is referred to as a measurement set. To obtain the experimental values, marker data is captured of a static motion capture trial with the test subject posed in a known, neutral position. Participants are required to stand upright with their feet facing forwards, head level and arms resting at their sides as recommended by the Vicon Motion Systems, "Essentials of Motion Capture" guidebook (Vicon Motion Systems 2006).

The second step in the scaling process replicates a participant's standing pose from the static trial within the scaled, virtual model by positioning the model to best match the virtual markers to the experimental marker locations. This is accomplished by a routine that seeks to minimize a weighted least squares error term for each ith marker, calculated as indicated in Equation 7.2 (Anderson et al. 2012).

$$Squared\ Error = \sum_{i=1}^{n_{markers}} w_i(\vec{x}_i^{subject} - \vec{x}_i^{model})^2 \qquad \textit{Equation 7.2}$$

Where w_i represents the weighting of the ith marker, $\vec{x}_i^{subject}$ is the 3D position of the ith marker recorded by the motion capture system and $\vec{x}_i^{model}$ is the 3D position of the ith marker as determined by the scaling routine in OpenSim.

To account for discrepancies between marker placement on the subject and the virtual model, the algorithm also adjusts the locations of virtual model markers to be more consistent with the experimental placements. Markers with high weights, as set by the operator, are more heavily penalized in the algorithm. Lower weighted markers are subsequently moved into more optimal positions relative to the higher confidence markers. Scaling is an iterative process and ends when the user is satisfied with the mathematical error term produced by the optimization algorithm as well as the visual match of the model with the static pose.

7.3.2: OpenSim - Inverse Kinematics Tool

Inverse kinematics is a routine that reproduces the movement of the subject within the scaled virtual model (Figure 7.3). For every frame of captured data, the algorithm calculates the joint angles (in the specified dimensions) of the model required to best match the virtual and experimental markers using the same weighted minimization formula (Equation 7.2) as in the scaling tool. Individual marker weights are operator determined (Delp et al. 2007; Bulluck 2010). Only joint coordinates specified in the routine will be tracked, others can be locked in a fixed position for the duration of the movement.

Figure 7.3: Inverse kinematics algorithm translates experimental kinematics to a simulation of a scaled musculoskeletal model (Anderson et al. 2012).

7.3.3: OpenSim - Analyze Tool

The Analyze tool in OpenSim allows for more detailed exploration of model parameters as a result of an existing (simulated) set of model states. These model states, obtained from the Inverse Kinematics routine, are usually filtered to reduce signal noise resulting of digital sampling. At each time point of the simulation, joint and body kinematics (positions, velocities and accelerations) as well as muscle and ligament lengths can be obtained (Anderson et al. 2012).

7.3.4: Ligament Strain

Strain in a ligament is defined as the change in length divided by its resting, or zero-load length. This is represented in Equation 7.3:

$$\varepsilon = (L - L_0)/L_0 \qquad \textit{Equation 7.3}$$

Where L represents the observed ligament length and L_0 represents the resting or zero-load length of the ligament. However, it is difficult to non-invasively determine the true zero-load length of a ligament in a healthy subject without the use of medical imaging methods (Bloemker et al. 2012). However, Blankevoort and Kuiper (1991) presented a generalised method of approximating the resting length of the ACL bundles. If a reference length (L_r) and strain (ε_r) of a ligament bundle is known with the knee joint placed at a reference position, the zero load length (L_0) of the bundle can be calculated using Equation 7.4:

$$L_0 = L_r/(\varepsilon_r + 1) \qquad \textit{Equation 7.4}$$

Blankevoort and Kuiper recorded the following reference strains in the ligament bundles with the knee positioned in a neutral (all knee angles set to zero degrees) position:

Table 7.1: Reference strains for the anteromedial and posterolateral bundles of the ACL

Ligament Bundle	Reference Strain
Anteromedial (AMB)	0.06
Posterolateral (PLB)	0.10

Table 7.1 Reference strains for the anteromedial and posterolateral bundles of the Anterior Cruciate Ligament, as reported by Blankevoort and Kuiper (1991).

The instantaneous length of the ligament bundles is a function of the relative distance between its attachment sites on the femur and tibia (Mommersteeg et al. 1996; Kar & Quesada 2012). To determine the relative distance between two points, their locations in coordinate space need to be expressed in the same frame of reference. The position of any point in one segment with respect to its position in a reference coordinate system can be represented as in Equation 7.5:

$$y = Rx + v \qquad \textit{Equation 7.5}$$

Where y is the position measured in the reference coordinate system and x is the position in the current body segment coordinate system. R and v represent the respective rotation and translation that define the transition from one coordinate system to another (Zhang 2010). Then L_r, the Euclidean distance between the insertion points, is expressed as in Equation 7.6:

$$Lr = \sqrt{(x_1 - x_2)^2 + (y_1 - y_2)^2 + (z_1 - z_2)^2} \qquad \textit{Equation 7.6}$$

7.3.5: Limitations of musculoskeletal modelling

There is currently limited research testing the reliability of inverse kinematics (Chapter 7.3.2) to accurately estimate joint kinematics based on the positions of markers attached to these joints. Inverse kinematics treats the body as a rigid-linked model when, in reality, tissue interactions at the joints as well as skin artefact on marker positions affects the accuracy of the minimization routine to track these kinematics. Recent studies of the elbow have shown that the inverse kinematics method in OpenSim outputs similar results to forward dynamic methods (Wells & Alderson 2012). However, the movement task was only a low velocity dynamic movement in a single plane of motion.

Ultimately, the accuracy of the obtained kinematics is dependent on minimising the accumulation of various mathematical errors throughout the pipeline. Errors occurring from the motion capture stage (Chapter 7.2) through to the kinematic analysis are cascaded to limit the accuracy of the calculation of ligament strains. These sources of error are discussed in more detail throughout Chapter 10.2.

7.4: Identification of linear relationships

Correlation measures both the quantity and strength of the linear relationship between two variables. It is a special case of bivariate linear regression (Chapter 7.5), with one predictor and one response variable. Where regression analyses the change in variance of a dependent variable as a linear function of the independent variable, correlation is simply the measure of linear association between these variables. It analyses the extent of which a scatter plot of the two variables represents a straight line (Allison 1999; Chatterjee et al. 2000; Salkind 2004). The measure of correlation is typically performed by Pearson's product-moment correlation coefficient, R (Pearson 1895). A positive correlation coefficient implies that both variables are linearly related in such a way that they increase and decrease in unison. A negative correlation implies an inverse linear relationship, one variable decreases as the other increases. A correlation of zero implies that there is no discernable linear relationship between the two variables. This is also the square root of the coefficient of determination (R^2) from the bivariate regression. This is analogous to Cohen's effect size where small, moderate and large correlations are defined as values greater than 0.1, 0.3 and 0.5 respectively.

The significance of the linear relationship is a function of the observed effect size as well as the number of observations. The more data pairs of predictor and response variables, the stronger the significance of the observed relationship (Fenton & Neil 2012). This can be seen on the table of critical values (Table 7.2) adapted from White et al. (1979). These values represent the minimum effect size required to achieve a statistically significant correlation, depending on the sample size (n) and the desired significance level (α).

Table 7.2: Critical Values of Pearson's R for specific levels of significance in a two-tailed test

n	Significance Level (α)			
	0.05	**0.02**	**0.01**	**0.001**
6	0.7067	0.7887	0.8343	0.9249
7	0.6664	0.7498	0.7977	0.8982
8	0.6319	0.7155	0.7646	0.8721
9	0.6021	0.6851	0.7348	0.8471
10	0.5760	0.6581	0.7079	0.8233
20	0.4227	0.4921	0.5368	0.6524
50	0.2732	0.3218	0.3541	0.4433

Table 7.2: Critical Values of Pearson's R for specific levels of significance in a two-tailed test for correlations between variables. Adapted from White et al. (1979).

7.5: Evaluation of predictive potential

7.5.1: Introduction

Regression is a widely used statistical analysis method for investigating functional relationships between variables. These relationships are defined in a model which expresses the dependent (response) variable (Y_i) as a linear function of one or more independent (predictor) variables ($X_{1i}, X_{2i}, \dots, X_{Pi}$). A simple regression model contains only one predictor variable whereas a multiple regression model is built with more than one predictor variable. The multiple regression function can be approximated by:

$$Y_i = B_0 + B_1 X_{1i} + B_2 X_{2i} + \cdots + B_P X_{Pi} + \varepsilon_i \ , \quad i = 1, 2, \dots, N \qquad \textit{Equation 7.7}$$

Where P is the number of predictor variables and i is the number of samples or observations used in the experiment. ε_i is the residual term, the random error for each sample which represents the difference between the true value of Y_i and that predicted by the regression model. This accounts for the failure of the model to perfectly fit the data. Constants $\mathrm{B}_0, \mathrm{B}_1, \dots, \mathrm{B}_\mathrm{p}$ are the regression coefficients which quantify the relationship between each predictor and the response variable. B_0 represents the intercept term of the linear model. The coefficients are obtained through a minimization routine known as ordinary least squares. This calculates the coefficients required to minimize the sum of squared residuals for each observation, creating a model that "best fits" the sample data (Allison 1999; Chatterjee et al. 2000; Miles & Shevlin 2001).

The coefficient of determination (R^2) describes how closely the model fits the data. It compares the sum of squared errors (SSE) of the regression model to those of a theoretical model using the mean of the dependent variable as the only predictor. This is represented in Equation 7.8.

$$R^2 = 1 - \frac{SSE(regression)}{SSE(mean\ only)} \qquad \textit{Equation 7.8}$$

This represents the total amount of variance observed in the dependent variable that is directly related to the variance of the combination of predictor variables used in the regression model. A confidence interval can be calculated to represent the upper and lower limits of the true value of this coefficient for the population of which the training sample was obtained (Cohen et al. 2013; Soper 2014). This is represented in Equation 7.9.

$$CI_{R^2} = R^2 \pm \mathrm{t}\left(\frac{(1-\propto)}{2},\ n-k-1\right) * SE \qquad \textit{Equation 7.9}$$

Where R^2 is the coefficient of determination from the regression model, $\propto$ is the desired level of confidence, n is the sample size, k is the number of predictor variables used and SE is the Olkin and Finn (1995) approximation of the standard error of the regression model.

To determine the significance of each coefficient in the model, hypothesis tests are performed to test the probability of obtaining the same model parameters by random chance. The results of these tests are a measure of the strength of the observed linear relationships.

7.5.2: Violation of Assumptions:

The R^2 value is not the only means of evaluating the performance of a regression model. The bias and efficiency of the model should also be analysed. A model is biased if it consistently over or underestimates the predicted response and inefficient if the variation of these estimates around their true values (i.e. the residuals) is inconsistent. Various assumptions are made about the residuals in a regression model. To ensure that the model is both unbiased and efficient, these assumptions need to be validated. These procedures are outlined in the following sections.

7.5.2.1: Linearity

The assumption of linearity requires the relationship between the response and predictor variables to be of a linear nature. To ensure that this is the case, the standardized residuals should be randomly distributed on a scatter plot. Any discernable pattern within these residuals violates the linearity assumption.

7.5.2.2: Mean Independence

For the model to satisfy the mean independence assumption, the residuals should be randomly distributed with no relationship to the predictor variables. Specifically, the mean value of the residuals is required to be zero. This provides an unbiased estimate of the intercept term, B_0.

7.5.2.3: Homoscedasticity (constant variance)

Homoscedasticity requires the variance observed in the residuals to be independent of the predictors. This requires the variance observed in the residuals to be consistent over the sample population. Heteroscedasticity, the violation of homoscedasticity, implies that the least squares estimation method is inefficient to model the relationships between the variables. Homoscedasticity can be confirmed on the same plot as used for the linearity test (Chapter 7.5.2.1). Homoscedastic residuals are evenly scattered whereas heteroscedastic residuals tend to follow a funnel-shaped distribution.

7.5.2.4: Uncorrelated Residuals

The fourth assumption is that the residuals are independent of one another. Thus, the value of Ɛ for any one sample is not correlated with the value of Ɛ for any of the others. This can happen if an unmeasured variable, that is a strong predictor of Y, is shared between two or more of the samples and is not controlled for in the regression model. This assumption is tested with the Durbin-Watson statistic (*d*), which provides a measure of the autocorrelation between residuals.

Table 7.3 contains the upper (*dU*) and lower (*dL*) limits for the Durbin-Watson statistic that are tabulated for different sample sizes (n) and number of independent variables (k), as defined by Savin (1977). If the Durbin-Watson statistic from the regression model is smaller than the lower limit, the null hypothesis - that the residuals are uncorrelated - is rejected. If it is greater than the upper limit then the null hypothesis is accepted. A value between these two limits denotes an inconclusive result.

Table 7.3: Critical Values of dL and dU for the Durbin-Watson Statistic at the 5% significance level

n	k = 1		k = 2		k = 3		k = 4	
	dL	dU	dL	dU	dL	dU	dL	dU
6	0.610	1.400	-	-	-	-	-	-
7	0.700	1.356	0.467	1.896	-	-	-	-
8	0.763	1.332	0.559	1.777	0.367	2.287	-	-
9	0.824	1.320	0.629	1.699	0.455	2.128	0.296	2.588
10	0.879	1.320	0.697	1.641	0.525	2.016	0.376	2.414

Table 7.3: Critical Values of dL and dU for the Durbin-Watson statistic at the 5 percent significance level (α = 0.05).

7.5.2.5: Normality

Normality assumes that the residuals are normally distributed. Provided the first four assumptions are not violated, normally distributed residuals allow for p values and confidence intervals to be accurately calculated (Allison 1999). Normality can be tested by plotting the observed cumulative distribution of the standardized residuals against the expected, normal distribution. This is known as a Probability-Probability (P-P) plot. If the residuals are normally distributed, this should closely approximate a straight line with intercept of zero and slope of one (Miles & Shevlin 2001).

7.5.3: Multicollinearity

Multicollinearity is when two or more of the independent variables are strongly correlated. While this does not violate any of the linear regression model assumptions or affect the calculation of the other regression coefficients, it drastically inflates the standard error for the collinear variables. This reduces the level of significance of the effect of these variables. Thus, variables which might otherwise be declared significant predictors in the model are declared insignificant.

Multicollinearities between predictors can be determined by the variance inflation factor (VIF). This value, calculated for each predictor, describes how the presence of collinearities have inflated the standard error of the variable. An orthogonal predictor, one with no collinearities, would have a variance inflation factor of one. A VIF of greater than four units typically indicates that collinearities are present within the model (Miles & Shevlin 2001).

7.5.4: Variable Entry

7.5.4.1: Introduction

If there are multiple candidate predictor variables with little information for the researcher to *make a priori* decisions as to which should be added to the model, variable entry methods are useful to determine which subset of candidate predictors variables best predicts the response variable. The best performing subset is known as the parsimonious model, which explains the most variance in the dependent variable with the fewest number of independent variables (Lovell 1983; Chatterjee et al. 2000) Essentially, the goal of this approach is to find the simplest possible model that also provides a strong fit to the data, since increasing the number of variables in the model may improve the bias but the potential for overfitting drastically increases.

Overfitting occurs when variables which have no predictive power on the response variable models the error term. Since the error - by definition - is random and cannot be predicted, this limits the effect of the

regression model (Miles & Shevlin 2001; Colton & Bower 2002). This leads to conclusions which cannot be translated to the population from which the observations were drawn (Burnham & Anderson 2002; Moyé 2008). This is especially true when there are a small number of observations used to build the model (Rencher & Pun 1980).

Forward regression is a variable entry method that begins with no variables in the model and predictors are added over multiple iterations. At each iteration, the predictor variable with the most significant individual effect is added to the model. This continues until no more variables are significant or all of the variables have been added to the model. Backwards regression operates in reverse, beginning with all the variables in the model and subtracting the least significant predictors at each interval. Stepwise regression is a combination of the two, adding and subtracting variables to the model at each step. However, these automatic variable selection methods may not always lead to the best performing model since they do not account for combinations of predictors which - individually may not be as strong but together result in the best combination (Yang 2013).

Another approach for optimizing the regression model is to analyse each of the possible combinations of predictors and isolate the best performing subset. This is referred to as the "best subset" method. This is often preferred by researchers over iterative methods which do not investigate all of the possible interactions between variables (King 2003; Fomby 2008).

7.5.4.2: Selection Criterion

The coefficient of determination (Equation 7.8) is not useful for judging the best performing subset since it can be artificially inflated by overfitting the observations. A widely recommended determinant of model performance is Akaike's Information Criterion (AIC) which can be used to avoid overfitting (Akaike 1974). It does not provide an absolute measure of performance, however, it only indicates the performance of one model relative to another. As defined by Burnham and Anderson (2002), it provides an *"estimate of the expected, relative distance between the fitted model and the unknown true mechanism (perhaps of infinite dimension) that actually generated the observed data"* A corrected form of AIC for smaller sample sizes, AICc, was published by Hurvich and Tsai (1989) and is recommended when the ratio of observations to predictors is small (less than 40).

7.5.4.3: Familywise Error Rate

The primary issue with variable entry methods is their tendency towards an exaggerated Type I error rate due to the multiple hypothesis testing performed on each of the other candidate subsets (Miles & Shevlin

2001; Fomby 2008; Mundry & Nunn 2009). Thus, the probability of incorrectly rejecting a true null hypothesis - that the model coefficients are significant - is inflated since it is calculated under the false assumption that no other candidate models were considered (Fomby 2008). This can be accounted for with the post-hoc correction method proposed by Lovell (1983). This is represented in Equation 7.10:

$$\propto = 1 - (1 - \hat{\propto})^{C/K} \qquad \textit{Equation 7.10}$$

Where C is the total number of candidate variables and K represents the number of candidates included in the final regression model. $\hat{\propto}$ is the level of significance set for the regression model and $\propto$ is the true, adjusted significance. Thus, the formula to calculate an appropriate $\hat{\propto}$ to maintain a desired adjusted significance level ($\propto$) is represented in Equation 7.11:

$$\hat{\propto} = 1 - (1 - \propto)^{K/C} \qquad \textit{Equation 7.11}$$

The significance of the final model should also be tested against this corrected value.

Chapter 8: Methods

Motion capture data of athletes performing side-step cutting movements was obtained through a collaboration with the University of Southern California. All testing took place at the Musculoskeletal Biomechanics Research Laboratory at the University of Southern California. Testing procedures were explained to each subject and written informed consent (parental assent where necessary) was obtained as approved by the Institutional Review Board for the University of Southern California (USC) Health Sciences Campus (Ref: HS - 04A005). The study was also approved by the University of Cape Town (UCT) Human Research Ethics Committee[15] (Ref: 172/2012). The letter of approval from the UCT Human Research Ethics Committee as well as the approved informed consent form from the USC study are in Appendix E.1 and E.2 respectively.

The experimental design, described in Chapters 8.1 and 8.2, is adapted from Sigward and Powers (2012).

8.1: Participants

In the Sigward (2012) study, one hundred and fifty six soccer players (76 male and 80 females) between the ages of 9 and 23 were recruited from school, club and recreational soccer teams. All participants were reported as healthy at the time of the study with no existing lower extremity injury. Athletes were not entered into the study if either of the following was reported:

- Prior ACL or any other previous injury or surgery that may affect joint laxity or function at the hip, knee or ankle
- Any medical or neurological condition that would hinder their ability to complete a side-step cutting movement.

To control the scope of the project (Chapter 6.5), all male, left-foot dominant and under-eighteen participant datasets were not used. Of the remaining group, a block of 11 adult (aged 18+) female, right-footed athletes was selected to be utilized in this study. This particular block was chosen as the participants all shared the same prefix in their unique ID number – indicating that they were from the same testing cohort. Following inspection of the data, another participant was removed due to insufficient

[15] This reflects ethical approval of the study concept and design, since the experimental protocol applied for in this study was not conducted due to the collaboration with USC.

marker data. The final participant dataset thus consisted of ten female, right footed athletes (average age = 19.60 ± 1.49 years, average BMI = 22.63 ± 2.07, average total experience 11.8 ± 3.12 years).

8.2: Experimental Setup

Each subject first recorded a static calibration trial (Chapter 7.3.1). Two groups of passive, retro-reflective markers (10mm diameter spheres) were placed on the subject for this trial, a static marker set and a dynamic marker set.

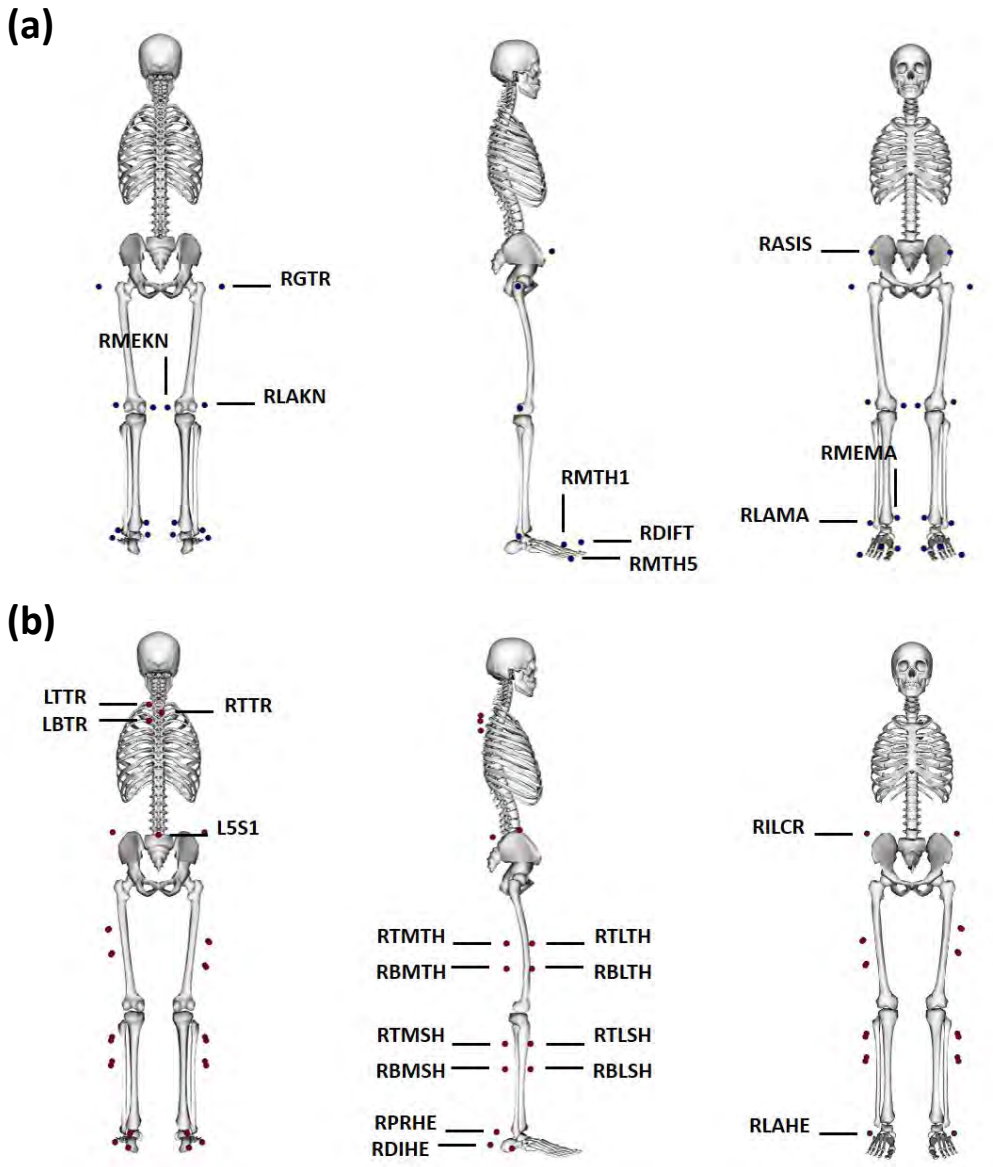

Figure 8.1: Markers locations for the static (a) and dynamic (b) marker sets (right sides shown only). Refer to Appendices B.3 and B.4 for the naming conventions used for these markers.

Markers were placed bilaterally at the following anatomical landmarks to form the static marker set: the anterior-superior iliac spines, greater trochanters, medial and lateral femoral epicondyles, medial and lateral malleoli and over the heads of the first and fifth metatarsals (Figure 8.1a). These landmarks are close to bony surfaces to minimize the effect of soft-tissue artefacts (Chapter 7.2). For the set of dynamic markers (Figure 8.1B), marker clusters fixed to rigid plates were secured bilaterally on the lateral surface of each subject's thigh, calf and heel with a final cluster placed posteriorly towards the top of the trunk. Three additional markers were placed on the left and right iliac crests and on the sacral spinous process inferior to the fifth lumbar vertebrae. The naming conventions used for the static and dynamic marker sets are detailed in Appendix B.3 and B.4 respectively.

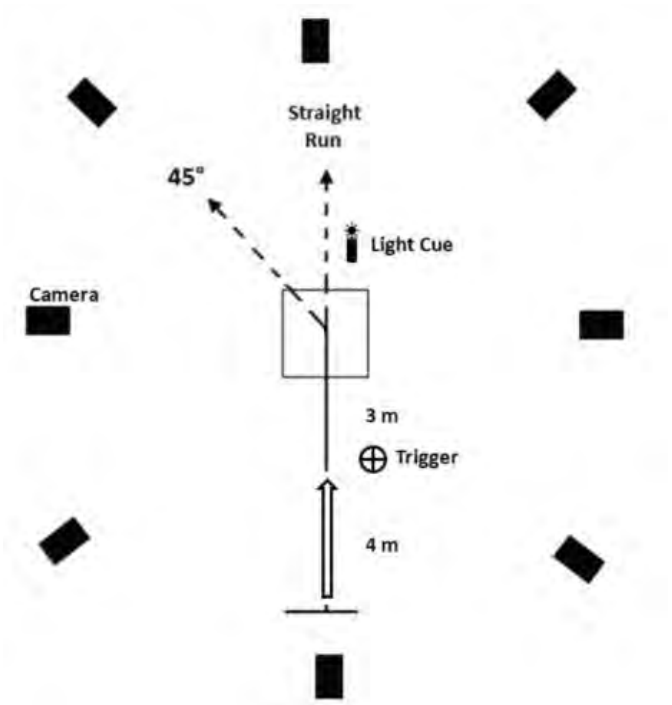

Figure 8.2: Top view of the motion capture experimental setup, adapted from Sigward et al (2012), consisting of 8 high-speed cameras, a force plate in the centre of the capture volume, the photoelectric trigger located 3 meters before the force plate, the light cue and the required cutting angle (45°).

The markers from the static set were only used for the static trial and were thus removed before the commencement of the side-step cutting trials. Each participant was required to run for 7 meters towards a force plate at a velocity of between 4.5–5.5m/s. The approach velocity was monitored with the use of a photoelectric circuit. A visual cue was randomly triggered 3 meters before the athlete arrived at the force

plate to prompt the execution of a 45° cut off their dominant leg. This is known as an "S-cut" movement[16]. If the cue did not trigger, the athlete continued running forwards. This was implemented to simulate an unanticipated cutting movement. Cones were placed at 35° and 55° from the forward direction to direct the athletes to the appropriate cutting angle. Since only right-footed athletes from the Sigward et al. (2012) study were included, each of these therefore used their right foot to land and pivot towards the left direction. The layout of the motion capture experiment is illustrated in Figure 8.2.

Each participant was allowed practice runs to become familiar with the equipment, procedures, and requirements before beginning the side-step trials. A trial was considered unsuccessful if the participant's foot did not completely land on the force plate, if the pre-requisite speed was not achieved or if the cut was not performed to the appropriate angle. Each participant was required to complete four successful side-step trials. Furthermore, to control for the possible effect of footwear interactions (Chapter 2.4.2), each participant was provided with the same brand of shoe (New Balance Inc., Boston, MA, USA).

An array of eight digital cameras was used in the motion analysis system (Vicon, Oxford Metrics LTD, Oxford, England), capturing marker data at a rate of 250 Hz. Ground reaction force data were obtained from an AMTI force platform at a sampling frequency of 1500 Hz (Model #OR6-61, Advanced Mechanical Technologies, Inc., Newton, MA, USA). Vicon Workstation software was used to edit and smooth the raw marker coordinate data, with a 12Hz fourth-order, zero-lag, Butterworth low-pass filter.

8.3: Pre-processing

A batch processing script was written by the author in Matlab (Mathworks, MA, USA) to convert raw Vicon files (.C3D) to the marker (.TRC) and force plate (.MOT) formatted files used in OpenSim. This script implements software routines from multiple, open-source toolboxes for Matlab[17,18,19]. This also utilized C3DServer (Motion Lab Systems, Baton Rouge, LA), a free software package for the development of C3D files. The coordinate system used by Vicon (ZXY) was converted to the OpenSim standard (YZX) through an orthonormal transformation and all distances were scaled from millimetres to meters. The coordinate

[16] In the original experimental of Sigward et al. (2012), participants were also required to perform additional cutting maneuvers at 110° from the original direction of movement. This is known as a "V-cut". These movements were not considered in this study.
[17] Matlab-OpenSim Interface Software by Glen Lichtwark, Ayman Habib and Rod Barratt (2011)
[18] Matlab Toolbox for C3DServer, Version 2, by Matthew R. Walker, Michael J. Rainbow (2006)
[19] XML Toolbox for Matlab by Jared Tuszynski (2007)

system used in OpenSim is described by Anderson et al. (2012) as follows: *"The x-axis of the model coordinate system points forward from the model, the y-axis points upward, and the z-axis points to the right of the model."* This is illustrated in Figure 8.3.

The timing of the stance phase was obtained for each trial, defined as the period from initial contact to toe-off (Hewett et al. 2005; Yu et al. 2006). This was calculated from the vertical (Y) component of the ground reaction force data from the force plate. The timing of the maximum vertical ground reaction force was also obtained. All motion capture data were trimmed to an arbitrarily selected window of interest corresponding to 300 milliseconds on either side of the initial contact point. The Matlab code for this routine is located at Appendix F.1.

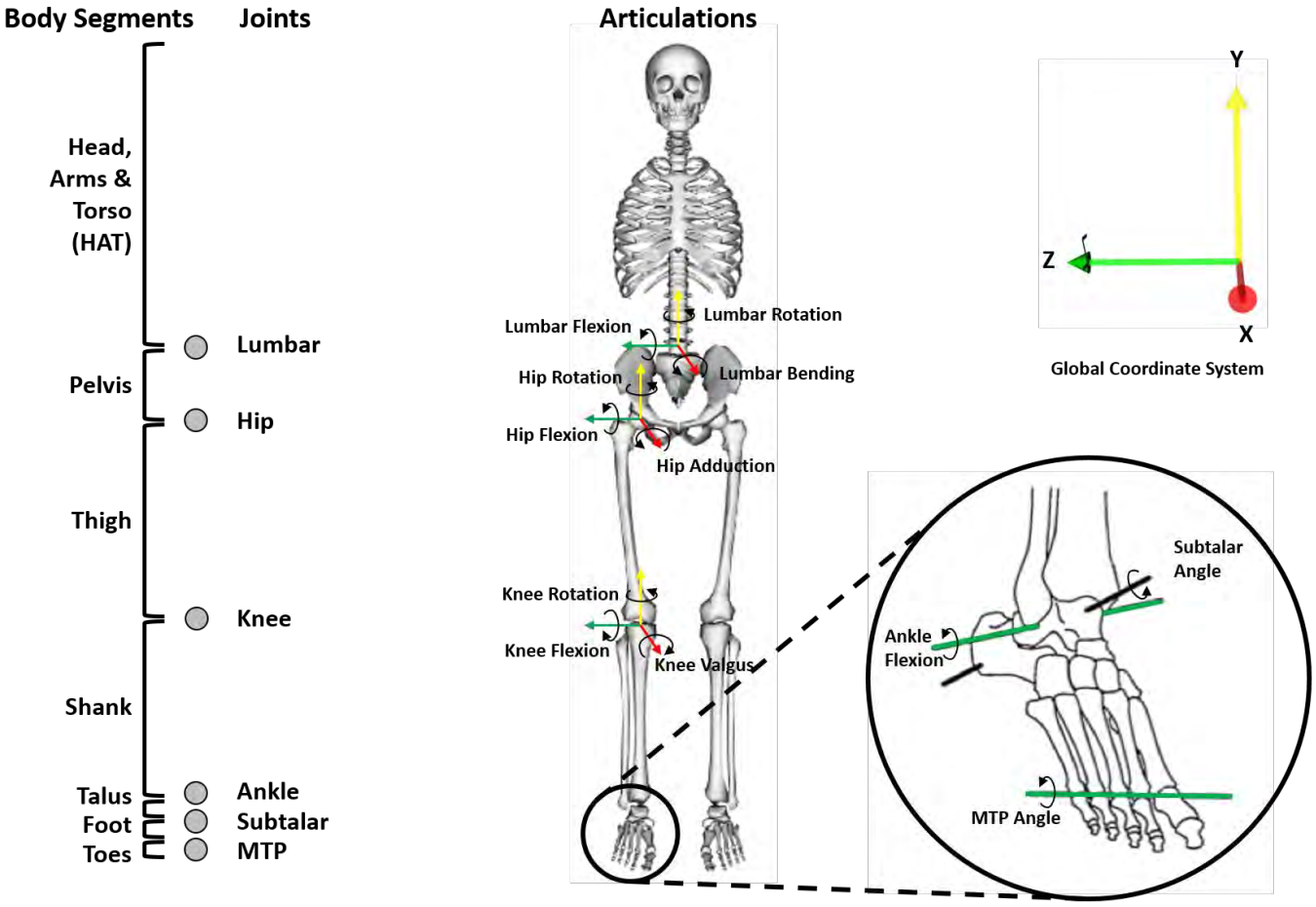

Figure 8.3: Parameters of the edited model, illustrating the body segments which are interconnected by articulating joints. The arrows indicate the positive direction of joint articulation (Table 8.1). Inset taken from Au et al. (2013).

8.4: Generic Musculoskeletal Model

A musculoskeletal model was developed in OpenSim version 3.0. This model was adapted from the generic Gait2392 model released with the OpenSim software under a Creative Commons License (Yamaguchi &

Zajac 1989; Delp et al. 1990; Anderson & Pandy 2001). Other studies that have used this model to research the ACL include Bulluck (2010), Kar & Quesada (2012) and Valente et al. (2013). More information about the parameters of this generic model can be found in Appendix B.5.

8.5: Model Editing and Development

8.5.1: Implementation

The muscle actuators from the generic model were removed and an additional two degrees of freedom, varus-valgus and internal-external Rotation, were added to both knee joints to maintain bilateral symmetry. Other studies to edit the generic Gait2392 model in this way include Kar and Queseda (2013), and Wienhandl et al. (2013). The Euler angle convention for this 3DOF joint was defined as a ZXY or flexion-extension/varus-valgus/internal-external rotation order (McLean et al. 2005; Kernozek et al. 2008; Zhang 2010). An illustration of the body segments and joints used in this model is represented in Figure 8.3, indicating the coordinates of interest (Chapter 6.5.4) and the directions of joint movement defined as the positive direction. This is also featured in Table 8.1.

Table 8.1:Model definitions of positive and negative directions of movement

Joint	Plane of Motion	Positive Direction	Negative Direction
Lumbar	Sagittal	Flexion	Extension
	Frontal	Bending (away from cutting direction)	Bending (towards cutting direction)
	Transverse	Rotation (towards cutting direction)	Rotation (away from cutting direction)
Hip	Sagittal	Flexion	Extension
	Frontal	Internal Rotation	External Rotation
	Transverse	Adduction	Abduction
Knee	Sagittal	Flexion	Extension
	Frontal	Internal Rotation	External Rotation
	Transverse	Valgus	Varus
Ankle	Sagittal	Flexion	Extension
Subtalar	Subtalar (Chapter B.5)	Supination	Pronation

Table 8.1: Model definitions of Positive and Negative directions of movement for the joints of interest (6.5.4) in this study. See Figure 8.3 for visual representation.

Virtual markers were added to the model to match the locations of the experimental markers used in the motion capture trials (Chapter 8.2). The anterior cruciate ligament was modelled as a dual-bundle, passive soft-tissue structure where each bundle is represented by a straight line element (Mommersteeg et al. 1996; Serpas et al. 2002; Shao et al. 2011). Using the OpenSim graphical user interface, the origins and

insertions of each bundle were manually attached to the relevant anatomical landmarks on the model, as detailed by Girgis et al. (1975), Odensten and Gilquist (1985), and Amis and Dawkins (1991) and illustrated in Figure 8.4. This was the same method implemented by Pflum et al. (2004), Shelburne et al. (2004), and Kar and Queseda (2012) to place the ligament within a virtual knee model in OpenSim. The ligament placement within the model knee is illustrated in Figure 8.4.

Source code segments of this model in the OpenSim format (.OSIM) for the knee joint, ligament bundles and virtual markers are located at Appendices F.2.1, F.2.2 and F.2.3 respectively.

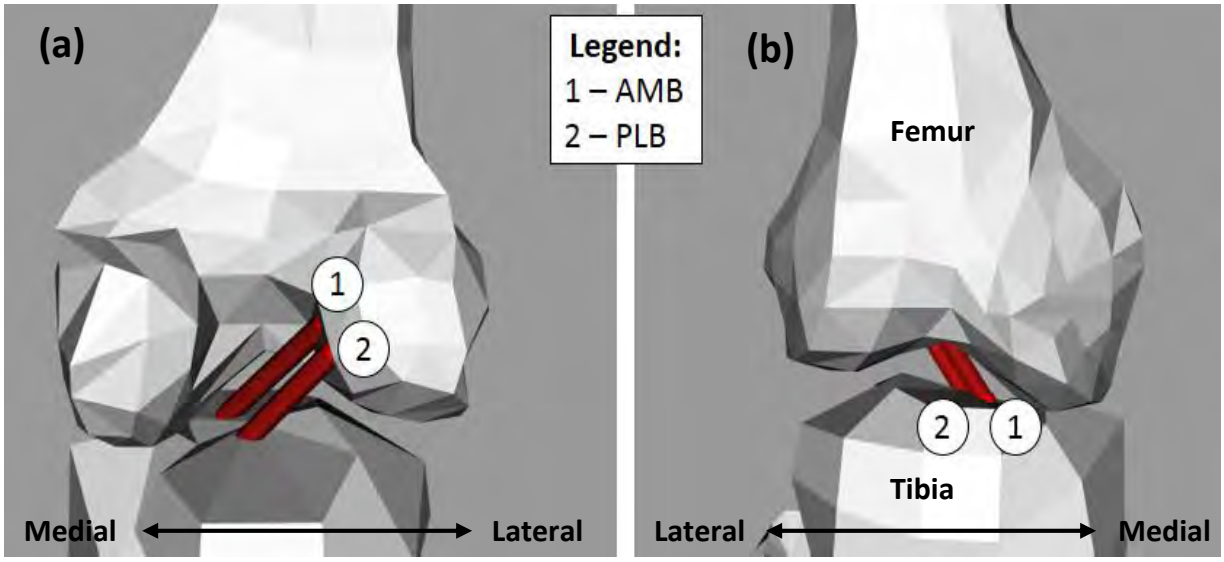

Figure 8.4: Posterior (a) and anterior (b) views of the modelled anteromedial (1 - AMB) and posterolateral (2 - PLB) ligaments.

8.5.2: Validation

The placements of the anteromedial and posterolateral bundles within the knee of the model were justified by comparing the ligaments' response to knee motion with results and observations published in literature. This process is detailed in Appendix C.1.

8.6: Model Scaling

8.6.1: Implementation

Individual marker sets were customized for each participant. Virtual marker locations in the generic edited model (Chapter 8.5.1) were manually adjusted over multiple iterations of a scale task run in the OpenSim graphical user interface. This was iterated until the mathematical error was sufficiently low and the resulting static pose best represented that of photographs taken of each subject during the static calibration trial. This resulted in a unique marker set for each participant to fit the variances between participants in experimental marker application (Chapter 7.3.1).

For the scaling measurement set, the pelvis segment is scaled by the ratio of distances between the left and right anterior superior iliac spine markers. The thigh measurement, the average bilateral distance from the greater trochanter to the lateral knee, is used to scale the femur. This measurement is also used to scale the torso, foot and toe segments as studies have shown strong relationships between height, foot size and thigh length (Özaslan et al. 2003; Grivas et al. 2008; Bhavna & Nath 2009; C-Motion Inc 2014). The average shank length, from the lateral femoral condyles to the lateral malleoli, is used to scale the tibia and talus body segments. The measurement set is depicted in Figure 8.5:

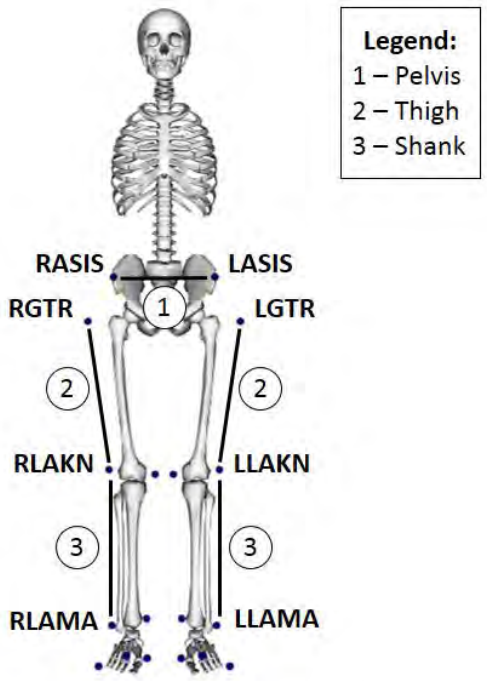

Figure 8.5: The set of measurements used for model scaling. The pelvis measurement (1) used to scale the pelvis, the thigh measurement (2) used to scale the femur, HAT, foot and toe segments and the shank measurement (3) used to scale the tibia and talus segments. For more information about model scaling, refer to 7.3.1. Refer to Appendices B.3 and B.4 for the naming conventions used for these markers.

The MTP joints in the model (Appendix B.5) were locked because there were insufficient dynamic markers placed on the toe segments (Chapter 8.2) to accurately track movement. For any simulated movements, the MTP angle is thus fixed at 0°. This is a widely recommended procedure for musculoskeletal simulations (Anderson et al. 2012; C-Motion Inc 2014).

The marker weights allocated to the dynamic set were significantly lower than those assigned to the static markers (Appendix B.6). This is because the static markers were placed on known, palpable anatomical landmarks whereas the dynamic set consisted primarily of rigid plates strapped to the soft tissue segments of the lower limb (Chapter 8.2). With multiple markers on each plate, the dynamic set is more suited to

accurate tracking of body segments during dynamic movements. The higher weights allocated to the static set allows them to be used as a reference to move the dynamic markers in the correct locations.

Weights were allocated heuristically during the iterations of the scale task. For each subject, 1 second of motion capture data taken from the middle of the static trial recording was averaged and input to the model scaling tool (Chapter 7.3.1). The result is the placement of the virtual model in the "static pose" with the virtual dynamic markers moved into the correct positions relative to the static markers.

8.6.2: Verification

Verification of the scaling routine was performed by determining if the mathematical errors from the minimization algorithm were below pre-defined thresholds (Appendix C.2). Furthermore, the static poses output for each subject model were compared - by visual inspection - for strength of matching with corresponding images captured during the static motion capture trial. This was confirmed by a third-party clinical specialist (Appendix C, Figure C.8).

8.7: Calculation of ACL Resting Length

8.7.1: Implementation

The ACL attachment sites on the femur and tibia (Chapter 8.5.1) are scaled automatically as part of the OpenSim scaling routine. A customized method was developed by the author in Matlab, using the OpenSim Application Programming Interface (API) to manually determine the zero-load lengths (Chapter 7.3.4) for each participant based on the scaled model proportions.

For each scaled subject, 3D coordinates of the AMB and PLB origin and insertion locations were obtained in the global reference frame with the knee set at 0° of rotation (Chapter 7.3.4). To account for the natural tibial translation at this position, defined by the knee joint constraints of the Gait2392 model (Figure B.2), this value was obtained from the scaled model in the global coordinate system (Equation 7.5) and added to the tibial insertions only. The ligament reference lengths were then calculated (Equation 7.6) and the zero load lengths obtained (Equation 7.4) using the reference strains reported by Blankevoort and Huiskes (1991) in Table 7.1. The relative distances between AMB and PLB insertions on the tibia and femur were also calculated for each scaled model. The Matlab code for this routine is located at Appendix F.3.

8.7.2: Validation

The obtained bundle resting lengths as well as the distances between AMB and PLB insertions on the scaled models were compared to values published in literature. These comparisons are detailed in Appendix C.3.

8.8: Inverse Kinematics and Analyze Tools

8.8.1: Implementation

A batch processing routine was developed by the author in Matlab using the OpenSim API to run inverse kinematic routines (Chapter 7.3.2) for each side-step trial. As in the scaling task (Chapter 8.6.1), marker weights for the inverse kinematics algorithm (dynamic marker set only) were set heuristically (Appendix B.7). This consisted of three functions, *Batch_IK* (F.4.1), *Run_IK* (F.4.2) and *IK_Errors* (F.4.3) which were used to cycle through each motion capture trial, run the inverse kinematics algorithm through OpenSim and then calculate the subsequent marker errors. The *Run_IK* routine was set up to load customized XML files, *Setup_IK* (Appendix F.4.4) and *IK_Tasks* (Appendix F.4.5) which contained details relevant to all of the motion capture trials, including the weights allocated to the markers.

An additional batch processing routine was developed in Matlab to run the OpenSim Analyze Tool (Chapter 7.3.3). This applied an 18Hz low pass filter to the output of the inverse kinematics routine and obtain the positions and angular velocities of each unconstrained joint as well as the ligament lengths during each cutting trial. This routine also implemented various post-processing methods on the kinematic and ligament data, which are described in more detail in Chapter 8.9. This was implemented through two functions, *Batch_Analyze* (Appendix F.5.1) and *Run_Analyze* (Appendix F.5.2) used to cycle through each motion capture trial and run the Analyze Tool through OpenSim. The *Run_Analyze* routine was set up to load a customized XML files, *Setup_Analyze* (Appendix F.5.3), which contained details of the analysis that were relevant to all of the motion capture trials.

8.8.2: Verification

Inverse kinematic results were verified by determining if the mathematical errors from the least squares minimization algorithm were below standard thresholds. Simulations were also visually inspected to determine if the kinematics represented those of a side-step movement. Consistency within subjects was also scrutinized since it was assumed that participants would employ similar techniques for each of their repeated movements. This was substantiated by a third-party clinical specialist. This process is described in detail in Appendix C.4.

8.9: Post-processing

8.9.1: Implementation

ACL strain during each of the four cutting trials was calculated for each participant using Equation 7.3. This implemented the subject-specific zero-load ligament lengths calculated as described in Chapter 8.7.

Kinematics of the right hip, knee, ankle and subtalar joints as well as the trunk were retained, all other joint angles and angular velocities were removed from the dataset since these are not part of the scope of this study (Chapter 6.5.4). Kinematic and Ligament data were trimmed over a window of interest from mid-swing up to and including mid-stance (Chapter 6.5). Mid-swing was defined as the moment of maximum knee flexion during the swing phase and mid-stance was defined as the midpoint of the total stance phase duration, between initial contact and toe off (Chapter 2.1). The resulting segment thus covers the terminal swing phase and the weight absorption phase of the side-step movement, as illustrated in

Figure 8.6.

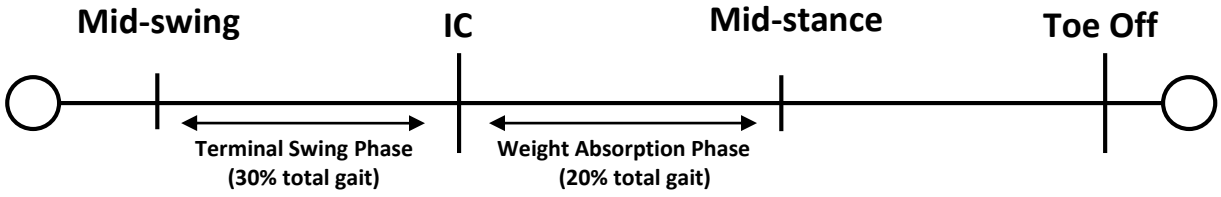

Figure 8.6: Illustration of trial segmentation windows, from the mid-swing point through to mid-stance of the side-step movement. This spans the terminal swing phase and the weight absorption phase (Chapter 2.1).

Kinematic and ligament data were then normalized by resampling the terminal swing phase data and the weight acceptance phase to 150 and 100 data points respectively to maintain their relative percentage of the running gait cycle[20] (Chapter 2.1). This ensures temporal alignment between trials, accounting for minor differences in timing between movements (McLean et al. 1999; Ford et al. 2005; Sigward & Powers 2006; Kernozek & Ragan 2008). Data from the repeated trials were averaged to form a single representative dataset for each subject (McLean et al. 2004; Frank et al. 2013; Kristianslund & Krosshaug 2013). Temporal normalization in the previous step ensures consistency between trials to better optimise this trial averaging method.

Dependent and independent variables were obtained from these representative datasets for each participant. Two independent variables were calculated from the mid-swing aspect of each of the eleven

[20] The running gait cycle was used instead of the walking gait cycle since it was deemed to be more similar to that of a side-step.

kinematic components of interest (Chapter 6.5.4). Maximum weight-absorption phase strains of each bundle were obtained as the dependent variables. These variables are illustrated in Figure 8.7.

The timing of the bundle strain peaks in addition to the timing of the maximum ground reaction force, relative to the total stance phase percentage, were also determined. For comparison with results from previous studies, the instantaneous positions and angular velocities at initial contact were also determined for each joint coordinate of interest.

8.9.2: Verification and Validation

Within session test-retest reliability of the simulations was calculated, as with Myer et al. (2005) and Ford et al. (2005), by analysing the intraclass correlation coefficients between individual trials of each subject for each of the trimmed and gait-cycle normalized datasets. This process is detailed in Appendix C.5. For more information about intraclass correlation coefficients, refer to Appendix B.8. This process justifies that averaging the repeated trials (Chapter 8.9.1) will maintain the exhibited kinematic patterns and is thus an accurate representation of each subject's side-step technique.

The gait-cycle-normalised, trial-averaged kinematics from mid-swing to mid-stance for each subject were validated through comparison with the corresponding values previously calculated (right hip, knee and ankle angles, only) on the same data by Sigward et al. (2012). Root mean square errors between the two datasets were calculated and normalized to the respective standard deviations according to methods published by McLean et al. (2004). This process is explained in Appendix C.6.

8.10: Statistical Analyses

All statistical comparisons were performed in Matlab and SPSS (IBM, New York, USA) where an alpha value of less than 0.05 denotes a significant result. Each ligament bundle was analysed as an independent structure (Figure 8.7) and, as such, post-hoc correction between separate hypotheses tests in this regard is not necessary (Hewett et al. 2005).

8.10.1: Descriptive Statistics

Descriptive statistics (means and standard deviations) were used to compare joint kinematics and ligament bundle strains with results from similar studies published in the literature.

8.10.2: Identifying Linear Relationships

To determine which mid-swing kinematics components are linearly related to the maximum stance phase ACL bundle strains, Pearson's Product-Moment Correlation coefficients (Chapter 7.3.5) were determined

between the dependent and independent variables (McLean et al. 2005; Dempsey et al. 2012; Valente et al. 2013).

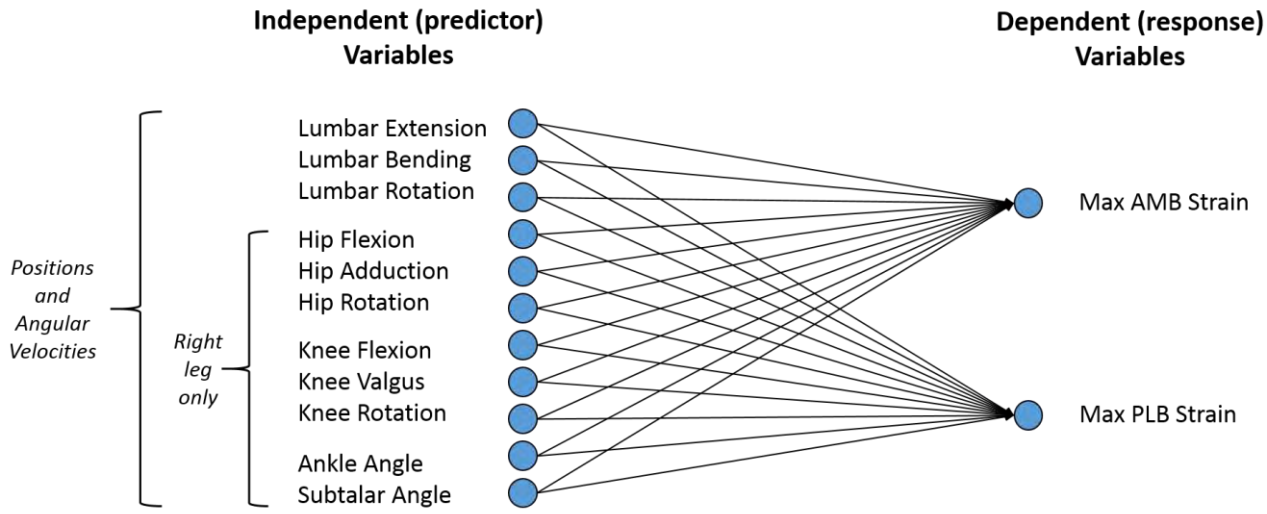

Figure 8.7: Visual representation of the 22 candidate predictor variables (positions and velocities of 11 joint angles at mid swing) and the 2 response variables (maximum strain in each ligament bundle occurring during the weight acceptance phase). This diagram also illustrates how the predictor variables are applied independently to each response variable in the statistical analysis.

Correlation coefficients were also determined between bundle strains and participant age, BMI and experience were calculated to control for these possible confounding factors (Chapter 2.4.1). Finally, correlations between bundle strains and the instantaneous joint angles and angular velocities at initial contact were obtained, merely for comparison with similar results from previous studies.

8.10.3: Evaluating Overall Predictability

Linear regression algorithms (Chapter 7.5) were implemented to investigate the effect of kinematic components to predict ligament strain in each bundle (Roberts et al. 2004; Sigward & Powers 2007; Frank et al. 2013; Kristianslund et al. 2013). For each model, only the most significant mid-swing kinematic variables, as defined by the results from the correlation tests (Chapter 8.10.2), were used as the candidate predictors.

The “best subset” method of variable entry (Chapter 7.5.4.1) was used to reduce the number of candidate variables to find the best possible set of predictors for each regression model. The corrected Akaike Information Criterion was used as the criterion to optimize subset selection and reduce overfitting (Chapter 7.5.4.2). The regression algorithm was implemented using the automatic linear modelling (LINEAR) tool in SPSS.

Post-hoc correction to compensate for multiple hypothesis testing was implemented using the method proposed by Lovell (1983) (Chapter 7.5.4.3). For verification, each regression model was inspected for the possible violation of the linear regression assumptions (Chapter 7.5.2). Variance inflation factors were also inspected to test for multicollinearity within the regression subsets (Chapter 7.5.3).

Chapter 9: Results

Eight participants each completed four successful side-step trials as required (Chapter 8.2). One participant only completed three successful side-step trials and one trial was removed from another participant's dataset during post processing due to defective marker data. However, the procedure of trial averaging (Chapter 8.9) resulted in one representative dataset for each subject.

9.1: Body Kinematics

Ensemble averages (mean ± standard deviation) of the joint angles and angular velocities displayed by the subject population during the side-step cutting movements, from mid-swing to mid-stance, are illustrated in Figure 9.1 through to Figure 9.22. These represent the general kinematic patterns displayed by the study population. Table 9.1 outlines the instantaneous means and standard deviations for these variables at the mid-swing and initial contact stages.

Table 9.1: Mean joint angles and angular velocities at mid-swing and initial contact

	Position (°)				Velocity (°/s)			
	Mid-swing		Initial contact		Mid-swing		Initial contact	
Lumbar								
Flexion	16.77 ±	5.37	15.05 ±	7.31	72.91 ±	48.59	61.96 ±	38.57
Bending[a]	0.28 ±	3.91	8.01 ±	3.48	2.50 ±	45.02	17.33 ±	29.89
Rotation[b]	5.30 ±	4.24	-12.16 ±	4.29	-102.21 ±	38.48	-61.20 ±	53.32
Hip								
Flexion	26.73 ±	5.23	37.72 ±	4.66	347.75 ±	84.13	-107.53 ±	56.77
Abduction	8.40 ±	3.49	3.43 ±	4.38	23.94 ±	57.11	19.73 ±	43.50
Int Rotation	3.46 ±	6.95	8.64 ±	9.30	168.49 ±	85.63	26.09 ±	113.70
Knee								
Flexion	94.22 ±	12.32	24.14 ±	6.98	-1.09 ±	5.78	124.22 ±	86.13
Varus	3.17 ±	8.88	-0.23 ±	2.83	42.81 ±	66.95	-34.36 ±	55.49
Int Rotation	-4.70 ±	9.72	0.10 ±	7.17	67.55 ±	67.27	31.73 ±	68.35
Ankle								
Dorsiflexion	-0.87 ±	5.96	8.55 ±	11.58	176.64 ±	42.19	-286.52 ±	122.81
Subtalar								
Supination	-8.49 ±	6.67	6.11 ±	5.70	39.64 ±	66.20	-12.53 ±	90.90

[a] Positive value denotes bending away from the cutting direction

[b] Positive value denotes rotation towards the cutting direction

Table 9.1: Mean (± standard deviations) joint angles and angular velocities of the subject population at both the mid-swing and initial contact stages of a side-step cutting movement. For continuous means and standard deviations throughout this period, refer to Figure 9.1 through to Figure 9.22. Positive values denote movements in the direction specified, negative values indicate rotations in the opposite direction. Refer to Table 8.1 for these definitions.

.

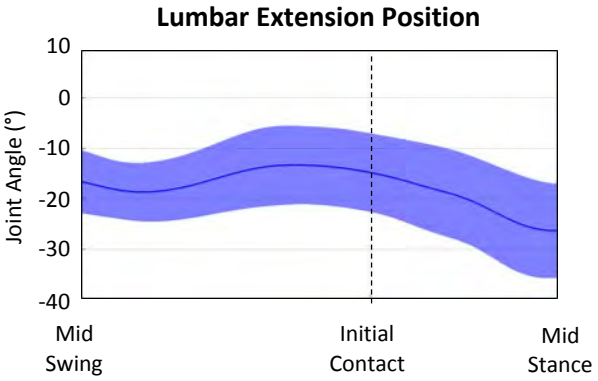

Figure 9.1: Mean lumbar extension position (± sd) from mid-swing to mid-stance of an unanticipated side-step cut.

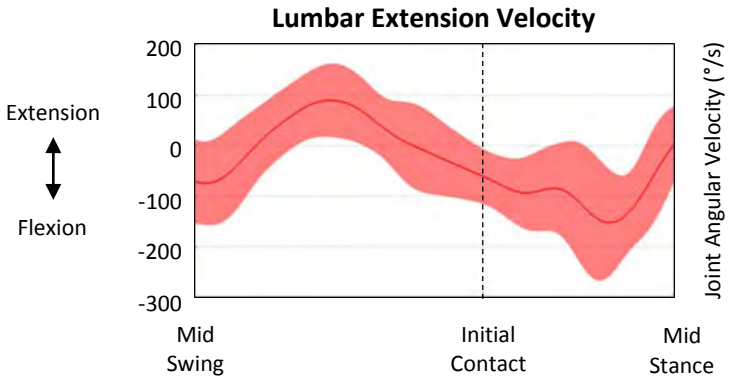

Figure 9.2: Mean lumbar extension velocity (± sd) from mid-swing to mid-stance of an unanticipated side-step cut.

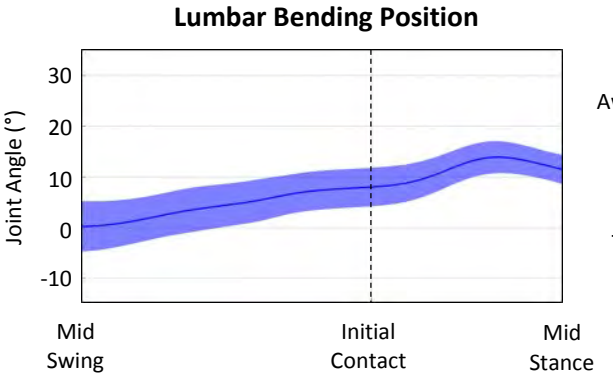

Figure 9.3: Mean lumbar bending position (± sd) from mid-swing to mid-stance of an unanticipated side-step cut.

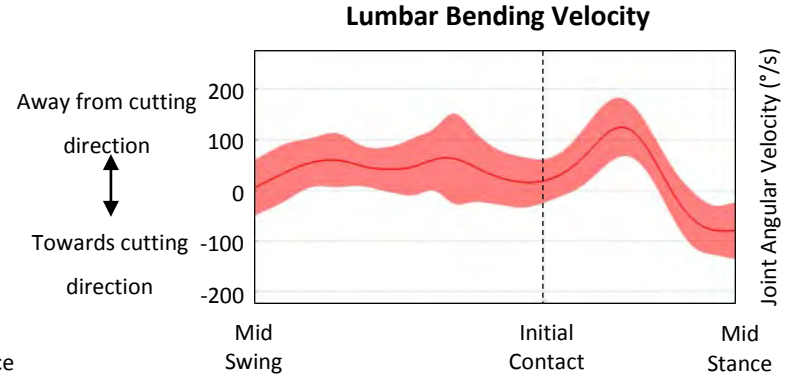

Figure 9.4: Mean lumbar bending velocity (± sd) from mid-swing to mid-stance of an unanticipated side-step cut.

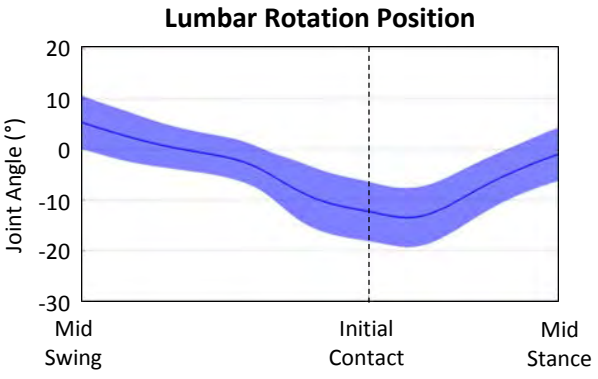

Figure 9.5: Mean lumbar rotation position (± sd) from mid-swing to mid-stance of an unanticipated side-step cut.

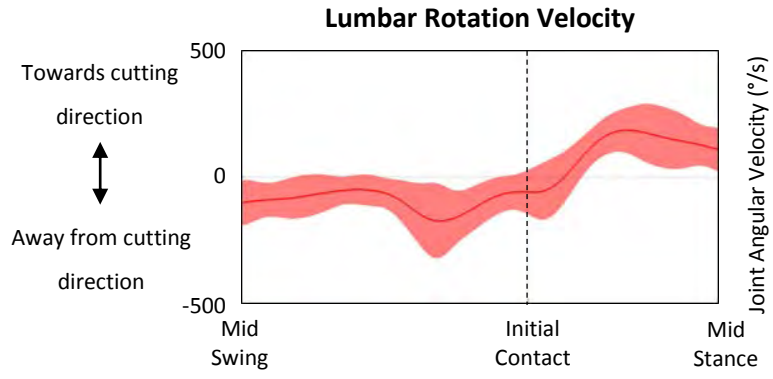

Figure 9.6: Mean lumbar rotation velocity (± sd) from mid-swing to mid-stance of an unanticipated side-step cut.

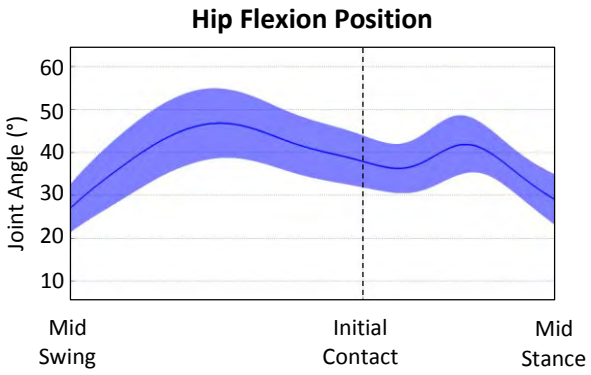

Figure 9.7: Mean hip flexion position (± sd) from mid-swing to mid-stance of an unanticipated side-step cut.

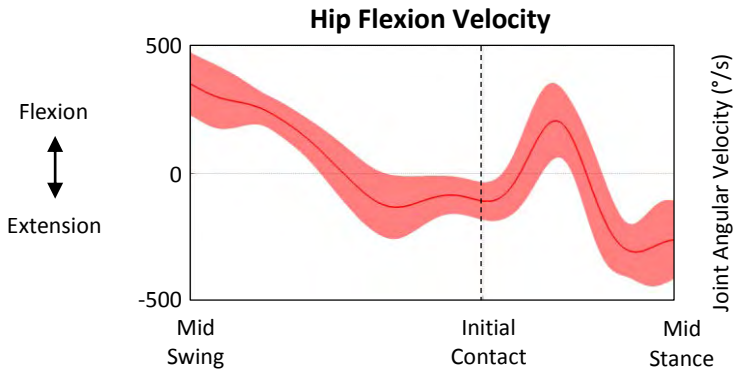

Figure 9.8: Mean hip flexion velocity (± sd) from mid-swing to mid-stance of an unanticipated side-step cut.

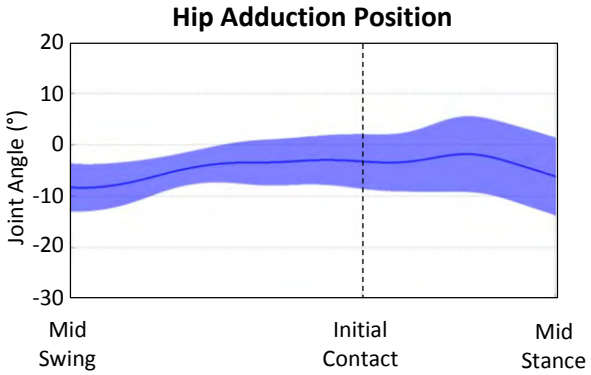

Figure 9.9: Mean hip adduction position (± sd) from mid-swing to mid-stance of an unanticipated side-step cut.

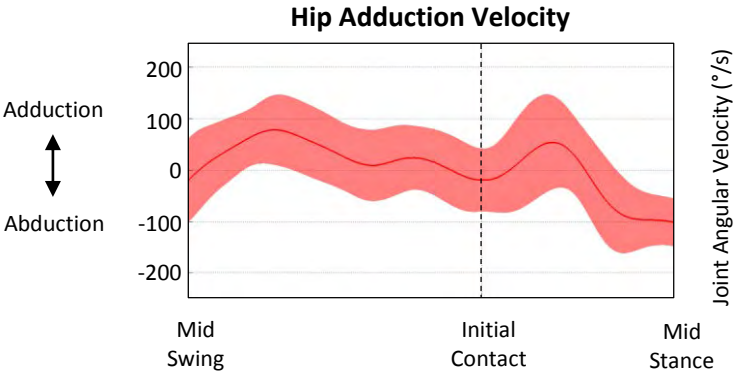

Figure 9.10: Mean hip adduction velocity (± sd) from mid-swing to mid-stance of an unanticipated side-step cut.

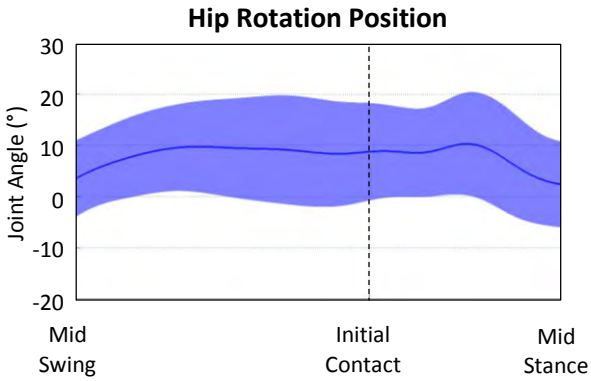

Figure 9.11: Mean hip rotation position (± sd) from mid-swing to mid-stance of an unanticipated side-step cut.

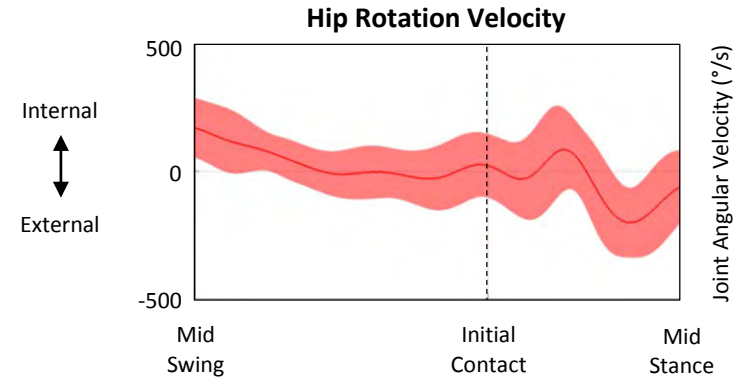

Figure 9.12: Mean hip rotation velocity (± sd) from mid-swing to mid-stance of an unanticipated side-step cut.

.

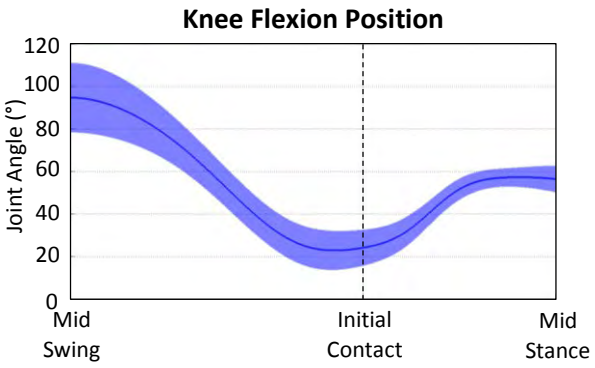

Figure 9.13: Mean knee flexion position (± sd) from mid-swing to mid-stance of an unanticipated side-step cut.

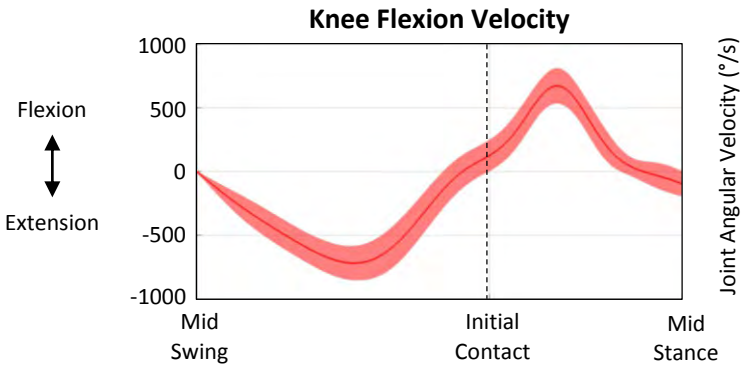

Figure 9.14: Mean knee flexion velocity (± sd) from mid-swing to mid-stance of an unanticipated side-step cut.

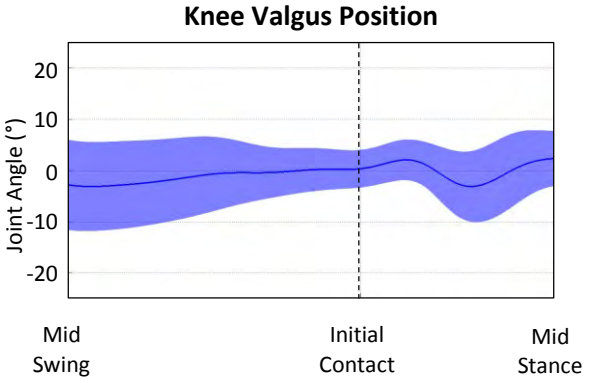

Figure 9.15: Mean knee valgus position (± sd) from mid-swing to mid-stance of an unanticipated side-step cut.

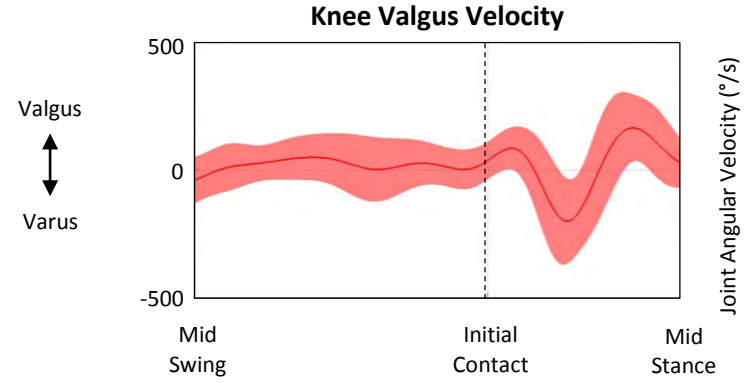

Figure 9.16: Mean knee valgus velocity (± sd) from mid-swing to mid-stance of an unanticipated side-step cut.

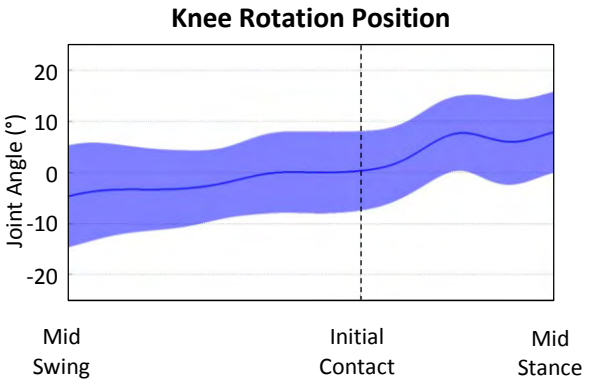

Figure 9.17: Mean knee rotation position (± sd) from mid-swing to mid-stance of an unanticipated side-step cut.

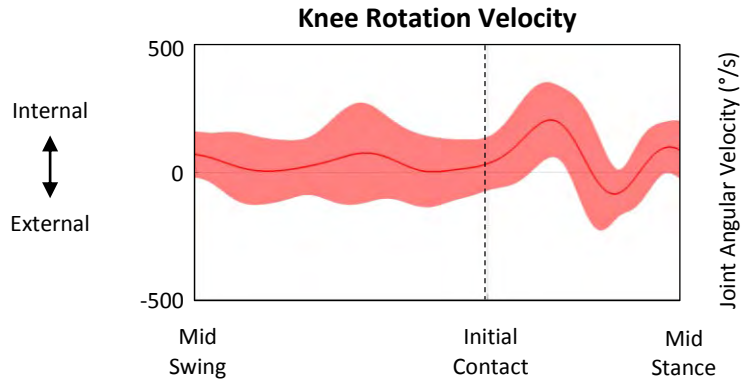

Figure 9.18: Mean knee rotation velocity (± sd) from mid-swing to mid-stance of an unanticipated side-step cut.

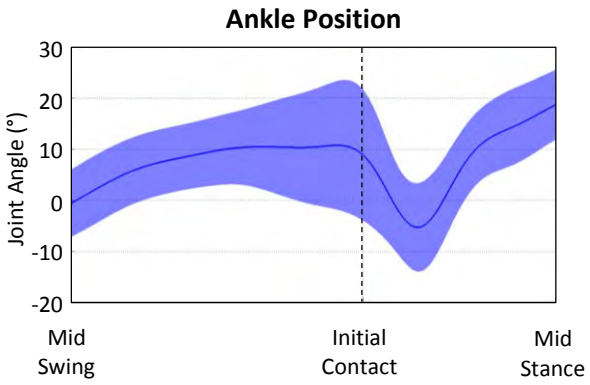

Figure 9.19: Mean ankle angle position (± sd) from mid-swing to mid-stance of an unanticipated side-step cut.

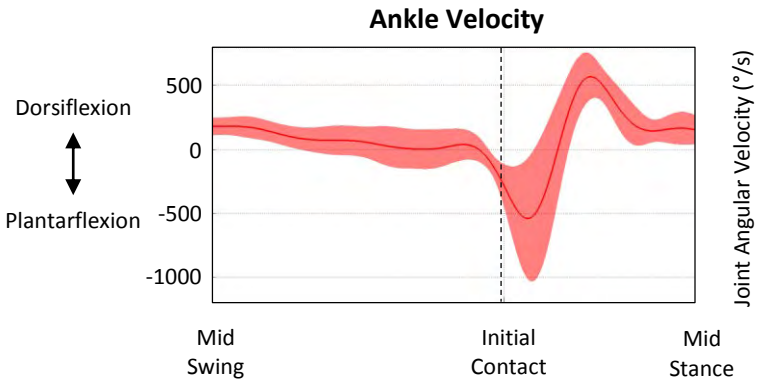

Figure 9.20: Mean ankle angular velocity (± sd) from mid-swing to mid-stance of an unanticipated side-step cut.

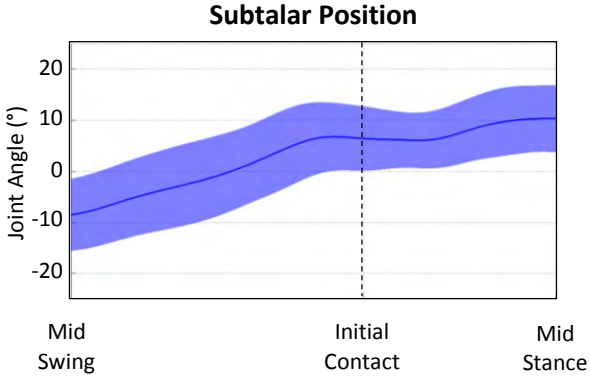

Figure 9.21: Mean subtalar angle position (± sd) from mid-swing to mid-stance of an unanticipated side-step cut.

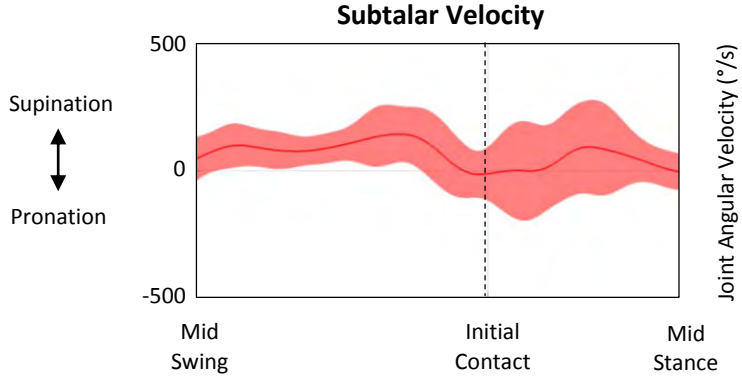

Figure 9.22: Mean subtalar angular velocity (± sd) from mid-swing to mid-stance of an unanticipated side-step cut.

9.2: Ligament Strains

Figure 9.23 illustrates the mean (± standard deviation) strains in both ligament bundles over the weight acceptance aspect of the stance phase (Chapter 2.1). One standard deviation above and below the mean is shaded on the graph with the timing of the average maximum vertical ground reaction force illustrated as a black dotted line.

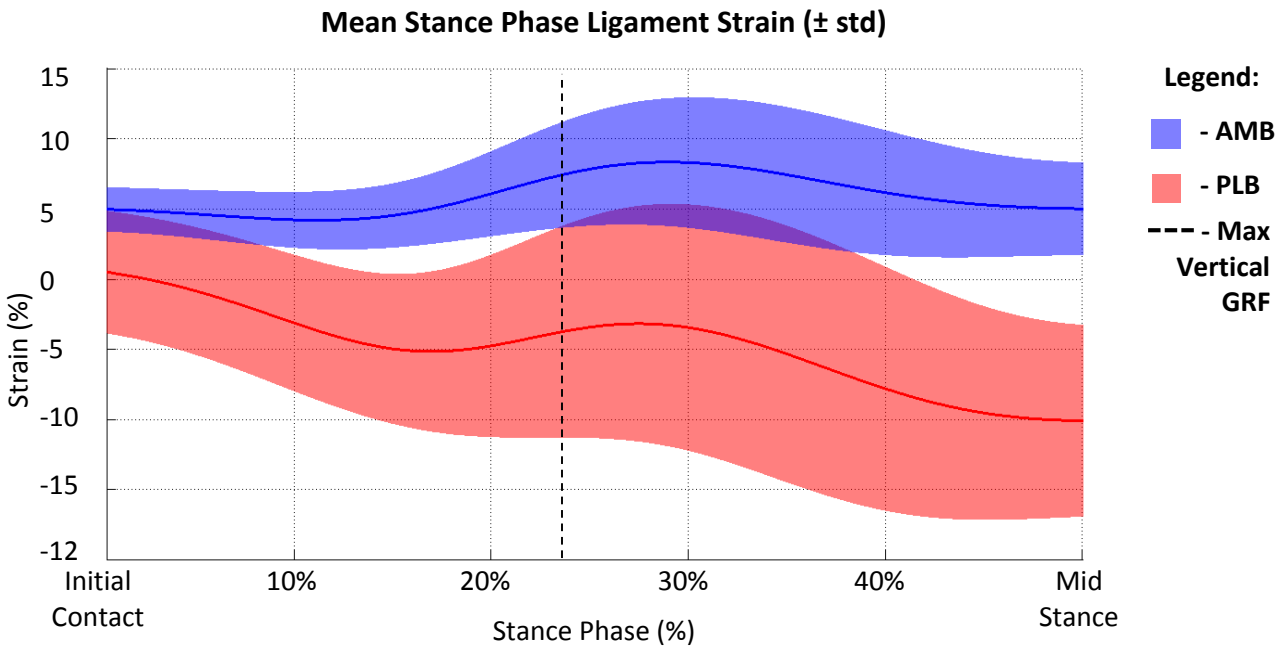

Figure 9.23: Mean strain in the anteromedial (AMB, blue) and posterolateral (PLB, red) bundles over the weight acceptance period of the stance phase, with one standard deviation either side of the mean shaded. The mean timing of the maximum vertical ground reaction force (Table 9.3) is illustrated as a black dotted line.

The average maximum stance-phase strains in each ligament bundle are presented in Table 9.2. This differs from what would appear to be the mean maximum values in Figure 9.23 because the true maximum values do not occur at the same point in time for each subject. Figure 9.23 is simply an illustration of the ensemble-average ligament strain at each stance-phase-normalised time point. The mean timing of these maximum strains as well as the timing of the mean onset of the maximum vertical ground reaction force are presented in Table 9.3.

Table 9.2: Mean maximum ligament bundle strains	
AMB_{MAX}	8.86 ± 4.36 %
PLB_{MAX}	-1.15 ± 7.72 %

Table 9.2: Mean maximum ligament strains in both the anteromedial (AMB) and posterolateral (PLB) bundles.

Table 9.3: Mean timing (relative to % stance phase)	
AMB_{MAX}	30.20 ± 4.58 %
PLB_{MAX}	26.90 ± 12.44 %
$GRF_{Vertical(MAX)}$	23.86 ± 17.18 %

Table 9.3: Mean timing (in units relative to the % of the total stance phase time) of the maximum bundle strains and vertical ground reaction forces occuring during the side-step trials.

9.3: Identification of Linear Relationships

Independent variables (Figure 8.7) that were found to be significantly correlated with anteromedial and posterolateral bundle strains are shown in Table 9.4, indicating the coefficient of the relationship and the associated level of significance. This table also includes the correlations between the ligament bundles and kinematic variables at initial contact[21]. Correlations between these variables, indicating potential multicollinearities (Chapter 7.5.3), are tabulated in Appendix D.1. Correlations between maximum ligament bundle strains and the potential confounding factors of age, body mass index and level of experience are detailed in Table 9.5.

Table 9.4: Variables significantly correlated with ligament bundle strain

	Ligaments		Mid-swing				Initial Contact	
	AMB	PLB	Hip Rotation Position	Knee Varus Position	Lumbar Bending Velocity	Knee Valgus Velocity	Knee Varus Position	Knee Extension Velocity
AMB	1	0.868**	.889**	.878**	.666*		.804**	.760*
PLB	0.868**	1	.718*	.754*	.708*	.670*	.730*	.661*

***. Correlation is significant at the 0.05 level (2-tailed).**

****. Correlation is significant at the 0.01 level (2-tailed).**

Table 9.4: Variables, including kinematics at both mid-swing and initial contact[21], that are significantly correlated with maximum weight-acceptance phase ligament strains in the anteromedial (AMB) and posterolateral (PLB) bundles. This also includes the correlations between these strains.

Table 9.5: Correlations of potentially confounding variables with ligament bundle strain

	Age	Body Mass Index	Total Experience
AMB Strain	-0.1134	0.5134	0.2582
PLB Strain	-0.0949	0.3553	-0.0999

***. Correlation is significant at the 0.05 level (2-tailed).**

****. Correlation is significant at the 0.01 level (2-tailed).**

Table 9.5: Correlations of potentially confounding variables (2.4.1) with maximum stance-phase ligament bundle strains.

[21] Initial contact kinematic variables are not to be included in the regression models, they are merely included for comparison with previous studies.

9.4: Regression Model Parameters

The parameters of the best performing subsets for each ligament bundle regression model are displayed in Table 9.6. This includes details of the predictor variables included in the subsets as well as the coefficients that are used form the regression equations. Scatter plots of the regression output (model predicted) strains against the observed (simulated) values with best fit lines are represented in Figure 9.24 and Figure 9.25 for the anteromedial and posterolateral bundles respectively. Comparisons of the five best performing subsets for each regression model are tabulated in Appendix D.2.

Table 9.6: Parameters of the best performing subsets for the AMB and PLB regression models

	AMB Model	PLB Model	
AIC	18.488	31.919	
R^2 (Study Population)	0.791	0.833	
R^2 (95% CI)	$0.599 < R^2 < 0.982$	$0.692 < R^2 < 0.974$	
Standard Error	2.118	3.576	
Significance Level ($\propto$)	0.05	0.05	
Adjusted Significance Level[22] ($\hat{\propto}$)	0.0170	0.0253	
Model Significance (p)	0.0006	0.0019	
Durbin-Watson	2.023	2.169	
Residual Mean	0.005	-0.017	
Residual Std.	1.006	1.033	
Significant Outliers	None	None	
	Predictors Included in the Regression Models		
Predictor Names	**Hip Rotation Position**	**Knee Varus Position**	**Knee Valgus Velocity**
Coefficient (Study Population)	0.559	0.553	0.061
Coefficient (95% CI)	$0.324 \leq B \leq 0.793$	$0.227 \leq B \leq 0.879$	$0.018 \leq B \leq 0.104$
Coefficient Significance (p)	0.0006	0.0051	0.0126
Variance Inflation Factor	1.000	1.052	1.052

Table 9.6: Parameters of the best performing subsets for the AMB and PLB regression models.

[22] Refer to Equation 7.11

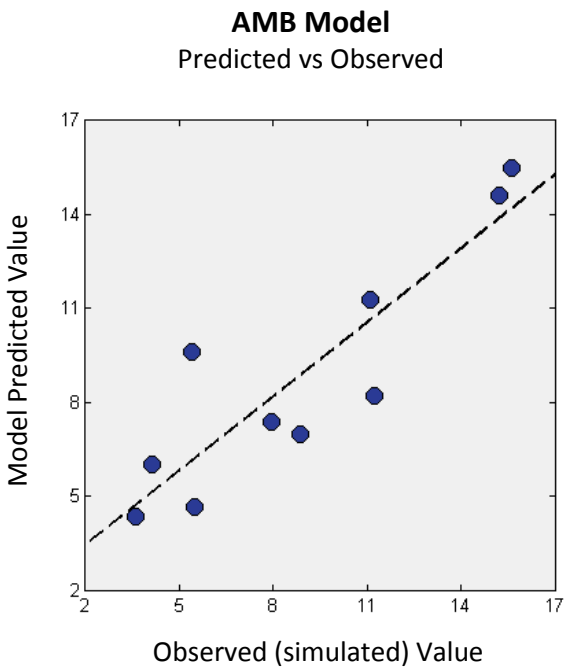

Figure 9.24: Comparison of the regression model predicted strain compared to the observed value for the anteromedial bundle. The line of best fit is displayed in black.

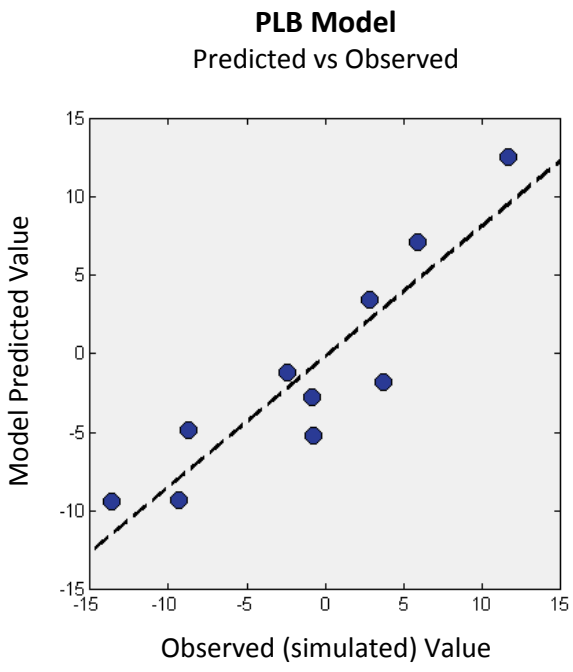

Figure 9.25: Comparison of the regression model predicted strain compared to the observed value for the posterolateral bundle. The line of best fit is displayed in black.

9.5: Regression Equations

The prediction equations for the best performing regression models are represented in Equation 9.1 and Equation 9.2 for the anteromedial and posterolateral bundles respectively.

$$AMB_{Max\ Strain} = 6.926 + 0.559(Hip\ Rotation\ Position_{Mid\ Swing})$$

Equation 9.1

$$PLB_{Max\ Strain} = -0.30 + 0.553(Knee\ Varus\ Position_{Mid\ Swing}) + 0.061(Knee\ Valgus\ Velocity_{Mid\ Swing})$$

Equation 9.2

9.6: Regression Residuals

Scatter plots (Chapter 7.5.2.1) showing the standardized residuals of each model are represented in Figure 9.26 and Figure 9.27 respectively. Similarly, Probability-Probability plots (Chapter 7.5.2.5) illustrating the observed cumulative distributions of the standardized residuals versus the cumulative normal distributions are represented in Figure 9.28 and Figure 9.29.

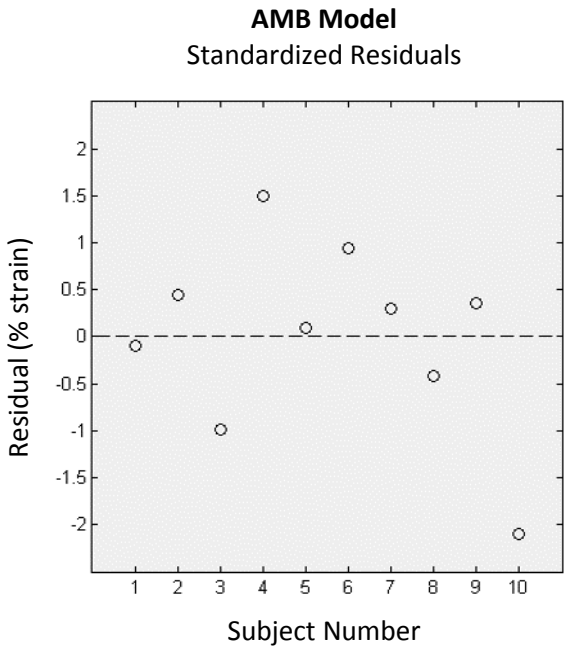

Figure 9.26: Scatter plot of standardized residuals (7.5.2.1) for the anteromedial bundle regression.

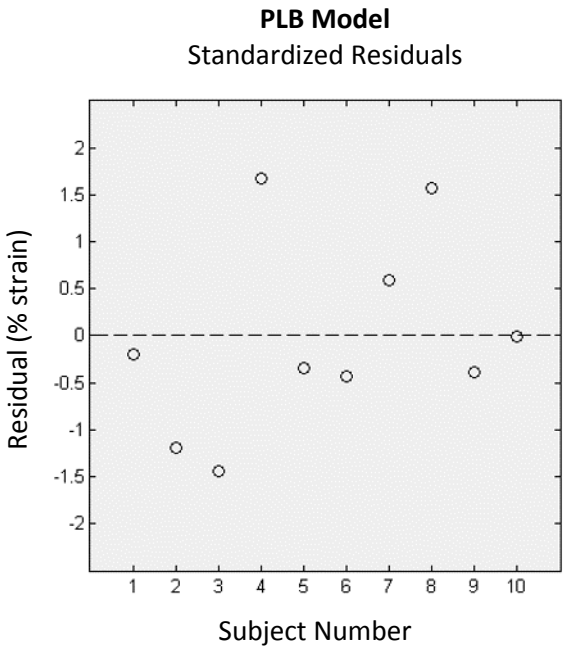

Figure 9.27: Scatter plot of standardized residuals (7.5.2.1) for the posterolateral bundle regression.

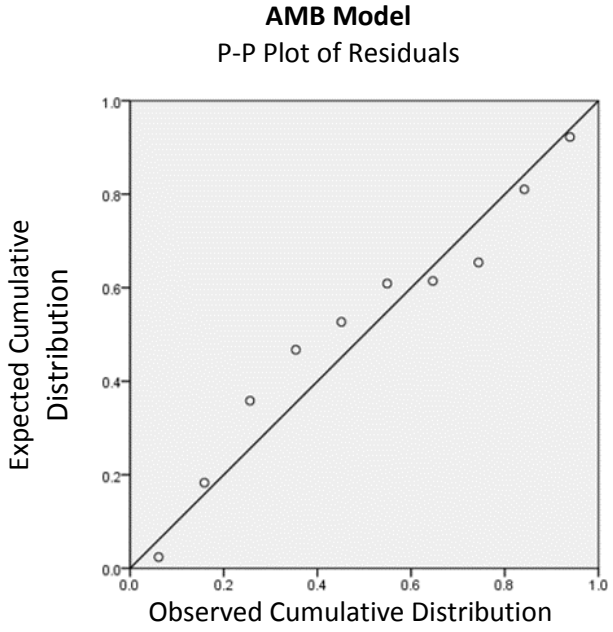

Figure 9.28: Probability-Probability Plot(7.5.2.5) of the residuals from the anteromedial bundle.

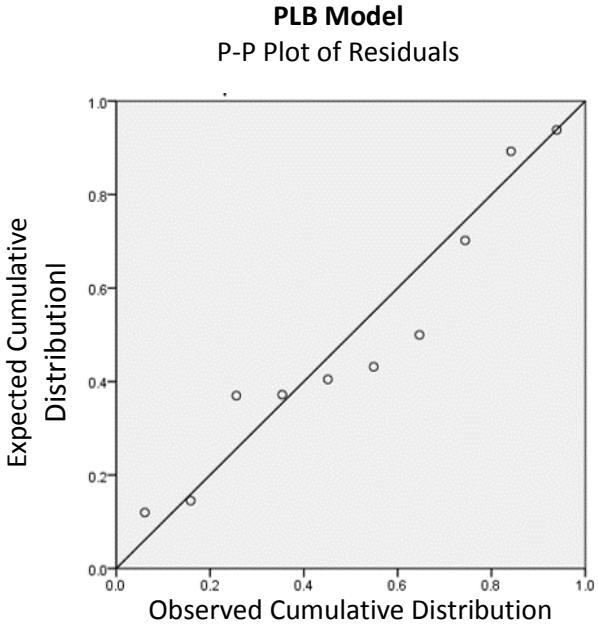

Figure 9.29: Probability-Probability Plot (7.5.2.5) of the residuals from the posterolateral bundle.

Chapter 10: Discussion

10.1: Analysis of Results

10.1.1: Kinematics

Comparison of the swing-phase kinematics obtained from the side-step trials with literature is difficult since no studies were found to have published this data (Chapter 5). However, many studies investigating side-step movements have published stance-phase body kinematics, primarily focusing on the point of initial contact. These studies implement multiple different model types with varying degrees of freedom and joint centre definitions, thus direct comparison is not always achievable. Furthermore, although useful in visualising rapid changes in joint angles, very few studies disclose the observed angular velocities.

10.1.1.1: Lumbar Joint

In the sagittal plane, the lumbar joint was predominantly in flexion throughout the movement, with an extension just prior to initial contact before moving back into a flexed position (Figure 9.1). This indicates that the participants were leaning forwards while running, straightened up as they performed the cut and then leaned forward again as they accelerated into the cutting direction. Participants also displayed a tendency to bend (Figure 9.3) and rotate (Figure 9.5) the trunk away from the new direction of travel (i.e. towards the planting foot) at initial contact before returning to a more neutral trunk position after the movement. This is likely a result of the lower limb first creating the change in direction, with the upper body then "following" the movement. Houck et al. (2006) reported lateral trunk bending at initial contact for unanticipated side-step cutting movements. Kristianslund et al. (2013) and Frank (2013) observed the same lumbar bending towards the planting foot, but observed their participants to demonstrate a tendency to rotate the trunk towards the cutting direction at initial contact. However, the population variance - in both studies - was such that some participants displayed lumbar rotation away from the cutting direction at this point. This is likely due to individual differences in technique or instruction, since some athletes may attempt to "fake" or "dummy" prior to the movement to confuse an imaginary opponent.

10.1.1.2: Hip Joint

The hip joint is flexed but extending prior to initial contact, where the force of impact and inertia of the body creates an additional flexion movement (Figure 9.7). This is especially visible on the hip flexion velocity, displayed in Figure 9.8. During the terminal swing-phase, the hip is also abducted (Figure 9.9) and internally rotated (Figure 9.11). This is likely as a result of the body beginning to dynamically align the

lower limb prior to contact with the ground to be in a position to create the change in direction required of the side-step (Rose & Gamble 2006). Houck (2006), Jorrakate and Vachalathiti. (2011) and Kristianslund et al. (2013) all observed participants to land with an abducted hip at initial contact. Houck did not analyse hip rotation but Jorrakate and Vachalathiti also observed a mean internal rotation of the hip. The participants in Kristianslund's study, however, demonstrated a mean tendency to land with the hip externally rotated although this was distributed across internal rotation as well. Kristianslund later went on to calculate that those participants who did land at higher degrees of hip internal rotation experienced greater frontal-plane knee moments.

10.1.1.3: Knee

The knee joint is at maximum flexion at mid-swing (Figure 9.13) before extending over the course of the terminal swing phase due to the combined inertial forces of the forward directed movement and the extending hip joint (Rose & Gamble 2006). The mean knee flexion angle at initial contact was 24.14 ± 6.98° (Table 9.1), indicating that participants landed with relatively extended knees which is known to typical within female athletes as well as a risk factor for injury (Chapter 2.6.2).

Following initial contact, the knee briefly flexes as the forces of impact are absorbed before extending again as the limb begins to push off the ground. In the frontal plane, the knee remains fairly static during the terminal swing phase and lands in a relatively neutral position. Following contact, there is a distinct, rapid valgus-varus-valgus rotation sequence that takes place. This is clearly visible in both the position (Figure 9.15) and angular velocity (Figure 9.16) kinematics. A similar sequence is evident in the transverse plane. The knee is externally rotated at mid-swing, neutral at initial contact but an internal-external-internal rotation sequence immediately follows contact with the ground (Figure 9.17 and Figure 9.18).

The same rotation sequences post-landing have previously been reported by Ford et al. (2005) and Sigward et al. (2006, 2007), both studies investigating simulated side-step movements through motion-capture, as well as Koga et al. (2010) who analysed video footage of actual non-contact ACL injury events. This rapid oscillation indicates a general instability in both the frontal and transverse planes as the ground reaction force propagates through the knee joint. It suggests that the participants displayed a "ligament dominance", relying on the ligaments to absorb the knee loads without adequate muscle contraction (Chapter 2.8). This also highlights the link between frontal and transverse plane movements in the knee, likely due to a combination of the ground reaction force and the mechanical interface between the contact surfaces of the tibia and femur (Chapter 2.2).

These rotation sequences, particularly the combined knee varus and internal rotation movements with the relatively extended knee, are likely the conditions that created the stance-phase loading patterns observed in the bundles of the ACL (Figure 9.23).

10.1.1.4: Ankle

The ankle joint dorsiflexes over the swing phase, preparing for the heel to impact with the ground (Figure 9.19). Once contact is made, the joint initially plantarflexes as the foot moves flat onto the ground before dorsiflexing as the body rotates over the planted foot (Rose & Gamble 2006). The subtalar joint changes from pronation at mid-swing to supination at initial contact, maintaining this position for the duration of the stance phase (Figure 9.21). This is likely due to the body leaning towards the new direction of movement with the foot planted flat on the ground. Supination is a combination of ankle inversion and internal rotation, also observed at the initial contact aspect of side-step movements by Ford et al. (2005) and Kristianslund et al. (2013) respectively.

10.1.2: Ligament Strain

The mean maximum strains observed in the study population were 8.86 ± 4.36% and -1.15 ± 7.72% for the anteromedial and posterolateral bundles respectively (Table 9.2). These peaks occurred at 30.20 ± 4.58% and 26.90 ± 12.44% of the total stance phase duration. This also coincides with the period of maximum ground reaction force observed during the movements, 23.86 ± 17.18% of the total stance phase duration (Table 9.3). This period of maximum strain in both ligament bundles falls within the early weight acceptance phase (Chapter 2.1) of the movement, when non-contact ACL injuries are known to occur (Chapter 2.5).

Cerulli (2003), using a strain gauge embedded in the ligament, observed average peak ACL strains of 5.47 ± 0.28% during a rapid deceleration movement. For jump landing tasks, Taylor (2011) observed average peak strains of 12 ± 7%. Kar and Queseda (2012) similarly recorded average peak strains of 12.2 ± 4.1%. These ligament strains (mean values and standard deviations) obtained from athletes during dynamic activity compare favourably with those calculated in this study. However, these studies did not investigate athletes attempting side-step cutting movements nor did they consider the ligament as a multi-bundle structure (Chapter 5). In a case study of a single participant performing a side-step movement, Zhang (2010) reported the maximum anteromedial bundle strain to be 7.68% with a maximum posterolateral bundle strain of 7.45%. These results fall approximately within one standard deviation of those obtained in this study.

Investigating the effect of increasing strain on the ligament bundles, Butler (1989) reported that strains exceeding 15% would be sufficient for ligament failure, or the point at which a rupture occurs. However, Butler separated the ligament bundles prior to testing. Other studies, keeping the bundles intact, recorded much higher strains required for failure. Noyes and Grood (1976) observed an average strain at ligament failure of 60.25 ± 6.78%. A more recent study by Chandrashekar et al. (2006) placed this value at 30 ± 6% for males and 27 ± 8% for females. It is likely that the bundles can withstand greater loads in combination, since each bundle contributes to resistance in different directions (Chapter 2.2). This is an indication of the multivariate nature of non-contact ACL injuries and the danger of combined loading in multiple directions.

The ligament strains observed in this study are clearly not of a magnitude to result an injury to the tissue, supported by the fact that no injuries were sustained by the participants during testing. Although, based on the findings of Butler (1989) and Chandrashekar et al. (2006), participants exhibiting strains greater than two standard deviations above the observed mean value could be considered to be at risk, particularly if the structure of the ligament is already compromised. This could likely occur in multiple ways, for example if one bundle was already partially ruptured, a reconstructed ligament was surgically inserted as a single bundle or even if the ligament tissue is inherently, anatomically weaker than average. This leads into the research question, proposed in Chapter 6.4, questioning the differences in loading between bundles during the weight-acceptance phase.

The ensemble-averaged ligament bundle strains during the weight-acceptance phase are illustrated in Figure 9.23. It indicates that the between-subject variance in posterolateral bundle strains is greater than that of the anteromedial bundle, for the duration of the stance-phase. This difference in variance is also clear in the standard deviations of mean maximum strain as well as the timing of this mean maximum value (Table 9.2, Table 9.3).

The strong positive correlation between bundle strains (Table 9.4) suggests that those participants who demonstrated high maximum anteromedial bundle strains also demonstrated high maximum posterolateral bundle strains, relative to the other participants in the study. This suggests that a subset of participants could be classified into a “high-risk” group who may demonstrate kinematic patterns - beyond just knee extension - that are responsible for the increased strain levels in both ligament bundles.

An important consideration is that the posterolateral bundle is shown to be predominantly in negative strain (shortened below its zero-load length) whereas the baseline for the anteromedial bundles is much

higher. This should be questioned, especially since the posterolateral bundle is under strain at low degrees of knee flexion (Chapter 1.1) – even without dynamic loading. However, the anteromedial bundle exhibits expected strain values so this is unlikely to be a result of the modelled kinematics or kinematic constraints. The low strain seen in the posterolateral bundles could arise due to incorrect ligament placement within the model or from errors in the calculation of the zero-load length.

Since the ligament placements within the musculoskeletal model were justified according to their responses to knee flexion (Appendix C.1), it is unlikely that this is the cause of this baseline difference. It is conceivable, though, that the posterolateral bundle strains are low as a result of an incorrect zero-load length definition. This could arise due the fact that generic reference strain definitions (Table 7.1) were used which, if incorrect for the posterolateral bundle, would linearly affect the observed strain values and result in a shift on the strain axis (Y). For example, a larger posterolateral bundle reference strain (which is realistic because the bundle is taut at the extended reference position) would result in a shorter zero-load length and thus an increase in "observed" posterolateral bundle strains during the side-step (for the exact same set of kinematics), matching better with anteromedial bundle strains.

It is necessary to draw attention to the fact that this will not affect the results of the correlation (10.1.3) or regression (10.1.4) analyses, since the shape of the posterolateral bundle response to the kinematics is still preserved. Changing the reference strain essentially results in a vertical (strain axis) shift and dilation of the posterolateral bundle response to the observed kinematics. The coefficients of the regression equations will be different, of course, but this does not affect the actual strength of the predictive relationship.

Conversely, supporting evidence for the observation of low posterolateral bundle strains is found in the rupture patterns of the ligaments, particularly when the ligament is partially torn (Amis & Dawkins 1991). Zantop et al. (2007) observed that the posterolateral bundle was found to be completely intact in 12% of all ACL injuries, suggesting that the anteromedial bundle is fundamentally at a higher risk of injury, potentially due to modifying factors in other planes of motion that could increase the strain in the anteromedial bundle and decrease strain in the posterolateral.

Ultimately, while both ligament bundles experience maximum values at a similar time during the side-step movement, there is evidence enough to suggest that researchers should continue to be regarded them as independent structures in future investigations.

10.1.3: Identification of Linear Relationships

The results from the correlation tests (Table 9.4) are primarily descriptive as no correction for multiple testing is implemented. Each kinematic variable is analysed independently to best inform selection for the linear regression algorithms (Chapter 8.10.2). Furthermore, since there has been no prior investigations into these relationships (Chapter 5), it was not possible to make "*a priori"* hypotheses for variable selection. The correlation analysis is merely used to identify the kinematic variables at mid-swing that demonstrate a linear relationship to the maximum stance phase ACL bundle strains as well as to independently test for potential age, BMI, and experience-related confounds. This also ensures that there are no spurious predictors added to the regression algorithm, reducing the number of potential candidate predictors to those that demonstrate a significant linear relationship. This is the same method as used by Roberts et al. (2004) and Frank et al. (2013), both studies using correlation analyses to inform variable selection for linear regression models.

10.1.3.1: Initial Contact Kinematic Variables

Two initial contact kinematic variables: knee varus position and knee extension velocity were found to be significantly correlated with ligament strains in both bundles and thus potential predictors of ACL loading (Table 9.4). Both McLean et al. (2005) and Kristianslund et al. (2013) showed that greater knee valgus angles at initial contact were predictive of large knee valgus moments during the stance-phase. Since both varus and valgus alignments at initial contact have been shown to place the ligament at risk (Chapter 2.6.2), it is conceivable that an increased varus position at initial contact could result in larger varus moment, particularly if the ground reaction force is located medially to the knee joint centre (Chapter 2.2).

An increased knee extension velocity at the point of contact would result in a more extended knee with a greater inertia, creating larger ground reaction forces (Chapter 2.2) and potentially requiring the ligaments to absorb the additional forces (Chapter 2.7.1). Yu et al. (2006) obtained a similar result, although the authors published the relationship between knee extension velocity at initial contact and the resulting ground reaction force vector without explicitly modelling the ligament bundles.

10.1.3.2: Mid-Swing Kinematic Variables

Four mid-swing kinematic variables were found to be significantly correlated with ligament bundle strains. Hip internal rotation position, knee varus position, and lumbar bending position (away from the cutting direction) were all observed to be positively correlated with maximum strains in both bundles (Table 9.4). Knee valgus velocity at mid-swing was only found to be positively correlated with strains in the

posterolateral bundle. All of these relationships can be classified as “strongly correlated” according to the criteria defined by Cohen (1988).

A more internally rotated hip would create a greater internal rotation of the entire lower limb, relative to the forward direction of movement. This is possibly as a result of the body preparing to execute the side-step by dynamically aligning the planting leg to push off the ground towards the new direction (Rose & Gamble 2006). It is also likely that greater hip rotation at mid-swing is followed by a greater hip rotation at initial contact, which has previously been suggested as a predictor of non-contact ACL injuries (Chapter 2.6.2).

In the case of lumbar bending away from the cutting direction (i.e. towards the planting foot), the trunk is directed away from the midline of the body. Since the trunk contains a large percentage of the total body mass, this will change the direction of the ground reaction force after initial contact, affecting the loads experienced at the knee (Chapter 2.6.1). Depending on the alignment of the lower body, this ground reaction force is very likely to increase the valgus moment at the knee. This indicates the dangers of deviating from the “balanced” strategy recommended as the position of least risk (Chapter 2.6.2) and may be a factor of the observed varus-valgus-varus rotation sequence discussed in Chapter 10.1.1.3.

The direct relationship of knee varus angle and knee valgus velocity at mid-swing with the resulting stance-phase bundle strain is a possible indicator of greater internal joint instability (Chapter 2.4.1) since the knee angles in the frontal plane are greater and change at a faster rate. This could be especially noticeable at the mid-swing aspect, where the knee is relatively unconstrained and the inertia of the swinging leg is the only force acting on the joint. This could also occur as a result of impaired proprioception, which is linked with functional instabilities within the knee (Chapter 2.4.1). In this case, the stability of the joint is compromised by its maneuverability (Chapter 1.1) and the participant may require the ligaments to absorb the additional forces within the joint (Chapter 2.7.1). This instability could also be a factor in the varus-valgus-varus stance-phase rotation sequence observed in the study population (Chapter 10.1.1.3).

An interesting observation is that - with the exception of mid-swing knee valgus velocity - the same kinematic variables are correlated with maximum weight-acceptance phase strains in both ligament bundles. This indicates that the strains in each bundle are closely related, which is understandable considering their co-location within the knee joint (Chapter 1.1). However, this is merely an observation since these correlations were calculated independently (Chapter 8.10.2).

None of BMI, age or experience were found to be significantly correlated with the maximum ligament strains exhibited by the participants (Table 9.5).

10.1.4: Evaluation of Predictive Ability

10.1.4.1: Model Parameters

For the anteromedial bundle regression model, the best performing subset of predictors included only a single variable, hip rotation position at mid-swing (Table 9.6). The R^2 value for the study population was calculated as 0.791 with a 95% confidence interval of the true value lying between 0.599 and 0.982. This means that, conservatively, the position of hip rotation at mid-swing explains at least 59.9% of the variance in the maximum anteromedial bundle strain occurring during the stance phase. The resulting regression equation (Equation 9.1) shows that every degree increase in hip rotation at mid-swing resulted in a 0.559% increase in anteromedial bundle strain, with a total standard error of 2.118%. Thus, the position of hip rotation at mid-swing can be used, with reasonable accuracy, to predict the maximum anteromedial bundle strain occurring more than 30% of the total gait cycle duration in the future (Chapter 2.1). The p-value for significance of this regression model, adjusted for hypothesis testing with multiple candidate subsets (Chapter 7.5.4.3), is well below 0.05.

Two mid-swing variables were included in the best performing posterolateral bundle model, knee varus position and knee valgus velocity (Table 9.6). The R^2 value for this model is 0.833 with a 95% confidence interval of 0.692 to 0.973. Thus, conservatively, these two variables in combination explain at least 69.2% of the variance in the maximum weight acceptance phase strain occurring in the posterolateral bundle. The regression equation for this model (Equation 9.2) equates every degree increase in knee varus position and every degree-per-second increase in knee valgus velocity at mid-swing to a 0.553% and 0.061% increase in posterolateral bundle strain respectively. The total standard error, 3.576%, is greater than that of the anteromedial bundle model. The adjusted p-values of the model as well as both predictor variables are all well below the 0.05 threshold for significance.

Although the posterolateral bundle regression model has a greater coefficient of determination than the anteromedial bundle model, it also has a greater standard error. This likely reflects the greater variance observed in the posterolateral bundle strains of the study population (Chapter 10.1.2).

These results indicate that hip rotation, knee varus position and, to a lesser extent, knee valgus velocity at mid-swing are all important factors related to the development of strain in the bundles of the ACL. However, errors potentially arising from the use of generic reference strain values suggest that the

regression equations may not necessarily be genuine estimates of the actual mathematical relationship. This is especially true in the case of the posterolateral bundle, where the strains were observed to be linearly offset below the zero-strain point (Chapter 10.1.2). However, this does not affect the R^2 value which represents the strength of the predictive ability of the models. Thus, the fundamental result of the regression models is still valid – that mid-swing kinematics can provide significant predictive information as to the future ligament strains in both bundles. This provides further evidence for the proposed concept of a kinematic "sequence of no return" that leads up to non-contact ACL injuries (Chapter 5.1).

10.1.4.2: Compliance with Linear Regression Assumptions

Neither model violates any of the assumption conditions required for linear regression modelling (Chapter 7.5.2). The standardized residuals, plotted in Figure 9.26 and Figure 9.27, appear to be arbitrarily distributed with no visible "funnel" pattern characteristic of homoscedasticity (Chapter 7.5.2.3). Thus we can infer that the relationship predicted by the model is of a linear nature (Chapter 7.5.2.1), which is understandable since only linearly-related variables were used as candidates (Chapter 10.1.3). The mean values of the residuals are close to 0 with standard deviations closely approximating 1 (Table 9.6), indicating mean independence within the residuals (Chapter 7.5.2.2). The Durbin-Watson statistics for each model (Table 9.6), are well above the critical values outlined in Table 7.3.

The correlations between the candidate variables (Table D.1) indicate that many of these predictors are strongly correlated with each other. This is understandable because a correlation with the ligament bundle strains was used as the criteria for selection as a candidate variable. However, there were no multicollinearities observed in the final regression models for each ligament. The anteromedial bundle model could not contain any multicollinearities since only one variable was used. The variance inflation factors (Table 9.6) for the two variables in the posterolateral bundle model are close to 1, suggesting that they are near orthogonal with no correlation. This is supported in Table D.1, with no significant correlation between knee varus position and knee valgus velocity at mid-swing.

The compliance of both regression models with the assumption conditions verifies the confidence in the results.

10.1.4.3: Application to broader population

The linear regression models are based on the observed relationships between the predictor and response variables from the samples in the study population. However, this study utilised a relatively small sample size of ten participants. This could potentially result in the model overfitting the sample data,

overestimating the obtained model coefficients. To then make inferences about other populations based on this estimate would be incorrect. In this case, the calculated R^2 values would only reflect the variance within the study sample, not the larger population of which that sample was obtained, that is explained by these predictor variables.

However, the calculation of confidence intervals (Table 9.6) for the true R^2 values accounts for the reduced sample size. This provides a much better estimate of where the true variance is likely to be and is thus better suited for estimating the overall predictive strength of the model (Colton & Bower 2002). Using the lower limit of the calculated confidence intervals as conservative estimates indicate that there are still strong predictive relationships between swing-phase kinematic variables and the resulting stance-phase strain in both ligament bundles and that this relationship extends beyond the samples used in this study. The lack of violation of regression assumptions (Chapter 10.1.4.2) and the use of the corrected Akaike's Information Criterion (Chapter 7.5.4.2) in model subset selection further support the fact that the small sample size did not result in overfitting. Additional research with larger, more diverse populations would confirm this.

Although, these confidence intervals are calculated under the assumption that the models were trained on samples that were randomly selected from - and thus statistically representative of - this broader population. In this study, the participants were not randomly selected from the Sigward (2012) dataset (Chapter 8.1). Furthermore, this is a population of female, right-footed soccer players, who might demonstrate completely different kinematic characteristics than other populations. Thus, these inferences based on the observed confidence intervals for R^2 can only realistically be made about broader samples of young, female, right-footed soccer players with no prior history of ACL injury. Further work is again required to justify the extension of these inferences to other populations.

10.1.4.4: Prediction vs Causation

The regression equations do not imply that the predictor variables "*cause"* strain in the ACL bundles. They do, however, suggest that the variance observed in these bundle strains is intrinsically, linearly related to the variance observed in the predictors (Chapter 7.5.1). To establish causality requires knowledge of three factors: association, direction of influence and isolation (Miles & Shevlin 2001). While the first two criteria can confidently be accepted, it is not possible - in this case - to satisfy the criterion of isolation. The kinematic variables input to the regression models (as well as multiple others that were not added) are fundamentally connected through the kinetic chain of the human body. It would be inaccurate to suggest that individual kinematic components at the mid-swing stage *causes* ACL strain during the weight-

acceptance phase. The actual relationship need not be known, it could be a result of multiple, interlinked factors - not necessarily a single, isolatable variable. What can be stated, with confidence, is that it is possible to make significant predictions about the future maximum weight-acceptance phase strain in the ligament bundles based on the observed values of body kinematics at mid-swing.

10.1.4.5: Model Design

The benefit, in this case, of using the best subsets approach over any of the step-by-step linear regression methods (Chapter 7.5.4.1) is that all of the possible candidate subsets are explored and compared, allowing for the most effective model to be found. This is valuable because the intention of this study is to investigate the possible existence of predictive relationships. The use of AICc (Chapter 7.5.4.2) as the best-fit criterion ensures that the model is not overfitting the data, relative to the other candidate subjects. This is especially important since the ratio of candidate predictors to samples is relatively small. Furthermore, the *post-hoc* correction method (Chapter 7.5.4.3) ensures that the performance of the final model is statistically significant. It also highlights the value of using the correlations to "prune" the list of possible candidates to only those that are linearly related with bundle strain. For example, if all 22 kinematic variables (Figure 8.7) were used in a best-subsets linear regression model for the anteromedial bundle then the adjusted significance for alpha would be 0.0023, assuming that the outcome would be the same. Similarly, the required threshold for significance of the posterolateral bundle model would be 0.0047. The anteromedial bundle model remains significant at this reduced threshold but the two coefficients of the posterolateral bundle model would not. Therefore, the null hypothesis for the posterolateral bundle model could not be rejected without the pre-processing step to trim the set of candidates. Values for the adjusted threshold for significance, depending on the total number of candidate predictors (C) and the number of predictors included in the best-performing subset (K) are indicated in Table 10.1.

Table 10.1: The adjusted significance level for α = 0.05

K	C						
	1	**2**	**3**	**4**	**5**	**10**	**22**
1	0.0500	0.0253	0.0170	0.0127	0.0102	0.0051	0.0023
2		0.0500	0.0336	0.0253	0.0203	0.0102	0.0047
3			0.0500	0.0377	0.0303	0.0153	0.0070
4				0.0500	0.0402	0.0203	0.0093

Table 10.1: Values of the adjusted significance level for alpha = 0.05, depending on the total number of candidate predictors (C) and the number of predictors included in the best-performing subset (K).

10.1.4.6: Existence of other predictive models

The comparisons of the five best performing variable subsets to create regression models for each ligament bundle are outlined in Table D.2 and Table D.3. These suggest that there is not necessarily a unique solution for the regression equation (Chapter 6) but that there are multiple possible combinations of candidate predictors that could potentially be used to predict future ligament strain with varying levels of accuracy. As such, all of these candidate variables and not just those included in the best performing subsets should be considered in future studies. The effects of the individual variables and the effects of combinations of these variables should be better quantified.

10.2: Limitations

A number of assumptions and simplifications had to be implemented to develop the musculoskeletal modelling, simulation and processing methods used in this study. The resulting limitations are discussed in the following chapters.

10.2.1: Measurement

Errors that occur during the data capturing of the motion capture trials (Chapter 7.2), can have a cascade effect through every stage of processing (Shrout & Fleiss 1979). However, the verification and validation methods implemented throughout the simulation process (Appendix C) indicate that these are negligible and unlikely to have significantly affected the results.

10.2.2: Modelling

The accuracy of a musculoskeletal model is dependent on how closely it approximates real life anatomical geometry and movement. This requires consideration of two factors. Firstly, what level of complexity is required to provide results that are sufficiently accurate? Secondly, what is the sensitivity of the model to subject-specific variables? Accounting for both of these factors ensures that the model is consistent enough to provide accurate comparisons between samples but still accommodates variations in parameters that are specific to the individual (Cleather & Bull 2012).

A major limitation to the musculoskeletal modelling approach used in this study is that the strain in the ACL is not measured directly (Chapter 7.3.4). While the musculoskeletal model is sensitive to individual variations in size and movement, it was not designed to account for possible physical interactions between the ligament bundles and the surrounding bone and soft-tissue elements. Neither does it represent individual subject variations in ligament origins and insertions, bone anthropometries or soft tissue

mechanics. Furthermore, reference strains used to calculate the zero-load lengths of the ligament bundles were generic and not calculated for each participant.

The ligaments are also simplified to be represented by one-dimensional line elements running directly from origin to insertion points when, in reality, they are more complex structures made up of multiple fibres of varying thickness and tensile properties. These fibres are not always parallel and tend to "fan" out as they insert on the tibia (Chapter 1.1). Similarly, the head, arms and trunk were represented in the model as a single, rigid body where - in reality - these are complex, dynamic structures which will certainly affect the biomechanics of movement.

The generic, unscaled model implements a complex knee joint which translates as a function of knee flexion angle to account for the physical interaction between joint tissues (Appendix B.5). The addition of two degrees of rotational freedom at the knee (Chapter 8.4) is limited by not also modelling the translations as a result of bone interactions in the frontal and transverse planes. Locking the MTP joint (Chapter 8.6.1) also restricts the complexity of the model at the foot, although movement at this joint during locomotion would likely be restricted by the athlete's footwear and it is doubtful to have significantly affected the simulations. The model was also limited by not accounting for changes in anterior tibial translation after impact with the ground, which is known to load the ACL (Chapter 2.2). Tibial translation was set as a function of the knee flexion angle to account for the shape of the articulating surfaces of the knee, a feature of the generic model (Appendix B.5).

The method of model scaling (Chapter 7.3.1) maintains bilateral symmetry in the subject-specific models. This procedure operates on the assumption that the participants have equal anthropometries in their left and right sides, which is not necessarily always accurate. However, since this study investigated kinematics of healthy athletes, it was assumed that this would be a minor limitation. This effect is further reduced due to the fact that only the right limb was used in the kinematic investigation and the marker weights for this limb in inverse kinematics were set considerably higher than those assigned to the left limb. Future studies that include analyses of both limbs would need to take this into consideration.

The effects of muscle activations were not considered in this study since the hypothesis was purely driven towards the identification of kinematic relationships (Chapter 6.5.4). Finally, while OpenSim is a useful tool for musculoskeletal modelling and simulation, the iterative model fitting process (Chapter 7.3.1) is highly time-consuming and is not currently beneficial to studies involving larger sample sizes.

10.2.3: Processing

Generalized reference strains were used to calculate the zero-load lengths for the ACL bundles (Chapter 7.3.4), without accounting for potential variations between individual subjects. This data is typically difficult to measure and is not very well reported in the literature (Blankevoort & Kuiper 1991).

Averaging the repeated trials to form representative datasets for each subject (Chapter 8.9) was another possible source of error. However, the use of this method is justified through the strong rest-retest reliability observed within-subjects (Appendix C.5) and the fact that multiple other studies have used the same trial-averaging approach for studying kinematics related to anterior cruciate ligament injuries (McLean et al. 1999; Ford et al. 2005; Sigward & Powers 2006; Kernozek & Ragan 2008).

10.2.4: Statistical Limitations

This study did not control for the effects of potentially confounding subject-specific variables such as joint laxity, static alignment, anatomical anthropometries (Chapter 2.4.1) or neuromuscular (Chapter 2.7) characteristics. The variables that were controlled for were footedness, experience, type of sport, gender, prior injury, age and BMI. These have all been identified as potential risk factors for non-contact ACL injuries (Chapter 2.4.1, Chapter 2.4.2). However the singular demographic of the study population could potentially limit the extension of the knowledge learned during this study to other groups. For example, it is possible that the predictive model developed in this study is gender-specific, since the study population consisted entirely of female subjects. Similarly, the model may only apply to a side-step cutting movement. The extension of the results to other movements such as a jump landing is yet unknown. Finally, the study population was not randomly selected (Chapter 8.1) and constituted a reasonably small sample size.

The sample population also represented a very experienced group of athletes, with an average of 11.8 ± 3.12 years of soccer experience. Although there was no correlation between experience and strain in either ligament bundle (Chapter 10.1.3), it remains to be seen what the effect would be with a vastly less experienced cohort.

The purpose of this project is not to predict or simulate actual ACL injury events. It is an investigation into the potential for swing phase kinematics to predict maximum ACL strain occurring during the early stance phase. Inferences about the events leading up to the onset of such injuries can then be made with the knowledge of these relationships. However, it is possible that the predictive relationships observed for side-stepping movements in healthy participants will not translate to those occurring during injury events,

although results from other studies do suggest that this is likely (McLean et al. 2005; Hewett et al. 2005; Myer et al. 2010).

10.3: Future Work

10.3.1: Study Population

Future investigations should attempt to replicate this study on a larger, randomly selected population. Provided the same effects were observed, this would improve the statistical power of the observations and allow for broader conclusions to be drawn. These studies should use modelling packages that include automated model fitting and marker placement methods. Following this, studies should attempt to replicate this study with different populations altogether. This should include investigations of participant groups of different ages, genders, activity/experience levels as well as other types of movements under varying testing conditions. Gender, in particular, should be explored in more detail to observe if these predictive relationships are also present in men who are at a fundamentally lower risk of sustaining non-contact ACL injuries (Chapter 2.4.1).

Electromyographic data of muscle activations should be used to supplement the kinematic input to the predictive models, since neuromuscular variables are known to be risk factors for non-contact ACL injuries (Chapter 2.7). Studies should seek to determine if similar predictive relationships exist between all of these biomechanical components and strain-rate, which is also thought to be an aspect of the injury event (Chapter 2.2).

Future iterations of this research should be attempted with kinematics obtained from actual injury situations. These can be reconstructed from video feeds, with more efficient extraction methods (Chapter 2.5), or even recorded directly from the body using sophisticated, non-invasive sensors (Yau et al. 2014). Alternatively, if kinematics cannot realistically or accurately be obtained from real injury situations, surrogate modelling techniques can be designed to artificially simulate injury events (McLean et al. 2003; Lin et al. 2009). These are beneficial for research purposes as unique simulations in the order of tens of thousands of iterations can be recreated from a small sample of motion capture trials.

10.3.2: Musculoskeletal Model

A major challenge that should be addressed is the development of models that are more sensitive to parameters unique to the individual such as the location of ligament origins and insertions as well as the zero-load ligament lengths (Chapter 7.3.4). These geometries could be obtained and precisely

reconstructed for each participant through medical imaging or other methods (Zhang et al. 2008; Bloemker et al. 2012).

Furthermore, subject specific variances in anatomical anthropometries such as the Q-angle, tibial slope and femoral notch width as well as the range-of-motion in the knee resulting from joint laxity should be accounted for in the model and used to supplement the prediction algorithm. This could also include the natural, resting joint angles of each subject such as subtalar pronation and knee recurvatum (Chapter 2.4.1). Other anthropometries, such as the lengths of each body segment, could be used for more accurate model scaling methods.

Further investigation is required to better characterize the differences between the different bundles of the ACL with regards to how they respond to knee loading. Finite element models of ligament bundles can be designed to gain a better understanding of non-uniform distributions of stresses through the tissue, particularly with regards to the changing positions and orientations of the fascicles which make up the ligament bundles. This is likely to be an important tool in understanding the causations of non-contact ACL injuries, although in the current literature it appears to be limited to studies of ligament response to static movements (Hirokawa et al. 1998; Zhang et al. 2008; Wang et al. 2009; Orsi et al. 2011).

The frontal and transverse plane rotations that were added to the knee in the generic OpenSim model (Appendix B.5) should be modified to include additional constraints based upon the interactions between bone and soft-tissue structures. This would create an anatomically accurate knee model with respect to the simulation of fluid movement in all planes of motion. In addition, more degrees of freedom should be added to the upper body to investigate how dynamic movement at the arms or head affect ligament loading. Biomechanical data from these additional joints should be included in future prediction algorithms, in addition to data from the opposite (non-landing) leg.

There is also a need for a more standardized approach with respect to musculoskeletal modelling practices, such that results from different studies can be directly and objectively compared.

10.3.3: Statistical Analysis

Expanding the study population (Chapter 10.3.1) would allow researchers to use a validation set of samples, which will provide more information as to the true value of a model. This data set could be withheld from the primary training data set and not used during candidate variable selection and the building of the regression models. The resulting regression equation can then be applied to this unused validation set to assess the true, unconditional predictive strength of the model. This is also useful for

determining if the regression model has overfit the training data (Picard & Cook 1984; Burnham & Anderson 2002; Yang 2007; Fomby 2008).

A similar, but alternate approach to the linear regression method implemented in this study would be to divide the study population into groups based on a pre-defined characteristic such as the level of strain exhibited during the motion capture trials or which players later went on to sustain non-contact ACL injuries after testing. A logistic regression algorithm could be trained, using swing phase kinematic or neuromuscular components, to predict which groups the players were allocated to. This would be useful as a screening tool as well as provide more information about potential kinematic risk factors by analysing which components are effective as predictors of non-contact ACL injury in the long term (Chapter 3.2).

Finally, more complex pattern recognition and statistical analysis techniques such as neural networks or support vector machines should be developed to improve upon the results obtained by this study. These methods should analyse biomechanical variables over a continuous range rather than instantaneous values at a specific point in the gait cycle. This will provide the information required to expand upon the "sequence of no return" concept (Chapter 5.1). It will also drastically increase the amount of predictive information available to the researcher and likely aid in the development of more sophisticated prediction algorithms and better understanding of injury aetiologies.

10.4: Applications

These findings have multiple, real-world applications towards the continued development of more effective injury prevention measures. The most immediate application would be the improvement of the accuracy and complexity of screening algorithms used to identify patients at a higher risk for injury (Chapter 3.2). Current screening algorithms only use instantaneous kinematic variables samples from the initial contact point. The use of continuous-valued swing-phase components in these algorithms would increase the amount of predictive information available, improving on the accuracy to identify potential at-risk athletes. This would allow researchers to collect more valuable data per trial, further improving the efficiency of these methods.

These results can also be translated into additional information for injury prevention training programs. A focus on swing-phase kinematics may also allow for more time during the movement to be applied to employing a safer landing strategy. Athletes can be coached in which strategies and techniques to employ in the approach to a cutting movement, leading up to foot contact with the ground. For example, based on the results from this study, athletes can be trained to reduce their internal hip rotation during cutting

movements. In addition, they should also be advised to strengthen the musculature at the knee to improve joint stability and reduce the movements in the frontal plane. Although, it would need to be determined how this change in technique might affect the ability of the athlete to complete the side step movement itself or what other repercussions might take place. Completing a side-step requires coordinated movement in multiple joints in multiple planes of motion. It is possible that it would be difficult to execute a side-step by limiting range-of-motion in certain joints, such as the hip. Conversely, if the side-step can still be performed with this restriction or new technique then it might result in additional, unwanted loading on other joints. However, existing technique training programs have not listed this as a limitation.

A completely novel application of these results is the implementation of more sophisticated statistical algorithms (neural networks, support vector machines etc.) - to predict non-contact ACL injury events based on a continuous stream of biomechanical information. These could be used in a real-time non-contact injury prediction algorithm which analyses the patterns of body biomechanics to predict when future ligament loading will exceed the known mechanical thresholds of the tissue. This would necessitate the development of an active knee brace to apply a mechanical resistance, similar in concept to a car airbag, to actively prevent or reduce the magnitude of the injury. This resistance would be applied at the time of initial contact, as the ground reaction force begins to propagate through the limb. This would be an implementation of a preventative measure more proximal to the injury event along the causation chain (Figure 2.4) and would potentially be more effective than the current preventative measures. Current braces (Chapter 3.1) do not contain any active components and, as such, are not able to measure variables known to affect ACL strains nor can they attempt to predict and correct for excessive ACL strain. Injury prevention training programs (Chapter 3.3) are designed to reduce the risk of injury, they cannot predict or prevent the actual injury event from taking place.

Chapter 11: Conclusions

11.1: Problem Statement

The prevalence and effects of non-contact anterior cruciate ligament injuries, particularly within female athlete populations is worrying and current prevention strategies have not yet provided sufficient evidence of their effects (Chapter 4). There does not appear to be an existing standardised program, best practice model or set of clinical application guidelines for the implementation of injury prevention programs (Griffin et al. 2006; Hootman et al. 2007; Renstrom et al. 2008).

Screening algorithms (Chapter 3.2) in combination with injury prevention training programs (Chapter 3.3) potentially offer the best current solution but there is a clear need to improve the accuracy and efficiency of these programs. This requires more sophisticated means of identifying and understanding the sequence of events that initiate non-contact ACL injuries, especially since these athletes frequently perform "at-risk" movements during athletic activity (Chapter 2.4.2).

Unfortunately, barring the unlikely event of an ACL injury occurring in a laboratory, investigators can currently only make assumptions for the non-contact injury mechanism by studying how body biomechanics affect ACL loading. However, these assumptions are only as strong as the model is an accurate representation of reality. With accurate modelling techniques, informed estimates can be made over what could ultimately damage the ligament. The results derived from these simulations have the potential to be applied in real-world applications, highlighting the value of computational models to formulate and test fundamental hypotheses (Delp et al. 2007). While the values output by simulations are only estimates of real life movements, the use of identical generic models and processing methods allows for strong relative comparisons to be performed (Escamilla et al. 2012).

11.2: Confirmation of Hypothesis

The results confirm the hypothesis in that kinematic components occurring during the swing-phase of a dynamic deceleration movement can be used to predict the future maximum strain in both bundles of the anterior cruciate ligament. This indicates that biomechanical variables occurring prior to initial contact in a dynamic deceleration movement are an important feature of non-contact injury mechanisms. Furthermore, these swing-phase variables should be considered as components of a "sequence of no return" that potentially leads up to non-contact injuries. In obtaining these results, multiple novel outcomes were achieved to address the gaps in the literature highlighted in Chapter 5. These novel outcomes are:

1. The description of swing-phase kinematics leading up to the onset of side-step movements (Chapter 10.1.1)
2. The description of strains occurring in both bundles of the ACL during a side-step movement for a sample population of athletes (Chapter 10.1.2)
3. Correlation coefficients indicating that kinematic components at mid-swing are linearly related to stance-phase ligament strains in both bundles (Chapter 10.1.3.2)
4. Linear regression equations demonstrating that these kinematic components can predict future stance-phase ligament strains in both bundles with statistical significance (Chapter 10.1.4).
5. The proof of concept of a kinematic "sequence of no return"

Other outcomes from the study were consistent with results already published in the literature, such as the body kinematics observed from the initial contact point through the weight acceptance phase (Chapter 10.1.1) and the linear relationships observed between kinematic variables at initial contact and ligament strain (Chapter 10.1.3.1). Together with the procedures used to verify and validate the modelling and simulation pipeline (Appendix C), these comparisons provide additional confidence in the reliability of the simulated kinematic and ligament data.

There was no categorical proof to support or oppose the research question regarding the implementation of a dual-bundle model of the ACL. While the maximum strains in the ligament bundles were highly correlated and the peaks occurred at similar times during the side-step movement, the differences in variance and baseline values is evidence to suggest that these bundles should continue be regarded as independent structures in future investigations until more conclusive evidence can be obtained (Chapter 10.1.2).

11.3: The Injury Mechanism

In this study, the results indicate that increases in hip internal rotation position, knee varus position and knee valgus velocity at mid-swing are significantly related to the development of increased strain in the bundles of the ACL during a side-step movement. These components thus make up the first feature of the "sequence of no return". Hip internal rotation results from the dynamic re-alignment of the lower limb prior to initial contact and knee varus position and valgus velocity are factors likely related to poor proprioception and/or increased joint laxity at the knee.

For the actual ACL loading methods, strain in the ACL was likely formed from a combination of varus and internal rotation of a relatively extended knee.

11.4: Applications

Ultimately, the goal of this project is to provide more information as to how biomechanics leading up to the point of contact during dynamic human movement relate to the subsequent anterior cruciate ligament loading. The outcome is to move towards reducing the risk and incidence of ACL injuries and the associated negative long-term effects, preserving long-term knee-vitality and ensuring quality of life for athletes and active individuals. While it is not yet possible to predict injury events in real time, the novel results from this study, including the proof of concept for a "sequence of no return", prove that this is possible and justifies continued exploration of this area. These findings should be used to guide the development of *a priori* hypotheses for future studies to be completed at higher levels of evidence.

Chapter 12: References

Adachi, N. et al., 2002. Mechanoreceptors in the anterior cruciate ligament contribute to the joint position sense. *Acta orthopaedica Scandinavica*, 73(3), pp.330–4. Available at: http://www.ncbi.nlm.nih.gov/pubmed/12143983.

Akaike, H., 1974. A New Look at the Statistical Model Identification. *IEEE Transactions on Automatic Control*. Available at: http://adsabs.harvard.edu/abs/1974ITAC...19..716A [Accessed August 26, 2014].

Alentorn-Geli, E. et al., 2009. Prevention of non-contact anterior cruciate ligament injuries in soccer players. Part 1: Mechanisms of injury and underlying risk factors. *Knee surgery, sports traumatology, arthroscopy : official journal of the ESSKA*, 17(7), pp.705–29. Available at: http://www.ncbi.nlm.nih.gov/pubmed/19452139 [Accessed November 6, 2013].

Allison, P.D., 1999. *Multiple Regression: A Primer*, Thousand Oaks, CA: Pine Forge Press, Inc.

Amis, A.A. & Dawkins, G.P.C., 1991. Functional anatomy of the Anterior Crucuate Ligament. *The Journal of bone and joint surgery. British volume*, 73-B(2), pp.260–267.

Anderson, A.F. et al., 2001. Correlation of Anthropometric Measurements, Strength, Anterior Cruciate Ligament Size, and Intercondylar Notch Characteristics to Sex Differences in Anterior Cruciate Ligament Tear Rates. *Am. J. Sports Med.*, 29(1), pp.58–66. Available at: http://ajs.sagepub.com/content/29/1/58 [Accessed August 30, 2014].

Anderson, F. et al., 2012. OpenSim User' s Guide. , pp.1–257. Available at: https://opensim.stanford.edu.

Anderson, F.C. & Pandy, M.G., 1999. A Dynamic Optimization Solution for Vertical Jumping in Three Dimensions. *Computer methods in biomechanics and biomedical engineering*, 2(3), pp.201–231. Available at: http://www.ncbi.nlm.nih.gov/pubmed/11264828 [Accessed March 14, 2013].

Anderson, F.C. & Pandy, M.G., 2001. Dynamic Optimization of Human Walking. *Journal of Biomechanical Engineering*, 123(5), p.381. Available at: http://biomechanical.asmedigitalcollection.asme.org/article.aspx?articleid=1406196 [Accessed July 11, 2014].

Arendt, E. a, Agel, J. & Dick, R., 1999. Anterior cruciate ligament injury patterns among collegiate men and women. *Journal of athletic training*, 34(2), pp.86–92. Available at: http://www.pubmedcentral.nih.gov/articlerender.fcgi?artid=1322895&tool=pmcentrez&rendertype=abstract.

Arnoczky, S.P., 1983. Anatomy of the anterior cruciate ligament. *Clinical orthopaedics and related research*, 172, pp.19–25.

Au, C. et al., 2013. Gait 2392 and 2354 Models. Available at: http://simtk-confluence.stanford.edu:8080/pages/viewpreviousversions.action?pageId=3376103.

Bahr, R. & Krosshaug, T., 2005. Understanding injury mechanisms: a key component of preventing injuries in sport. *British journal of sports medicine*, 39(6), pp.324–9. Available at: http://www.pubmedcentral.nih.gov/articlerender.fcgi?artid=1725226&tool=pmcentrez&rendertype=abstract [Accessed January 29, 2013].

Barenius, B. et al., 2014. Increased Risk of Osteoarthritis After Anterior Cruciate Ligament Reconstruction: A 14-Year Follow-up Study of a Randomized Controlled Trial. *The American journal of sports medicine*, 42(5), pp.1049–57. Available at: http://ajs.sagepub.com/content/42/5/1049.short [Accessed May 26, 2014].

Beard, D.J. et al., 1993. Proprioception after rupture of the Anterior Cruciate Ligament. *Journal of Bone and Joint Surgery (Br)*, 75-B(2), pp.311–315.

Besier, T.F. et al., 2001. Anticipatory effects on knee joint loading during running and cutting maneuvers. *Medicine & Science in Sports & Exercise*, 1(3), pp.1176–1181.

Besier, T.F. et al., 2001. Anticipatory effects on knee joint loading during running and cutting maneuvers. *Medicine and science in sports and exercise*, 33(7), pp.1176–81.

Besier, T.F., Lloyd, D.G. & Ackland, T.R., 2003. Muscle activation strategies at the knee during running and cutting maneuvers. *Medicine and science in sports and exercise*, 35(1), pp.119–27. Available at: http://europepmc.org/abstract/MED/12544645 [Accessed July 11, 2014].

Bhavna & Nath, S., 2009. Use of Lower Limb Measurements in Reconstructing Stature among Shia Muslims. *Internet Journal of Biological Anthropology*, 2.2.

Birmingham, T.B. et al., 2008. A randomized controlled trial comparing the effectiveness of functional knee brace and neoprene sleeve use after anterior cruciate ligament reconstruction. *The American journal of sports medicine*, 36(4), pp.648–55. Available at: http://www.ncbi.nlm.nih.gov/pubmed/18192493 [Accessed February 21, 2013].

Blankevoort, L. & Kuiper, J., 1991. Articular contact in a three-dimensional model of the knee. *Journal of Biomechanics*, 24(2), pp.1019–1031. Available at: http://www.sciencedirect.com/science/article/pii/002192909190019J [Accessed July 12, 2014].

Bloemker, K.H. et al., 2012. Computational Knee Ligament Determined Zero-Load Lengths Modeling Using Experimentally Determined Zero-Load Lengths. *The Open Biomedical Engineering Journal*, 6, pp.33–41.

Borotikar, B.S. et al., 2008. Combined effects of fatigue and decision making on female lower limb landing postures: central and peripheral contributions to ACL injury risk. *Clinical biomechanics (Bristol, Avon)*, 23(1), pp.81–92. Available at: http://www.sciencedirect.com/science/article/pii/S0268003307001684 [Accessed June 23, 2014].

Boyer, J., 2011. ACL Injury Prevention. , pp.1–8.

Broome, J., 1993. Qalys. *Journal of public economics*, 50(2), pp.149–167. Available at: http://linkinghub.elsevier.com/retrieve/pii/004727279390047W [Accessed August 7, 2014].

Bulluck, J.M., 2010. *Influence of thigh muscle forces on Anterior Cruciate Ligament forces during single-leg landing from three different heights*. East Carolina University.

Burnham, K.P. & Anderson, D.R., 2002. *Model Selection and Multimodel Inference* Second Edi., Fort Collins, CO: Springer New York.

Butler, D.L., 1989. Anterior cruciate ligament: Its normal response and replacement. *Journal of orthopaedic research*, 7(6), pp.910–921. Available at: http://www.ncbi.nlm.nih.gov/pubmed/2677288.

Cappozzo, A., 1991. Three-dimensional analysis of human walking: Experimental methods and associated artifacts. *Human Movement Science*, 10(5), pp.589–602.

Carey, J.L. et al., 2006. Outcomes of anterior cruciate ligament injuries to running backs and wide receivers in the National Football League. *The American journal of sports medicine*, 34(12), pp.1911–7. Available at: http://www.ncbi.nlm.nih.gov/pubmed/16870822 [Accessed November 10, 2013].

Cerulli, G. et al., 2003. In vivo anterior cruciate ligament strain behaviour during a rapid deceleration movement: case report. *Knee surgery, sports traumatology, arthroscopy : official journal of the ESSKA*, 11(5), pp.307–11. Available at: http://www.ncbi.nlm.nih.gov/pubmed/14523613 [Accessed October 24, 2013].

Chandrashekar, N. et al., 2006. Sex-based differences in the tensile properties of the human anterior cruciate ligament. *Journal of biomechanics*, 39(16), pp.2943–50. Available at: http://www.ncbi.nlm.nih.gov/pubmed/16387307 [Accessed February 20, 2013].

Chatterjee, S., Hadi, A.S. & Price, B., 2000. *Regression analysis by example* Third., New York: Wiley.

Chaudhari, A.M. & Andriacchi, T.P., 2006. The mechanical consequences of dynamic frontal plane limb alignment for non-contact ACL injury. *Journal of biomechanics*, 39(2), pp.330–8. Available at: http://www.ncbi.nlm.nih.gov/pubmed/16321635 [Accessed February 19, 2013].

Chaudhari, A.M., Hearn, B.K. & Andriacchi, T.P., 2005. Sport-dependent variations in arm position during single-limb landing influence knee loading: implications for anterior cruciate ligament injury. *The American journal of sports medicine*, 33(6), pp.824–30. Available at: http://www.ncbi.nlm.nih.gov/pubmed/15827366 [Accessed March 12, 2015].

Chew, K.T.L. et al., 2007. Current evidence and clinical applications of therapeutic knee braces. *American journal of physical medicine & rehabilitation / Association of Academic Physiatrists*, 86(8), pp.678–86. Available at: http://www.ncbi.nlm.nih.gov/pubmed/17667199 [Accessed February 21, 2013].

Cleather, D.J. & Bull, a. M., 2012. The development of lower limb musculoskeletal models with clinical relevance is dependent upon the fidelity of the mathematical description of the lower limb. Part 2: patient-specific geometry. *Proceedings of the Institution of Mechanical Engineers, Part H: Journal of*

Engineering in Medicine, 226(2), pp.133–145. Available at: http://pih.sagepub.com/lookup/doi/10.1177/0954411911432105 [Accessed March 2, 2013].

Close, J. et al., 1967. The Function of the Subtalar Joint. *Clinical orthopaedics and related research*, 50, pp.159–180.

C-Motion Inc, 2014. OpenSim - Visual3D Wiki Documentation.

Cohen, J. et al., 2013. *Applied multiple regression/correlation analysis for the behavioral sciences*, Routledge. Available at: http://books.google.ca/books?hl=en&lr=&id=gkalyqTMXNEC&oi=fnd&pg=PP1&dq=Applied+Multiple+Regression/Correlation+Analysis+for+the+Behavioral+Sciences+(3rd+edition)&ots=tQCSU5rbaf&sig=uXFtRHgmcwD6sqH7gGpEG1LXIIA [Accessed October 10, 2014].

Cohen, S.B. et al., 2009. MRI measurement of the 2 bundles of the normal anterior cruciate ligament. *Orthopedics*, 32(9). Available at: http://www.ncbi.nlm.nih.gov/pubmed/19750997 [Accessed August 30, 2014].

Colby, S. et al., 2000. Electromyographic and kinematic analysis of cutting maneuvers. Implications for anterior cruciate ligament injury. *The American journal of sports medicine*, 28(2), pp.234–40. Available at: http://www.ncbi.nlm.nih.gov/pubmed/10751001.

Colton, J. & Bower, K., 2002. Some misconceptions about R 2. *International Society of Six Sigma Professionals, EXTRAOrdinary Sense*, 3(2). Available at: http://minitab.com/uploadedFiles/Content/News/Published_Articles/r2_misconceptions.pdf [Accessed August 19, 2014].

Coplan, J., 1989. Rotational motion of the knee: a comparison of normal and pronating subjects. *Journal of Orthopaedic & Sports Physical Therapy*. Available at: http://www.jospt.org/doi/abs/10.2519/jospt.1989.10.9.366 [Accessed November 17, 2014].

Delp, S.L. et al., 1990. An interactive graphics-based model of the lower extremity to study orthopaedic surgical procedures. *IEEE transactions on bio-medical engineering*, 37(8), pp.757–767.

Delp, S.L. et al., 2007. OpenSim: open-source software to create and analyze dynamic simulations of movement. *IEEE transactions on bio-medical engineering*, 54(11), pp.1940–50. Available at: http://www.ncbi.nlm.nih.gov/pubmed/18018689.

DeMorat, G., 2004. Aggressive Quadriceps Loading Can Induce Noncontact Anterior Cruciate Ligament Injury. *American Journal of Sports Medicine*, 32(2), pp.477–483. Available at: http://journal.ajsm.org/cgi/doi/10.1177/0363546503258928 [Accessed February 21, 2013].

Dempsey, A. et al., 2012. *Whole body kinematics and knee moments that occur during an overhead catch and landing task in sport*. Griffith University. Available at: http://www.sciencedirect.com/science/article/pii/S0268003311003007 [Accessed November 8, 2013].

Dempsey, A.R. et al., 2009. Changing sidestep cutting technique reduces knee valgus loading. *The American journal of sports medicine*, 37(11), pp.2194–200. Available at: http://www.ncbi.nlm.nih.gov/pubmed/19509415 [Accessed February 27, 2015].

DeVita, P., 1994. The selection of a standard convention for analyzing gait data based on the analysis of relevant biomechanical factors. *Journal of biomechanics*, 27(4), pp.501–8. Available at: http://www.ncbi.nlm.nih.gov/pubmed/8188730 [Accessed August 8, 2014].

Dong, W. et al., 2008. A low-cost motion tracker and its error analysis. *2008 IEEE International Conference on Robotics and Automation*, pp.311–316. Available at: http://ieeexplore.ieee.org/lpdocs/epic03/wrapper.htm?arnumber=4543226.

Donnelly, C.J. et al., 2012. Optimizing whole-body kinematics to minimize valgus knee loading during sidestepping: implications for ACL injury risk. *Journal of biomechanics*, 45(8), pp.1491–7. Available at: http://www.ncbi.nlm.nih.gov/pubmed/22387123 [Accessed February 9, 2013].

Dugan, S. a & Bhat, K.P., 2005. Biomechanics and analysis of running gait. *Physical medicine and rehabilitation clinics of North America*, 16(3), pp.603–21. Available at: http://www.ncbi.nlm.nih.gov/pubmed/16005396 [Accessed August 8, 2014].

Duthon, V.B. et al., 2006. Anatomy of the anterior cruciate ligament. *Knee surgery, sports traumatology, arthroscopy : official journal of the ESSKA*, 14(3), pp.204–13. Available at: http://www.ncbi.nlm.nih.gov/pubmed/16235056 [Accessed February 19, 2013].

Escamilla, R.F. et al., 2012. Anterior cruciate ligament strain and tensile forces for weight-bearing and non-weight-bearing exercises: a guide to exercise selection. *The Journal of orthopaedic and sports physical therapy*, 42(3), pp.208–20. Available at: http://www.ncbi.nlm.nih.gov/pubmed/22387600 [Accessed January 31, 2013].

Fenton, N. & Neil, M., 2012. *Risk assessment and decision analysis with Bayesian networks*, Available at: http://books.google.com/books?hl=en&lr=&id=p9CmmpIVzJEC&oi=fnd&pg=PP1&ots=JzjRjABMCS&sig=hgEwWAvu3JatO-2750udXlTajfU [Accessed August 26, 2014].

Firestein, G.S. et al., 2008. *Kelley's Textbook of Rheumatology* 8th Editio., Saunders.

Fomby, T., 2008. *MULTIPLE LINEAR REGRESSION AND SUBSET SELECTION*, Dallas, TX.

Ford, K.R. et al., 2005. Gender Differences in the Kinematics of Unanticipated Cutting in Young Athletes. *Medicine & Science in Sports & Exercise*, 37(1), pp.124–129. Available at: http://content.wkhealth.com/linkback/openurl?sid=WKPTLP:landingpage&an=00005768-200501000-00020 [Accessed February 18, 2013].

Frank, B. et al., 2013. Trunk and hip biomechanics influence anterior cruciate loading mechanisms in physically active participants. *The American journal of sports medicine*, 41(11), pp.2676–83. Available at: http://www.ncbi.nlm.nih.gov/pubmed/23884306 [Accessed November 10, 2013].

Fregly, B.J. et al., 2012. Grand challenge competition to predict in vivo knee loads. *Journal of orthopaedic research : official publication of the Orthopaedic Research Society*, 30(4), pp.503–13. Available at: http://www.ncbi.nlm.nih.gov/pubmed/22161745 [Accessed March 6, 2013].

Fu, F. & Cohen, S., 2008. *Current concepts in ACL reconstruction*, Available at: http://books.google.co.za/books?hl=en&lr=&id=WpciU74pRWAC&oi=fnd&pg=PR5&dq=Current+Concepts+in+ACL+Reconstruction&ots=YKKoyaHc8L&sig=m-HN_kTv7b69m_wK5W7pWXcC3ps [Accessed August 30, 2014].

Fujie, H., Sekito, T. & Orita, A., 2004. A Novel Robotic System for Joint Biomechanical Tests: Application to the Human Knee Joint. *Journal of Biomechanical Engineering*, 126(1), p.54. Available at: http://biomechanical.asmedigitalcollection.asme.org/article.aspx?articleid=1411251 [Accessed March 18, 2013].

Ghez, C., 2011. The Control of Movement. In *Neuroanatomy for the Neuroscientist*. Springer.

Gianotti, S.M. et al., 2009. Incidence of anterior cruciate ligament injury and other knee ligament injuries: a national population-based study. *Journal of science and medicine in sport / Sports Medicine Australia*, 12(6), pp.622–7. Available at: http://www.ncbi.nlm.nih.gov/pubmed/18835221 [Accessed November 11, 2013].

Girgis, F.G., Marshall, J.L. & Al Monajem, A.R.S., 1975. The Cruciate Ligaments of the Knee Joint. *Clinical orthopaedics and related research*, 106, pp.216–231.

Golden, G.M., Pavol, M.J. & Hoffman, M. a, 2009. Knee joint kinematics and kinetics during a lateral false-step maneuver. *Journal of athletic training*, 44(5), pp.503–10. Available at: http://www.pubmedcentral.nih.gov/articlerender.fcgi?artid=2742460&tool=pmcentrez&rendertype=abstract.

Grandstrand, S.L. et al., 2006. The effects of a commercially available warm-up program on landing mechanics in female youth soccer players. *Journal of strength and conditioning research / National Strength & Conditioning Association*, 20(2), pp.331–5. Available at: http://www.ncbi.nlm.nih.gov/pubmed/16686560 [Accessed June 23, 2014].

Griffin, L. & Agel, J., 2000. Noncontact anterior cruciate ligament injuries: risk factors and prevention strategies. *Journal of the American Academy of Orthopaedic Surgeons*, 8(3), pp.141–150. Available at: https://jaaos.org/content/8/3/141.full [Accessed June 9, 2014].

Griffin, L.Y. et al., 2006. Understanding and preventing noncontact anterior cruciate ligament injuries: a review of the Hunt Valley II meeting, January 2005. *The American journal of sports medicine*, 34(9), pp.1512–32. Available at: http://www.ncbi.nlm.nih.gov/pubmed/16905673 [Accessed February 18, 2013].

Grivas, T.B. et al., 2008. Correlation of foot length with height and weight in school age children. *Journal of forensic and legal medicine*, 15(2), pp.89–95. Available at: http://www.ncbi.nlm.nih.gov/pubmed/18206824 [Accessed July 12, 2014].

Hagel, B. & Meeuwisse, W., 2004. Risk Compensation. *Clinical Journal of Sport Medicine*, 14(4), pp.193–196. Available at: http://content.wkhealth.com/linkback/openurl?sid=WKPTLP:landingpage&an=00042752-200407000-00001.

Hartigan, E.H., Axe, M.J. & Snyder-Mackler, L., 2010. Time line for noncopers to pass return-to-sports criteria after anterior cruciate ligament reconstruction. *The Journal of orthopaedic and sports physical therapy*, 40(3), pp.141–54. Available at: http://www.ncbi.nlm.nih.gov/pubmed/20195019 [Accessed January 31, 2013].

Hashemi, J. et al., 2011. Hip extension, knee flexion paradox: a new mechanism for non-contact ACL injury. *Journal of biomechanics*, 44(4), pp.577–85. Available at: http://www.ncbi.nlm.nih.gov/pubmed/21144520 [Accessed February 19, 2013].

Hashemi, J. et al., 2010. Increasing pre-activation of the quadriceps muscle protects the anterior cruciate ligament during the landing phase of a jump: an in vitro simulation. *The Knee*, 17(3), pp.235–41. Available at: http://www.ncbi.nlm.nih.gov/pubmed/19864146 [Accessed March 10, 2015].

Hemmerich, A. et al., 2006. Hip , Knee , and Ankle Kinematics of High Range of Motion Activities of Daily Living. *JOURNAL OF ORTHOPAEDIC RESEARCH*, 24(4), pp.770–781.

Hennekens, C. & Buring, J., 1987. *Epidemiology in medicine* 1st ed. S. L. Mayrent., ed., Boston: Little, Brown and Co. Available at: http://www.sidalc.net/cgi-bin/wxis.exe/?IsisScript=SIBE01.xis&method=post&formato=2&cantidad=1&expresion=mfn=004399 [Accessed August 7, 2014].

Hewett, T.E. et al., 2005. Biomechanical measures of neuromuscular control and valgus loading of the knee predict anterior cruciate ligament injury risk in female athletes: a prospective study. *The American journal of sports medicine*, 33(4), pp.492–501.

Hewett, T.E. et al., 1996. Plyometric Training in Female Athletes: Decreased Impact Forces and Increased Hamstring Torques. *The American Journal of Sports Medicine*, 24(6), pp.765–773. Available at: http://journal.ajsm.org/cgi/doi/10.1177/036354659602400611 [Accessed June 9, 2014].

Hewett, T.E. et al., 1999. The effect of neuromuscular training on the incidence of knee injury in female athletes. A prospective study. *The American journal of sports medicine*, 27(6), pp.699–706. Available at: http://www.ncbi.nlm.nih.gov/pubmed/10569353.

Hewett, T.E. et al., 2010. Understanding and preventing ACL injuries: Current Biomechanical and Epidemiologic considerations - update 2010. , 5(4), pp.234–251.

Hewett, T.E., Myer, G.D. & Ford, K.R., 2006. Anterior cruciate ligament injuries in female athletes: Part 1, mechanisms and risk factors. *The American journal of sports medicine*, 34(2), pp.299–311. Available at: http://www.ncbi.nlm.nih.gov/pubmed/16423913 [Accessed February 21, 2013].

Hicks, J. & Uchida, T., 2012. Checklist - Evaluating your Simulation. Available at: http://simtk-confluence.stanford.edu:8080/display/OpenSim/Checklist+-+Evaluating+your+Simulation.

Hirokawa, S., Yamamoto, K. & Kawada, T., 1998. A photoelastic study of ligament strain. *IEEE transactions on rehabilitation engineering : a publication of the IEEE Engineering in Medicine and Biology Society*, 6(3), pp.300–8. Available at: http://www.ncbi.nlm.nih.gov/pubmed/9749907.

Hollis, J.M. et al., 1991. The effects of knee motion and external loading on the length of the anterior cruciate ligament (ACL): a kinematic study. *Journal of biomechanical engineering*, 113(2), pp.208–14. Available at: http://www.ncbi.nlm.nih.gov/pubmed/1875695 [Accessed August 12, 2014].

Hootman, J.M., Dick, R. & Agel, J., 2007. Epidemiology of Collegiate Injuries for 15 Sports: Summare and Recommendations for Injury Prevention Initiatives. *Journal of athletic training*, 42(2), pp.311–319.

Houck, J.R., Duncan, A. & De Haven, K.E., 2006. Comparison of frontal plane trunk kinematics and hip and knee moments during anticipated and unanticipated walking and side step cutting tasks. *Gait & posture*, 24(3), pp.314–22. Available at: http://www.ncbi.nlm.nih.gov/pubmed/16293416 [Accessed September 1, 2014].

Huang, H.J. & Ahmed, A. a, 2011. Tradeoff between stability and maneuverability during whole-body movements. *PloS one*, 6(7), p.e21815. Available at: http://www.pubmedcentral.nih.gov/articlerender.fcgi?artid=3136469&tool=pmcentrez&rendertype=abstract [Accessed February 21, 2013].

Huiskes, R. & Blankevoort, L., 1992. Anatomy and Biomechanics of the Anterior Cruciate Ligament: A Three-Dimensional Problem. , pp.92–110.

Hurvich, C. & Tsai, C., 1989. Regression and time series model selection in small samples. *Biometrika*, 76(2), pp.297–307. Available at: http://www.stat.tamu.edu/~suhasini/teaching613/hurvich_tsai89.pdf [Accessed August 26, 2014].

Indrayan, A., 2013. Clinical Agreement in Quantitative Measurements: Limits of Disagreement and the Intraclass Correlation. In S. A. R. Doi & G. M. Williams, eds. *Methods of Clinical Epidemiology*. Springer Series on Epidemiology and Public Health. Berlin, Heidelberg: Springer Berlin Heidelberg, pp. 17–27. Available at: http://link.springer.com/10.1007/978-3-642-37131-8 [Accessed August 28, 2014].

Ireland, M.L., 1999. Anterior cruciate ligament injury in female athletes: epidemiology. *Journal of athletic training*, 34(2), pp.150–4. Available at: http://www.pubmedcentral.nih.gov/articlerender.fcgi?artid=1322904&tool=pmcentrez&rendertype=abstract.

James, C.R. et al., 2004. Gender Differences among Sagittal Plane Knee Kinematic and Ground Reaction Force Characteristics during a Rapid Sprint and Cut Maneuver. *Research Quarterly for Exercise and Sport*, 75(1), pp.31–38. Available at: http://www.tandfonline.com/doi/abs/10.1080/02701367.2004.10609131 [Accessed September 1, 2014].

Jorrakate, C. & Vachalathiti, R., 2011. Lower extremity joint posture and peak knee valgus moment during side-step cutting performed by males and females. *Journal of Physical Therapy Science*, 23(4),

pp.585–589. Available at: http://jlc.jst.go.jp/JST.JSTAGE/jpts/23.585?from=Google [Accessed August 19, 2014].

Kadaba, M.P., Ramakrishnan, H.K. & Wootten, M.E., 1990. Measurement of lower extremity kinematics during level walking. *Journal of orthopaedic research : official publication of the Orthopaedic Research Society*, 8(3), pp.383–92.

Kaminski, T.W. & Perrin, D.H., 1996. Effect of prophylactic knee bracing on balance and joint position sense. *Journal of athletic training*, 31(2), pp.131–6. Available at: http://www.pubmedcentral.nih.gov/articlerender.fcgi?artid=1318443&tool=pmcentrez&rendertype=abstract.

Kar, J. & Quesada, P.M., 2013. A musculoskeletal modeling approach for estimating anterior cruciate ligament strains and knee anterior-posterior shear forces in stop-jumps performed by young recreational female athletes. *Annals of biomedical engineering*, 41(2), pp.338–48. Available at: http://www.ncbi.nlm.nih.gov/pubmed/23015067 [Accessed March 6, 2013].

Kar, J. & Quesada, P.M., 2012. A numerical simulation approach to studying anterior cruciate ligament strains and internal forces among young recreational women performing valgus inducing stop-jump activities. *Annals of biomedical engineering*, 40(8), pp.1679–91. Available at: http://www.ncbi.nlm.nih.gov/pubmed/22527014 [Accessed February 20, 2013].

Kawano, K. et al., 2007. Analyzing 3D Knee Kinematics Using Accelerometers , Gyroscopes and Magnetometers. *IEEE*, (1 1).

Kernozek, T.W. & Ragan, R.J., 2008. Estimation of anterior cruciate ligament tension from inverse dynamics data and electromyography in females during drop landing. *Clinical biomechanics (Bristol, Avon)*, 23(10), pp.1279–86. Available at: http://www.ncbi.nlm.nih.gov/pubmed/18790553 [Accessed February 15, 2013].

Kernozek, T.W., Torry, M.R. & Iwasaki, M., 2008. Gender differences in lower extremity landing mechanics caused by neuromuscular fatigue. *The American journal of sports medicine*, 36(3), pp.554–65. Available at: http://www.ncbi.nlm.nih.gov/pubmed/18006677 [Accessed February 20, 2013].

Kim, H.-Y., 2013. Statistical notes for clinical researchers: Evaluation of measurement error 1: using intraclass correlation coefficients. *Restorative dentistry & endodontics*, 38(2), pp.98–102. Available at: http://www.pubmedcentral.nih.gov/articlerender.fcgi?artid=3670985&tool=pmcentrez&rendertype=abstract.

King, J., 2003. Running a best-subsets logistic regression: An alternative to stepwise methods. *Educational and Psychological Measurement*, 63, pp.392–403. Available at: http://epm.sagepub.com/content/63/3/392.short [Accessed August 17, 2014].

Kinikli, G.İ. et al., 2014. Bracing After Anterior Cruciate Ligament Reconstruction: Systematic Review and Meta-Analysis. *Turkiye Klinikleri Journal of Sports Sciences*, 6(1), pp.28–38. Available at:

http://www.turkiyeklinikleri.com/article/en-bracing-after-anterior-cruciate-ligament-reconstruction-systematic-review-and-meta-analysis-68540.html [Accessed June 23, 2014].

Kirk, a. G., O'Brien, J.F. & Forsyth, D. a., 2005. Skeletal Parameter Estimation from Optical Motion Capture Data. *2005 IEEE Computer Society Conference on Computer Vision and Pattern Recognition (CVPR'05)*, 2, pp.782–788. Available at: http://ieeexplore.ieee.org/lpdocs/epic03/wrapper.htm?arnumber=1467522.

Koga, H. et al., 2010. Mechanisms for noncontact anterior cruciate ligament injuries: knee joint kinematics in 10 injury situations from female team handball and basketball. *The American journal of sports medicine*, 38(11), pp.2218–25. Available at: http://www.ncbi.nlm.nih.gov/pubmed/20595545 [Accessed February 11, 2013].

Kristianslund, E. et al., 2013. Sidestep cutting technique and knee abduction loading: implications for ACL prevention exercises. *British journal of sports medicine*. Available at: http://www.ncbi.nlm.nih.gov/pubmed/23258848 [Accessed November 10, 2013].

Kristianslund, E. & Krosshaug, T., 2013. Comparison of drop jumps and sport-specific sidestep cutting: implications for anterior cruciate ligament injury risk screening. *The American journal of sports medicine*, 41(3), pp.684–8. Available at: http://www.ncbi.nlm.nih.gov/pubmed/23287439 [Accessed November 10, 2013].

Krosshaug, T., Slauterbeck, J.R., et al., 2007. Biomechanical analysis of anterior cruciate ligament injury mechanisms: three-dimensional motion reconstruction from video sequences. *Scandinavian journal of medicine & science in sports*, 17(5), pp.508–19. Available at: http://www.ncbi.nlm.nih.gov/pubmed/17181770 [Accessed February 14, 2013].

Krosshaug, T., Nakamae, A., et al., 2007. Mechanisms of anterior cruciate ligament injury in basketball: video analysis of 39 cases. *The American journal of sports medicine*, 35(3), pp.359–67. Available at: http://www.ncbi.nlm.nih.gov/pubmed/17092928 [Accessed February 1, 2013].

Lalkhen, a. G. & McCluskey, a., 2008. Clinical tests: sensitivity and specificity. *Continuing Education in Anaesthesia, Critical Care & Pain*, 8(6), pp.221–223. Available at: http://bjarev.oxfordjournals.org/cgi/doi/10.1093/bjaceaccp/mkn041 [Accessed July 14, 2014].

Laughlin, W. a et al., 2011. The effects of single-leg landing technique on ACL loading. *Journal of biomechanics*, 44(10), pp.1845–51. Available at: http://www.ncbi.nlm.nih.gov/pubmed/21561623 [Accessed February 20, 2013].

Lee, S.J. et al., 2014. Effects of pivoting neuromuscular training on pivoting control and proprioception. *Medicine and science in sports and exercise*, 46(7), pp.1400–9. Available at: http://europepmc.org/abstract/MED/24389517 [Accessed June 23, 2014].

Levine, D., Richards, J. & Whittle, M.W. eds., 2012. *Whittle's Gait Analysis* Fifth Edit., Churchill, Livingstone, Elsevier.

Lim, B.-O. et al., 2009. Effects of sports injury prevention training on the biomechanical risk factors of anterior cruciate ligament injury in high school female basketball players. *The American journal of sports medicine*, 37(9), pp.1728–34. Available at: http://www.ncbi.nlm.nih.gov/pubmed/19561174 [Accessed June 5, 2014].

Lin, C.-F. et al., 2009. A stochastic biomechanical model for risk and risk factors of non-contact anterior cruciate ligament injuries. *Journal of biomechanics*, 42(4), pp.418–23. Available at: http://www.ncbi.nlm.nih.gov/pubmed/19200994 [Accessed March 5, 2013].

Lin, K., Huang, Y.-L. & Huang, C.-H., 2011. The Effect of Taping on Knee Kinematics in Healthy People during Side Hop. *Defense Science Research Conference and Expo (DSR)*, pp.1–3.

Lloyd, D.G. & Besier, T.F., 2003. An EMG-driven musculoskeletal model to estimate muscle forces and knee joint moments in vivo. *Journal of Biomechanics*, 36(6), pp.765–776. Available at: http://linkinghub.elsevier.com/retrieve/pii/S0021929003000101 [Accessed January 29, 2013].

Lo, J. et al., 2008. Forces in anterior cruciate ligament during simulated weight-bearing flexion with anterior and internal rotational tibial load. *Journal of biomechanics*, 41(9), pp.1855–61. Available at: http://www.ncbi.nlm.nih.gov/pubmed/18513729 [Accessed February 20, 2013].

Lohmander, L.S. et al., 2004. High prevalence of knee osteoarthritis, pain, and functional limitations in female soccer players twelve years after anterior cruciate ligament injury. *Arthritis and rheumatism*, 50(10), pp.3145–52. Available at: http://www.ncbi.nlm.nih.gov/pubmed/15476248 [Accessed August 7, 2013].

Loudon, J.K. & Jenkins, W., 1996. The relationship between static posture and ACL injury in female athletes. *The Journal of orthopaedic and sports physical therapy*, 24(2), pp.91–7. Available at: http://www.ncbi.nlm.nih.gov/pubmed/8832472.

Lovell, M.C., 1983. Data Mining. *The Review of Econometrics and Statistics*, 65(1), pp.1–12.

Lu, T.W. & O'Connor, J.J., 1999. Bone position estimation from skin marker co-ordinates using global optimisation with joint constraints. *Journal of biomechanics*, 32(2), pp.129–34. Available at: http://www.ncbi.nlm.nih.gov/pubmed/10052917.

Luites, J.W.H. et al., 2007. Description of the attachment geometry of the anteromedial and posterolateral bundles of the ACL from arthroscopic perspective for anatomical tunnel placement. *Knee surgery, sports traumatology, arthroscopy : official journal of the ESSKA*, 15(12), pp.1422–31. Available at: http://www.pubmedcentral.nih.gov/articlerender.fcgi?artid=2082657&tool=pmcentrez&rendertype=abstract [Accessed March 25, 2013].

Majewski, M., Susanne, H. & Klaus, S., 2006. Epidemiology of athletic knee injuries: A 10-year study. *The Knee*, 13(3), pp.184–8. Available at: http://www.ncbi.nlm.nih.gov/pubmed/16603363 [Accessed July 17, 2014].

Mandelbaum, B.R. et al., 2005. Effectiveness of a neuromuscular and proprioceptive training program in preventing anterior cruciate ligament injuries in female athletes: 2-year follow-up. *The American*

journal of sports medicine, 33(7), pp.1003–10. Available at: http://www.ncbi.nlm.nih.gov/pubmed/15888716 [Accessed February 1, 2013].

Markolf, K.L. et al., 1995. Combined knee loading states that generate high anterior cruciate ligament forces. *Journal of orthopaedic research : official publication of the Orthopaedic Research Society*, 13(6), pp.930–5.

Mather, R.C. et al., 2014. Cost-effectiveness Analysis of Early Reconstruction Versus Rehabilitation and Delayed Reconstruction for Anterior Cruciate Ligament Tears. *The American journal of sports medicine*, p.0363546514530866–. Available at: http://ajs.sagepub.com/content/early/2014/05/06/0363546514530866.abstract [Accessed June 23, 2014].

McDevitt, E.R., 2004. Functional Bracing After Anterior Cruciate Ligament Reconstruction: A Prospective, Randomized, Multicenter Study. *American Journal of Sports Medicine*, 32(8), pp.1887–1892. Available at: http://journal.ajsm.org/cgi/doi/10.1177/0363546504265998 [Accessed November 11, 2013].

McGinty, G., Irrgang, J.J. & Pezzullo, D., 2000. Biomechanical considerations for rehabilitation of the knee. *Clinical biomechanics (Bristol, Avon)*, 15(3), pp.160–6. Available at: http://www.ncbi.nlm.nih.gov/pubmed/10656977.

McGraw, K. & Wong, S., 1996. Forming inferences about some intraclass correlation coefficients. *Psychological methods*, I(1), pp.30–46. Available at: http://psycnet.apa.org/journals/met/1/1/30/ [Accessed August 12, 2014].

McIntosh, A.S., 2005. Risk compensation, motivation, injuries, and biomechanics in competitive sport. *British journal of sports medicine*, 39(1), pp.2–3. Available at: http://www.pubmedcentral.nih.gov/articlerender.fcgi?artid=1725025&tool=pmcentrez&rendertype=abstract [Accessed August 10, 2013].

McLean, S.G. et al., 1999. Knee joint kinematics during the sidestep cutting maneuver: potential for injury in women. *Medicine & Science in Sports & Exercise*, 31, pp.959–968.

McLean, S.G. et al., 2004. Sagittal plane biomechanics cannot injure the ACL during sidestep cutting. *Clinical biomechanics (Bristol, Avon)*, 19(8), pp.828–38. Available at: http://www.ncbi.nlm.nih.gov/pubmed/15342155 [Accessed February 9, 2013].

McLean, S.G., Huang, X. & van den Bogert, A.J., 2005. Association between lower extremity posture at contact and peak knee valgus moment during sidestepping: implications for ACL injury. *Clinical biomechanics (Bristol, Avon)*, 20(8), pp.863–70. Available at: http://www.ncbi.nlm.nih.gov/pubmed/16005555 [Accessed February 21, 2013].

McLean, S.G., Huang, X. & van den Bogert, A.J., 2008. Investigating isolated neuromuscular control contributions to non-contact anterior cruciate ligament injury risk via computer simulation methods. *Clinical biomechanics (Bristol, Avon)*, 23(7), pp.926–36. Available at: http://www.ncbi.nlm.nih.gov/pubmed/18485552 [Accessed March 5, 2013].

McLean, S.G., Su, A. & van den Bogert, A.J., 2003. Development and Validation of a 3-D Model to Predict Knee Joint Loading During Dynamic Movement. *Journal of Biomechanical Engineering*, 125(6), p.864. Available at: http://biomechanical.asmedigitalcollection.asme.org/article.aspx?articleid=1411034 [Accessed March 14, 2013].

Meeuwisse, W.H., 1994. Assessing causation in sport injury: A Multifactorial Model. *Clinical Journal of Sport Medicine*, 4, pp.166–170.

Meyer, E.G. & Haut, R.C., 2005. Excessive compression of the human tibio-femoral joint causes ACL rupture. *Journal of biomechanics*, 38(11), pp.2311–6. Available at: http://www.ncbi.nlm.nih.gov/pubmed/16154419 [Accessed February 21, 2013].

Miles, J. & Shevlin, M., 2001. *Applying regression and correlation: A guide for students and researchers* First., London: Sage.

Mirza, F. et al., 2000. Management of injuries to the anterior cruciate ligament: results of a survey of orthopaedic surgeons in Canada. *Clinical journal of sport medicine : official journal of the Canadian Academy of Sport Medicine*, 10(2), pp.85–8. Available at: http://www.ncbi.nlm.nih.gov/pubmed/10798788.

Mommersteeg, T.J.A. et al., 1996. Characterization of the mechanical behaviour of human knee ligaments: a numerical-experimental approach. *Journal of biomechanics*, 29(2), pp.151–160.

Morgan, K.D., Donnelly, C.J. & Reinbolt, J.A., 2014. Elevated gastrocnemius forces compensate for decreased hamstrings forces during the weight-acceptance phase of single-leg jump landing: implications for anterior cruciate ligament injury risk. *Journal of biomechanics*, 47(13), pp.3295–302. Available at: http://www.ncbi.nlm.nih.gov/pubmed/25218505 [Accessed December 15, 2014].

Moyé, L. a, 2008. Disciplined analyses in clinical trials: the dark heart of the matter. *Statistical methods in medical research*, 17(3), pp.253–64. Available at: http://www.ncbi.nlm.nih.gov/pubmed/17925318 [Accessed August 14, 2014].

Mundry, R. & Nunn, C.L., 2009. Stepwise model fitting and statistical inference: turning noise into signal pollution. *The American naturalist*, 173(1), pp.119–23. Available at: http://www.ncbi.nlm.nih.gov/pubmed/19049440 [Accessed July 15, 2014].

Myer, G.D. et al., 2010. Clinical Correlates to Laboratory Measures for use in Non-Contact Anterior Cruciate Ligament Injury Risk Prediction Algorithm. *Clinical Biomechanics*, 25(7), pp.693–699.

Myer, G.D. et al., 2007. Differential neuromuscular training effects on ACL injury risk factors in“high-risk” versus “low-risk” athletes. *BMC musculoskeletal disorders*, 8(1), p.39. Available at: http://www.biomedcentral.com/1471-2474/8/39 [Accessed June 9, 2014].

Myer, G.D. et al., 2005. Neuromuscular training improves performance and lower-extremity biomechanics in female athletes. *Journal of strength and conditioning research / National Strength & Conditioning Association*, 19(1), pp.51–60. Available at: http://www.ncbi.nlm.nih.gov/pubmed/15705045 [Accessed June 10, 2014].

Myklebust, G. et al., 2003. Prevention of anterior cruciate ligament injuries in female team handball players: a prospective intervention study over three seasons. *Clinical journal of sport medicine : official journal of the Canadian Academy of Sport Medicine*, 13(2), pp.71–8. Available at: http://www.ncbi.nlm.nih.gov/pubmed/12629423.

Nisell, R., Nemeth, G. & Ohlsdn, H., 1986. Joint forces in extension of the knee: Analysis of a mechanical model. *Acta Orthopaedica*, 57(1), pp.41–46.

Novacheck, T., 1998. The biomechanics of running. *Gait & posture*, 7(1), pp.77–95. Available at: http://www.ncbi.nlm.nih.gov/pubmed/10200378.

Noyes, F. & Grood, E., 1976. The strength of the anterior cruciate ligament in humans and Rhesus. *J. Bone Joint Surg. Am*, 58, pp.1074–1082. Available at: http://www.researchgate.net/publication/22151724_The_strength_of_the_anterior_cruciate_ligament_in_humans_and_Rhesus_monkeys/file/60b7d51e9853622db0.pdf [Accessed June 9, 2014].

Noyes, F.R. et al., 1989. Partial tears of the Anterior Cruciate Ligament - Progression to complete ligament deficiency. *British Editorial Society of Bone and Joint Surgery*, 71-B(5), pp.825–833.

Noyes, F.R. & Barber-Westin, S.D., 2014. Neuromuscular retraining intervention programs: do they reduce noncontact anterior cruciate ligament injury rates in adolescent female athletes? *Arthroscopy : the journal of arthroscopic & related surgery : official publication of the Arthroscopy Association of North America and the International Arthroscopy Association*, 30(2), pp.245–55. Available at: http://www.arthroscopyjournal.org/article/S0749806313011614/fulltext [Accessed June 23, 2014].

Nuber, G., 1997. Dynamic and static properties of the human knee joint in axial rotation. *Proceedings of the 19th Annual International Conference of the IEEE Engineering in Medicine and Biology Society. "Magnificent Milestones and Emerging Opportunities in Medical Engineering" (Cat. No.97CH36136)*, 4(C), pp.1738–1741. Available at: http://ieeexplore.ieee.org/lpdocs/epic03/wrapper.htm?arnumber=757059.

O'Connor, J. & Zavatsky, A., 1995. ACL function in the normal knee. *Biomecanica*, III(5), pp.121–132.

Odensten, M. & Gillquist, J., 1985. Functional anatomy of the anterior cruciate ligament and a rationale for reconstruction. *The Journal of bone and joint surgery. American volume*, 67(2), pp.257–62. Available at: http://www.ncbi.nlm.nih.gov/pubmed/3968118.

Oh, Y.K. et al., 2012. What strains the anterior cruciate ligament during a pivot landing? *The American journal of sports medicine*, 40(3), pp.574–83. Available at: http://www.ncbi.nlm.nih.gov/pubmed/22223717 [Accessed August 14, 2014].

Olkin, I. & Finn, J., 1995. Correlations redux. *Psychological Bulletin*. Available at: http://psycnet.apa.org/journals/bul/118/1/155/ [Accessed October 6, 2014].

Olsen, O.-E., 2004. Injury Mechanisms for Anterior Cruciate Ligament Injuries in Team Handball: A Systematic Video Analysis. *American Journal of Sports Medicine*, 32(4), pp.1002–1012. Available at: http://ajs.sagepub.com/cgi/doi/10.1177/0363546503261724 [Accessed February 15, 2013].

Orchard, J. et al., 2001. Intrinsic and Extrinsic Risk Factors for Anterior Cruciate Ligament Injury in Australian Footballers. *The American Journal of Sports Medicine*, 29(2), pp.196–200.

Orchard, J.W. & Powell, J.W., 2003. Risk of knee and ankle sprains under various weather conditions in American football. *Medicine and science in sports and exercise*, 35(7), pp.1118–23. Available at: http://www.ncbi.nlm.nih.gov/pubmed/12840631 [Accessed June 9, 2014].

Orsi, A. et al., 2011. Development of a Failure Locus for a 3-Dimensional Anterior Cruciate Ligament : A Finite Element Analysis. In *Bioengineering Conference (NEBEC), 2011 IEEE 37th Annual Northeast*. pp. 2–3.

Otsubo, H. et al., 2012. The arrangement and the attachment areas of three ACL bundles. *Knee surgery, sports traumatology, arthroscopy : official journal of the ESSKA*, 20(1), pp.127–34. Available at: http://www.ncbi.nlm.nih.gov/pubmed/21695467 [Accessed August 10, 2014].

Ounpuu, S., 1994. The biomechanics of walking and running. *Clinics in sports medicine*, 13(4), pp.843–63. Available at: http://www.ncbi.nlm.nih.gov/pubmed/7805110 [Accessed August 12, 2014].

Özaslan, A. et al., 2003. Estimation of stature from body parts. *Forensic Science International*, 132(1), pp.40–45. Available at: http://www.fsijournal.org/article/S0379073802004255/fulltext [Accessed July 12, 2014].

Pandy, M.G., 2001. Computer modelling and simulation of human movement. *Annual Review of Biomedical Engineering*, 3, pp.245–273.

Pandy, M.G., Sasaki, K. & Kim, S., 2007. A Three-Dimensional Musculoskeletal Model of the Human Knee Joint. Part 1: Theoretical Construction. *Computer Methods in Biomechanics and Biomedical Engineering*, 1(2), pp.87 – 108.

Parikh, R. et al., 2008. Understanding and using sensitivity, specificity and predictive values. *Indian journal of ophthalmology*, 56(1), pp.45–50. Available at: http://www.pubmedcentral.nih.gov/articlerender.fcgi?artid=2636062&tool=pmcentrez&rendertype=abstract [Accessed August 2, 2014].

Pearson, K., 1895. Note on regression and inheritance in the case of two parents. *Proceedings of the Royal Society of ….* Available at: http://rspl.royalsocietypublishing.org/content/58/347-352/240.full.pdf [Accessed August 28, 2014].

Perry, J.F., Rohe, D.A. & Garcia, A.O., 1996. *The Kinesiology Workbook* Second. J.-F. Vilain, ed., Philadelphia, PA: F. A. Davis Company.

Petersen, W. & Zantop, T., 2007. Anatomy of the anterior cruciate ligament with regard to its two bundles. *Clinical orthopaedics and related research*, 454(454), pp.35–47.

Pflum, M. a. et al., 2004. Model Prediction of Anterior Cruciate Ligament Force during Drop-Landings. *Medicine & Science in Sports & Exercise*, 36(11), pp.1949–1958. Available at:

http://content.wkhealth.com/linkback/openurl?sid=WKPTLP:landingpage&an=00005768-200411000-00019 [Accessed February 20, 2013].

Picard, R. & Cook, R., 1984. Cross-validation of regression models. *Journal of the American Statistical …*, 79(387), pp.575–583. Available at: http://amstat.tandfonline.com/doi/abs/10.1080/01621459.1984.10478083 [Accessed August 19, 2014].

Pietrosimone, B.G. et al., 2008. A systematic review of prophylactic braces in the prevention of knee ligament injuries in collegiate football players. *Journal of athletic training*, 43(4), pp.409–15. Available at: http://www.pubmedcentral.nih.gov/articlerender.fcgi?artid=2474821&tool=pmcentrez&rendertype=abstract.

Podraza, J.T. & White, S.C., 2010. Effect of knee flexion angle on ground reaction forces, knee moments and muscle co-contraction during an impact-like deceleration landing: implications for the non-contact mechanism of ACL injury. *The Knee*, 17(4), pp.291–5. Available at: http://www.ncbi.nlm.nih.gov/pubmed/20303276 [Accessed February 13, 2013].

Van de Pol, G.J. et al., 2009. Varus alignment leads to increased forces in the anterior cruciate ligament. *The American journal of sports medicine*, 37(3), pp.481–7. Available at: http://www.ncbi.nlm.nih.gov/pubmed/19088054 [Accessed October 24, 2013].

Pollard, C.D. et al., 2006. The influence of in-season injury prevention training on lower-extremity kinematics during landing in female soccer players. *Clinical journal of sport medicine : official journal of the Canadian Academy of Sport Medicine*, 16(3), pp.223–7. Available at: http://www.ncbi.nlm.nih.gov/pubmed/16778542 [Accessed June 23, 2014].

Von Porat, a, 2004. High prevalence of osteoarthritis 14 years after an anterior cruciate ligament tear in male soccer players: a study of radiographic and patient relevant outcomes. *Annals of the Rheumatic Diseases*, 63(3), pp.269–273. Available at: http://ard.bmj.com/cgi/doi/10.1136/ard.2003.008136 [Accessed August 7, 2013].

Quatman, C.E. & Hewett, T.E., 2009. The anterior cruciate ligament injury controversy: is “valgus collapse” a sex-specific mechanism? *British journal of sports medicine*, 43(5), pp.328–35. Available at: http://www.ncbi.nlm.nih.gov/pubmed/19372087 [Accessed February 21, 2013].

Rahnama, N., Reilly, T. & Lees, a, 2002. Injury risk associated with playing actions during competitive soccer. *British journal of sports medicine*, 36(5), pp.354–9. Available at: http://www.pubmedcentral.nih.gov/articlerender.fcgi?artid=1724551&tool=pmcentrez&rendertype=abstract.

Ramsey, D.K. et al., 2001. Assessment of functional knee bracing: an in vivo three-dimensional kinematic analysis of the anterior cruciate ligament deficient knee. *Clinical Biomechanics*, 16, pp.61–70.

Ren, Y. et al., 2010. Developing a 6-DOF robot to investigate multi-axis ACL injuries under valgus loading coupled with tibia internal rotation. *Conference proceedings : ... Annual International Conference of*

the IEEE Engineering in Medicine and Biology Society. IEEE Engineering in Medicine and Biology Society. Conference, 2010, pp.3942–5. Available at: http://www.ncbi.nlm.nih.gov/pubmed/21097089.

Rencher, A. & Pun, F., 1980. Inflation of R2 in best subset regression. *Technometrics*, 22(1), pp.49–53. Available at: http://amstat.tandfonline.com/doi/abs/10.1080/00401706.1980.10486100 [Accessed August 19, 2014].

Renstrom, P. et al., 2008. Non-contact ACL injuries in female athletes: an International Olympic Committee current concepts statement. *British journal of sports medicine*, 42(6), pp.394–412. Available at: http://www.ncbi.nlm.nih.gov/pubmed/18539658 [Accessed February 15, 2013].

Roberts, D., Andersson, G. & Friden, T., 2004. Knee joint proprioception in ACL-deficient knees is related to cartilage injury, laxity and age. *Acta orthopaedica Scandinavica*, 75(1), pp.78–83.

Rose, J. & Gamble, J.G. eds., 2006. *Human Walking* Third Edit., Lippincott, Williams and Wilkins.

Rovere, G.D., Haupt, H.A. & Yates, C.S., 1987. Prophylactic knee bracing in college football. *The American Journal of Sports Medicine*, 15(2), pp.111–116. Available at: http://ajs.sagepub.com/content/15/2/111.abstract [Accessed June 23, 2014].

Rozzi, S.L. et al., 1999. Knee joint laxity and neuromuscular characteristics of male and female soccer and basketball players. *The American journal of sports medicine*, 27(3), pp.312–9. Available at: http://www.ncbi.nlm.nih.gov/pubmed/10352766.

Salarian, A., 2008. Intraclass Correlation Coefficient (ICC).

Salkind, N.J., 2004. *Statistics for People who (think They) Hate Statistics* Second., Thousand Oaks, CA: Sage.

Sandholm, A., Pronost, N. & Thalmann, D., 2009. MotionLab : A Matlab toolbox for extracting and processing experimental motion capture data for neuromuscular simulations. In *Modelling the Physiological Human*. Springer Berlin Heidelberg, pp. 110–124.

Schönauer, C., Pintaric, T. & Kaufmann, H., 2011. Full Body Motion Capture: A Flexible Marker-Based Solution.

Scranton, P.E. et al., 1997. A review of selected noncontact anterior cruciate ligament injuries in the National Football League. *Foot & ankle international / American Orthopaedic Foot and Ankle Society [and] Swiss Foot and Ankle Society*, 18(12), pp.772–6.

Scuderi, G.R., 2010. *The Knee: A Comprehensive Review*, World Scientific. Available at: http://books.google.ca/books/about/The_Knee.html?id=-IKTj6TrKEQC&pgis=1 [Accessed November 17, 2014].

Senter, C. & Hame, S.L., 2006. Biomechanical analysis of tibial torque and knee flexion angle: implications for understanding knee injury. *Sports medicine (Auckland, N.Z.)*, 36(8), pp.635–41. Available at: http://www.ncbi.nlm.nih.gov/pubmed/16869706 [Accessed August 6, 2014].

Serpas, F., Yanagawa, T. & Pandy, M., 2002. Forward-Dynamics Simulation of Anterior Cruciate Ligament forces developed during isokinetic dynamometry. *Computer Methods in Biomechanics and Biomedical Engineering*, 5(1), pp.33–43.

Seth, A. et al., 2011. OpenSim: a musculoskeletal modeling and simulation framework for in silico investigations and exchange. *Procedia IUTAM*, 2, pp.212–232. Available at: http://linkinghub.elsevier.com/retrieve/pii/S2210983811000228 [Accessed February 11, 2013].

Shao, Q. et al., 2011. Estimation of ligament loading and anterior tibial translation in healthy and ACL-deficient knees during gait and the influence of increasing tibial slope using EMG-driven approach. *Annals of biomedical engineering*, 39(1), pp.110–21. Available at: http://www.pubmedcentral.nih.gov/articlerender.fcgi?artid=3010217&tool=pmcentrez&rendertype=abstract [Accessed February 20, 2013].

Shelbourne, K., 1998. The relationship between intercondylar notch width of the femur and the incidence of anterior cruciate ligament tears A prospective study. *The American Journal of Sports Medicine*, 26(3), pp.402–408. Available at: http://ajs.sagepub.com/content/26/3/402.short [Accessed June 9, 2014].

Shelbourne, K.D., Benner, R.W. & Gray, T., 2014. Return to Sports and Subsequent Injury Rates After Revision Anterior Cruciate Ligament Reconstruction With Patellar Tendon Autograft. *The American journal of sports medicine*, 42(6), pp.1395–1400. Available at: http://ajs.sagepub.com/content/42/6/1395.short [Accessed June 1, 2014].

Shelburne, K.B. et al., 2004. Pattern of anterior cruciate ligament force in normal walking. *Journal of biomechanics*, 37(6), pp.797–805. Available at: http://www.ncbi.nlm.nih.gov/pubmed/15111067 [Accessed February 14, 2013].

Shelburne, K.B., Pandy, M.G. & Torry, M.R., 2004. Comparison of shear forces and ligament loading in the healthy and ACL-deficient knee during gait. *Journal of Biomechanics*, 37(3), pp.313–319. Available at: http://linkinghub.elsevier.com/retrieve/pii/S0021929003002926 [Accessed March 26, 2013].

Shrout, P. & Fleiss, J., 1979. Intraclass correlations: uses in assessing rater reliability. *Psychological bulletin*, 86(2), pp.420–428. Available at: http://psycnet.apa.org/journals/bul/86/2/420/ [Accessed August 21, 2014].

Sigward, S.M. et al., 2012. Influence of sex and maturation on knee mechanics during side-step cutting. *Medicine and science in sports and exercise*, 44(8), pp.1497–503. Available at: http://www.pubmedcentral.nih.gov/articlerender.fcgi?artid=3399059&tool=pmcentrez&rendertype=abstract [Accessed August 6, 2014].

Sigward, S.M. & Powers, C.M., 2007. Loading characteristics of females exhibiting excessive valgus moments during cutting. *Clinical biomechanics (Bristol, Avon)*, 22(7), pp.827–33. Available at: http://www.ncbi.nlm.nih.gov/pubmed/17531364 [Accessed February 21, 2013].

Sigward, S.M. & Powers, C.M., 2006. The influence of gender on knee kinematics, kinetics and muscle activation patterns during side-step cutting. *Clinical biomechanics (Bristol, Avon)*, 21(1), pp.41–8. Available at: http://www.ncbi.nlm.nih.gov/pubmed/16209900 [Accessed February 5, 2013].

Silvers, H.J. & Mandelbaum, B.R., 2011. ACL Injury Prevention in the Athlete. *Sport-Orthopädie - Sport-Traumatologie - Sports Orthopaedics and Traumatology*, 27(1), pp.18–26. Available at: http://linkinghub.elsevier.com/retrieve/pii/S0949328X11000111 [Accessed February 21, 2013].

Simpson, M.M.R., 2006. Benign joint hypermobility syndrome: evaluation, diagnosis, and management. *JAOA: Journal of the American …*, 106(9), pp.531–536. Available at: http://www.jaoa.org/content/106/9/531.short [Accessed November 17, 2014].

Sitler, M. et al., 1990. The efficacy of a prophylactic knee brace to reduce knee injuries in football. A prospective, randomized study at West Point. *The American journal of sports medicine*, 18(3), pp.310–5.

Solomonow, M., 2004. Ligaments: a source of work-related musculoskeletal disorders. *Journal of electromyography and kinesiology : official journal of the International Society of Electrophysiological Kinesiology*, 14(1), pp.49–60. Available at: http://www.ncbi.nlm.nih.gov/pubmed/14759750 [Accessed November 10, 2013].

Soper, D.., 2014. R-square Confidence Interval Calculator. Available at: http://www.danielsoper.com/statcalc.

Stevenson, J.H. et al., 2014. Assessing the Effectiveness of Neuromuscular Training Programs in Reducing the Incidence of Anterior Cruciate Ligament Injuries in Female Athletes: A Systematic Review. *The American journal of sports medicine*, p.0363546514523388–. Available at: http://ajs.sagepub.com/content/early/2014/02/25/0363546514523388.short [Accessed June 6, 2014].

Stone, A. et al., 2014. Knee and hip mechanics during side-step cutting: a comparison between dominant and non-dominant limbs. In *Northwest Biomechanics Symposium*. Oregon, USA, p. 1.

Stredney, D.L., 1982. *The representation of anatomical structures through computer animation for scientific, educational and artistic applications*. The Ohio State University.

Strehl, A. & Eggli, S., 2007. The value of conservative treatment in ruptures of the anterior cruciate ligament (ACL). *The Journal of trauma*, 62(5), pp.1159–62. Available at: http://www.ncbi.nlm.nih.gov/pubmed/17495718.

Sugimoto, D. et al., 2014. Dosage effects of neuromuscular training intervention to reduce anterior cruciate ligament injuries in female athletes: meta- and sub-group analyses. *Sports medicine (Auckland, N.Z.)*, 44(4), pp.551–62. Available at: http://www.ncbi.nlm.nih.gov/pubmed/24370992 [Accessed June 8, 2014].

Swinnen, B., 2014. Planes Of Motion. Available at: http://functionalresistancetraining.com/articles/planes-of-motion.

Takahashi, M. et al., 2006. Anatomical study of the femoral and tibial insertions of the anteromedial and posterolateral bundles of human anterior cruciate ligament. *The American journal of sports medicine*, 34(5), pp.787–92. Available at: http://www.ncbi.nlm.nih.gov/pubmed/16452272 [Accessed March 20, 2013].

Taylor, K. a et al., 2011. Measurement of in vivo anterior cruciate ligament strain during dynamic jump landing. *Journal of biomechanics*, 44(3), pp.365–71. Available at: http://www.pubmedcentral.nih.gov/articlerender.fcgi?artid=3053134&tool=pmcentrez&rendertype=abstract [Accessed February 27, 2013].

Tiberio, D., 1987. The effect of excessive subtalar joint pronation on patellofemoral mechanics: a theoretical model. *Journal of Orthopaedic & Sports Physical Therapy*. Available at: http://www.jospt.org/doi/abs/10.2519/jospt.1987.9.4.160 [Accessed November 17, 2014].

Toutoungi, D.E., Zavatsky, a B. & O'Connor, J.J., 1997. Parameter sensitivity of a mathematical model of the anterior cruciate ligament. *Proceedings of the Institution of Mechanical Engineers. Part H, Journal of engineering in medicine*, 211(3), pp.235–46. Available at: http://www.ncbi.nlm.nih.gov/pubmed/9256000.

Tsuda, E. et al., 2001. Direct Evidence of the Anterior Cruciate Ligament-Hamstring Reflex Arc in Humans. *The American Journal of Sports Medicine*, 29(1), pp.83–87.

Uhorchak, J.M. et al., 2003. Risk factors associated with noncontact injury of the anterior cruciate ligament: a prospective four-year evaluation of 859 West Point cadets. *The American journal of sports medicine*, 31(6), pp.831–42. Available at: http://www.ncbi.nlm.nih.gov/pubmed/14623646.

Valente, G., Taddei, F. & Jonkers, I., 2013. Influence of weak hip abductor muscles on joint contact forces during normal walking: probabilistic modeling analysis. *Journal of biomechanics*, 46(13), pp.2186–2193. Available at: http://www.ncbi.nlm.nih.gov/pubmed/23891175 [Accessed August 7, 2013].

Vescovi, J.D. & VanHeest, J.L., 2010. Effects of an anterior cruciate ligament injury prevention program on performance in adolescent female soccer players. *Scandinavian journal of medicine & science in sports*, 20(3), pp.394–402. Available at: http://www.ncbi.nlm.nih.gov/pubmed/19558381 [Accessed May 24, 2014].

Vicon Motion Systems, 2006. Essentials of Motion Capture v1.2. , pp.1–62.

Waldén, M. et al., 2011. Anterior cruciate ligament injury in elite football: a prospective three-cohort study. *Knee surgery, sports traumatology, arthroscopy : official journal of the ESSKA*, 19(1), pp.11–9. Available at: http://www.ncbi.nlm.nih.gov/pubmed/20532869 [Accessed August 7, 2013].

Wang, T., Hao, Z. & Wan, C., 2009. The Effect of Anterior Cruciate Ligament Injury on the Biomechanical Behavior of Human Knee Joint. *2009 2nd International Conference on Biomedical Engineering and Informatics*, pp.1–5. Available at: http://ieeexplore.ieee.org/lpdocs/epic03/wrapper.htm?arnumber=5305872.

Weinhandl, J.T. et al., 2013. Anticipatory effects on anterior cruciate ligament loading during sidestep cutting. *Clinical biomechanics (Bristol, Avon)*, 28(6), pp.655–63. Available at: http://www.ncbi.nlm.nih.gov/pubmed/23810662 [Accessed November 18, 2013].

Weinhandl, J.T. et al., 2012. Hamstrings weakness increases ACL loading during sidestep cutting. In *American Society of Biomechanics Annual Meeting*. Norfolk, VA, pp. 1–2. Available at: http://www.asbweb.org/conferences/2012/abstracts/317.pdf [Accessed November 8, 2013].

Wells, D. & Alderson, J., 2012. ASSESSING THE ACCURACY OF INVERSE KINEMATICS IN OPENSIM TO ESTIMATE ELBOW FLEXION-EXTENSION DURING CRICKET BOWLING: *ISBS-Conference …*. Available at: http://www.researchgate.net/profile/Jacqueline_Alderson/publication/236026172_ASSESSING_THE_ACCURACY_OF_INVERSE_KINEMATICS_IN_OPENSIM_TO_ESTIMATE_ELBOW_FLEXION-EXTENSION_DURING_CRICKET_BOWLING_MAINTAINING_THE_RIGID_LINKED_ASSUMPTION/links/00463515d97c4b63f5000000.pdf [Accessed March 19, 2015].

White, J., Yeats, A. & Skipworth, G., 1979. *Tables for statisticians*, Available at: http://books.google.com/books?hl=en&lr=&id=LlkpoZVPzCoC&oi=fnd&pg=PA1&dq=tables+for+statisticians&ots=TZATaZhikK&sig=beF1a2aGlu-WN9zZ6c5e6Va-HoU [Accessed August 26, 2014].

WHO, 1995. Physical status: the use and interpretation of anthropometry. Report of a WHO Expert Committee. *World Health Organization technical report series*, 854, pp.1–452. Available at: http://www.ncbi.nlm.nih.gov/pubmed/8594834 [Accessed October 8, 2014].

Wilde, G., 1994. *Target risk: dealing with the danger of death, disease and damage in everyday decisions*, Toronto: PDE Publications. Available at: http://scholar.google.co.za/scholar?q=Target+Risk.+Dealing+with+the+danger+of+death,+disease+and+damage+in+everyday+decisions&btnG=&hl=en&as_sdt=0,5#0 [Accessed August 6, 2014].

Winter, D.A., 2009. *Biomechanics and Motor Control of Human Movement* Fourth., Wiley.

Wismans, J. et al., 1980. A three-dimensional mathematical model of the knee-joint. *Journal of biomechanics*, 13(8), pp.677–85. Available at: http://www.ncbi.nlm.nih.gov/pubmed/7419534.

Wojtys, E.M., Kothari, S.U. & Huston, L.J., 1994. Anterior cruciate ligament functional brace use in sports. *The American journal of sports medicine*, 24(4), pp.539–46. Available at: http://www.ncbi.nlm.nih.gov/pubmed/8827316.

Woo, S.L. et al., 1999. Biomechanics of Knee Ligaments. *The American journal of sports medicine*, 27(4), pp.533–543.

Woodford-Rogers, B., 1994. Risk factors for anterior cruciate ligament injury in high school and college athletes. *Journal of athletic …*. Available at: http://www.ncbi.nlm.nih.gov/pmc/articles/PMC1317810/ [Accessed November 17, 2014].

Wright, R.W. & Fetzer, G.B., 2007. Bracing after ACL reconstruction: a systematic review. *Clinical orthopaedics and related research*, 455(455), pp.162–8.

Wu, J.-L., Seon, J.K., et al., 2010. In situ forces in the anteromedial and posterolateral bundles of the anterior cruciate ligament under simulated functional loading conditions. *The American journal of sports medicine*, 38(3), pp.558–63. Available at: http://www.pubmedcentral.nih.gov/articlerender.fcgi?artid=3740365&tool=pmcentrez&rendertype=abstract [Accessed March 7, 2015].

Wu, J.-L., Hosseini, A., et al., 2010. Kinematics of the anterior cruciate ligament during gait. *The American journal of sports medicine*, 38(7), pp.1475–82. Available at: http://www.pubmedcentral.nih.gov/articlerender.fcgi?artid=3740375&tool=pmcentrez&rendertype=abstract [Accessed March 7, 2015].

Yam, C., Nixon, M.S. & Carter, J.N., 2004. Automated person recognition by walking and running via model-based approaches. *Pattern Recognition*, 37(5), pp.1057–1072. Available at: http://linkinghub.elsevier.com/retrieve/pii/S0031320303003996 [Accessed August 1, 2014].

Yamaguchi, G.T. & Zajac, F.E., 1989. A planar model of the knee joint to characterize the knee extensor mechanism. *Journal of biomechanics*, 22(1), pp.1–10. Available at: http://www.ncbi.nlm.nih.gov/pubmed/2914967.

Yang, H., 2013. The Case for Being Automatic: Introducing the Automatic Linear Modeling (LINEAR) Procedure in SPSS Statistics. *Multiple Linear Regression Viewpoints*, 39(2), pp.27–37.

Yang, Y., 2007. Consistency of cross validation for comparing regression procedures. *The Annals of Statistics*, 35(6), pp.2450–2473. Available at: http://projecteuclid.org/euclid.aos/1201012968 [Accessed August 14, 2014].

Yau, A. et al., 2014. *Electronic Knee Wrap for Injury Prediction*, Philadelphia, PA.

Yeow, C.H. et al., 2010. Effect of an anterior-sloped brace joint on anterior tibial translation and axial tibial rotation: a motion analysis study. *Clinical biomechanics (Bristol, Avon)*, 25(10), pp.1025–30. Available at: http://www.ncbi.nlm.nih.gov/pubmed/20797811 [Accessed February 21, 2013].

Yoo, Y.-S. et al., 2010. Changes in ACL length at different knee flexion angles: an in vivo biomechanical study. *Knee surgery, sports traumatology, arthroscopy : official journal of the ESSKA*, 18(3), pp.292–7. Available at: http://www.ncbi.nlm.nih.gov/pubmed/19915824 [Accessed May 21, 2013].

Yu, B., Lin, C.-F. & Garrett, W.E., 2006. Lower extremity biomechanics during the landing of a stop-jump task. *Clinical biomechanics (Bristol, Avon)*, 21(3), pp.297–305. Available at: http://www.ncbi.nlm.nih.gov/pubmed/16378667 [Accessed February 11, 2013].

Zantop, T. et al., 2007. Intraarticular rupture pattern of the ACL. *Clinical orthopaedics and related research*, 454(454), pp.48–53. Available at: http://www.ncbi.nlm.nih.gov/pubmed/17202917 [Accessed November 11, 2013].

Zazulak, B.T. et al., 2007. The effects of core proprioception on knee injury: a prospective biomechanical-epidemiological study. *The American journal of sports medicine*, 35(3), pp.368–73. Available at: http://www.ncbi.nlm.nih.gov/pubmed/17267766 [Accessed May 27, 2014].

Zhang, X. et al., 2008. A subject-specific finite element model of the anterior cruciate ligament. *Conference proceedings : ... Annual International Conference of the IEEE Engineering in Medicine and Biology Society. IEEE Engineering in Medicine and Biology Society. Conference*, 2008(2), pp.891–4. Available at: http://www.ncbi.nlm.nih.gov/pubmed/19162800.

Zhang, Y., 2010. Biomechanical Analysis of Anterior Cruciate Ligament Elongations. *2010 4th International Conference on Bioinformatics and Biomedical Engineering*, pp.1–4. Available at: http://ieeexplore.ieee.org/lpdocs/epic03/wrapper.htm?arnumber=5518054.

Zhang, Y., Liu, G. & Xie, S.Q., 2011. Biomechanical simulation of anterior cruciate ligament strain for sports injury prevention. *Computers in biology and medicine*, 41(3), pp.159–63. Available at: http://www.ncbi.nlm.nih.gov/pubmed/21292250 [Accessed February 20, 2013].

Appendix A: Supplementary Material - Literature Review

A.1: Nomogram for screening of ACL Injury Risk

For each of the five variables outlined in Figure A.1, the user is required to draw a vertical line upwards at the appropriate position and record the value from the "points" axis at the top. The score for each variable is summed and then a vertical line drawn down from the corresponding section of the "Total Points" line down to the "Probability of High Knee Load" line. This will identify the probability that the patient will demonstrate a high knee valgus load during a dynamic movement.

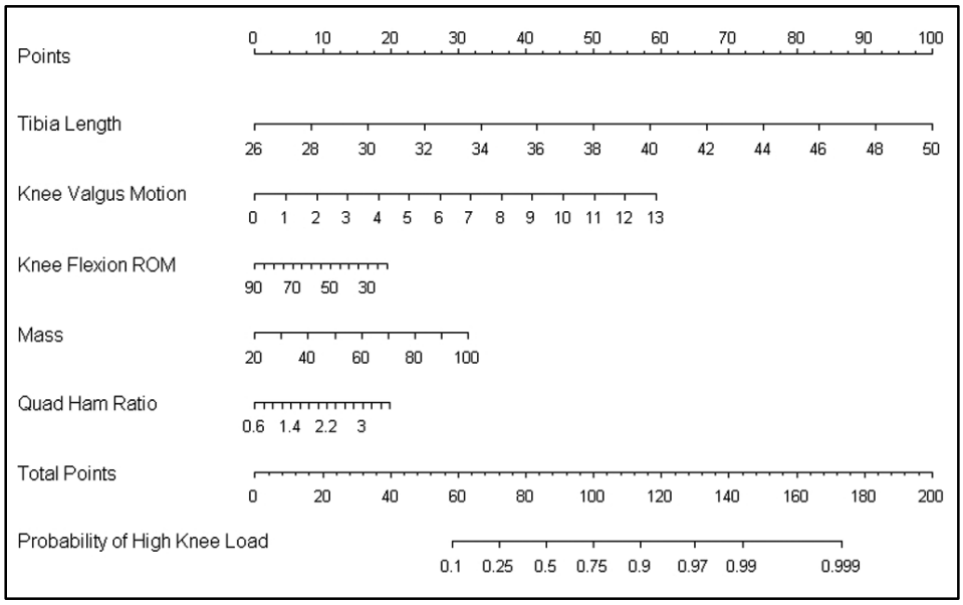

Figure A.1: The nomogram developed from the Myer et al. (2010) screening model to predict ACL risk.

A.2: Sample Injury Prevention Training Program

Appendix 1. Jump Training Program

Exercise	Duration or Repetitions by Week	
Phase I: Technique	**Week 1**	**Week 2**
1. Wall jumps	20 sec	25 sec
2. Tuck jumps*	20 sec	25 sec
3. Broad jumps stick (hold) landing	5 reps	10 reps
4. Squat jumps*	10 sec	15 sec
5. Double-legged cone jumps*	30 sec/30 sec	30 sec/30 sec (side-to-side and back-to-front)
6. 180° jumps	20 sec	25 sec
7. Bounding in place	20 sec	25 sec
Phase II: Fundamentals	**Week 3**	**Week 4**
1. Wall jumps	30 sec	30 sec
2. Tuck jumps*	30 sec	30 sec
4. Jump, jump, jump, vertical jump	5 reps	8 reps
5. Squat jumps*	20 sec	20 sec
6. Bounding for distance	1 run	2 runs
7. Double-legged cone jumps*	30 sec/30 sec	30 sec/30 sec (side-to-side and back-to-front)
8. Scissors jump	30 sec	30 sec
9. Hop, hop, stick landing*	5 reps/leg	5 reps/leg
Phase III: Performance	**Week 5**	**Week 6**
1. Wall jumps	30 sec	30 sec
2. Step, jump up, down, vertical	5 reps	10 reps
3. Mattress jumps	30 sec/30 sec	30 sec/30 sec (side-to-side and back-to-front)
4. Single-legged jumps distance*	5 reps/leg	5 reps/leg
5. Squat jumps*	25 sec	25 sec
6. Jump into bounding*	3 runs	4 runs
7. Hop, hop, stick landing	5 reps/leg	5 reps/leg

Before jumping exercises: Stretching (15-20 minutes), skipping (2 laps), side shuffle (2 laps).
Posttraining: Cool-down walk (2 minutes), stretching (5 minutes).
*These jumps performed on mats.
Note: Each jump exercise is followed by a 30-second rest period.

Appendix 2. Glossary of Jump Training Exercises

1. **180° Jumps:** Two-footed jump. Rotate 180° in mid-air. Hold landing for 2 seconds and then repeat in reverse direction.
2. **Bounding for Distance:** Start bounding in place and slowly increase distance with each step, keeping knees high.
3. **Bounding in Place:** Jump from one leg to the other straight up and down, progressively increasing rhythm and height.
4. **Broad Jumps-Stick (hold) Landing:** Two-footed jump as far as possible. Hold landing for 5 seconds.
5. **Cone Jumps:** Double-legged jump with feet together. Jump side-to-side over cones quickly. Repeat forward and backward.
6. **Hop, Hop Stick:** Single-legged hop. Stick second landing for 5 seconds. Increase distance of hop as technique improves.
7. **Jump into Bounding:** Two-footed broad jump. Land on single leg, then progress into bounding for distance.
8. **Jump, Jump, Jump, Vertical:** Three broad jumps with vertical jump immediately after landing the third broad jump.
9. **Mattress Jumps:** Two-footed jump on mattress, tramp, or other easily compressed device. Perform side-to-side and back-to front.
10. **Scissors Jump:** Start in stride position with one foot well in front of other. Jump up, alternating foot positions in mid-air.
11. **Single-Legged Jumps, Distance:** Single-legged hop for distance. Hold landing (knees bent) for 5 seconds.
12. **Squat Jumps:** Standing jump raising both arms overhead, land in squatting position touching both hands to floor.
13. **Step, Jump Up, Down, Vertical:** Two-footed jump onto 6- to 8-inch step. Jump off step with two feet, then vertical jump.
14. **Tuck Jumps:** From standing position jump, and bring both knees up to chest as high as possible. Repeat quickly.
15. **Wall Jumps (Ankle Bounces):** With knees slightly bent and arms raised overhead, bounce up and down off toes.

Appendix 3. Stretching and Weight Training Program

Stretches[a]	Weight-training exercises[b]
1. Calf stretch 1	1. Abdominal curl
2. Calf stretch 2: soleus	2. Back hyperextension
3. Quadriceps	3. Leg press
4. Hamstring	4. Calf raise
5. Hip flexors	5. Pullover
6. Iliotibial band/lower back	6. Bench press
7. Posterior deltoids	7. Latissimus dorsi pulldown
8. Latissimus dorsi	8. Forearm curl
9. Pectorals/biceps	9. Warm-down/short stretch

[a] Stretching consists of 3 sets of 30 seconds each.
[b] Weight training consists of 1 set of each exercise, generally 12 repetitions for upper body exercises and 15 repetitions for the trunk and lower body exercise.

Figure A.2: Injury Prevention Training Program (Hewett et al. 1999).

A.3: Similar Studies

Table A.1: List of studies performing cause-and-effect analyses of ACL loading during dynamic movements using non-invasive methods

Authors	Effect Investigated:	ACL Loading Method	Ligament Model	Movement
Mclean et al. (1999)	Gender, Experience	Knee Kinematic Variability	No	Side-step
Besier et al. (2001)	Anticipation of Movement	Knee Moments	No	Running & Side-step[c]
Besier et al. (2003)	Anticipation of Movement	Muscle Activations	No	Running & Side-step[c]
McLean et al. (2003)	Neuromuscular Control	Knee Moments	No	Side-step
McLean et al. (2004)	Neuromuscular Control	Knee Moments	No	Side-step
Shelburne et al. (2004)	Simulated ACL Injury	Anterior Tibial Translation & ACL Force	Dual	Walking
James et al. (2004)	Gender	Ground Reaction Force and Knee Kinematics	No	Side-step
Hewett et al. (2005)	ACL Injury (Prospective)	Neuromuscular Activations & Knee Valgus Moments	No	Landing
McLean et al. (2005)	Body Alignment at Initial Contact	Knee Valgus Moments	No	Side-step
Yu et al. (2006)	Stance-phase Kinematics and Kinetics[1]	Ground Reaction Forces	No	Landing
Ford et al. (2005)	Gender	Lower Limb Kinematics & Knee Moments	No	Side-step[b]
Sigward and Powers (2006)	Gender	Lower Limb Kinematics, Knee Moments & Muscle Activations	No	Side-step
Houck et al. (2006)	Anticipation of movement	Trunk Kinematics, Hip and Knee Moments	No	Side-step[c] & Walking[c]
Sigward and Powers (2007)	Body Alignment at Initial Contact, Ground Reaction Force	Knee Valgus Moments	No	Side-step
McLean et al. (2008)	Neuromuscular Control	Anterior Tibial Shear Force & Knee Valgus Moments	No	Side-step
Kernozek et al. (2008)	Gender and Fatigue	Lower Limb Kinematics & Knee Moments	No	Landing
Kernozek and Ragan (2008)	Observational	ACL Force	Single	Landing
Golden et al. (2009)	Width of Cut	Knee Kinematics and Moments	No	Side-step & Running

Podraza and White (2010)	Knee Flexion Angle at Initial Contact	Ground Reaction Forces, Knee Moments & Muscle Activations	No	Landing
Shao et al. (2011)	Tibial Slope	Anterior Tibial Translation & ACL Force	Single	Walking
Jorrakate and Vachalathiti (2011)	Body Alignment at Initial Contact, Knee Valgus Moment at Initial Contact, Gender,	Knee Valgus Moments	No	Side-step
Laughlin et al. (2011)	Body Alignment at Initial Contact	Muscle, Joint and ACL Forces	Single	Landing
Dempsey et al. (2012)	Body Alignment at Initial Contact	Knee Moments	No	Landing
Donnelly et al. (2012)	Body Alignment at Initial Contact	Knee Valgus Moments	No	Side-step[c]
Sigward et al. (2012)	Gender, Age	Lower Limb Kinematics, Knee Moments & Ground Reaction Forces	No	Side-step[b]
Kar and Quesada (2012)	Jumping Height	Knee Valgus Moments, ACL Strain and Force	Single	Landing
Frank et al. (2013)	Trunk and Hip Kinematics, Moments	Knee Moments	No	Side-step
Kristianslund et al. (2013)	Technique Factors	Knee Valgus Moments	No	Side-step
Kristianslund and Krosshaug (2013)	Type of movement	Knee kinematics and Moments	No	Side-step & Landing
Weinhandl (2013)	Anticipation of movement	ACL Force	Single	Side-step[c]
Valente (2013)	Weak Hip Adductor Muscles	Joint Contact Forces	No	Walking

Table A.1: List of studies, in chronological order, performing cause-and-effect analyses of ACL loading during dynamic movements. This including the loading method that were investigated, if an ACL ligament was modelled in the study, what type of dynamic movement(s) were performed by the participants and whether or not these were planned or unplanned. Studies that implemented invasive methods as well as those that only analysed static movements were not considered in the review. "Side-step" is used to describe any plant and pivot movement and "landing" is used for any movement that involves a jump or a step off from a raised platform.

Table A.2: List of studies performing observational analyses of variables related to non-contact anterior cruciate ligament injuries during dynamic movements using non-invasive methods

Authors	Observed Variable	Ligament Model	Movement
Colby et al. (2000)	Knee Kinematics, Muscle Activations	No	Side-step, Landing, Stopping
Cerulli et al. (2003)	ACL Strain	Single	Landing
Shelburne et al. (2004)	ACL Force	Dual	Walking
Pflum et al. (2004)	ACL Force	Dual	Landing
Zhang et al. (2010)	ACL Strain	Dual	Landing
Zhang et al. (2011)	ACL Strain	Dual	Side-step, Landing, Running
Taylor et al. (2011)	ACL Strain	Single	Landing
Kar and Quesada (2013)	Knee Kinematics, Knee Moments, ACL Strain and Force	Single	Landing

Table A.2: List of studies, in chronological order, which performed observational analyses of variables related to non-contact anterior cruciate ligament injuries during dynamic movements using non-invasive methods. The variable that was observed in the study is indicated, as well as the type of ligament bundle model included (if any) and the type of dynamic movement that was performed by the test subjects. "Side-step" is used to describe any plant and pivot movement and "landing" is used for any movement that involves a jump or a step off from a raised platform. Studies that implemented invasive methods as well as those that only analysed static movements were not considered in the review.

Appendix B: Supplementary Material - Methods

B.1: Motion capture methods not considered

Invasive or potentially harmful methods such as fluoroscopic imaging (Kozanek 2009) or radiostereometry, which requires the use of metal beads embedded in the bone tissue (Nisell et al. 1986), were not considered for this study.

Goniometers are devices used to measure joint angles (Kaminski & Perrin 1996). They can be bulky and restricting and tend to be used primarily in static range-of-motion, or single coordinate trials rather than experiments involving multi-axial human movement (Lloyd & Besier 2003) (Nuber 1997). Recent investigations into the use of Inertial Measurement Units (IMUs), which combines Accelerometers, Gyroscopes and Magnetometers to estimate relative joint angles, have shown promising results. These are cheap and small, with high temporal resolution and theoretically unlimited recording space. However, they tend to accumulate large errors due to sensor drift (Kawano et al. 2007; Dong et al. 2008). This technique may improve but at present it is not very well defined with no standardized, commercially available platform and ultimately requires more work to be validated as a viable option.

Kinematics can also be retrospectively reconstructed from multiple camera views of video footage. This can be implemented using either automated, model-based approaches (Krosshaug, Slauterbeck, et al. 2007; Koga et al. 2010) or manually with expert physicians subjectively estimating the joint angles at each frame (Olsen 2004; Krosshaug, Nakamae, et al. 2007). This is the only realistic way to obtain kinematic information from an actual injury event (Renstrom et al. 2008). However, matching one video sequence can take up to two months and this method is highly dependent on the accuracy of the reconstruction process (Krosshaug, Slauterbeck, et al. 2007; Koga et al. 2010). There is little confidence over the reported kinematics obtained by this method as it is typically limited by camera occlusion, poor picture quality, low frame rate and a distinct lack of anatomical reference points with which to validate the results. It is also difficult to estimate the actual time of injury without objective ground reaction force data (Krosshaug, Slauterbeck, et al. 2007). With current methods and technologies, video analysis is more useful for studying aspects such as player behaviours rather than the actual mechanics of the injury event (Olsen 2004).

B.2: ACL Modelling Methods not considered

Dynamic robotic systems can simulate recorded loading or kinematic conditions on cadaver knee joints without dissecting the joint itself to allow for natural motion of the knee (Woo et al. 1999). These can

measure the kinematics in a response to applied loads or the loads resulting from applied kinematics (Ren et al. 2010; Lo et al. 2008). However, the cadaver knee - typically a specimens from an older human - does not always truly reflect the mechanical properties of the knee in vivo, specifically those of a young, athletic population. Cadaver studies should thus be interpreted with caution (Noyes & Grood 1976; Fujie et al. 2004).

The tensile force in the ACL at any point in time can be determined by resolving the kinetics (forces and moments) acting upon the knee (Kernozek & Ragan 2008; Shao et al. 2011). This requires the knowledge of all the external forces acting upon the body as well as those generated by the musculature surrounding the knee. If the modulus of elasticity of the ligament is known, strain can then be determined from this force.

B.3: Naming Convention for the Static Marker Set

RMTH1 - Right 1st Metatarsal
RMTH5 - Right 5th Metatarsal
RDIFT - Right Distal Foot
RMEMA - Right Medial Malleolus
RLAMA - Right Lateral Malleolus
RMEKN - Right Medial Femoral Epicondyle
RLAKN - Right Lateral Femoral Epicondyle
RGTR - Right Greater Trochanter
RASIS - Right Ant/Sup Iliac Spine

LMTH1 - Left 1st Metatarsal
LMTH5 - Left 5th Metatarsal
LDIFT - Left Distal Foot
LMEMA - Left Medial Malleolus
LLAMA - Left Lateral Malleolus
LMEKN - Left Medial Femoral Epicondyle
LLAKN - Left Lateral Femoral Epicondyle
LGTR - Left Greater Trochanter
LASIS - Left Ant/Sup Iliac Spine

B.4: Naming Convention for the Dynamic Marker Set

RTTR - Right Top Trunk
LTTR - Left Top Trunk
LBTR - Left Bottom Trunk

RILCR - Right Iliac Crest
LILCR - Left Iliac Crest
L5S1 - L5S1

RTMTH - Right Top Medial Thigh (Posterior)
RTLTH - Right Top Lateral Thigh (Anterior)
RBMTH - Right Bottom Medial Thigh
RBLTH - Right Bottom Lateral Thigh

LTMTH - Left Top Medial Thigh
LTLTH - Left Top Lateral Thigh
LBMTH - Left Bottom Medial Thigh
LBLTH - Left Bottom Lateral Thigh

RTMSH - Right Top Medial Shank
RTLSH - Right Top Lateral Shank
RBMSH - Right Bottom Medial Shank
RBLSH - Right Bottom Lateral Shank

LTMSH - Left Top Medial Shank
LTLSH - Left Top Lateral Shank
LBMSH - Left Bottom Medial Shank
LBLSH - Left Bottom Lateral Shank

RPRHE - Right Proximal Heel
RDIHE - Right Distal Heel
RLAHE - Right Lateral Heel

LPRHE - Left Proximal Heel
LDIHE - Left Distal Heel
LLAHE - Left Lateral Heel

B.5: The Gait2392 Musculoskeletal Model

The Gait2392 model was created by Darryl Thelen (University of Wisconsin-Madison) and Ajay Seth, Frank C. Anderson, and Scott L. Delp (Stanford University). The unscaled model is built from 12 rigid body segments and is 1.8 meters tall with a mass of 75.16 kg. The reference frames on each individual segment are fixed (Au et al. 2013). Anthropometric data were primarily obtained from an earlier model by Delp et al (1990). However, shank (tibia and fibula) and foot data were adopted from Stredney et al. (1982) with lower back data from Anderson and Pandy (1999).

The pelvis segment forms the base of the model and is designated 6 degrees-of-freedom to translate and rotate freely in the simulated coordinate space (Kevin B Shelburne et al. 2004). The remaining body segments branch out from the pelvis in a kinetic chain, with the location of each segment in the model defined in the reference frame of its parent (Anderson & Pandy 1999). The centre of rotation of the pelvis is located at the midpoint of the imaginary line drawn between the left and right anterior superior iliac spines.

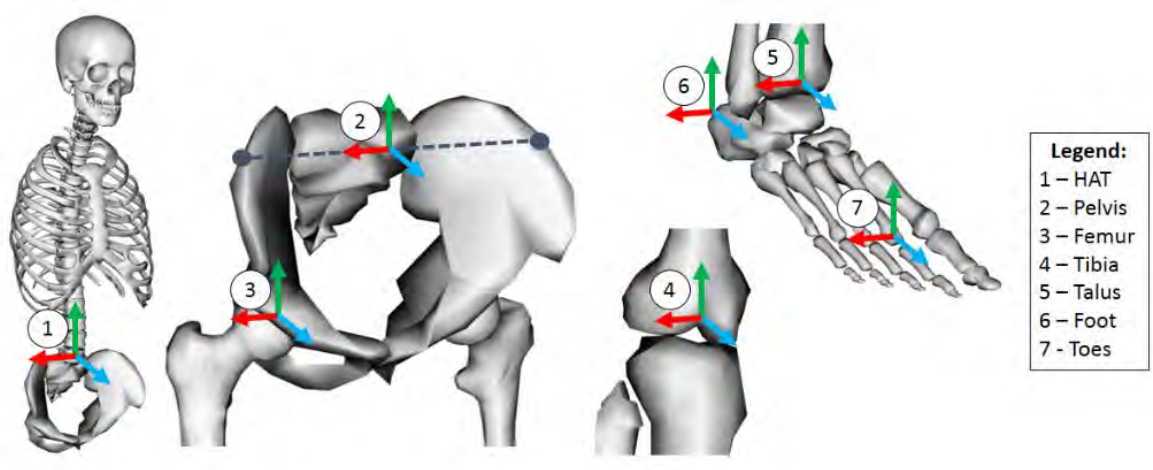

Figure B.1: Body reference frames and centres of rotation for the generic Gait2392 Model. Blue Arrow = X, Green Arrow = Y, Red Arrow = Z.

The head, arms and torso (HAT) are modelled as a single, rigid body. The HAT connects to the pelvis at the lumbar joint, located at the centre of the 3rd lumbar vertebrae. This interface is characterized as a three degree-of-freedom joint.

The reference frame of each femur bone is at the centre of the femoral head. These articulate with the pelvis at the left and right hip joint, modelled as three degree-of-freedom ball-and-socket joints.

The shank segment, including both the tibia and fibula, links with the femur at the knee joint. At rest, the centre of rotation of this segment is located on the femur at the midpoint between the medial and lateral epicondyles. To simulate the gliding and rolling motion of the femoral head on the tibial plateau, the femoral condyles are represented as ellipses with the tibial plateau modelled as a flat line. As the knee moves through flexion and extension, the tibia translates in the X and Y coordinates to remain in constant contact with the femoral condyles. However, this particular model is not designed to account for tissue interactions in the other two degrees of rotation. A diagram of the model and the corresponding translations are represented graphically in the figures below. The patellar segment was removed by Ajay Seth in a later edition of the model to avoid imposing kinematic constraints at the knee (Au et al. 2013).

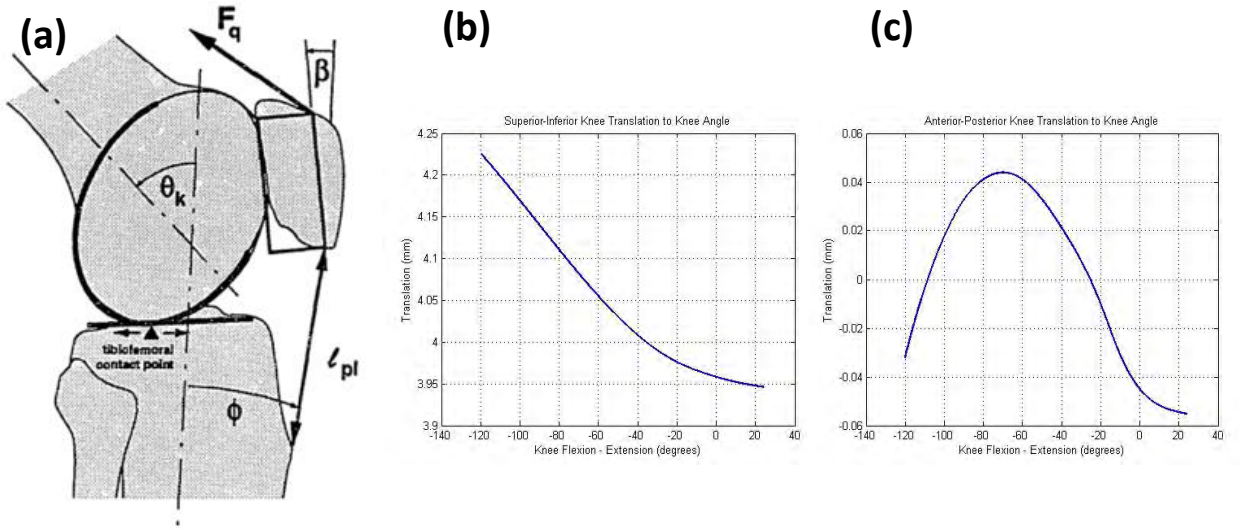

Figure B.2: Knee geometry for determining the tibiofemoral contact point in the Delp (1990) model. A lateral view (a) indicating the modelling of the tibiofemoral contact point as the interaction between an ellipse and a plane. The superior-inferior translation in the y-axis (a) and the anterior posterior translation in the x-axis (c) as a function of the degree of flexion of the knee joint in order to achieve this tibiofemoral contact model.

The ankle-foot complex is represented by three body segments, the talus, foot and toes. The talus is located inferior to the shank, halfway between the medial and lateral malleoli. It connects to the tibia and the foot at the ankle and subtalar joints respectively. The foot is modelled with the calcaneus, navicular, cuboid, cuneiforms, and metatarsal bones together as a single unit. The centre of rotation of this group is located at the most interior, lateral point on the posterior aspect of the calcaneus. The toe segment, with the phalanges modelled as a single unit, articulates with the foot at the metatarsophalangeal (MTP) joint. The frame of reference located on the foot at the base of the second metatarsal. The ankle, subtalar, and

MTP joints are each modelled as single degree-of-freedom “hinge” joints. The ankle joint controls dorsiflexion and plantarflexion of the foot, whereas the subtalar joint controls supination and pronation of the foot. Supination is a combination of inversion, plantar flexion and internal rotation. Pronation is a combination of eversion, dorsiflexion and external rotation (Close et al. 1967).

The Gait2392 model also features 92 muscle actuators, represented by a series of line segments with origins and insertions based on the anatomical landmarks of the bone surface models (Au et al. 2013).

B.6: Marker Weights for Model Scaling

Marker weights used in the model scaling routine	
Markers:	**Weight:**
Static Marker Set	
Pelvis	
RASIS, LASIS	10000
Hip	
RGTR, LGRT	5000
Knee	
RMEKN, RLAKN, LMEKN, LLAKN	10000
Ankle	
RMEMA, RLAMA, LLEMA, LLAMA	10000
Foot	
RMTH1, RMTH5, RDIFT, LMTH1, LMTH5, LDIFT	5000
Dynamic Marker Set	1

Table B.1: Marker weights used in the model scaling routine.

B.7: Marker Weights for Inverse Kinematics

Marker weights used in the inverse kinematics routine	
Markers:	Weight:
Upper Body	
Pelvis	
RILCR, LILCR, L5S1	5
Trunk	
RTTR, LTTR, LBTR	2
Right (dominant) leg	
Right Thigh	
RTMTH, RTLTH, RBMTH, RBLTH	10
Right Shank	
RTMSH, RTLSH, RBMSH, RBLSH	10
Right Heel	
RPRHE, RDIHE, RLAHE	2
Left (non-dominant) leg	1

Table B.2: Marker weights used in the inverse kinematics routine.

B.8: Intraclass Correlation Coefficients

Reliability is defined by Kim (2013) as, *"the degree to which a measurement technique can secure consistent results upon repeated measuring on the same objects either by multiple raters or test-retest trials by one observer at different time points."* Intraclass correlation coefficients (ICCs) are statistical measures for determining reliability between different measurements of the same variables (McGraw & Wong 1996). It represents the percentage of the total variance that is accounted for by the variance between measurements. This is represented in Equation B.1:

$$ICC = \frac{\delta_M^2}{\delta_M^2 + \delta_e^2} \qquad \textit{Equation B.1}$$

Where δ_M^2 and δ_e^2 represent the variance between measurements and the error variance respectively (Indrayan 2013).

There are multiple types of ICC, as described by Shrout and Fleiss (1979), and McGraw and Wong (1996). Deciding which is appropriate for the task at hand requires consideration of the data to be tested. The data typically consists of repeated observations of a test with multiple variables (targets). Three decisions need to be made to choose the appropriate form of the ICC, these are detailed in Chapter 1.3.2 through Chapter 1.3.4.

B.8.1: Decision 1 - Effects Model (One-way vs Two-way)

The first consideration is the selection of an appropriate statistical model to represent the data. This refers to the perceived origin of variances within the data. If variance only exists within the targets, a one-way design is used. If variance exists both within the targets and between the individual observations, a two-way design is used. An additional aspect of the two way model is its description as a random or mixed design. The fundamental difference in this regard is that in the mixed design, every available observation is included in the model. The two-way random design differs in that it only incorporates a random sample from a larger population of observations (McGraw & Wong 1996). This is more of a theoretical construct, since it does not affect the value of the coefficient, merely the interpretation. Results from the random model will apply to the entire population whereas the mixed model cannot be generalized and only applies to the set of observations. This distinction only applies to the two-way model, the one-way model requires a randomized design.

Shrout and Fleiss (1979) use a strong analogy to differentiate between the three model types, using the concept of K independent "judges" making ratings (targets) for each of their observation.

Scenario 1: "Each target is rated by a different set of K judges, randomly selected from a larger population of judges"

Scenario 2: "A random sample of K judges is selected from a larger population, and each judge rates N[23] targets"

Scenario 3: "Each target is rated by each of the same K judges, who are the only judges of interest."

Scenario 1 would be best represented by the one-way model, since it is impossible to account for the variance in the judge selection method. The only source of variance is within the ratings themselves. Scenario 2 and Scenario 3 apply to the two-way random and mixed designs respectively.

B.8.2: Decision 2 - Type of Index (Consistency vs Absolute Agreement)

Intraclass correlation coefficients can be chosen to account for, or ignore, the relative difference between observations. The first type of ICC index measures the reliability using a definition of consistency whereas the other analyses the level of absolute agreement between observations. Continuing with the analogy from Appendix B.8.1, suppose one judge consistently rated higher than the others. A consistent index would not penalize this difference, it would only assess the consistency or linear relationship between the observations. Absolute agreement is a stricter criterion because it requires the linear relationship to exist but also penalizes observations that differ in value (McGraw & Wong 1996). Consequently, the coefficient calculated with the absolute agreement index is always lower than one calculated with an index of consistency (Kim 2013).

B.8.3: Decision 3 - Measurement of Interest (Single vs Average)

There are two types of measurements that can be performed with ICCs. Single measurements provide the expected reliability of any individual observation compared to the population. Average measurements calculate the expected reliability of the mean of the observation, in comparison to the included population. This is useful to determine how reliably the mean observation represents the original set of measured data.

[23] Where N is a randomly selected subset of the total number of ratings

Table B.3: Critical Values of the Intraclass Correlation Coefficient to determine the strength of the agreement

Intraclass Correlation Coefficient	Strength of Agreement
ICC < 0.25	Poor
0.25 < ICC < 0.50	Fair
0.50 < ICC < 0.75	Moderate
0.75 < ICC < 0.90	Good
0.90 < ICC	Excellent

Table B.3: Critical Values of the Intraclass Correlation Coefficient to determine the strength of the agreement (Indrayan 2013).

B.8.4: Effect Size

Like Pearson's product-moment correlation coefficient (Chapter 7.3.5), R, the intraclass correlation coefficient is also analogous to Cohen's effect size. However, the ICC differs from R in the sense that R is a measure of the linearity between two observations and the ICC is an additivity index. It measures the level at which variables can be equated to one another through the addition of a constant term. The ICC penalizes changes in variance between observations whereas R does not (McGraw & Wong 1996). Indrayan (2013) defines the strength of the agreement between the observations as a function of the Intraclass correlation coefficient, as displayed in Table B.3. An F-test is also performed to determine if the acquired coefficient is significant, beyond that of random chance.

Appendix C: Supplementary Material - Model Verification and Validation

C.1: ACL Bundle Placement

Ligament placement within the model was validated by inspection, comparing the modelled ligament lengthening response to knee flexion (Figure C.1a) with results (Figure C.1b) published by Amis and Dawkins (1991).

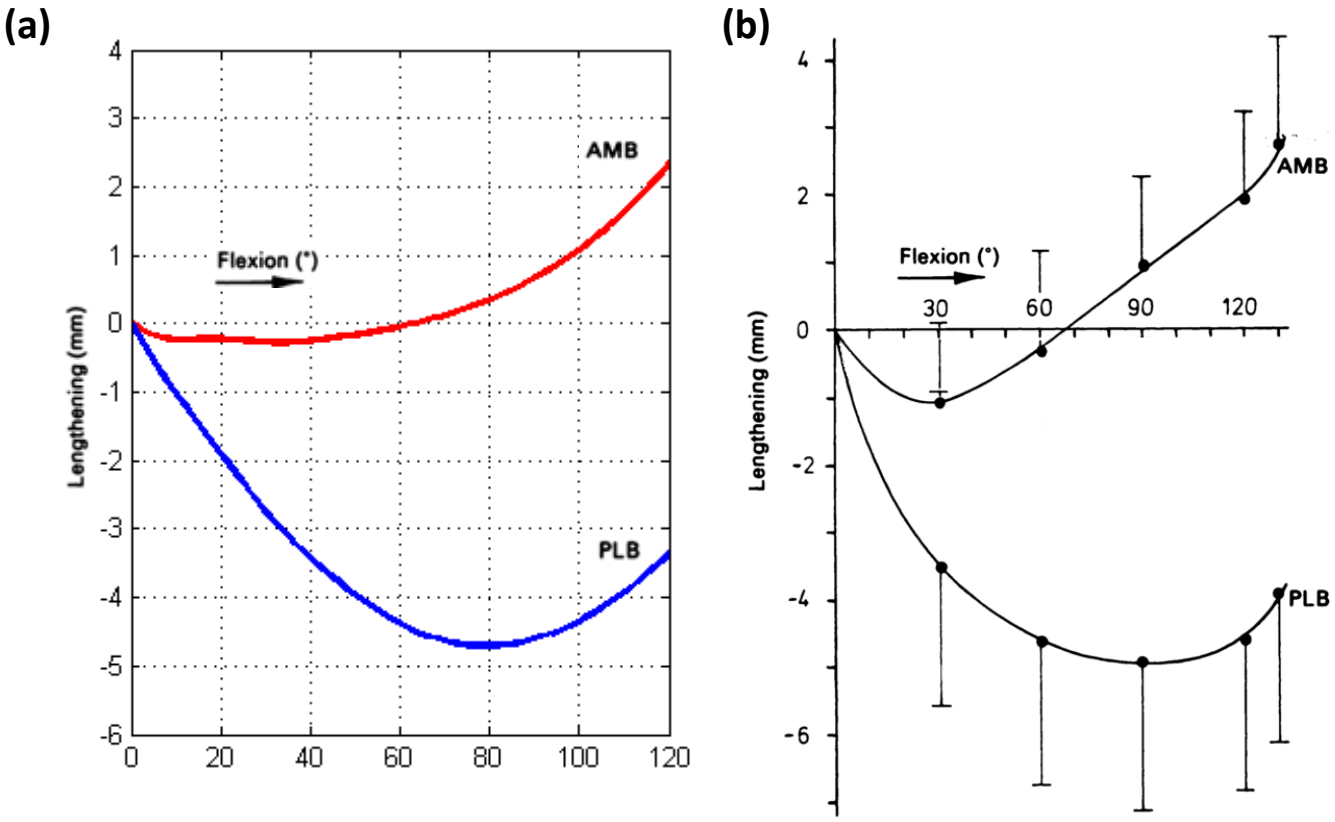

Figure C.1: ACL bundle lengthening in the anteromedial (AMB) and posterolateral (PLB) bundles as a result of knee flexion, for the musculoskeletal model (a) compared to results published for the same bundles by Amis and Dawkins (1991) (b).

Furthermore, the AMB and PLB bundles of the ACL are known to twist around each other during knee flexion (Pandy et al. 2007; Otsubo et al. 2012). This characteristic feature is shown in the modelled ligament in Figure C.2.

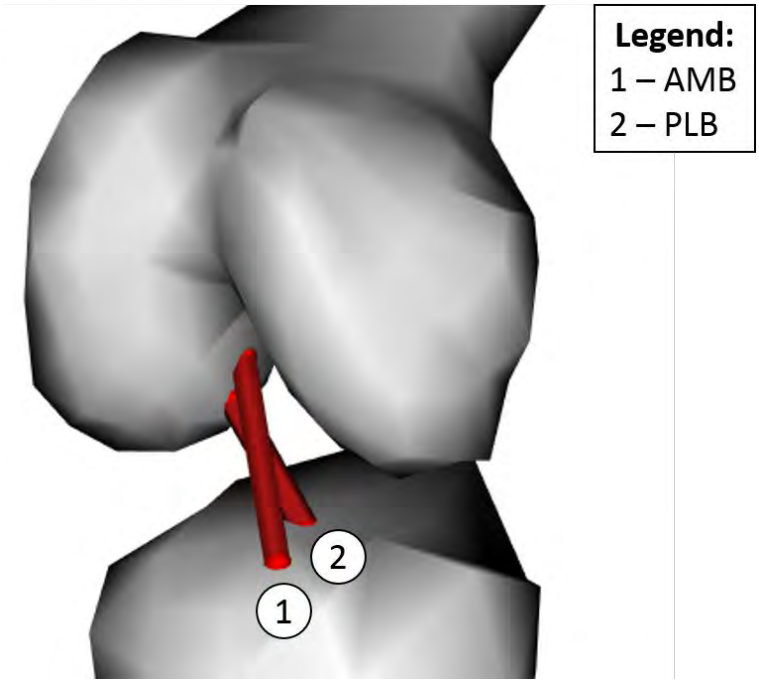

Figure C.2: The cross-over of the anteromedial (AMB) and posterolateral (PLB) bundles of the ACL at 90 of knee flexion.

Figure C.1 and Figure C.2 show that the modelled ligament origins and insertions are good approximations of their real values. This approximation can be considered to be reliable, as demonstrated by Zhang et al. (2010). Zhang, also using the Gait2392 model, calculated that small three-dimensional perturbations of less than 5mm in origin and insertion points of the ACL had little effect on bundle elongation patterns. This is illustrated for the anteromedial and posterolateral bundles in Figure C.3a and Figure C.3b respectively.

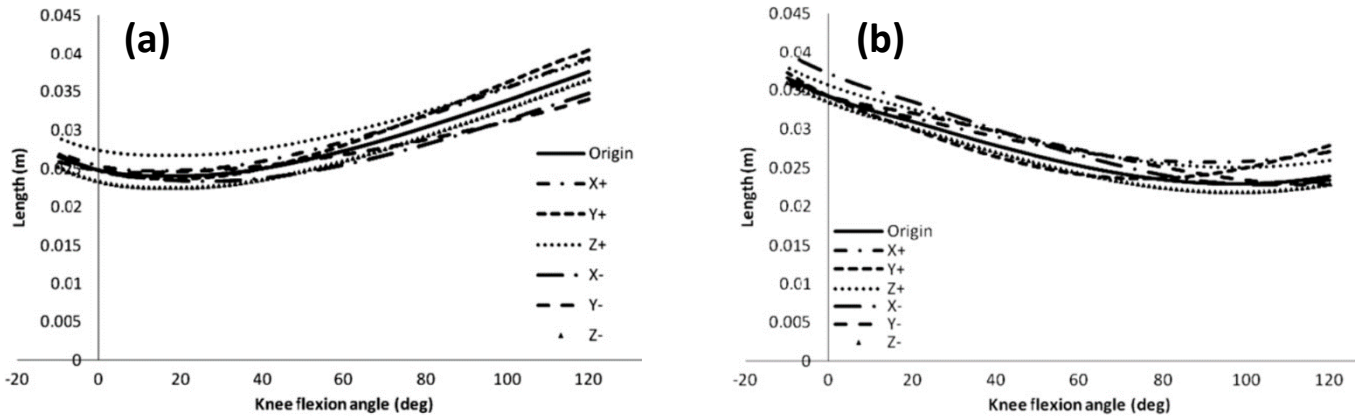

Figure C.3: Elongations in anteromedial (a) and posterolateral (b) bundles as a function of knee flexion and perturbations in origin and insertion coordinates (Zhang 2010).

C.2: Model Scaling

Maximum and root mean square marker errors output by the scaling routine for each subject in are represented in Figure C.4a and Figure C.4b respectively, with the mean errors displayed in red. The OpenSim Best Practice Guide recommends that maximum marker errors for static markers should be less than 20 mm with RMS error smaller than 10 mm (Hicks & Uchida 2012; Anderson et al. 2012). It is clear that the numerical accuracy of the scaling algorithm across the subject population is satisfactory.

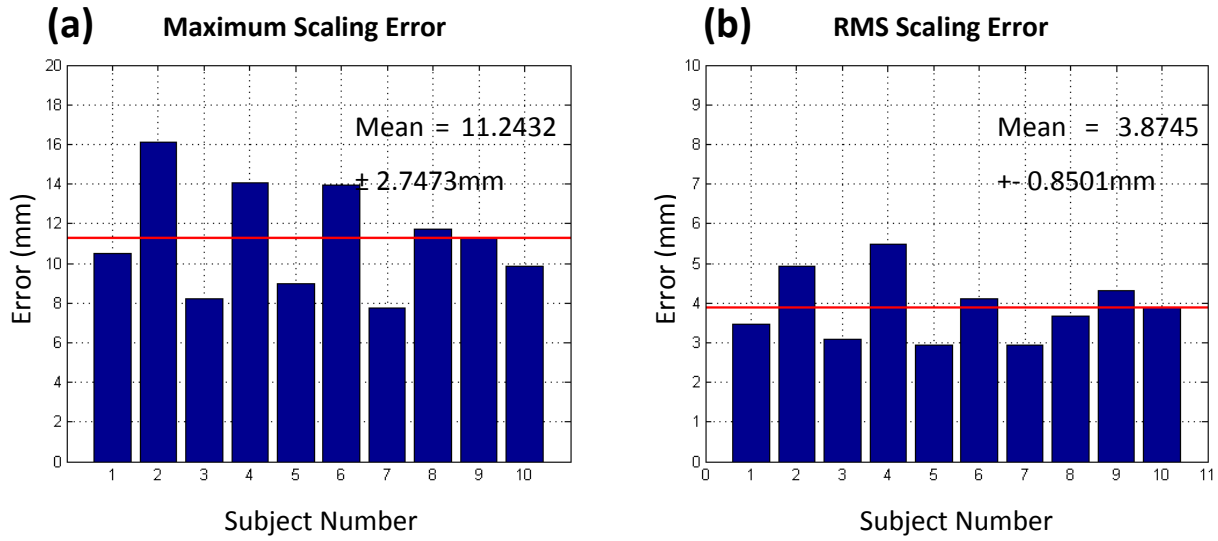

Figure C.4: Maximum (a) and root mean square (b) mathematical errors of the scaling algorithm for each subject.

Verification was completed by inspection, through a visual comparison of each static poses output to photographs taken of the participants during the static trial. The images[24] were compared for goodness of fit with regards to size, pose reconstruction and marker placement. This was corroborated by a specialist at the MRC/UCT Research Unit for Exercise Science & Sports Medicine. Refer to Figure C.8 for this report. This further justifies the set of marker weightings used in the scaling algorithm, which were determined heuristically.

[24] Due to ethical considerations, the photographs of the participants undertaking the static pose could not be published.

C.3: Calculation of ACL Resting Length

Figure C.5a illustrates a box-plot of the zero load (resting) lengths of the anteromedial and posterolateral bundles calculated for the subject population. Figure C.5b illustrates a box plot of the respective distances between bundles at the tibial insertion and femoral origins. The mean (± one standard deviation) anteromedial and posterolateral bundle resting lengths are displayed in Table C.1 along with similar measurements from other studies.

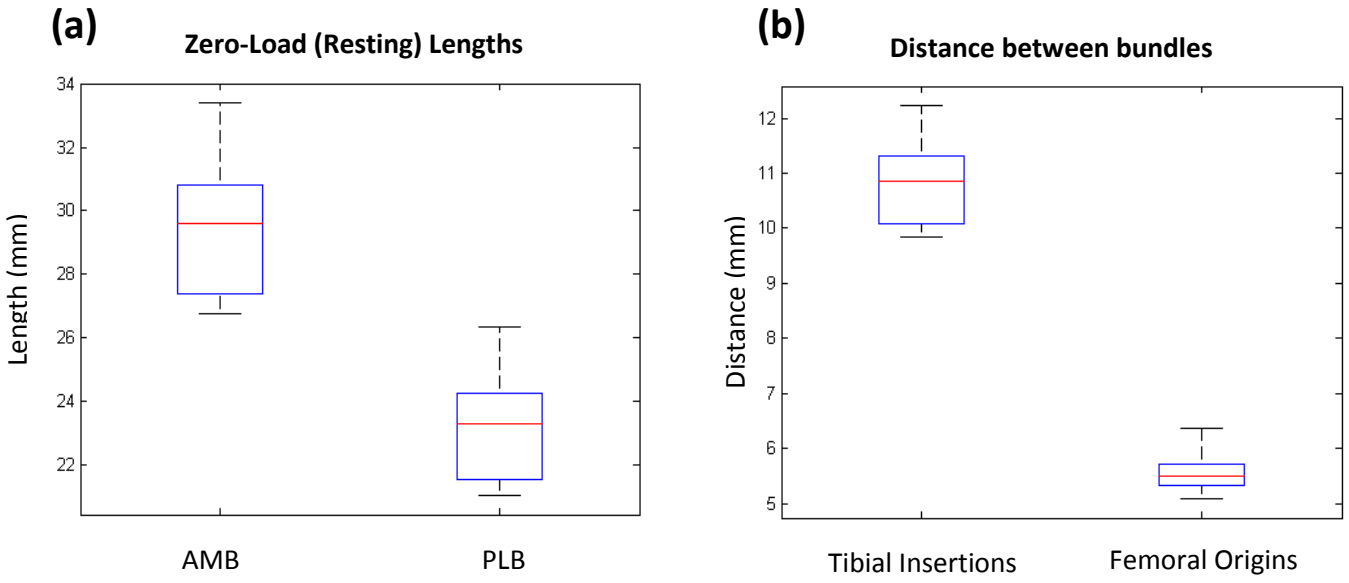

Figure C.5: Zero load ligament lengths for the anteromedial (AMB) and posterolateral (PLB) bundles of the ACL (a) and the relative distances between the origins and insertions of these bundles on the tibia and femur respectively (b).

Table C.1: Zero load ligament lengths reported in different studies

		Bundle		
Study:	**Gender:**	**AMB**	**PLB:**	**Not Specified**
Current Study	Female	29.47 ± 2.16	23.18 +- 1.71	
Chandrashekar et al. (2006)	Female			27.04 ± 2.90
Kar & Quesada (2012)	Female			32.30 ± 3.00
Yoo et al. (2010)	Male	38.40 ± 1.80	29.20 ± 1.90	
Cohen et al. (2009)	Not Specified	36.90 ± 2.80	20.50 ± 2.40	
Odensten & Gillquist (1985)	Not Specified			31.00 ± 3.00

Table C.1: Zero load ligament lengths reported in different studies, classified according to the gender of the study population and the type of ligament bundle that was analysed.

The obtained ligament resting lengths compare well with those reported in the literature, as illustrated in Table C.1. In all cases, as in this study, the anteromedial bundle is longer than the posterolateral bundle. The lengths obtained in this study are slightly smaller than those reported by Cohen et al. (2009) and Yoo et al. (2010). This is likely because of the gender of the population analysed. Females have significantly shorter ligaments than males (Anderson et al. 2001; Fu & Cohen 2008).

Takahashi et al. (2006) performed an anatomical study of the femoral and tibial insertions of the ACL bundles in cadaver samples. The distance between the two bundle origins on the Femur was approximately 7mm, with 13mm separating the two bundle insertions on the Tibia. This compares favourably with the mean distance between insertions (Figure C.5b) calculated over the test population. The mean distance calculated between bundles at their femoral origins was 5.55 ± 0.36mm and the mean distance between the tibial insertions was 10.82 ± 0.78mm. Takahashi's results are slightly higher, which is to be expected because their sample population was evenly divided between males and females whereas this study only utilized female participants.

The strength of these comparisons provides additional confidence to the accuracy of the model design (Appendix C.1) and scaling (Appendix C.2) processes, including the weights assigned to the markers (Appendix B.6) for these tasks.

C.4: Inverse Kinematics Mathematical Accuracy

For model verification, Inverse Kinematic Errors were calculated over the window of interest as the difference between the simulated marker positions and those recorded by the motion capture system. Maximum (Figure C.6) and root mean square (Figure C.7) IK errors were graphed for each trial, with the mean errors plotted in red, to determine if these were less than 40mm and 20mm respectively as recommended by the OpenSim Best Practice Guide (Hicks & Uchida 2012; Anderson et al. 2012).

Observing these graphs, it is evident that the mathematical error terms associated with the Inverse Kinematics minimization routine are well within acceptable limits. Furthermore, they appear to be relatively consistent within-subjects, which indicates a strong measure of reliability of the experimental protocol. The simulated kinematics were initially verified by inspection. Each simulated movement was analysed individually to determine if it represented that of a side-step with no obvious errors. Then, the repeated trials for each subject were viewed together to observe for similarities. This was corroborated by a specialist at the UCT/MRC Research Unit for Exercise Science & Sports Medicine (Figure C.8). This process further justified the set of marker weightings used in the inverse kinematics algorithm.

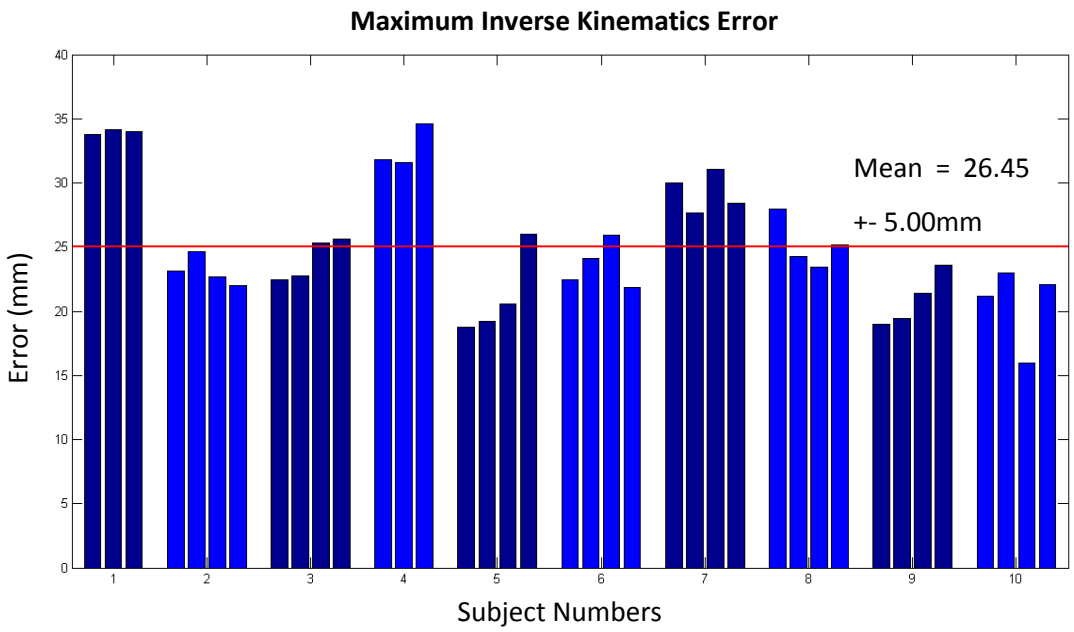

Figure C.6: Maximum mathematical errors of the inverse kinematics algorithm for each subject.

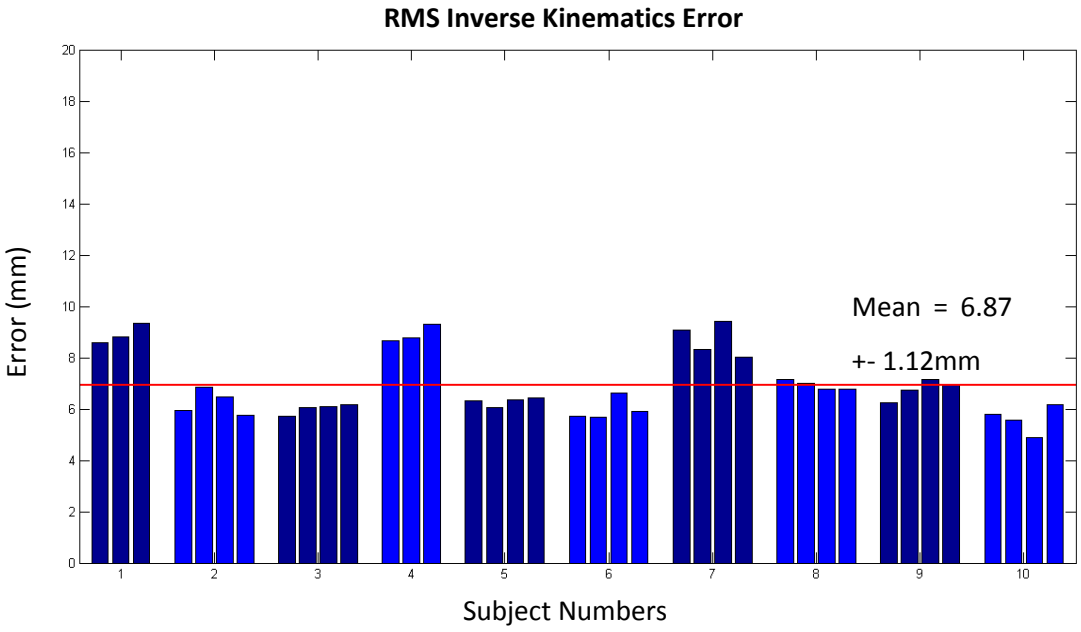

Figure C.7: Root mean square mathematical errors of the inverse kinematics algorithm for each subject.

Department of Human Biology
UCT/MRC Research Unit for Exercise Science & Sports Medicine
Faculty of Health Sciences, University of Cape Town
Private Bag, Rondebosch 7700, South Africa
Tel: +27-21-650-4575 Fax: +27-21-686-7530

Date: 21st August 2014

To

Whoever it may concern,

As a part of his Master's degree in Biomedical Engineering, Mr. Shaun Fickling carried out biomechanical modelling on data collected from subjects performing a typical "side step". This is to confirm that I have visually checked the biomechanical models he has produced from the data and all models exhibit the following:

Static Analysis: - There is a good match in scaling, body position/static pose and marker placement between the participant and the respective model.

Dynamic Analysis: - Trials for every subject are consistent with regards to general movement technique and the movements are good representations of a side step.

Yours truly,

Mr. Nikhil V. Divekar, *MSc (MED) Biomedical Engineering*
Technical Manager: Biomechanics Laboratory,
MRC/UCT Research Unit for Exercise Science and Sports Medicine
University of Cape Town

Phone: +27-21-6504575 **Cell**: +27-813089516
Email: Nikhil.Divekar@gmail.com

Figure C.8: Letter of Verification from the UCT/MRC Research Unit for Exercise Science & Sports Medicine.

C.5: Test-retest reliability

To assess the within-session test-retest reliability of the multiple side-step trials attempted by each participant, Intraclass Correlation Coefficients (Appendix B.8) were calculated for every participant over each of the gait cycle normalized kinematic variables of interest. The design of the intraclass correlation coefficient model was a two-way, mixed effect, average measure of absolute agreement. This was achieved through the use of a freely available software routine written for Matlab by Arash Salarian (Salarian 2008) and based on work published by McGraw and Wong (1996). Intraclass correlation coefficients are also used by Myer et al. (2005), Ford et al. (2005), Carey et al. (2006) and Yoo (2010) to evaluate inter-observer reliability. The results are tabulated in Table C.2. If not otherwise denoted, all results are significant with $p < 0.05$.

Table C.2: Intraclass Correlation Coefficients evaluating the test-retest reliability of the kinematics obtained from multiple side-step cutting trials

	Subject Number										
	1	**2**	**3**	**4**	**5**	**6**	**7**	**8**	**9**	**10**	**Mean**
Hip Flexion	84.22	85.76	97.37	73.65	95.66	69.38	88.50	83.16	64.51	95.47	83.77
Hip Adduction	68.89	16.54	79.85	71.27	90.67	-19.71*	77.64	82.58	23.72	57.90	54.94
Hip Rotation	59.07	77.32	86.86	70.39	68.70	63.16	65.51	78.35	83.04	90.03	74.24
Knee Flexion	86.87	99.15	99.64	98.08	98.71	98.31	99.61	98.55	91.85	98.30	96.91
Knee Valgus	81.52	81.24	90.99	76.28	95.05	85.00	75.74	88.84	74.45	61.95	81.11
Knee Rotation	87.27	98.40	98.24	90.22	85.15	78.54	92.19	93.29	78.44	89.55	89.13
Ankle Flexion	86.29	98.79	97.54	95.37	96.94	93.47	48.80	97.72	93.49	75.54	88.40
Subtalar Angle	81.77	97.48	96.59	86.98	94.20	96.45	87.64	92.10	96.49	95.81	92.55
Lumbar Extension	62.82	87.38	93.10	91.87	89.90	62.77	88.19	87.80	59.38	77.16	80.04
Lumbar Bending	75.46	94.86	94.15	69.30	94.85	96.00	98.17	98.13	83.27	72.49	87.67
Lumbar Rotation	69.58	87.47	96.49	88.88	94.04	87.05	94.09	87.76	63.33	93.13	86.18
Mean	76.71	84.04	93.71	82.94	91.26	73.67	83.28	89.84	73.82	82.48	83.17

***No significant relationship**

Table C.2: Intraclass Correlation Coefficients evaluating the test-retest reliability of the kinematics obtained from multiple side-step cutting trials.

The results in Table C.2 indicate that the overall within-subject test-retest reliability of the motion capture trials is moderate to excellent (Table B.3) across subjects as well as kinematic variables. The only kinematic variable that does not consistently indicate a strong absolute agreement is Hip Adduction Position, specifically for subjects 2, 6 and 9. It is possible that these subjects displayed different hip adduction strategies during their repeated trials. Considering the unanticipated nature of these trials, this is not unlikely. However, for each of these subjects, the coefficients for all of the other kinematic variables show very strong reliability. Thus, the mean value of the trials for each coordinate can be considered to be a strong representation of the separate trials. This justifies the method of averaging across trials to form a single, representative dataset for each participant.

C.6: Validation of Averaged Kinematic Datasets

Individual coordinate RMS error terms between the two datasets were calculated for every subject and averaged across the subjects at each sample (Figure C.9, Step 1). These were then divided by the between-subject standard deviations at each sample (Figure C.9, Step 2) and finally averaged across the samples (Figure C.9, Step 3) to provide a mean, normalized RMS error term for each coordinate. The criterion for model validation, as in McLean et al. (2004), was that the mean difference between data sets should be smaller than two between-trial standard deviations.

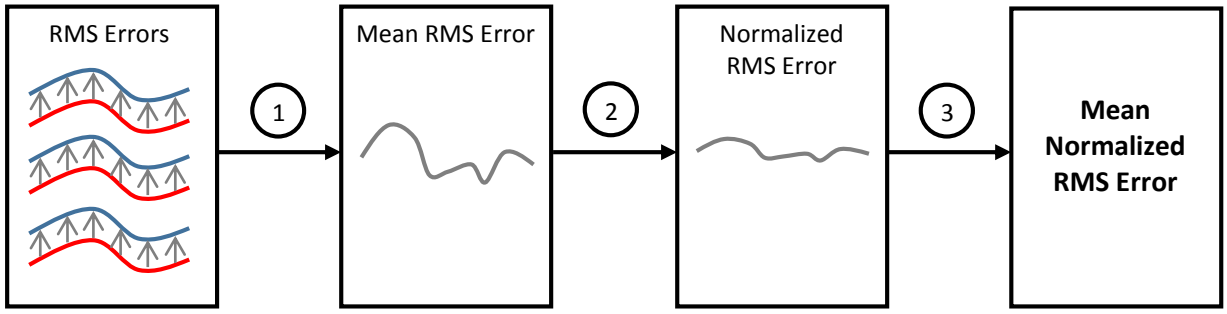

Figure C.9: Pipeline for determining the mean normalized RMS Error, adapted from McLean et al. (2004).

These errors are represented in Table C.3. Comparisons between the calculated kinematics (population mean ± standard deviation) plotted against those obtained by Sigward et al. (2012) are illustrated in Figure C.10 through to Figure C.16.

Table C.3: Mean normalized RMS errors (±sd) between current and previously obtained results	
Coordinate:	**Normalized RMS Error (mm):**
Hip Flexion	1.2186 ± 0.2174
Hip Adduction	0.8338 ± 0.3223
Hip Rotation	0.7499 ± 0.1469
Knee Flexion	0.6334 ± 0.4077
Knee Valgus	1.4884 ± 0.3427
Knee Rotation	1.4772 ± 0.2617
Ankle Angle	0.8286 ± 0.1489
Mean	1.0328 ± 0.2639

Table C.3: Mean normalized RMS errors (±sd) between current and previous obtained results.

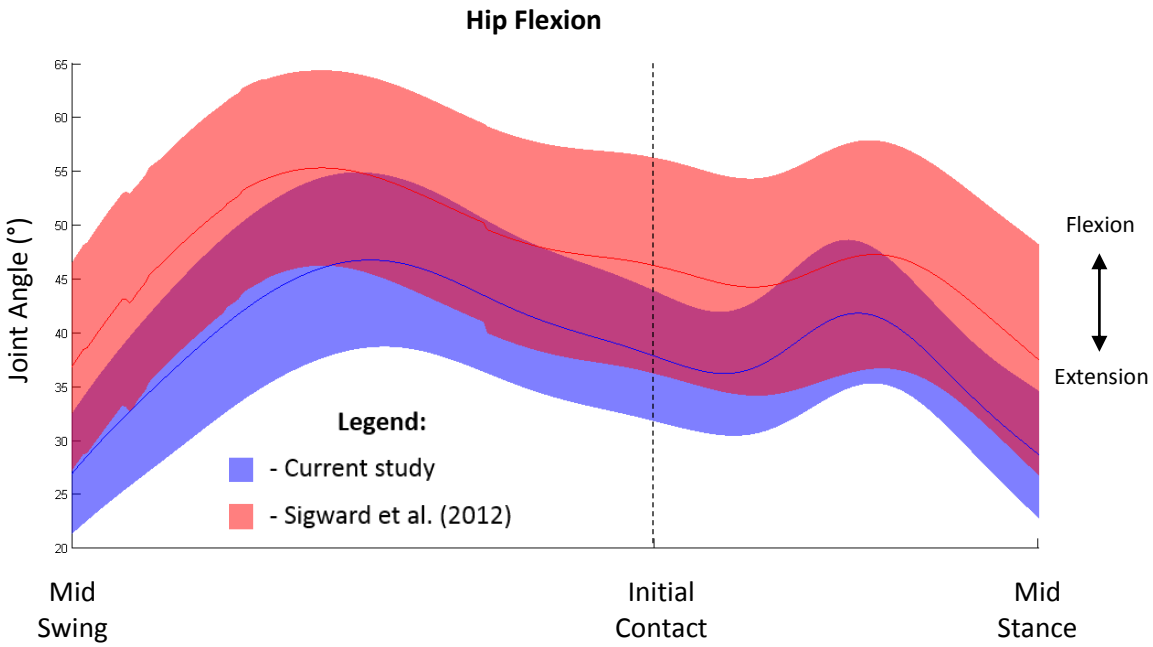

Figure C.10: Hip flexion kinematics obtained from the current study (blue) plotted against hip flexion kinematics obtained from the Sigward et al. (2012) study (red).

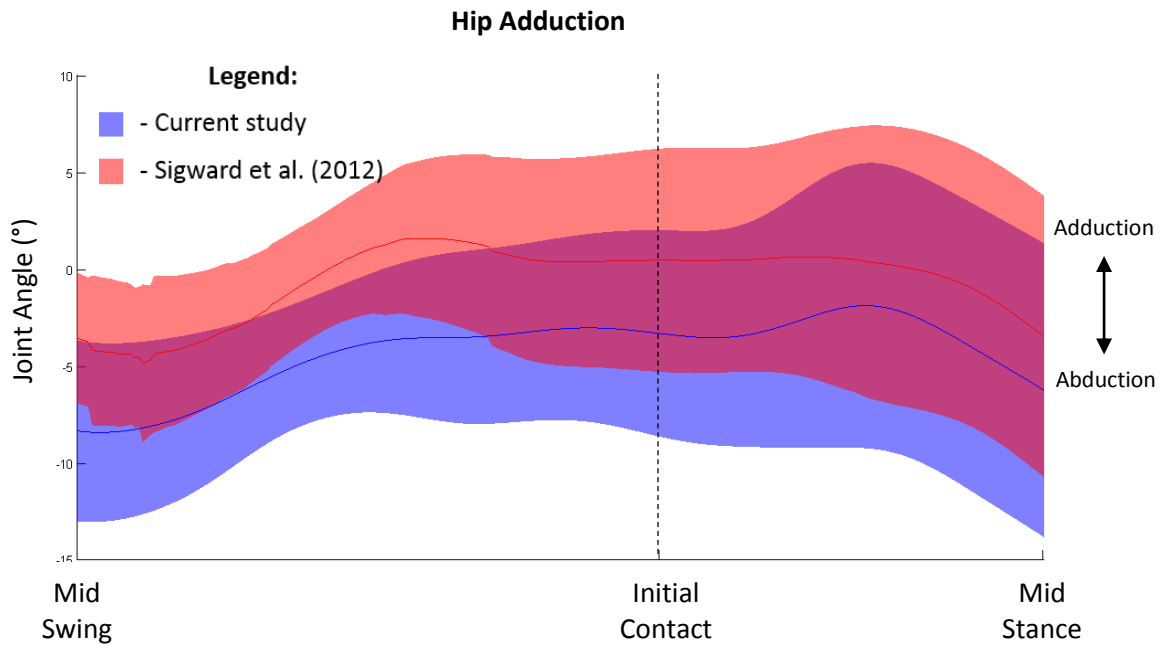

Figure C.11: Hip adduction kinematics obtained from the current study (blue) plotted against hip adduction kinematics obtained from the Sigward et al. (2012) study (red).

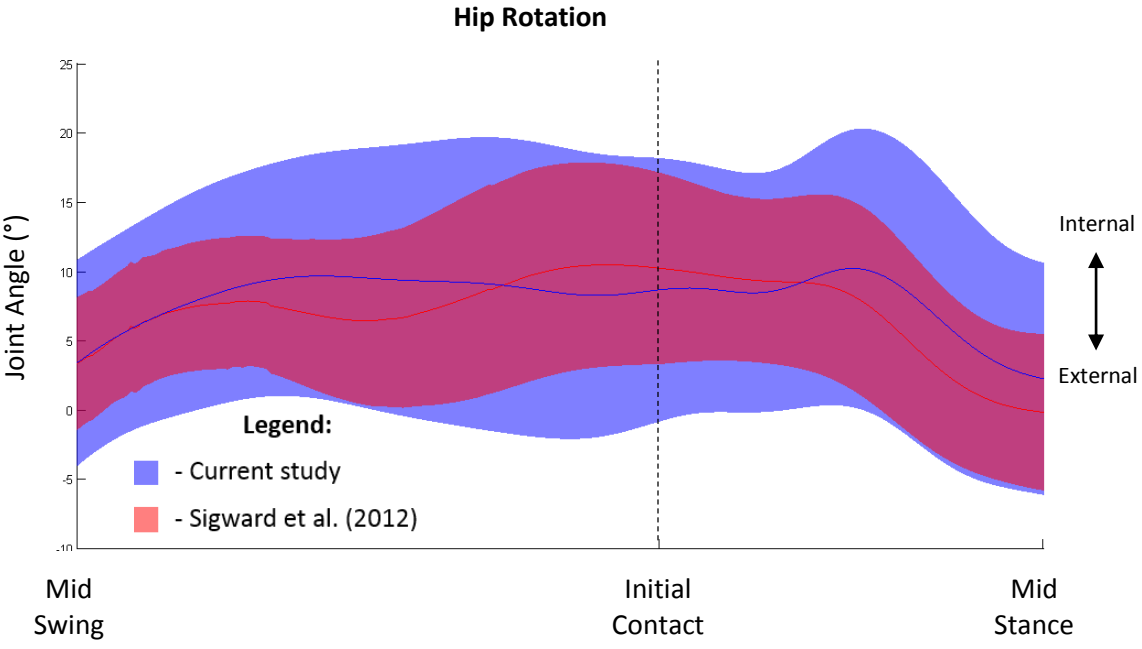

Figure C.12: Hip rotation kinematics obtained from the current study (blue) plotted against hip rotation kinematics obtained from the Sigward et al. (2012) study (red).

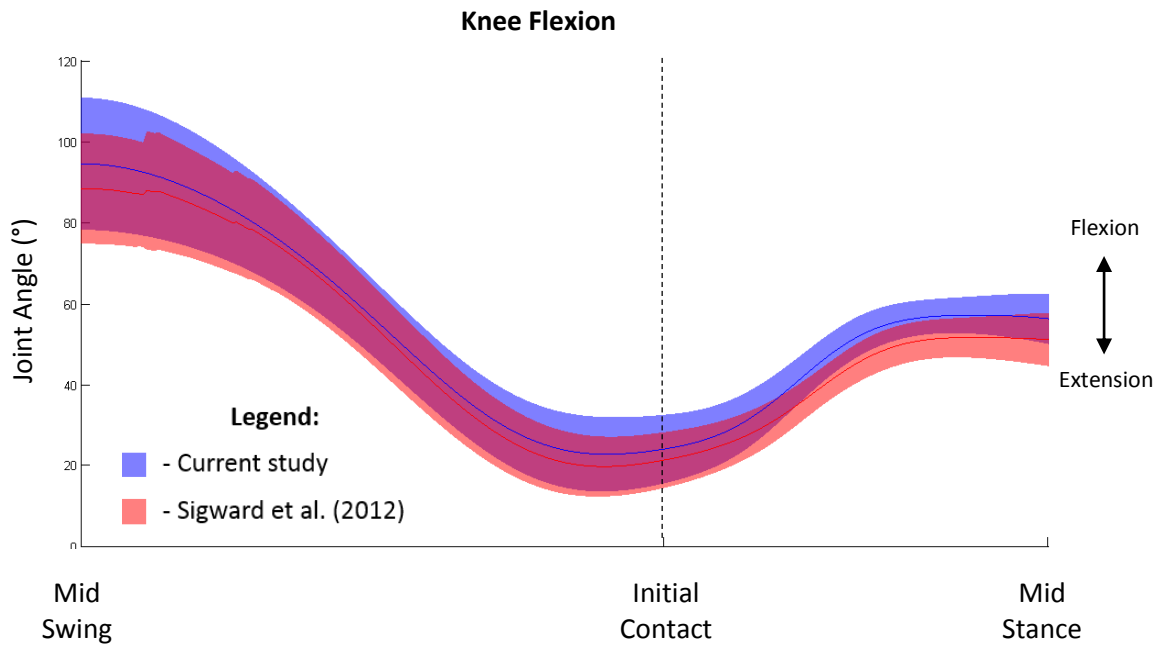

Figure C.13: Knee flexion kinematics obtained from the current study (blue) plotted against knee flexion kinematics obtained from the Sigward et al. (2012) study (red).

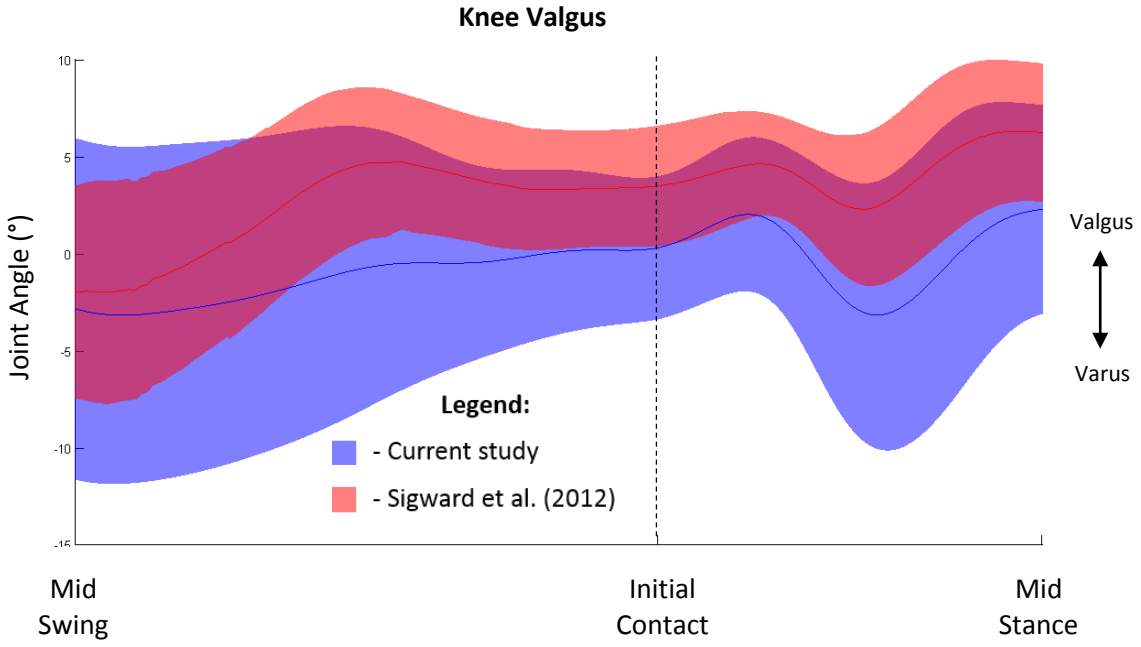

Figure C.14: Knee valgus kinematics obtained from the current study (blue) plotted against knee valgus kinematics obtained from the Sigward et al. (2012) study (red).

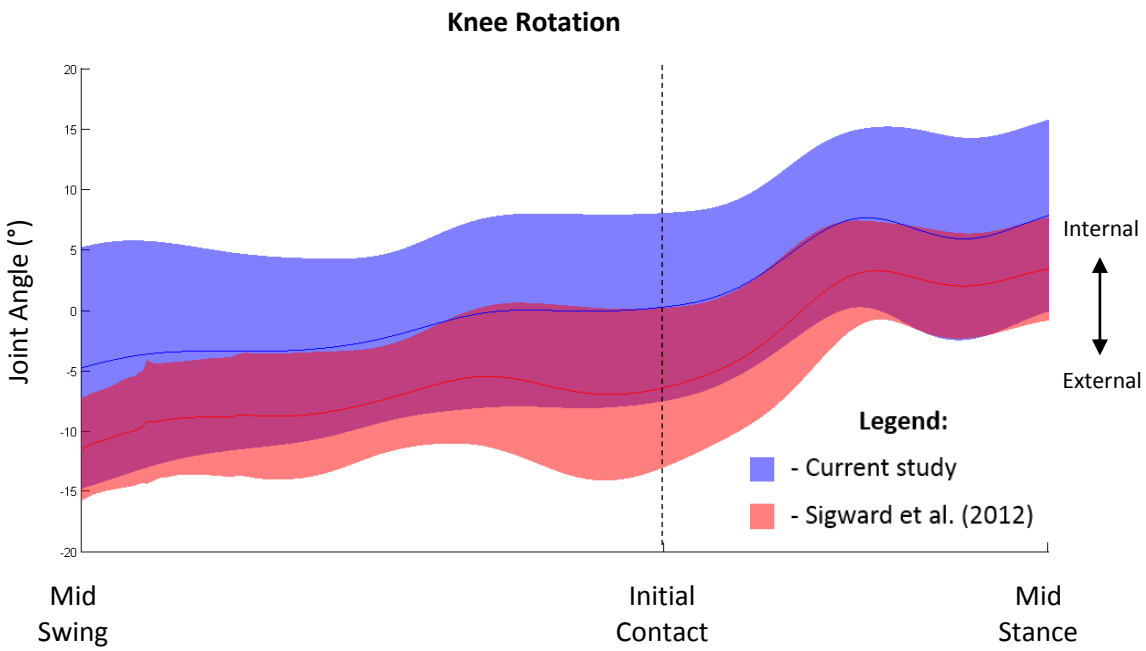

Figure C.15: Knee rotation kinematics obtained from the current study (blue) plotted against knee rotation kinematics obtained from the Sigward et al. (2012) study (red).

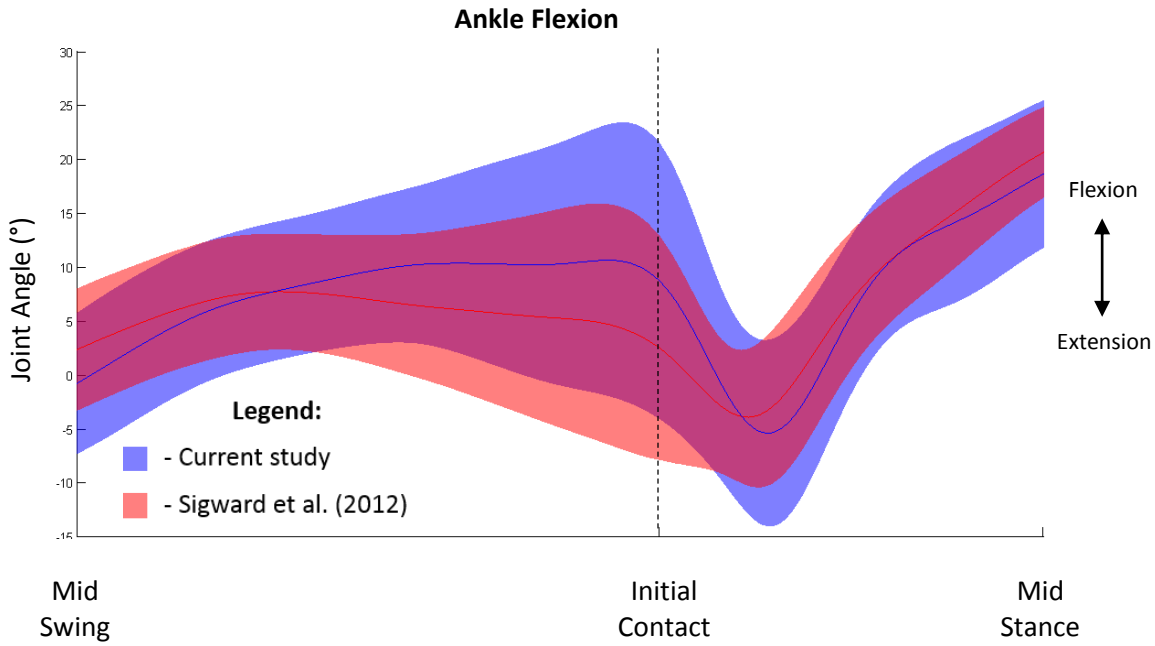

Figure C.16: Ankle flexion kinematics obtained from the current study (blue) plotted against ankle flexion kinematics obtained from the Sigward et al. (2012) study (red).

The normalized RMS errors listed in Table C.3 are within the pre-requisite two standard deviations, indicating that the kinematics obtained in this study agree strongly with those previously obtained by Sigward et al. (2012). Figure C.10 through to Figure C.16 provide graphical demonstrations of this agreement for each kinematic coordinate. These figures demonstrate that the error between the datasets is consistent for each of the coordinates, except for Hip Rotation. Figure C.12 suggests that the Hip Rotation kinematic patterns do not match well between the studies. Although the normalized root mean square error is less than one standard deviation (Table C.3), the error between the two sets of results for Hip Rotation is not consistent from mid-swing through to mid-stance as observed in the other kinematic coordinates. However, at the mid-swing, initial contact and mid-stance aspects of the movement, the agreement between the two datasets is strong.

This can be explained due to differences in the parameters of the models used by each of the studies. Firstly, two different software packages were used to obtain the results. Sigward et al. (2012) used Visual-3D (C-Motion, Inc., Rockville, MD) whereas this study used OpenSim (Chapter 7.3). Visual-3D and OpenSim have inherently different methods of processing motion capture data. Visual-3D automatically performs the scaling and inverse kinematics routines whereas OpenSim is more user driven, requiring the operator to manually place markers on the model and specify individual marker weights. Furthermore, the locations and orientations of joint centres are different between the two packages (C-Motion Inc 2014). The joint centres in OpenSim are fixed to the model, whereas Sigward et al. (2012) derived coordinate systems of the body segments from the static trial data. Finally, the musculoskeletal model used in this study differs to that developed by Sigward et al. The lower limbs were modelled as a frustra of cones, with the pelvis represented by an ellipsoid.

Thus, considering the inverse kinematic errors are well within tolerance (Appendix C.4), the confirmed visual representations of the simulations (Figure C.8), the test-retest reliability of the repeated trials (Appendix C.5), and the strong agreement with the results obtained by a previous (albeit with a different model) study (Appendix C.6), the obtained kinematics from mid-swing to mid-stance are an accurate representation of the real life movements performed by the athletes, validating the modelling pipeline.

Appendix D: Supplementary Material - Results:

D.1: Correlations between kinematic variables

Table D.1 displays the correlations beween the kinematic variables at mid-swing and initial contact that were found to be significantly correlated with maximum stance phase anteromedial or posterolateral strain (Chapter 9.3).

Correlations between kinematic variables

		Mid-swing				Initial Contact	
		Hip Rotation Position	Knee Varus Position	Knee Valgus Velocity	Lumbar Bending Velocity	Knee Varus Position	Knee Extension Velocity
Mid-swing	Hip Rotation Position	1	.884**	.367	.685*	.842**	.706*
	Knee Varus Position	.884**	1	.223	.595	.921**	.442
	Knee Valgus Velocity	.367	.223	1	.387	.210	.803**
	Lumbar Bending Velocity	.685*	.595	.387	1	.788**	.484
Initial Contact	Knee Varus Position	.842**	.921**	.210	.788**	1	.414
	Knee Extension Velocity	.706*	.442	.803**	.484	.414	1

***. Correlation is significant at the 0.05 level (2-tailed).**

****. Correlation is significant at the 0.01 level (2-tailed).**

Table D.1: Correlations between kinematic variables.

D.2: Model Building Summaries

Table D.2 and Table D.3 represent the five best performing subsets of predictor variables for the anteromedial and posterolateral bundles respectively. Each table indicates which predictor variables were included in the subset as well as the information criterion, R^2 value and standard error from the subsequent regression model.

Table D.2: Best performing subsets for the Anteromedial bundle (AMB) regression model

	1	2	3	4	5
Hip Rotation Position	X		X		X
Knee Varus Position		X	X	X	
Lumbar Bending Velocity				X	X
Information Criterion	18.488	19.424	20.740	22.200	22.476
R^2	0.791	0.770	0.829	0.802	0.797
Standard Error	2.118	2.219	2.045	2.200	2.230

Table D.2: Summary of the best performing models from the regression model for the anteromedial bundle.

Table D.3: Best performing subsets for the Posterolateral bundle (PLB) regression model

	1	2	3	4	5
Knee Varus Position	X	X	X	X	
Knee Valgus Velocity	X	X		X	X
Lumbar Bending Velocity		X			
Hip Rotation Position				X	X
Information Criterion	31.919	36.146	37.135	37.448	37.581
R^2	0.883	0.860	0.568	0.841	0.706
Standard Error	3.576	3.535	5.378	3.773	4.746

Table D.3: Summary of the best performing models from the regression model for the posterolateral bundle.

Appendix E: Human Research Ethics

E.1: University of Cape Town Human Research Ethics Committee

UNIVERSITY OF CAPE TOWN

Health Sciences Faculty
Human Research Ethics Committee
Room E52-24 Groote Schuur Hospital Old Main Building
Observatory 7925
Telephone [021] 406 6338 • **Facsimile** [021] 406 6411
e-mail: shuretta.thomas@uct.ac.za

15 May 2012

HREC REF: 172/2012

Dr L John
Human Biology
Anatomy Building

Dear Dr John

PROJECT TITLE: AN ALGORITHM FOR THE ANTICIPATION OF NON-CONTACT ANTERIOR CRUCIATE LIGAMENT INJURIES.

Thank you for responding to the issues raised by the Faculty of Health Sciences Human Research Ethics Committee in your letter dated 10th May 2012.

It is a pleasure to inform you that the HREC has **formally approved** the above-mentioned study.

Approval is granted for one year till the 30th May 2013.

Please submit a progress form, using the standardised Annual Report Form if the study continues beyond the approval period. Please submit a Standard Closure form if the study is completed within the approval period.
(Forms can be found on our website: www.health.uct.ac.za/research/humanethics/forms)

Please note that the ongoing ethical conduct of the study remains the responsibility of the principal investigator.

Please quote the HREC. REF in all your correspondence.

Yours sincerely

PROFESSOR M BLOCKMAN
CHAIRPERSON, HSF HUMAN ETHICS
Federal Wide Assurance Number: FWA00001637.
Institutional Review Board (IRB) number: IRB00001938

This serves to confirm that the University of Cape Town Human Research Ethics Committee complies to the Ethics Standards for Clinical Research with a new drug in patients, based on the Medical Research Council (MRC-SA), Food and Drug Administration (FDA-USA), International Convention on Harmonisation Good Clinical Practice (ICH GCP) and Declaration of Helsinki guidelines.
The Human Research Ethics Committee granting this approval is in compliance with the ICH Harmonised Tripartite Guidelines E6: Note for Guidance on Good Clinical Practice (CPMP/ICH/135/95) and FDA Code Federal Regulation Part 50, 56 and 312.

s.thomas

E.2: University of Southern California Institutional Review Board

Informed Consent Form

TITLE OF PROJECT: Do lower extremity kinematics, kinetics, and muscular control strategies differ between males and females across different stages of development while performing sports specific activities?

PRINCIPAL INVESTIGATOR: Christopher Powers PhD

DEPARTMENT: Biokinesiology and Physical Therapy

24-HOUR TELEPHONE NUMBER: (323) 442-2948

WHY IS THIS STUDY BEING DONE?

It has been determined that a major stabilizing ligament in the knee (anterior cruciate ligament) is more commonly injured by female athletes than male athletes. You are invited to participate in a research study that will look at the differences between males and females during athletic cutting, pivoting and landing maneuvers. This information will be used to help determine factors that contribute to anterior cruciate ligament knee injuries in females. This study will include 160 subjects (80 female athletes and 80 male athletes).

WHAT IS INVOLVED IN THE STUDY?

You will be asked to fill out a medical history form to see whether you are healthy and to see if you have a history of any injuries that would interfere with the study or that the investigators feel would make it unsafe for you to be in this study. You will be asked to fill out a questionnaire that will help us determine your level of physical maturity (i.e. if you have gone through or are going through your growth spurt). You will also be asked to fill out an activities questionnaire to see if you have experience in performing athletic maneuvers.

If you are eligible, based on these questions, and are willing to be in the study you will be scheduled for one visit at the USC Department of Biokinesiology and Physical Therapy's, Musculoskeletal Biomechanics Research Laboratory.

The one visit to the USC Biomechanics Research Laboratory will take place during a 2-week period and will require approximately 1.5 hours of your time.

If you are a subject in the study, you will be asked do the following for your visit to the USC Biomechanics Laboratory:

1. You will have your weight, height, and leg length measured.

2. You will be taught how to perform 5 different tasks normally done during sports activities. You will be asked to run forward and change directions after stepping on a marked spot. You will do this in two different directions. You will also be asked to jump up and land on a particular spot. In addition, you will be asked to kick a stationary soccer ball and to dribble/kick a soccer ball. You will be given time to practice each of these activities.

3. After practicing these activities small reflective markers will be taped to your skin on your legs and hips. In addition, reflective markers will be taped to your shoes. Furthermore, we will measure muscle activation during these tasks by taping electrodes to muscles on your leg.

4. You will then perform the activities again while being taped on a video recorder that sees the markers. We will record the trials of you performing each of the five activities. We will continue until five trials of complete data are collected.

5. If you are tired or have any pain or discomfort performing the activity you must tell the investigator and stop the activity.

WHAT ARE THE POSSIBLE RISKS AND DISCOMFORTS?

The study described above may involve the following risks and or discomforts:

1. There may be some muscle soreness of the thighs and legs from performing the exercises.

2. Even though you will have practiced the activity until you feel comfortable with it, there is a small risk of knee ankle or hip sprains or unexpected falls resulting in a fracture (broken bone).
3. Even though you will be performing these maneuvers in a controlled environment at a controlled speed there is risk of injury to your anterior cruciate ligament and other knee ligaments.

WHAT ARE THE POSSIBLE BENEFITS OF TAKING PART IN THIS STUDY?

There are no benefits to you from this study. We may learn about possible causes of anterior cruciate ligament injuries in athletes.

WHAT OTHER OPTIONS ARE THERE?

This is not a treatment study. An alternative would be not to participate in this study

WILL YOUR INFORMATION BE KEPT PRIVATE?

Every effort will be made to maintain the confidentiality of your medical records for this study by the investigator and the Institutional Review Board (IRB) to the extent permitted by law.

WHOM DO YOU CALL IF YOU HAVE QUESTIONS OR CONCERS?

This study will be supervised by Dr. Christopher Powers PT, PhD at the USC Department of Biokinesiology and Physical Therapy (phone: [323] 442-1928). Any questions you may have regarding the study or injuries sustained during the testing should be addressed to Dr. Powers. If you have questions regarding your rights as a study subject, you may contact the Institutional Review Board Office at (323) 223-2340. You will be given a copy of this form to keep.

ARE THERE ANY PAYMENTS TO YOU FOR TAKING PART IN THE STUDY?

You will be paid $25 for participating in this study.

WILL YOU RECEIVE NEW INFORMATION ABOUT THIS STUDY?

Any new information that is developed during the course of this research that may be related to your willingness to continue or discontinue participation in this study will be provided to you.

UNDER WHAT CIRCUMSTANCES CAN YOUR PARTICIPATION BE TERMINATED?

You may be terminated from this study without your consent if you fail to follow the investigator's instructions.

WHAT ARE YOUR RIGHTS AS A PARTICIPANT, AND WHAT WILL HAPPEN IF YOU DECIDE NOT TO PARTICIPATE?

Your participation in this study is voluntary. Your decision whether or not to participate in this study will not interfere with your future care at this institution. If you decide to participate, you are free to withdraw your consent and discontinue your participation at any time.

WHAT HAPPENS IF YOU GET INJURED OR NEED EMERGENCY CARE?

If you require medical treatment as a result of injury from your participation in this study, the financial responsibility for such care will be yours. Thus, you or your third party provider is financially responsible for such medical treatment and the University of Southern California can offer no monetary compensation.

AGREEMENT:

I have read (or someone has read to me) the information provided above. I have been given a chance to ask questions. All my questions were answered. I have decided to sign this form in order to take part in this study.

Subject's Signature_____ Date_____

Witness' Signature_____ Date_____

I have personally explained the research to the subject or the subject's legally authorized representative and answered all questions. I believe that he/she understands the information described in this informed consent and freely consents to participate.

Investigator's Signature_____ Date_____

Form Valid For Enrollment From
9/17/2008 To 8/18/2009
Institutional Review Board
HS-04A005

Appendix F: Software Code

F.1: Pre-processing

```
function File_Conversion
% Written by Shaun Fickling (The University of Cape Town)

% This function first converts a single C3D file into the required TRC and
% MOT files and then creates specific setup files for the Scaling, IK, RRA,
% CMC and Forward Dynamics tools.

%% Assumptions:
% Right legged trial (i.e. force plate data on right leg only)


%% Acknowledgements:

%% 1. MATLAB-OpenSim Interface Software
% By Glen Lichtwark
% The University of Queensland

%% 2. MATLAB TOOLBOX FOR C3DSERVER – VERSION 2
% Matthew R. Walker, Michael J. Rainbow
% Motion Analysis Laboratory
% Shriners Hospitals for Children – Erie PA (USA)
% Version 2: April 21, 2006

%% 3. XML Toolbox for Matlab
% Copyright (c) 2007 Jarek Tuszynski
%
% Permission is hereby granted, free of charge, to any person
% obtaining a copy of this software and associated documentation
% files (the "Software"), to deal in the Software without
% restriction, including without limitation the rights to use,
% copy, modify, merge, publish, distribute, sublicense, and/or sell
% copies of the Software, and to permit persons to whom the
% Software is furnished to do so, subject to the following
% conditions:
%
% The above copyright notice and this permission notice shall be
% included in all copies or substantial portions of the Software.
%
% THE SOFTWARE IS PROVIDED "AS IS", WITHOUT WARRANTY OF ANY KIND,
% EXPRESS OR IMPLIED, INCLUDING BUT NOT LIMITED TO THE WARRANTIES
% OF MERCHANTABILITY, FITNESS FOR A PARTICULAR PURPOSE AND
% NONINFRINGEMENT. IN NO EVENT SHALL THE AUTHORS OR COPYRIGHT
% HOLDERS BE LIABLE FOR ANY CLAIM, DAMAGES OR OTHER LIABILITY,
% WHETHER IN AN ACTION OF CONTRACT, TORT OR OTHERWISE, ARISING
% FROM, OUT OF OR IN CONNECTION WITH THE SOFTWARE OR THE USE OR
% OTHER DEALINGS IN THE SOFTWARE.

%% Initialise

  clear;
  clc;
```

```
Results_Path = 'C:\Pipeline\OpenSim_Files\Pipeline_Results\';
Generic_Path = 'C:\Pipeline\OpenSim_Files\Generic_Setup_Files\';
Model_Path = 'C:\Pipeline\OpenSim_Files\Models\';

Fields = {'Hip_Ang', 'Hip_Add', 'Hip_Rot', 'Knee_Ang', 'Knee_Val', 'Knee_Rot', 'Ank_Ang' };
Analog_Fields = {'VL', 'MH', 'LH', 'GMED', 'GMAX', 'MG'};

USC.All = struct('Hip_Ang', [], 'Hip_Add', [],'Hip_Rot', [],'Knee_Ang', [],'Knee_Val', [],'Knee_Rot', [],'Ank_Ang', []);
Scut_List = {};
Vcut_List = {};


%% Select C3D Folder to Process

% Here the user needs to specify whether or not the file being converted
% is of a Static or Dynamic Motion Capture Trial
Dynamic = true;  %default
Cut = [];
type = menu('Choose type of trial to be converted','Static','Dynamic - Scut');

if (type == 1)  %Static Trial Conversion
   [Path_Name] = uigetdir('*.c3d', 'Please select the folder containing the Static Trials');
   Dynamic = false; %Static
   Cut = '\';
elseif (type == 2) %Dynamic Scut Trial Conversion
   [Path_Name] = uigetdir('*.c3d', 'Please select the folder containing the Scut Dynamic Trials');
   Cut = '\Scut\';
else
   disp('No option chosen, please try again');
   return;
end

Path_Name = [Path_Name '\'];
% Path_Name should contain the path of the subject-specific C3D data (i.e. C:\Pipeline\Input\Subject Data\TestSubject\)
% From the C3D data we create the .trc, _grf.mot, _grf.xml and
% Scaleset.xml (manual scaling) files which will be saved in the same directory

Listing = dir(Path_Name);
Listing = Listing(3:end); %Cuts out the first two null values in Listing

%% PROCESS EACH FILE IN THE FOLDER (Main Loop)
for i = 1:(length(Listing))

File_Name = Listing(i).name;
disp(['Processing File: ' File_Name]);

% Remove ".c3d" from end of File_Name to get the name and trial number of the subject
Full = strtok(File_Name, '.');
Len = length(Full);

Subject_Name = Full(1:Len-2); %This is necessary because the subject name isn't in the C3D file, but is part of the filename

if (~Dynamic)  %Static Trial
   Trial_Number = 'Static';
elseif (Dynamic) %Dynamic Trial
   Trial_Number = ['Step_' Full(Len-1:Len)]; %Used to seperate individual trials from the same subject
```

```
    end

    Subject_Specific_Path = 'C:\Pipeline\OpenSim_Files\Subject_Specific\';
    Subject_Path = [Subject_Specific_Path Subject_Name  Cut Trial_Number '\'];

    % The Variable 'Subject_Path' contains the location of the subject-specific model files used for each simulation
    % The output files from the Scale, IK, RRA and CMC Pipeline tools are also located here

%% Check if directory already exists

if (isdir(Subject_Path))
    rmdir(Subject_Path, 's'); %Remove all old files and directory
end

    mkdir(Subject_Path); %create new directory
    cd (Subject_Path);

    % Create directory and set the current directory to the location of the Subject Specific files.
    % Thus everything output by this Conversion pipeline will be saved in
    % this location

%% Load C3D File
% loads the c3dfiles into MATLAB variables
  Data = [];
  A_Data = [];
  FP_Info = [];
  MP_Info = [];

  [Data, A_Data, FP_Info, MP_Info] = loadc3dfile([Path_Name, File_Name]);

  %Check that everything has been loaded correctly. If not, retry
  while ((isempty(Data)) || (isempty(A_Data)) || (isempty(FP_Info)) || (isempty(MP_Info)) )
    disp('Matrix Empty, attempting again...');
    Data = [];
    A_Data = [];
    FP_Info = [];
    MP_Info = [];
    [Data, A_Data, FP_Info, MP_Info] = loadc3dfile([Path_Name, File_Name]);
  end
% Static_FP_Info.Number = 0; %Discard Forceplate data for the static trial

%% Sort C3D Files
% data sorted into new fields depending on whether it is Marker data, Angle data, Moment data etc. eg. data.Marker.ASIS
rather than data.ASIS"
    Marker_List = {};
    if (~Dynamic)
        Marker_List = {'RMTH1'; 'RMTH5'; 'RDIFT'; 'RMEMA'; 'RLAMA'; 'RMEKN'; 'RLAKN'; 'RGTR'; 'RASIS';...
                    'LMTH1'; 'LMTH5'; 'LDIFT'; 'LMEMA'; 'LLAMA'; 'LMEKN'; 'LLAKN'; 'LGTR'; 'LASIS';...
                    'RILCR'; 'LILCR'; 'L5S1'; 'RTMTH'; 'RTLTH'; 'RBMTH'; 'RBLTH'; 'RTMSH'; 'RTLSH';...
                    'RBMSH'; 'RBLSH'; 'RPRHE'; 'RDIHE'; 'RLAHE'; 'LTMTH'; 'LTLTH'; 'LBMTH'; 'LBLTH';...
                    'LTMSH'; 'LTLSH'; 'LBMSH'; 'LBLSH'; 'LPRHE'; 'LDIHE'; 'LLAHE'; 'LTTR'; 'RTTR'; 'LBTR'};
    else
        Marker_List = {'L5S1'; 'RILCR'; 'RTMTH'; 'RTLTH'; 'RBMTH'; 'RBLTH'; 'RTMSH'; 'RTLSH';...
                    'RBMSH'; 'RBLSH'; 'RPRHE'; 'RDIHE'; 'RLAHE'; 'LILCR'; 'LTMTH'; 'LTLTH'; 'LBMTH'; 'LBLTH';...
                    'LTMSH'; 'LTLSH'; 'LBMSH'; 'LBLSH'; 'LPRHE'; 'LDIHE'; 'LLAHE'; 'LTTR'; 'RTTR'; 'LBTR'};
    end
```

```
   Data = sort_c3d((Data), Marker_List);

%% Add Subject Data (from file) to MP_Info
%Subject name, mass, height and gender (1 = F, 0 = M) can be found in the Subject_Details MAT file

 load('Subject_Data.mat'); %Loads the CellArray
 row = [];
 col = [];
 [row, col] = size(Subject_Data);

 for j = 1:row
    temp = cell2mat(Subject_Data(j,1));
    if strcmp(temp, Subject_Name)
       MP_Info.Height = cell2mat(Subject_Data(j,2));
       MP_Info.Bodymass = cell2mat(Subject_Data(j,3));
       MP_Info.Gender = cell2mat(Subject_Data(j,4));
    end
 end

 MP_Info.Name = Subject_Name;
 Data.Name = Subject_Name;

 Data.Trial_Number = Trial_Number;

%% Define start and end points and
   if (~Dynamic)
      Data.Start_Frame = Data.Start_Frame + round(Data.Rate); %Give the subject time to settle (i.e. cut off 0.5 seconds in the
beginning)
      Data.End_Frame = Data.End_Frame - round(Data.Rate);                %(i.e. cut off the final 0.5 seconds)
   elseif (Dynamic)
      % For the Dynamic Trial:
      % Find the time of first foot contact. E(1)
      % Start = E(1) - 0.7sec
      % End = E(1) + 0.7sec

      %NOTE: The USC data uses the second force plate because all the subjects are stepping off their right legs!

      E = [];
      clear a
      a = find(A_Data.CH_2FZ < 0.01*min(A_Data.CH_2FZ));
         if ~isempty(a)
            P = round((a(1)*Data.Rate/A_Data.Rate)):round((a(end)*Data.Rate/A_Data.Rate));
            E(1) = min([min(E) P(1)]); %First foot contact (i.e. Beginning of Stance Phase)
            E(2) = max([max(E) P(end)]); %Last Foot Contact (i.e. End of Stance Phase)
         end

      Window = ceil((Data.Rate)*0.30);
      %The number of frames corresponding to 300 milliseconds - arbitrary

      % redefine start and end frames from the events to write the appropriate TRC
      % and MOT files for the OpenSim simulations
      Data.Start_Frame = E(1) - Window - 1; %300ms of swing phase
      Data.End_Frame = E(1) + Window; %300ms of stance phase. we don't take E2 into account, we only care about the 0.25 sec
before and after IC
```

```
    %at 250hz, this creates 152 data points. The first 76 = Swing, last 76 = stance

    Data.SP_Start = E(1) - Data.Start_Frame + 1;
    Data.SP_End = E(2) - Data.Start_Frame + 1;

    %Position of Maximum Vertical GRF
    [~, MaxPos] = min(A_Data.CH_2FZ(a));
    Data.Max_GRF = round(a(MaxPos)*(Data.Rate/A_Data.Rate)) - Data.Start_Frame + 1;

    %NOTE: In the conversion to TRC, the c3d2xml function takes the difference in frame rate between data and a_data into
account.
  end

%% Convert to TRC

  TRC_File_Name = [Subject_Name '_' Trial_Number '.trc'];
  [DataOut] = c3d2trc(Data, A_Data, FP_Info, MP_Info, TRC_File_Name, Dynamic);

    %Trim Marker Data
    for k = (1: length(Marker_List))
      try
        Temp = DataOut.Markers.(Marker_List{k});
        Temp = Temp(DataOut.Start_Frame:DataOut.End_Frame,:);
        DataOut.Markers.(Marker_List{k}) = [];
        DataOut.Markers.(Marker_List{k}) = Temp;
      catch
        disp([Marker_List{k} ' not found']);
      end
    end

    if(Dynamic)
    %Functions needed for the Dynamic Trial only

      % Setup GRF xml file (Dynamic Only)

      ExForce{1} = 'ExternalForce_1';
      ApBodies{1} = 'calcn_r';

      GRFFile = [Subject_Path Subject_Name '_' Trial_Number '_grf.mot'];
      MOTFile = [Subject_Path Subject_Name '_' Trial_Number '_ik.mot'];

      ForceIdentifier{1} = '2_ground_force_v';
      PointIdentifier{1} = '2_ground_force_p';
      TorqueIdentifier{1} = '2_ground_torque_';

      grf2xml(DataOut,'ExternalLoadNames',ExForce,'AppliedToBodies',ApBodies,...
        'GRFFile',GRFFile,'MOTFile',MOTFile,'LowPassFilterForKinematics',15,...
        'ForceIdentifier', ForceIdentifier, 'PointIdentifier', PointIdentifier,...
        'TorqueIdentifier', TorqueIdentifier);


    % Save and trim USC Results
    [Kin] = Get_USC_Data(File_Name, Data.Start_Frame, Data.End_Frame);

    for m = 1:length(Fields)
```

```
            USC.All.(Fields{m}) = [USC.All.(Fields{m}) Kin.(Fields{m})];
        end

        Scut_List = [Scut_List File_Name];



        end

    % Save Important Data to file
        if (Dynamic) % Mass & Height not needed
            save('Data.mat', '-struct', 'DataOut', 'Rate', 'Name', 'Trial_Number', 'Markers', 'True_Start', 'True_End', 'SP_End',
'SP_Start', 'Max_GRF');
        else       % Marker Data not needed
            save('Data.mat', '-struct', 'DataOut', 'Start_Frame', 'End_Frame', 'Rate', 'Name', 'Trial_Number', 'Mass', 'Height');
        end

        disp(['Completed Processing File: ' File_Name]);

    %end %End of if(Trial Deleted)
    end % End of Main Processing Loop


    %Save Full Set of Data to Results Path
    if (Dynamic)
    save([Results_Path 'USC.mat'], 'USC');
    save([Results_Path 'Scut_List.mat'], 'Scut_List');
    end

    disp('Processing Complete');

end % End of Function
```

F.2: Edited Gait2392 OpenSim Model

F.2.1: Knee Joint

```
<Body name="tibia_r">
        <mass>3.7075</mass>
        <mass_center> 0 -0.1867 0</mass_center>
        <inertia_xx>0.0504</inertia_xx>
        <inertia_yy>0.0051</inertia_yy>
        <inertia_zz>0.0511</inertia_zz>
        <inertia_xy>0</inertia_xy>
        <inertia_xz>0</inertia_xz>
        <inertia_yz>0</inertia_yz>
        <Joint>
                <CustomJoint name="knee_r">
                        <parent_body>femur_r</parent_body>
                        <location_in_parent>0 0 0</location_in_parent>
                        <orientation_in_parent>0 0 0</orientation_in_parent>
                        <location>0 0 0</location>
                        <orientation>0 0 0</orientation>
                        <CoordinateSet>
                                <objects>
                                        <Coordinate name="knee_flexion_r">
                                                <motion_type>rotational</motion_type>
                                                <default_value>0</default_value>

                                                <default_speed_value>0</default_speed_value>

                                                <range>-2.0943951 0.17453293</range>
                                                <clamped>false</clamped>
                                                <locked>false</locked>
                                                <prescribed_function />
                                                <prescribed>false</prescribed>
                                        </Coordinate>
                                        <Coordinate name="knee_valgus_r">
                                                <motion_type>rotational</motion_type>
                                                <default_value>0</default_value>
                                                <default_speed_value>0</default_speed_value>
                                                <range>-0.523598775 0.523598775</range>
                                                <clamped>false</clamped>
                                                <locked>false</locked>
                                                <prescribed_function />
                                                <prescribed>false</prescribed>
                                        </Coordinate>
                                        <Coordinate name="knee_rotation_r">
                                                <motion_type>rotational</motion_type>
                                                <default_value>0</default_value>
                                                <default_speed_value>0</default_speed_value>
                                                <range>-0.523598775 0.523598775</range>
                                                <clamped>false</clamped>
                                                <locked>false</locked>
                                                <prescribed_function />
                                                <prescribed>false</prescribed>
                                        </Coordinate>
                                </objects>
                                <groups />
                        </CoordinateSet>
                        <reverse>false</reverse>
```

```
<SpatialTransform>
	<TransformAxis name="rotation1">
		<coordinates>knee_flexion_r</coordinates>
			<axis>0 0 1</axis>
			<function>
				<LinearFunction>
					<coefficients> 1 0</coefficients>
				</LinearFunction>
			</function>
	</TransformAxis>
	<TransformAxis name="rotation2">
		<coordinates>knee_valgus_r</coordinates>
			<axis>-1 0 0</axis>
			<function>
				<LinearFunction>
					<coefficients> 1 0</coefficients>
				</LinearFunction>
			</function>
	</TransformAxis>
	<TransformAxis name="rotation3">
		<coordinates>knee_rotation_r</coordinates>
			<axis>0 1 0</axis>
			<function>
				<LinearFunction>
					<coefficients> 1 0</coefficients>
				</LinearFunction>
			</function>
	</TransformAxis>
	<TransformAxis name="translation1">
		<coordinates>knee_flexion_r</coordinates>
			<axis>1 0 0</axis>
			<function>
				<SimmSpline>
					<x> -2.0944 -1.74533 -1.39626 -1.0472 -
0.698132 -0.349066 -0.174533 0.197344 0.337395 0.490178 1.52146 2.0944</x>
					<y> -0.0032 0.00179 0.00411 0.0041 0.00212 -
0.001 -0.0031 -0.005227 -0.005435 -0.005574 -0.005435 -0.00525</y>
				</SimmSpline>
			</function>
	</TransformAxis>
	<TransformAxis name="translation2">
		<coordinates>knee_flexion_r</coordinates>
			<axis>0 1 0</axis>
			<function>
				<SimmSpline>
					<x> -2.0944 -1.22173 -0.523599 -0.349066 -
0.174533 0.159149 2.0944</x>
					<y> -0.4226 -0.4082 -0.399 -0.3976 -0.3966 -
0.395264 -0.396</y>
				</SimmSpline>
			</function>
	</TransformAxis>
	<TransformAxis name="translation3">
		<coordinates></coordinates>
			<axis>0 0 1</axis>
			<function>
				<Constant>
					<value>0</value>
```

```
                                        </Constant>
                                    </function>
                                </TransformAxis>
                            </SpatialTransform>
                        </CustomJoint>
                    </Joint>
                    <VisibleObject>
                        <GeometrySet>
                            <objects>
                                <DisplayGeometry>
                                    <geometry_file>tibia.vtp</geometry_file>
                                    <color> 1 1 1</color>
                                    <texture_file />
                                    <transform> -0 0 -0 0 0 0</transform>
                                    <scale_factors> 1 1 1</scale_factors>
                                    <display_preference>4</display_preference>
                                    <opacity>1</opacity>
                                </DisplayGeometry>
                                <DisplayGeometry>
                                    <geometry_file>fibula.vtp</geometry_file>
                                    <color> 1 1 1</color>
                                    <texture_file />
                                    <transform> -0 0 -0 0 0 0</transform>
                                    <scale_factors> 1 1 1</scale_factors>
                                    <display_preference>4</display_preference>
                                    <opacity>1</opacity>
                                </DisplayGeometry>
                            </objects>
                            <groups />
                        </GeometrySet>
                        <scale_factors> 1 1 1</scale_factors>
                        <transform> -0 0 -0 0 0 0</transform>
                        <show_axes>false</show_axes>
                        <display_preference>4</display_preference>
                    </VisibleObject>
                    <WrapObjectSet>
                        <objects />
                        <groups />
                    </WrapObjectSet>
</Body>
```

F.2.2: Ligaments

```
<ForceSet>
    <objects>
        <Thelen2003Muscle name="AMB">
            <isDisabled>false</isDisabled>
            <min_control>0</min_control>
            <max_control>1</max_control>
            <GeometryPath>
                <PathPointSet>
                    <objects>
                        <PathPoint name="AMB-P1">
                        <location> -0.009 -0.405 0.007</location>
                            <body>femur_r</body>
                        </PathPoint>
                        <PathPoint name="AMB-P2">
```

```
                                        <location> 0.009 -0.032 -0.005</location>
                                                <body>tibia_r</body>
                                        </PathPoint>
                                </objects>
                                <groups />
                        </PathPointSet>
                        <PathWrapSet>
                                <objects />
                                <groups />
                        </PathWrapSet>
                        <VisibleObject name="display">
                                <GeometrySet>
                                        <objects />
                                        <groups />
                                </GeometrySet>
                                <scale_factors> 1 1 1</scale_factors>
                                <transform> -0 0 -0 0 0 0</transform>
                                <show_axes>false</show_axes>
                                <display_preference>4</display_preference>
                        </VisibleObject>
                </GeometryPath>
                <optimal_force>1</optimal_force>
                <max_isometric_force>100</max_isometric_force>
                <optimal_fiber_length>0.01</optimal_fiber_length>
                <tendon_slack_length>0.24</tendon_slack_length>
                <pennation_angle_at_optimal>0</pennation_angle_at_optimal>
                <max_contraction_velocity>10</max_contraction_velocity>
                <activation_time_constant>0.01</activation_time_constant>
                <deactivation_time_constant>0.04</deactivation_time_constant>
                <FmaxTendonStrain>0.033</FmaxTendonStrain>
                <FmaxMuscleStrain>0.6</FmaxMuscleStrain>
                <KshapeActive>0.5</KshapeActive>
                <KshapePassive>4</KshapePassive>
                <Af>0.3</Af>
                <Flen>1.8</Flen>
        </Thelen2003Muscle>
        <Thelen2003Muscle name="PLB">
                <isDisabled>false</isDisabled>
                <min_control>0</min_control>
                <max_control>1</max_control>
                <GeometryPath>
                        <PathPointSet>
                                <objects>
                                        <PathPoint name="PLB-P1">
                                        <location> -0.014 -0.409 0.009</location>
                                                <body>femur_r</body>
                                        </PathPoint>
                                        <PathPoint name="PLB-P2">
                                        <location> 0.002 -0.033 -0.005</location>
                                                <body>tibia_r</body>
                                        </PathPoint>
                                </objects>
                                <groups />
                        </PathPointSet>
                        <PathWrapSet>
                                <objects />
                                <groups />
                        </PathWrapSet>
```

```
                                        <VisibleObject name="display">
                                                <GeometrySet>
                                                        <objects />
                                                        <groups />
                                                </GeometrySet>
                                                <scale_factors> 1 1 1</scale_factors>
                                                <transform> -0 0 -0 0 0 0</transform>
                                                <show_axes>false</show_axes>
                                                <display_preference>4</display_preference>
                                        </VisibleObject>
                                </GeometryPath>
                                <optimal_force>1</optimal_force>
                                <max_isometric_force>100</max_isometric_force>
                                <optimal_fiber_length>0.01</optimal_fiber_length>
                                <tendon_slack_length>0.24</tendon_slack_length>
                                <pennation_angle_at_optimal>0</pennation_angle_at_optimal>
                                <max_contraction_velocity>10</max_contraction_velocity>
                                <activation_time_constant>0.01</activation_time_constant>
                                <deactivation_time_constant>0.04</deactivation_time_constant>
                                <FmaxTendonStrain>0.033</FmaxTendonStrain>
                                <FmaxMuscleStrain>0.6</FmaxMuscleStrain>
                                <KshapeActive>0.5</KshapeActive>
                                <KshapePassive>4</KshapePassive>
                                <Af>0.3</Af>
                                <Flen>1.8</Flen>
                        </Thelen2003Muscle>
                </objects>
                <groups />
</ForceSet>
```

F.2.3: Model Markers

```
<MarkerSet>
        <objects>
                <Marker name="RMTH1">
                        <body>toes_r</body>
                        <location> 0.006 0.015 -0.05</location>
                        <fixed>false</fixed>
                </Marker>
                <Marker name="RMTH5">
                        <body>toes_r</body>
                        <location> 0.025 0 0.07</location>
                        <fixed>false</fixed>
                </Marker>
                <Marker name="RMEMA">
                        <body>tibia_r</body>
                        <location> 0.006 -0.3888 -0.038</location>
                        <fixed>false</fixed>
                </Marker>
                <Marker name="RLAMA">
                        <body>tibia_r</body>
                        <location> -0.01 -0.41 0.053</location>
                        <fixed>false</fixed>
                </Marker>
                <Marker name="RMEKN">
                        <body>femur_r</body>
                        <location> 0.01 -0.41 -0.06</location>
```

```
            <fixed>false</fixed>
</Marker>
<Marker name="RLAKN">
            <body>femur_r</body>
            <location> -0.01 -0.4 0.06</location>
            <fixed>false</fixed>
</Marker>
<Marker name="RGTR">
            <body>femur_r</body>
            <location> -0.016 -0.015 0.115</location>
            <fixed>false</fixed>
</Marker>
<Marker name="RASIS">
            <body>pelvis</body>
            <location> 0.02 0.03 0.128</location>
            <fixed>false</fixed>
</Marker>
<Marker name="RDIFT">
            <body>toes_r</body>
            <location> 0.06 0.035 0</location>
            <fixed>false</fixed>
</Marker>
<Marker name="LMTH1">
            <body>toes_l</body>
            <location> 0.006 0.015 0.05</location>
            <fixed>false</fixed>
</Marker>
<Marker name="LMTH5">
            <body>toes_l</body>
            <location> 0.025 0 -0.07</location>
            <fixed>false</fixed>
</Marker>
<Marker name="LMEMA">
            <body>tibia_l</body>
            <location> 0.006 -0.3888 0.038</location>
            <fixed>false</fixed>
</Marker>
<Marker name="LLAMA">
            <body>tibia_l</body>
            <location> -0.01 -0.41 -0.053</location>
            <fixed>false</fixed>
</Marker>
<Marker name="LMEKN">
            <body>femur_l</body>
            <location> 0.01 -0.41 0.06</location>
            <fixed>false</fixed>
</Marker>
<Marker name="LLAKN">
            <body>femur_l</body>
            <location> -0.01 -0.4 -0.06</location>
            <fixed>false</fixed>
</Marker>
<Marker name="LGTR">
            <body>femur_l</body>
            <location> -0.016 -0.015 -0.115</location>
            <fixed>false</fixed>
</Marker>
<Marker name="LASIS">
```

```
            <body>pelvis</body>
            <location> 0.02 0.03 -0.128</location>
            <fixed>false</fixed>
</Marker>
<Marker name="LDIFT">
            <body>toes_l</body>
            <location> 0.06 0.035 0</location>
            <fixed>false</fixed>
</Marker>
<Marker name="L5S1">
            <body>pelvis</body>
            <location> -0.16 0.076 0</location>
            <fixed>false</fixed>
</Marker>
<Marker name="RILCR">
            <body>pelvis</body>
            <location> -0.07 0.09 0.15</location>
            <fixed>false</fixed>
</Marker>
<Marker name="RTMTH">
            <body>femur_r</body>
            <location> -0.04 -0.2 0.08</location>
            <fixed>false</fixed>
</Marker>
<Marker name="RTLTH">
            <body>femur_r</body>
            <location> 0.04 -0.2 0.08</location>
            <fixed>false</fixed>
</Marker>
<Marker name="RBMTH">
            <body>femur_r</body>
            <location> -0.04 -0.28 0.07</location>
            <fixed>false</fixed>
</Marker>
<Marker name="RBLTH">
            <body>femur_r</body>
            <location> 0.04 -0.28 0.07</location>
            <fixed>false</fixed>
</Marker>
<Marker name="RTMSH">
            <body>tibia_r</body>
            <location> -0.04 -0.12 0.07</location>
            <fixed>false</fixed>
</Marker>
<Marker name="RTLSH">
            <body>tibia_r</body>
            <location> 0.04 -0.12 0.07</location>
            <fixed>false</fixed>
</Marker>
<Marker name="RBMSH">
            <body>tibia_r</body>
            <location> -0.04 -0.2 0.07</location>
            <fixed>false</fixed>
</Marker>
<Marker name="RBLSH">
            <body>tibia_r</body>
            <location> 0.04 -0.2 0.07</location>
            <fixed>false</fixed>
```

```
</Marker>
<Marker name="RPRHE">
        <body>foot_r</body>
        <location> -0.02 0.06 0</location>
        <fixed>false</fixed>
</Marker>
<Marker name="RDIHE">
        <body>foot_r</body>
        <location> -0.04 0.02 0.005</location>
        <fixed>false</fixed>
</Marker>
<Marker name="RLAHE">
        <body>foot_r</body>
        <location> 0.03 0.02 0.05</location>
        <fixed>false</fixed>
</Marker>
<Marker name="LILCR">
        <body>pelvis</body>
        <location> -0.07 0.09 -0.15</location>
        <fixed>false</fixed>
</Marker>
<Marker name="LTMTH">
        <body>femur_l</body>
        <location> -0.04 -0.16 -0.08</location>
        <fixed>false</fixed>
</Marker>
<Marker name="LTLTH">
        <body>femur_l</body>
        <location> 0.04 -0.16 -0.08</location>
        <fixed>false</fixed>
</Marker>
<Marker name="LBMTH">
        <body>femur_l</body>
        <location> -0.04 -0.24 -0.07</location>
        <fixed>false</fixed>
</Marker>
<Marker name="LBLTH">
        <body>femur_l</body>
        <location> 0.04 -0.24 -0.07</location>
        <fixed>false</fixed>
</Marker>
<Marker name="LTMSH">
        <body>tibia_l</body>
        <location> -0.04 -0.12 -0.07</location>
        <fixed>false</fixed>
</Marker>
<Marker name="LTLSH">
        <body>tibia_l</body>
        <location> 0.04 -0.12 -0.07</location>
        <fixed>false</fixed>
</Marker>
<Marker name="LBMSH">
        <body>tibia_l</body>
        <location> -0.04 -0.2 -0.07</location>
        <fixed>false</fixed>
</Marker>
<Marker name="LBLSH">
        <body>tibia_l</body>
```

```
                <location> 0.04 -0.2 -0.07</location>
                <fixed>false</fixed>
            </Marker>
            <Marker name="LPRHE">
                <body>foot_l</body>
                <location> -0.02 0.06 0</location>
                <fixed>false</fixed>
            </Marker>
            <Marker name="LDIHE">
                <body>foot_l</body>
                <location> -0.04 0.02 -0.005</location>
                <fixed>false</fixed>
            </Marker>
            <Marker name="LLAHE">
                <body>foot_l</body>
                <location> 0.03 0.02 -0.05</location>
                <fixed>false</fixed>
            </Marker>
            <Marker name="RTTR">
                <body>torso</body>
                <location> -0.1 0.375 0.01</location>
                <fixed>false</fixed>
            </Marker>
            <Marker name="LTTR">
                <body>torso</body>
                <location> -0.1 0.4 -0.03</location>
                <fixed>false</fixed>
            </Marker>
            <Marker name="LBTR">
                <body>torso</body>
                <location> -0.1 0.35 -0.03</location>
                <fixed>false</fixed>
            </Marker>
        </objects>
        <groups />
</MarkerSet>
```

F.3: ACL Resting Length

```
function [AMB_ZLL, PLB_ZLL, Tibial, Femoral] = ACL_Resting_Length(ScaleSet)

Generic_Path = 'C:\Pipeline\OpenSim_Files\Generic_Setup_Files\';

%% Initialise Constants
AMBf = [-0.009 -0.406 0.008]; %AMB origin in Femur
AMBt = [0.013 -0.033 -0.008]; %AMB insertion in Tibia
PLBf = [-0.014 -0.409 0.009]; %PLB origin in Femur
PLBt = [0.002 -0.033 -0.005]; %PLB insertion inTibia

AMB_Er = 0.06; %AMB reference strain
PLB_Er = 0.1; %PLB reference strain

F2G = [-0.0707 -0.0661 0.0835]; %i.e. the position of the femur in respect of the ground (pelvis) reference plane

Knee_Angle = 0; %Used to find inherent, anatomical knee translation as a function of knee angle
```

```
load([Generic_Path 'Knee Translations.mat']); %A-P and S-I translations

%% Fetch Scale Factors From ScaleSet

Pelvis_Scale = str2double(strtok((ScaleSet(2).Scale.scales)));
Femur_Scale = str2double(strtok((ScaleSet(3).Scale.scales)));
Tibia_Scale = str2double(strtok((ScaleSet(4).Scale.scales)));

%% AMB

%Scale Origin/Insertion Points as a function of the body segment that they are attached to
AMBf_Scaled = AMBf*Femur_Scale;
AMBt_Scaled = AMBt*Tibia_Scale;

% Calculate Tibial Translation Matrix (as a function of the Knee Angle (0 degrees) at Reference Position)
Trans_X = fixpt_interp1(Tx.x, Tx.y, Knee_Angle, float('single'), 1, float('single'), 1, 'Floor');
Trans_Y = fixpt_interp1(Ty.x, Ty.y, Knee_Angle, float('single'), 1, float('single'), 1, 'Floor');

Tibial_Translation = [Trans_X, Trans_Y, 0]; %i.e. the position of the tibia relative to the femur

%Change to Global Coordinate System (by adding Scaled Translations)
AMBf_Scaled_Ground = AMBf_Scaled + (F2G*Pelvis_Scale);
AMBt_Scaled_Ground = AMBt_Scaled + (Tibial_Translation*Femur_Scale) + (F2G*Pelvis_Scale);

%% PLB

%Scale Origin/Insertion Points
PLBf_Scaled = PLBf*Femur_Scale;
PLBt_Scaled = PLBt*Tibia_Scale;

% Calculate Tibial Translation Matrix (as a function of Predefined Knee Angle at Resting Length)
Trans_X = fixpt_interp1(Tx.x, Tx.y, Knee_Angle, float('single'), 1, float('single'), 1, 'Floor');
Trans_Y = fixpt_interp1(Ty.x, Ty.y, Knee_Angle, float('single'), 1, float('single'), 1, 'Floor');

Tibial_Translation = [Trans_X, Trans_Y, 0];

%Change to Global Coordinate System (by adding Scaled Translations)
PLBf_Scaled_Ground = PLBf_Scaled + (F2G*Pelvis_Scale);
PLBt_Rotated_Ground = PLBt_Scaled + (Tibial_Translation*Femur_Scale) + (F2G*Pelvis_Scale);

% Calculate Reference Length - The length of the ligament at the reference position
AMB_Ref_Length = sqrt(sum((AMBf_Scaled_Ground-AMBt_Scaled_Ground).^2));
PLB_Ref_Length = sqrt(sum((PLBf_Scaled_Ground-PLBt_Rotated_Ground).^2));

%Calculate Zero Load Length
AMB_ZLL = AMB_Ref_Length / (AMB_Er + 1);
PLB_ZLL = PLB_Ref_Length / (PLB_Er + 1);

%% Distance Between Femoral Insertions

Femoral = sqrt(sum((AMBf_Scaled-PLBf_Scaled).^2));

%% Distance Between Tibial Insertions
Tibial = sqrt(sum((AMBt_Scaled-PLBt_Scaled).^2));
```

```
end
```

F.4: Inverse Kinematics

F.4.1: Batch IK

```
function Batch_IK(File_List)
%   This function calls an IK routine multiple times after receiving a list
%   of file names to process (and the type of file, Scut or Vcut)

Generic_Path = 'C:\Pipeline\OpenSim_Files\Generic_Setup_Files\';
Results_Path = 'C:\Pipeline\OpenSim_Files\Pipeline_Results\';
Subject_Specific_Path = 'C:\Pipeline\OpenSim_Files\Subject_Specific\';

Kinematics.Sorted = {};
Kinematics.Mean = {};
Kinematics.Errors = {};
Kinematics.Raw = {};
Kinematics.Coordinate_List = {};

for i = 1:(length(File_List))

   File_Name = File_List{i};

   % Remove ".c3d" from end of File_Name to get the name of the subject
   Full = strtok(File_Name, '.');
   Len = length(Full);

   Subject_Name = Full(1:Len-2); %This is necessary because the subject name isn't in the C3D file, but is part of the filename
   Trial_Number = ['Step_' Full(Len-1:Len)]; %Used to seperate individual trials from the same subject

   Subject_Path = [Subject_Specific_Path Subject_Name '\Scut\' Trial_Number '\'];

   cd(Subject_Path);

   load('Data.mat');

   % Inverse Kinematics
   Run_IK();

   %Group like Coordinates into Master File
   %Get kinematics

   IK = [Subject_Name '_' Trial_Number '_ik.mot'];
   IK_in = importdata(IK);
   Kinematics.Coordinate_List = IK_in.colheaders(2:end);
   Kinematics.Raw{1,i} = IK_in.data(:, 2:end); %Skips the first column, time

   %Create Master File (Only once)
   if (i == 1)
      Kinematics.Sorted = cell2struct(cell(1,length(Kinematics.Coordinate_List)),Kinematics.Coordinate_List,2);
   end
```

```
    for j = 1:length(Kinematics.Coordinate_List) %Coordinates are always saved in the same order
        Kinematics.Sorted.(Kinematics.Coordinate_List{j}) = [Kinematics.Sorted.(Kinematics.Coordinate_List{j}),
Kinematics.Raw{1,i}(:, j)];      %The results are stored in columns 7-13
    end

end %End of main processing loop


% Calculate Mean and SD of IK results
    Kinematics.Mean = cell2struct(cell(1,length(Kinematics.Coordinate_List)),Kinematics.Coordinate_List,2);

    for j = 1:length(Kinematics.Coordinate_List) %Coordinates are always saved in the same order
        m = nanmean(Kinematics.Sorted.(Kinematics.Coordinate_List{j}), 2);
        st = nanstd(Kinematics.Sorted.(Kinematics.Coordinate_List{j}),0, 2);
        Kinematics.Mean.(Kinematics.Coordinate_List{j}) = [m st];
    end

    % Save
    save([Results_Path  'IK Results.mat'], 'Kinematics');

end
```

F.4.2: Run IK

```
function Run_IK
%   This function runs a single Inverse Kinematics Routine
%   The Assumption is that the current path contains all the necessary data
%% Initialise
tic;
import org.opensim.modeling.*;
import org.opensim.utils.*;

load('Data.mat');

Current_Path = [pwd '\'];
Generic_Path = 'C:\Pipeline\OpenSim_Files\Generic_Setup_Files\';
Static_Path = ['C:\Pipeline\OpenSim_Files\Subject_Specific\' Name '\Static\'];

cd(Generic_Path); %So that the out and err log files are saved in this location.

 %Clear Log File
 fid = fopen('out.log', 'w');
 fclose(fid);

disp(['Initialising inverse Kinematics for subject ' Name ', trial number ' Trial_Number '...']);

%% Setup IK Tool
Scaled_Model = Model([Static_Path Name '_Scaled.osim']);
Scaled_Model.initSystem;

IK_Tool = InverseKinematicsTool([Generic_Path 'Generic_Setup_InverseKinematics.xml']);

%Setup IK Tasks
copyfile([Generic_Path 'Generic_IK_Tasks.xml'], Current_Path);
```

```
IK_Tasks = IK_Tool.getIKTaskSet();
Ob = IK_Tasks.makeObjectFromFile([Current_Path 'Generic_IK_Tasks.xml']);
IK_Tasks.assign(Ob);

%Check if markers were manually deleted - remove them from tasks

if (exist('Deleted_Markers', 'var'))
   for k = 1:length(Deleted_Markers)
      disp(['Removing ' Deleted_Markers{k} ' from IK Tasks']);
      task = IK_Tasks.get(Deleted_Markers{k});
      task.setApply(0);
   end
end

IK_Tasks.print([Current_Path Name '_' Trial_Number '_IK_Tasks.xml']); %save to location

IK_Tool.setName([Name ' IK']);

IK_Tool.setModel(Scaled_Model);

T_Start = 0; %((True_Start - 1)/Rate); %we subtract one data point because MATLAB treats the first unit as 1 but Opensim as 0

T_End = 1; %((True_End - 1)/Rate);

T_Start = (round(double(T_Start)*10^4)/(10^4)); %gets rid of noise when casting from single to double
T_End = round(double(T_End)*10^4)/(10^4);

IK_Tool.setInputsDir(Current_Path);
IK_Tool.setResultsDir(Current_Path);

IK_Tool.setMarkerDataFileName([Current_Path Name '_' Trial_Number '.trc']);
IK_Tool.setStartTime(T_Start);
IK_Tool.setEndTime(T_End);

IK_Tool.setOutputMotionFileName([Current_Path Name '_' Trial_Number '_ik.mot']);

IK_Tool.print([Current_Path Name '_' Trial_Number '_Setup_IK.xml']); %For checking with the OpenSim GUI

disp('Running Inverse Kinematics...');
IK_Tool.run();

%% End

   %Clear Log File
   fid = fopen('out.log', 'w');
   fclose(fid);
   cd(Current_Path);
   toc;
end
```

F.4.3: IK Errors

```
function IK_Err = Marker_Errors(Begin, End)
Current_Path = [pwd '\'];
```

```
load('Data.mat');

IK = importdata([Current_Path 'ik_model_marker_locations.sto']);

Marker_List = {'L5S1','RILCR', 'RTMTH', 'RTLTH', 'RBMTH', 'RBLTH', 'RTMSH', 'RTLSH',...
               'RBMSH', 'RBLSH', 'RPRHE', 'RDIHE', 'RLAHE', 'LILCR', 'LTMTH', 'LTLTH', 'LBMTH', 'LBLTH',...
               'LTMSH', 'LTLSH', 'LBMSH', 'LBLSH', 'LPRHE', 'LDIHE', 'LLAHE', 'LTTR', 'RTTR', 'LBTR'};

max_err = 0;
if (exist('Deleted_Markers', 'var'))
for m = 1:length(Deleted_Markers) %If Deleted_Markers is empty, this routine is skipped without an error

   %Remove Marker from Marker List
   term = find(strcmp(Deleted_Markers{m}, Marker_List));
   if ~isempty(term)
      Marker_List{term} = [];
   end
end

Marker_List = Marker_List(~cellfun('isempty',Marker_List));
end

for  i = 1: (length(Marker_List))
  Name = Marker_List{i};

  Mocap_3D = [];
  IK3D = [];

  Mocap_X = (Markers.(Name)((Begin+1):(End+1), 1))/1000;  %We add a data point because opensim calculates (n-1) marker
locations.
  Mocap_Y = (Markers.(Name)((Begin+1):(End+1), 2))/1000;
  Mocap_Z = (Markers.(Name)((Begin+1):(End+1), 3))/1000;

  %Remove positions where data was set to NaN
  %Mocap_X = Mocap_X((True_Start):(True_End), :);
  %Mocap_Y = Mocap_Y((True_Start):(True_End), :);
  %Mocap_Z = Mocap_Z((True_Start):(True_End), :);

  Mocap_3D = sqrt((Mocap_X.^2) + (Mocap_Y.^2) + (Mocap_Z.^2));

  pos = find(strcmp(IK.colheaders, [Name '_tx']));

  IK_X = IK.data(Begin:End, pos);
  IK_Y = IK.data(Begin:End, (pos+1));
  IK_Z = IK.data(Begin:End, (pos+2));

  IK_3D = sqrt((IK_X.^2) + (IK_Y.^2) + (IK_Z.^2));

  IK_Err.Marker_Errors(:,i) =  IK_3D - Mocap_3D;
  if (max(max(abs(IK_Err.Marker_Errors(:,i)))) > max_err)

    IK_Err.MaxMark = Name;
    max_err = max(max(abs(IK_Err.Marker_Errors(:,i))));
  end
```

```
end

IK_Err.MaxErr =  max_err;
IK_Err.MeanMaxErr = mean(max(IK_Err.Marker_Errors, [], 2));
Err = (IK_Err.Marker_Errors).^2;

%Calculate RMS Errors
Col_Count = sum(~isnan(Err),2);
Row_Count = sum(~isnan(Err),1);
Total_Count = sum(sum(~isnan(Err)));

%Calculates the Total RMS Error, irrespective of Marker Weightings
IK_Err.Total_RMS = sqrt( nansum(nansum(Err))/(Total_Count));

IK_Err.Marker_List = Marker_List;

end
```

F.4.4: Setup_IK

```
<? xml version="1.0" encoding="UTF-8" ?>
<OpenSimDocument Version="30000">
  <InverseKinematicsTool name="">
    <results_directory></results_directory>
    <input_directory></input_directory>
    <model_file></model_file>
    <constraint_weight>infinity</constraint_weight>
    <accuracy>5e-005</accuracy>
            <marker_file></marker_file>
            <report_marker_locations> true </report_marker_locations>
    <coordinate_file>Unassigned</coordinate_file>
    <time_range>0 0</time_range>
    <report_errors>true</report_errors>
    <output_motion_file></output_motion_file>
  </InverseKinematicsTool>
</OpenSimDocument>
```

F.4.5: IK Tasks

```
<? xml version="1.0" encoding="UTF-8" ?>
<OpenSimDocument Version="30000">
          <IKTaskSet name="IK_Tasks">
                    <objects>
                              <IKMarkerTask name="L5S1">
                                        <apply>true</apply>
                                        <weight>5</weight>
                              </IKMarkerTask>
                              <IKMarkerTask name="RILCR">
                                        <apply>true</apply>
                                        <weight>5</weight>
                              </IKMarkerTask>
                              <IKMarkerTask name="RTMTH">
                                        <apply>true</apply>
                                        <weight>10</weight>
```

```
</IKMarkerTask>
<IKMarkerTask name="RTLTH">
        <apply>true</apply>
        <weight>10</weight>
</IKMarkerTask>
<IKMarkerTask name="RBMTH">
        <apply>true</apply>
        <weight>10</weight>
</IKMarkerTask>
<IKMarkerTask name="RBLTH">
        <apply>true</apply>
        <weight>10</weight>
</IKMarkerTask>
<IKMarkerTask name="RTMSH">
        <apply>true</apply>
        <weight>10</weight>
</IKMarkerTask>
<IKMarkerTask name="RTLSH">
        <apply>true</apply>
        <weight>10</weight>
</IKMarkerTask>
<IKMarkerTask name="RBMSH">
        <apply>true</apply>
        <weight>10</weight>
</IKMarkerTask>
<IKMarkerTask name="RBLSH">
        <apply>true</apply>
        <weight>10</weight>
</IKMarkerTask>
<IKMarkerTask name="RPRHE">
        <apply>true</apply>
        <weight>2</weight>
</IKMarkerTask>
<IKMarkerTask name="RDIHE">
        <apply>true</apply>
        <weight>2</weight>
</IKMarkerTask>
<IKMarkerTask name="RLAHE">
        <apply>true</apply>
        <weight>2</weight>
</IKMarkerTask>
<IKMarkerTask name="LILCR">
        <apply>true</apply>
        <weight>5</weight>
</IKMarkerTask>
<IKMarkerTask name="LTMTH">
        <apply>true</apply>
        <weight>1</weight>
</IKMarkerTask>
<IKMarkerTask name="LTLTH">
        <apply>true</apply>
        <weight>1</weight>
</IKMarkerTask>
<IKMarkerTask name="LBMTH">
        <apply>true</apply>
        <weight>1</weight>
</IKMarkerTask>
<IKMarkerTask name="LBLTH">
```

```
                        <apply>true</apply>
                        <weight>1</weight>
                    </IKMarkerTask>
                    <IKMarkerTask name="LTMSH">
                        <apply>true</apply>
                        <weight>1</weight>
                    </IKMarkerTask>
                    <IKMarkerTask name="LTLSH">
                        <apply>true</apply>
                        <weight>1</weight>
                    </IKMarkerTask>
                    <IKMarkerTask name="LBMSH">
                        <apply>true</apply>
                        <weight>1</weight>
                    </IKMarkerTask>
                    <IKMarkerTask name="LBLSH">
                        <apply>true</apply>
                        <weight>1</weight>
                    </IKMarkerTask>
                    <IKMarkerTask name="LPRHE">
                        <apply>true</apply>
                        <weight>1</weight>
                    </IKMarkerTask>
                    <IKMarkerTask name="LDIHE">
                        <apply>true</apply>
                        <weight>1</weight>
                    </IKMarkerTask>
                    <IKMarkerTask name="LLAHE">
                        <apply>true</apply>
                        <weight>1</weight>
                    </IKMarkerTask>
                    <IKMarkerTask name="RTTR">
                        <apply>true</apply>
                        <weight>2</weight>
                    </IKMarkerTask>
                    <IKMarkerTask name="LTTR">
                        <apply>true</apply>
                        <weight>2</weight>
                    </IKMarkerTask>
                    <IKMarkerTask name="LBTR">
                        <apply>true</apply>
                        <weight>2</weight>
                    </IKMarkerTask>
                </objects>
                <groups />
            </IKTaskSet>
</OpenSimDocument>
```

F.5: Analyze Tool

F.5.1: Batch Analyze

```
function Batch_Analyze(File_List)
%   This function calls an IK routine multiple times after receiving a list
%   of file names to process
tic
Generic_Path = 'C:\Pipeline\OpenSim_Files\Generic_SErrorsup_Files\';
```

```
Results_Path = 'C:\Pipeline\OpenSim_Files\Pipeline_Results\';
Subject_Specific_Path = 'C:\Pipeline\OpenSim_Files\Subject_Specific\';

Position.Sorted = {};
Position.Mean = {};
Position.Raw = {};
Position.Coordinate_List = {};

IK_Err = {};
Velocity = {};

ACL.Length.Raw = {};
ACL.Length.Sorted = struct('AMB', [], 'PLB', []);
ACL.Length.Mean = struct('AMB', [], 'PLB', []);
ACL.Strain.Raw = {};
ACL.Strain.Sorted = struct('AMB', [], 'PLB', []);
ACL.Strain.Mean = struct('AMB', [], 'PLB', []);

ACL.List = {'AMB', 'PLB'};

load([Results_Path 'USC.mat']);
USC.Trimmed = struct('Hip_Ang', [], 'Hip_Add', [],'Hip_Rot', [],'Knee_Ang', [],'Knee_Val', [],'Knee_Rot', [],'Ank_Ang', []);
USC.Mean = {};
Fields = {'Hip_Ang', 'Hip_Add', 'Hip_Rot', 'Knee_Ang', 'Knee_Val', 'Knee_Rot', 'Ank_Ang' };

for i = 1:(length(File_List))

   File_Name = File_List{i};
   disp(['Loaded file ' File_Name '...']);

   % Remove ".c3d" from end of File_Name to gErrors the name of the subject
   Full = strtok(File_Name, '.');
   Len = length(Full);

   Subject_Name = Full(1:Len-2); %This is necessary because the subject name isn't in the C3D file, but is part of the filename
   Trial_Number = ['Step_' Full(Len-1:Len)]; %Used to seperate individual trials from the same subject

   Subject_Path = [Subject_Specific_Path Subject_Name '\Scut\' Trial_Number '\'];

   cd(Subject_Path);

   %Run
   disp(['Running Position and ACL Analysis on ' File_Name '...']);
   Run_Analyze();

   load('Data.mat');

   %Save IK Output to Master File
   An_Pos = importdata([Subject_Name '_' Trial_Number '_Analysis_Kinematics_q.sto']);
   An_Vel = importdata([Subject_Name '_' Trial_Number '_Analysis_Kinematics_u.sto']);
   An_Len = importdata([Subject_Name '_' Trial_Number '_Analysis__Length.sto']);

   Position.Coordinate_List = An_Pos.colheaders(2:end);
   Velocity.Coordinate_List = An_Vel.colheaders(2:end);
```

```
%Normalise kinematic & ACL data to stance phase and trim window

IK = [Subject_Name '_' Trial_Number '_ik.mot'];
IK_in = importdata(IK);

%trim over window of interest
Position.Raw{1,i} = An_Pos.data(1:152, 2:end);%interp1(1:126, An_Pos.data(:, 2:end), xq); %Skips the first column, time - replace 1:126 with length(kin)...
Velocity.Raw{1,i} = An_Vel.data(1:152, 2:end); %interp1(1:126, An_Vel.data(:, 2:end), xq);
ACL.Length.Raw{1,i} = An_Len.data(1:152, 2:end);%interp1(1:126, An_Len.data(:, 2:end), xq);

%convert knee flexion to positive axis (OpenSim sees it as -)
Position.Raw{1,i}(:, 10) = - Position.Raw{1,i}(:, 10);
Velocity.Raw{1,i}(:, 10) = - Velocity.Raw{1,i}(:, 10);

SP_Duration = SP_End - SP_Start;
[~, Cut_Begin] = max(Position.Raw{1,i}(:, 10));

Cut_End = SP_Start + (SP_Duration/2);

xq1 = linspace(Cut_Begin, SP_Start, 151);  %Swing phase
xq2 = linspace(SP_Start, Cut_End, 100);    %stance phase


Position.Trimmed{1,i} = [interp1(1:77, Position.Raw{1,i}(1:77, :), xq1); interp1(77:152, Position.Raw{1,i}(77:152, :), xq2)  ];
Velocity.Trimmed{1,i} = [interp1(1:77, Velocity.Raw{1,i}(1:77, :), xq1); interp1(77:152, Velocity.Raw{1,i}(77:152, :), xq2)  ];
ACL.Length.Trimmed{1,i} = [interp1(1:77, ACL.Length.Raw{1,i}(1:77, :), xq1); interp1(77:152, ACL.Length.Raw{1,i}(77:152, :), xq2) ];

Position.Trimmed{1,i}(151, :) = []; %delete repeated IC data point
Velocity.Trimmed{1,i}(151, :) = [];
ACL.Length.Trimmed{1,i}(151, :) = [];

% Save and trim USC Results
 for m = 1:length(Fields)
    Col = USC.All.(Fields{m})(1:152, i);
    temp = [interp1(1:77, Col(1:77, :), xq1)';  interp1(77:152, Col(77:152, :), xq2)'];
    temp(151, :) = [];
    USC.Trimmed.(Fields{m}) = [USC.Trimmed.(Fields{m}), temp];
 end

% Trim Inverse Kinematic errors over the necessary window and gErrors RMS Errorsc.
% Calculate and Save IK Marker Errors
IK = Marker_Errors(floor(Cut_Begin), ceil(Cut_End));
IK_Err.All{i} = IK.Marker_Errors;
IK_Err.Marker_List{i} = IK.Marker_List;
IK_Err.RMS{i} = IK.Total_RMS;
IK_Err.Max{i} = IK.MaxErr;
IK_Err.MeanMax{i} = IK.MeanMaxErr;

%Group like Positions into Master File
%Create Master File (Only once)
if (i == 1)
   Position.Sorted = cell2struct(cell(1,length(Position.Coordinate_List)),Position.Coordinate_List,2);
   Velocity.Sorted = cell2struct(cell(1,length(Velocity.Coordinate_List)),Velocity.Coordinate_List,2);
end
```

```
    for j = 1:length(Position.Coordinate_List) %Coordinates are always saved in the same order
        Position.Sorted.(Position.Coordinate_List{j}) = [Position.Sorted.(Position.Coordinate_List{j}), Position.Trimmed{1,i}(:, j)];
        Velocity.Sorted.(Velocity.Coordinate_List{j}) = [Velocity.Sorted.(Velocity.Coordinate_List{j}), Velocity.Trimmed{1,i}(:, j)];
    end

    %Calculate ACL Strain
    load([Results_Path 'Scale Output.mat']);
    pos = find(strcmp(Subject_Names, Subject_Name));

    AMB_Rest = ACL_Lengths.Data(pos,1);
    PLB_Rest = ACL_Lengths.Data(pos,2);

    ACL.Strain.Trimmed{1,i}(:,1) = (ACL.Length.Trimmed{1,i}(:,1) - AMB_Rest)/(AMB_Rest);
    ACL.Strain.Trimmed{1,i}(:,2) = (ACL.Length.Trimmed{1,i}(:,2) - PLB_Rest)/(PLB_Rest);


    for j = 1:length(ACL.List) %Coordinates are always saved in the same order
        ACL.Length.Sorted.(ACL.List{j}) = [ACL.Length.Sorted.(ACL.List{j}), ACL.Length.Trimmed{1,i}(:, j)];
        ACL.Strain.Sorted.(ACL.List{j}) = [ACL.Strain.Sorted.(ACL.List{j}), ACL.Strain.Trimmed{1,i}(:, j)];
    end

    disp('Processing Completed');
    disp('');
end

    % Calculate Mean and SD of Position & Velocity Kinematics
    Position.Mean = cell2struct(cell(1,length(Position.Coordinate_List)),Position.Coordinate_List,2);
    Velocity.Mean = cell2struct(cell(1,length(Velocity.Coordinate_List)),Velocity.Coordinate_List,2);

    for j = 1:length(Position.Coordinate_List) %Coordinates are always saved in the same order
        m = nanmean(Position.Sorted.(Position.Coordinate_List{j}), 2);
        st = nanstd(Position.Sorted.(Position.Coordinate_List{j}),0, 2);
        Position.Mean.(Position.Coordinate_List{j}) = [m st];

        m2 = nanmean(Velocity.Sorted.(Velocity.Coordinate_List{j}), 2);
        st2 = nanstd(Velocity.Sorted.(Velocity.Coordinate_List{j}),0, 2);
        Velocity.Mean.(Velocity.Coordinate_List{j}) = [m2 st2];
    end

    % Calculate Mean and SD of ACL Length and Strain
    for j = 1:length(ACL.List) %Coordinates are always saved in the same order
        Lm = nanmean(ACL.Length.Sorted.(ACL.List{j}), 2);
        Ls = nanstd(ACL.Length.Sorted.(ACL.List{j}),0, 2);
        ACL.Length.Mean.(ACL.List{j}) = [Lm Ls];

        Sm = nanmean(ACL.Strain.Sorted.(ACL.List{j}), 2);
        Ss = nanstd(ACL.Strain.Sorted.(ACL.List{j}),0, 2);
        ACL.Strain.Mean.(ACL.List{j}) = [Sm Ss];

    end

    for m = 1:length(Fields)
        Kin_Mean = nanmean(  USC.Trimmed.(Fields{m}), 2);
        Kin_Std =  nanstd(   USC.Trimmed.(Fields{m}), 1,2);
```

```
    USC.Mean.(Fields{m}) = [Kin_Mean Kin_Std];
  end

  save([Results_Path 'USC.mat'], 'USC');
  save([Results_Path  'Analysis Results.mat'], 'Position', 'Velocity', 'ACL', 'IK_Err');

  toc

end
```

F.5.2: Run Analyze

```
function Run_Analyze

%  This function runs a single Static Optimisation Routine
%  The Assumption is that the current path contains all the necessary data

import org.opensim.modeling.*
import org.opensim.utils.*
load('Data.mat');

Current_Path = [pwd '\'];
Generic_Path = 'C:\Pipeline\OpenSim_Files\Generic_Setup_Files\';
Model_Path = ['C:\Pipeline\OpenSim_Files\Subject_Specific\' Name '\Static\' Name '_Scaled.osim'];
Extension = [Current_Path Name '_' Trial_Number];

cd(Generic_Path);

%clear log file
fid = fopen('out.log', 'w');
fclose(fid);

AT = AnalyzeTool([Generic_Path 'Generic_Setup_Analyze.xml']);
AT.setModelFilename(Model_Path);

T_Start = 0;
T_End = 0.604;

T_Start = round(double(T_Start)*10^4)/(10^4); %gets rid of noise when casting from single to double
T_End = round(double(T_End)*10^4)/(10^4);

AT.setInitialTime(T_Start);
AT.setFinalTime(T_End);

AT.setCoordinatesFileName([Extension '_ik.mot']);
%AT.setExternalLoadsFileName([Extension '_grf.xml']);

AT.setResultsDir(Current_Path);
AT.setName([Name '_' Trial_Number '_Analysis']);

Print_File = [Extension '_Setup_Analyze.xml'];
AT.print(Print_File);
```

```
clear AT;

%load and run
AT = AnalyzeTool(Print_File);
AT.run();

%clear log file
fid = fopen('out.log', 'w');
fclose(fid);

%delete unneeded files

copyfile([Extension '_Analysis__Length.sto'], 'temp.sto');
copyfile([Extension '_Analysis_Kinematics_q.sto'], 'temp1.sto');
copyfile([Extension '_Analysis_Kinematics_u.sto'], 'temp2.sto');
delete([Extension '_Analysis*.sto']);

copyfile('temp.sto', [Extension '_Analysis__Length.sto']);
copyfile('temp1.sto', [Extension '_Analysis_Kinematics_q.sto']);
copyfile('temp2.sto', [Extension '_Analysis_Kinematics_u.sto']);
delete('temp.sto');
delete('temp1.sto');
delete('temp2.sto');

cd(Current_Path);
end
```

F.5.3: Setup Analyze

```
<? xml version="1.0" encoding="UTF-8" ?>
<OpenSimDocument Version="30000">
        <AnalyzeTool name="">
                <model_file></model_file>
                <replace_force_set>false</replace_force_set>
                <results_directory>.</results_directory>
                <output_precision>20</output_precision>
                <solve_for_equilibrium_for_auxiliary_states>false</solve_for_equilibrium_for_auxiliary_states>
                <maximum_number_of_integrator_steps>20000</maximum_number_of_integrator_steps>
                <maximum_integrator_step_size>1</maximum_integrator_step_size>
                <minimum_integrator_step_size>1e-008</minimum_integrator_step_size>
                <integrator_error_tolerance>1e-005</integrator_error_tolerance>
                <AnalysisSet name="Analyses">
                        <objects>
                                <Kinematics name="Kinematics">
                                        <on>true</on>
                                        <step_interval>1</step_interval>
                                        <in_degrees>true</in_degrees>
                                </Kinematics>
                                <MuscleAnalysis name="">
                                        <on>true</on>
                                        <step_interval>1</step_interval>
                                        <in_degrees>true</in_degrees>
                                        <muscle_list> AMB PLB </muscle_list>
                                        <moment_arm_coordinate_list />
                                        <compute_moments>false</compute_moments>
                                </MuscleAnalysis>
```

```
                    </objects>
                    <groups />
                </AnalysisSet>
                <lowpass_cutoff_frequency_for_coordinates>18</lowpass_cutoff_frequency_for_coordinates>
            </AnalyzeTool>
</OpenSimDocument>
```